

**„Some cycle others do not“
New views on cyclin function in the multinucleate hyphae of
*A. gossypii***

Inauguraldissertation

zur

Erlangung der Würde eines Doktors der Philosophie

vorgelegt der

Philosophisch-Naturwissenschaftlichen Fakultät

der Universität Basel

von

Anne Katrin Hungerbühler
aus Zürich

Basel, 2007

Genehmigt von der Philosophisch-Naturwissenschaftlichen Fakultät

auf Antrag von

Prof. Dr. Peter Philippsen, Prof. Dr. Yves Barral und Prof. Dr. Jean Pieters

Basel, den 6. Juni 2006

Prof. Dr. Hans-Jakob Wirz

TABLE OF CONTENTS

GENERAL INTRODUCTION 1

CHAPTER I

CYCLIN CHARACTERIZATION IN *A. GOSSYPII*

Abstract	11
Introduction	11
Results	12
Conserved gene set of cyclins found in <i>A. gossypii</i>	12
Cyclin function is conserved between <i>S. cerevisiae</i> and <i>A. gossypii</i>	12
Deletion of the G1 cyclin <i>AgCLN3</i>	14
The G1 cyclin deletion <i>Agcln1/2Δ</i> shows hyphal morphology defects	15
Deletion of the mitotic cyclin <i>AgCLB1/2</i> results in growth arrest as unipolar germling containing two to four nuclei	15
<i>AgCLB3/4</i> functions as a sporulation cyclin	17
The S-phase cyclin <i>AgCLB5/6</i> is essential in <i>A. gossypii</i>	22
Cell cycle specific arrest phenotype in the cyclin deletion mutants in <i>A. gossypii</i>	22
Discussion	26

CHAPTER II

REGULATION OF CELL CYCLE PROGRESSION BY NONCYCLING CYCLINS IN THE MULTINUCLEATED, FILAMENTOUS FUNGUS *A. GOSSYPII*

Abstract	33
Introduction	33
Results	34
G1 cyclins are nuclear and present across all spindle stages	34
Mitotic cyclins are nuclear and present during the entire nuclear division cycle	38
Mitotic cyclins are present in nuclei that are distinct from the site of expression	38
Asynchrony persists when cyclins are displaced from nuclei with two exogenous NESs	41
Mitotic cyclin degradation does not correlate with mitotic exit	45
Mitotic cyclin destruction box mutants do not show altered cell cycle progression	45
<i>AgSic1p</i> contributes to accurate nuclear division	47
<i>AgSic1p</i> localization changes across the nuclear division cycle	47
Discussion	50

CHAPTER III

THE S-PHASE CYCLIN AS A MAJOR CELL CYCLE REGULATOR IN *A. GOSSYPII*

Abstract	57
Introduction	57
Results	58
The S-phase cyclin AgClb5/6p levels oscillate during the cell cycle	58
Comparison of the S-phase cyclin AgClb5/6p with its homologues in <i>S. cerevisiae</i>	59
Forcing AgClb5/6p into the nucleus by the addition of two exogenous NLSs does not have an effect on cell cycle progression	59
A nondegradable form of AgClb5/6p causes severe growth defects in <i>A. gossypii</i>	63
Discussion	69

CHAPTER IV

CHARACTERIZATION OF KARYOPHERINS AND NUCLEOPORINS IN *A. GOSSYPYII*

Abstract	77
Introduction	77
Results	78
Deletion of the importin α , <i>AgSRP1</i>	78
Deletion of the importin β , <i>AgKAP95</i> , <i>AgPSE1</i> and <i>AgKAP123</i>	78
Phenotypic analysis of the deletion of the Ran binding protein (<i>AgYRB1</i>) and the Ran GTPase activating protein (<i>AgRNA1</i>)	82
Heterologous complementation assay of RNA1	82
Domain comparison of three <i>S. cerevisiae</i> and <i>A. gossypii</i> nucleoporins	82
Characterization of three nucleoporin deletions in <i>A. gossypii</i>	88
Asymmetric localization of the nucleoporin <i>AgNUP116/100</i>	88
Discussion	88

MATERIAL AND METHODS

<i>A. gossypii</i> strains and growth conditions	95
DNA manipulations	95
Generation of deletions	95
pAG plasmid construction	96
Generation of GFP-Fusions	96
Epitope-tagging with 13myc	96
LacI-LacO constructs	97
Construction of the D-box mutants (<i>AgCLB1/2</i>)	97
Construction of the overexpressed <i>AgCLB1/2</i>	98
Construction of D-box mutants (<i>AgCLB5/6</i>) under their endogenous promoter or the <i>GAL1</i> promoter	98
Forced localization cassettes (<i>AgCLB1/2</i> and <i>AgCLB5/6</i>)	99
Immunofluorescence, Hoechst/Actin and Calcofluor staining	100
Protein extraction and Western blotting	100
Microscopy	101

REFERENCES	117
APPENDIX (1-3)	124
ACKNOWLEDGEMENTS	163
CURRICULUM VITAE	165
ERKLÄRUNG	167

GENERAL INTRODUCTION

General Introduction

In order to divide, eukaryotic cells proceed through a sequence of phases called the cell cycle, during which the cell grows (G1), DNA duplicates (S-phase), daughter chromosomes segregate to opposite poles and the nucleus divides (M-phase). Eventually, the cytoplasm also divides giving rise to two identical daughter cells (cytokinesis). Processes of the cell cycle have to be coordinated both temporally and spatially to ensure that each division produces two viable progeny. In unicellular organisms, such as bacteria or yeasts, each cell division produces a complete new organism, while in multicellular organisms; many rounds of cell division are required to create a new individual.

The core machinery of the nuclear division cycle has been identified and intensively studied in the budding yeast. In *S. cerevisiae* the progression through the cell cycle can easily be followed by its morphological changes (Figure 1 A). In early G1-phase actin cables and patches display a random, unpolarized distribution. At a point late in G1-phase, called "Start" (Tyers, 1996), *S. cerevisiae* commits irreversibly to cell division. Start is operationally defined as the mating pheromone arrest point, nutritional arrest point, and the CDC28 execution point (Pringle and Hartwell, 1981). Following Start, cortical actin patches assemble at the "pre-bud" site, and cables are oriented toward that site. After actin polarization a visible bud is formed by apical growth at late G1 and in the beginning of S-phase. As the bud enlarges, cortical actin patches concentrate in the newly formed bud. After DNA replication but before chromosome segregation, when the bud has reached a certain size, a change in bud growth occurs, called the apical/isotropic switch. In larger buds, the mother/bud asymmetry in actin distribution breaks down and the actin structures are randomly distributed over the entire cell. At the end of the cell cycle, cortical actin patches become concentrated on both sides of the neck, cables orient towards the neck and also secretion and cell wall synthesis occurs primarily at the neck to promote cytokinesis and septation (summarized in (Lew et al., 1997), Figure 1 A).

As a mean to determine the events of the cell cycle in more detail, observation of spindle pole bodies (SPBs, fungal equivalent of the centrosomes) revealed being useful. In G1, a single SPB is embedded in the nuclear envelope, which nucleates growth of both, cytoplasmic and nuclear microtubules. During the time of bud emergence, a new SPB is constructed adjacent

to the old SPB (Donaldson and Kilmartin, 1996). When DNA replication is completed, (bud diameter $\sim 0.4 \times$ mother cell diameter, (Byers and Goetsch, 1975)), one SPB migrates away, to the other side of the nucleus. This SPB separation requires microtubules (Jacobs et al., 1988) resulting in the assembly of a short bipolar spindle, connecting the two SPBs, indicative of "G2/M-phase". During a period in which the short spindle remains relatively constant, the nucleus migrates to the mother-bud neck and orients along the mother-bud axis (Jacobs et al., 1988). The spindle then elongates, marking anaphase and finally shortly before cytokinesis, the spindle breaks down ((Kilmartin and Adams, 1984), summarized in (Lew et al., 1997), Figure 1 A).

One of the key problems in the field of cell cycle is the coordination of the different events. Cell cycle events must occur in proper order with respect to each other and in addition they have to take place once and only once in each cycle. The complex molecular events of the eukaryotic cell cycle is coordinated by a small number of heterodimeric protein kinases, the cyclin dependent kinase, called CDK. Cyclical changes in CDK activities are required for regulating cell cycle steps both positively and negatively to ensure accurate cell cycle progression. As a second coordinating mechanism, the checkpoint controls monitor the progress of key cell cycle events and act to delay cell cycle progression if one of these events has not been completed. Thus, checkpoint controls ensure that even if some perturbation delays the performance of a particular event, the cell cycle is able to occur in proper order.

CDKs are inactive as monomers and their activity is regulated by controlling levels of the associated cyclins (Morgan, 1995). Cyclins have first been identified in the early sea-urchin embryo and were named for their cyclical accumulation during the cell cycle (Evans et al., 1983). These proteins have been conserved throughout eukaryotes and their increases and decreases in concentration and activity ensures oscillation in the CDK activity, and thereby orderly progression through the cell cycle. The cyclins form a very diverse family of proteins, which contain the defined feature of the cyclins, the "cyclin-box", that is a necessary and sufficient domain, for binding and activation of CDKs (Morgan, 1995).

The main CDK implicated for cell cycle control in *S. cerevisiae* is Cdc28p (Nasmyth, 1993), which forms complexes with nine cyclins (ScCln1-

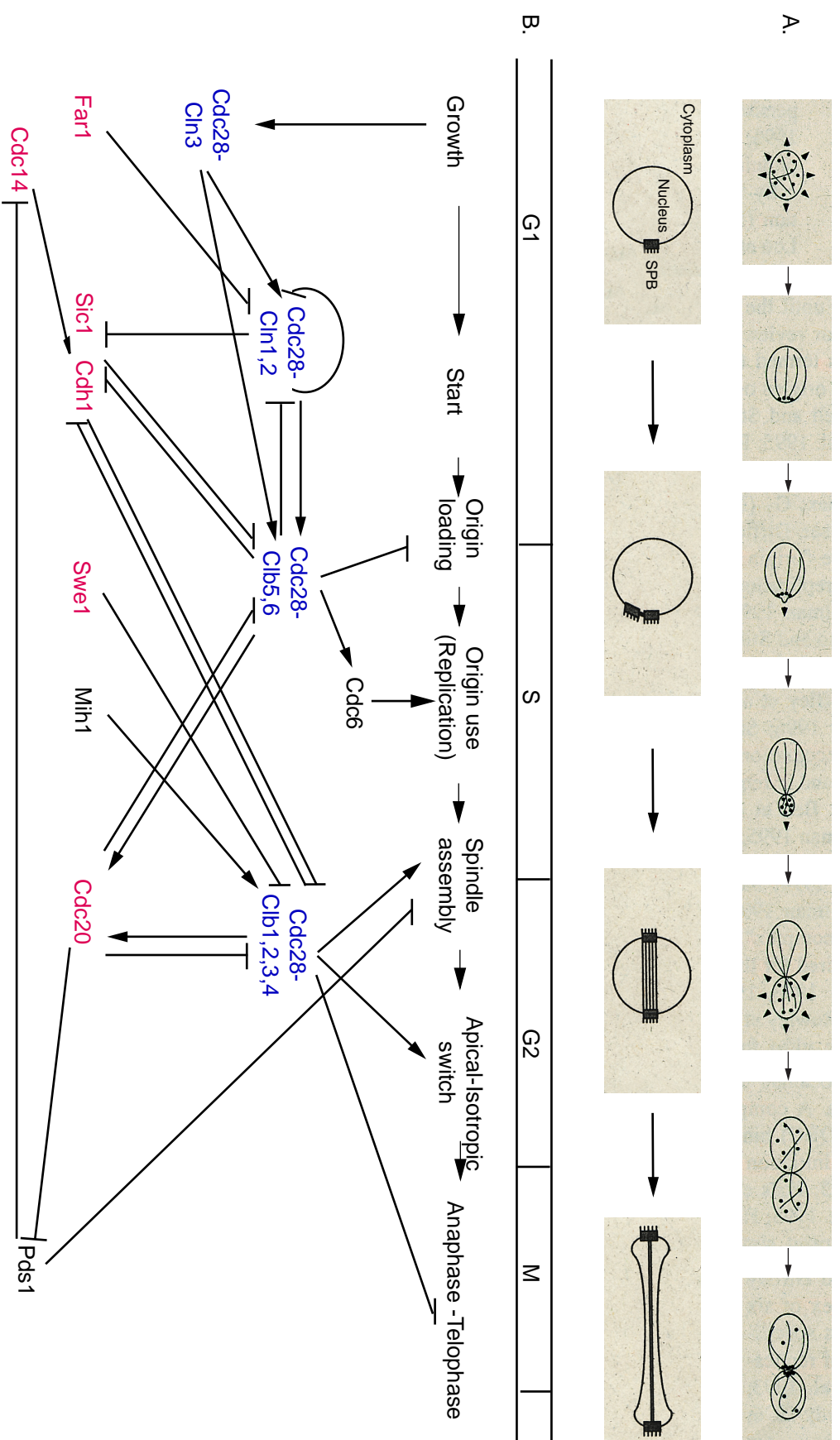


Figure 1
Control of cell cycle progression by the core cell cycle machinery.

A. Major landmark events of the *S. cerevisiae* cell cycle, showing the rearrangements of the actin cytoskeleton and secretory machinery on top, and the SPB duplication on the bottom. Lines represent actin cables, dots, actin patches. Pictures adapted from D.J. Lew et al., 1997.

B. Regulatory machinery responsible for the regulation of the core cell cycle. Activation is indicated by an arrow, presumably achieved by phosphorylation and dephosphorylation. Inhibition is indicated by a flat line and occurs by multiple mechanisms: inhibition, phosphorylation, or proteolysis due to ubiquitination. In blue are the Cdk-cyclin complexes, in red inhibitors.

3p, ScClb1-6p). With one exception (*ScCLN3*), the *S. cerevisiae* cyclins are encoded by pairs of closely related genes (*ScCLN1,2*; *ScCLB1,2*; *ScCLB3,4* and *ScCLB5,6*), which share partially redundant functions. Their products accumulate at specific times during the cell cycle, leading to waves of activation of distinct cyclin/Cdc28p complexes.

The activity of cyclin/Cdc28p complexes can be regulated posttranslationally by phosphorylation of Cdc28p and by association with other proteins. Cdc28p phosphorylation may occur on either of two sites: threonine 169 (T169), possibly required for activity (Deshaies and Kirschner, 1995) and tyrosine 19 (Y19) which inhibits kinase activity (Booher et al., 1993). The kinase ScSwe1p is responsible for the phosphorylation of Y19 in Clb1-4p/Cdc28p complexes (Booher et al., 1993; Lim et al., 1996), which is counteracted by the phosphatase ScMih1p (Booher et al., 1993; Russell et al., 1989). In the unperturbed cell cycle, Y19 phosphorylation of Clb1-4p/Cdc28p does not display a significant role. However, in cells which are impaired in their ability to form a bud, the morphogenesis checkpoint is triggered, causing Y19 phosphorylation to delay cell cycle progression until a bud has been formed (Lew and Reed, 1995).

The kinase activity of cyclin/Cdc28p complexes can also be controlled by the binding of "CDK inhibitor proteins", such as ScFar1p and ScSic1p (Peter and Herskowitz, 1994). ScFar1p is involved in the specific inhibition of Cln/Cdc28p complexes, whereas ScSic1p specifically inhibits Clb/Cdc28p (Peter and Herskowitz, 1994; Schwob et al., 1994). Therefore their activities are complementing each other. ScFar1p and ScSic1p accumulate periodically during the cell cycle, with maximal accumulation in early G1 (Schwob et al., 1994), when most cyclins (except Cln3p) are absent. Their inhibitory activity is based on their ability to exclude substrates from the Cdc28p active site, thereby blocking any cell cycle progression (Verma et al., 1997). Periodic activity changes of the CDK are controlled by many different processes such as timely complex building with distinct cyclins, inhibitory phosphorylation and inhibition by CDK inhibitors (Figure 1 B). Therefore temporally regulated expression, localization and degradation of cyclins and regulatory proteins ensure accurate progression through the cell cycle.

The core machinery and regulators of the nuclear division cycle have been closely investigated in the budding yeast and other uninucleated model organisms. However, also multinucleated cells are found in a variety of organisms and are integral to processes as diverse as the early development of the fruit fly, musculoskeletal and blood system,

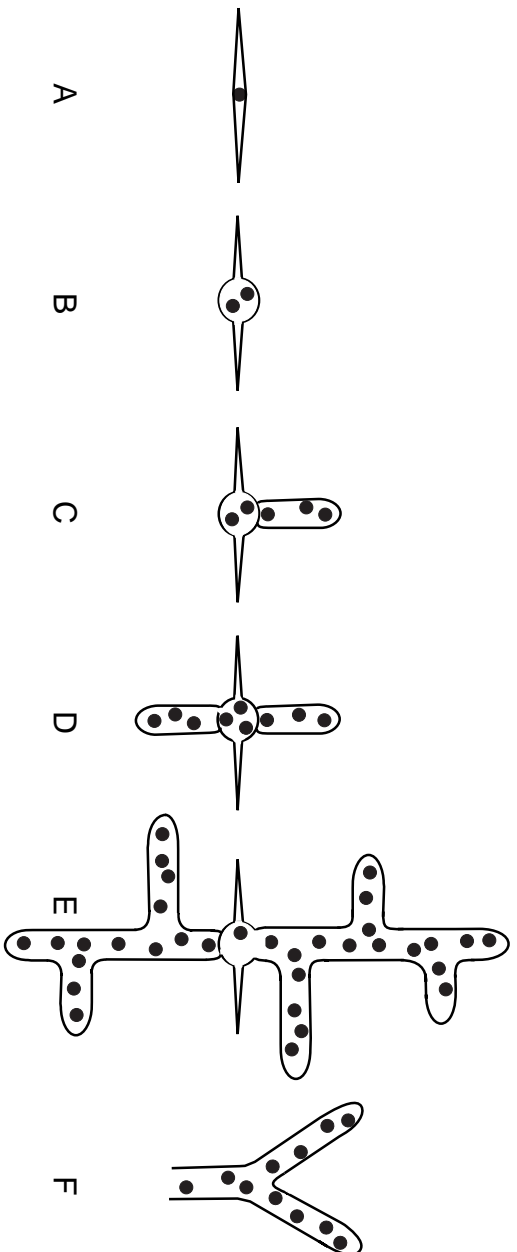
placenta formation and metastasizing tumor cells. So far, it remains completely unclear how a multinucleate cell regulates nuclear division.

We are studying nuclear division in the multinucleate model organism, *Ashbya gossypii*. This filamentous fungus is an Ascomycete, in the order of *Endomycetales* in the family of *Saccharomycetaceae* (Prillinger et al., 1997) which was first described in 1926 by Ashby and Nowell (Ashby and Nowell, 1926). *A. gossypii* was isolated as a cotton pathogen in the West Indies and Tanganyika Territory and causes a disease stigmatomycosis which affects the development of the hair cells in cotton bolls. Additionally, *A. gossypii* is a pathogen on citrus and tomatoes, where it causes the infected fruits to dry out and collapse (Phaff and Starmer, 1987). Needle shaped spores and parts of the mycelium are transferred from plant to plant by insects. Of particular biotechnological interest is the fact that *A. gossypii* is a natural overproducer of riboflavin (vitamin B2) and is together with *Candida famata* and *Bacillus subtilis* in use for industrial riboflavin production (Bacher et al., 1983).

A. gossypii grows filamentous and is able to form from a single spore within seven days a huge network, covering a 8 cm Petri dish. Its spores are needle shaped with a sticky filament at one end that probably attaches to carriers or to host plants. Spores germinate in response to as yet unknown environmental signals. Germination starts with isotropic growth in the center of the spore, forming a germ bubble. After the "isotropic-polarized" switch, polarization at one side of the bubble is established, and a first hypha is built, which is followed by a second on the opposite side. These main branches produce lateral branches to form a young mycelium (Figure 2). Mature mycelia speed up and grow by apical tip splitting. Spores are produced by mature hyphae and are found in sporangia. Our domesticated lab strain of *A. gossypii* is always haploid and has never been shown to mate or be responsive to mating pheromones, thus it is not yet known if these spores are the products of meiotic or mitotic events. These spores are mononucleated and as soon as germination occurs, also nuclear division is happening, leading to hyphae which are filled with hundreds of nuclei, present in one common cytoplasm.

In most multinucleate cells, mitosis tends to occur either synchronously, where all nuclei divide simultaneously, as in the slime mold *Physarum polycephalum* (Nygaard et al., 1960) or parasynchronously with a linear wave of nuclear division spreading across a cell, as in the filamentous fungus *Aspergillus nidulans*

A.



B.

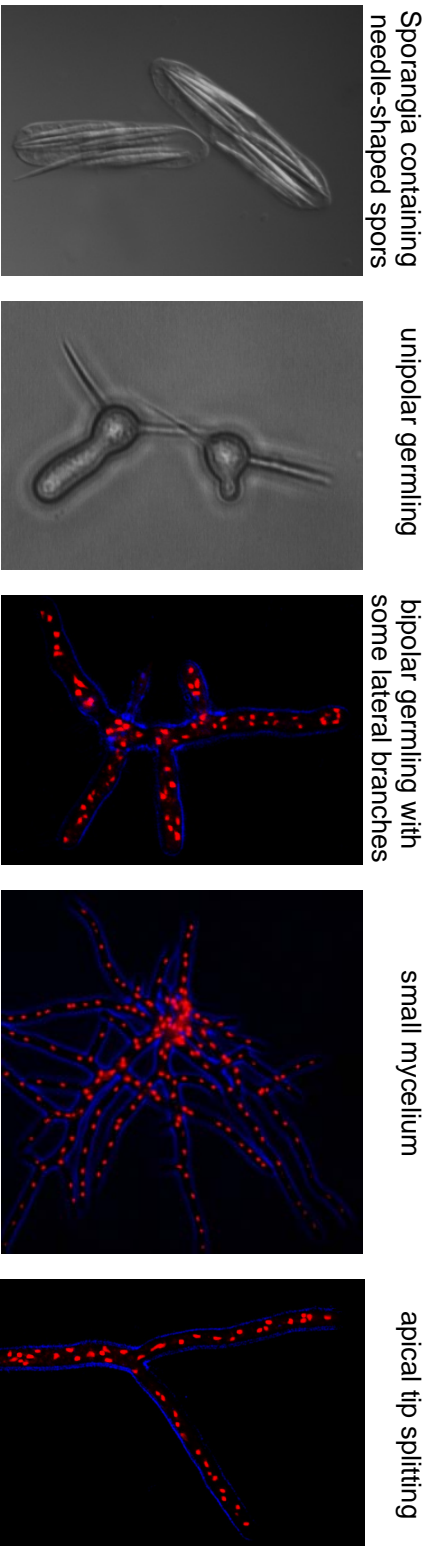


Figure 2

Morphological development of *A. gossypii*.

A. *A. gossypii* develops from a mononucleated, needle shaped spore [A]. During an isotropic growth phase, the germ bubble is produced containing several nuclei [B]. After a "isotropic-polarized" switch a unipolar germling is produced [C], followed by a second germtube at the opposite end of the germbubble [D] and lateral branches [E]. After 20 h the mature mycelium accelerates growth speed and grows exclusively by apical tip splitting [F].

B. Microscopy pictures representing the various growth stages in *A. gossypii* wild-type cells. In overlays, DNA is red (Hoechst staining) and brightfield is blue.

(Clutterbuck, 1970). However, only few cases have been reported, where asynchronous mitosis has been observed, as in the filamentous fungi *Neurospora crassa* and *Podospora anserina* (Minke et al., 1999), unpublished data). In these cells, nuclei of different cell cycle stage were coexisting in a common cytoplasm. Interestingly, also *A. gossypii* has been shown to divide its nuclei in an asynchronous manner. Nuclei in the hyphae of *A. gossypii* were investigated by in vivo time-lapse video microscopy, where single nuclei were followed. These nuclei oscillate rapidly and tumble through the cytoplasm in three dimensions, frequently exchanging places through by-passing one another (Alberti-Segui et al., 2001), Figure 3A and B). In these growing hyphae, multiple mitoses were observed, which happened asynchronously, independent of neighboring nuclei in close physical proximity (Figure 3A and B). The distance between nuclei varied between $< 1.0 \mu\text{m}$, when nuclei passed each other, and $7 \mu\text{m}$, with a mean of $3.6 \pm 0.1 \mu\text{m}$ (Gladfelter et al., 2006). Nuclear division can happen irrespective of the distance from the hyphal tip, however, the majority of mitoses occurs at branching sites, or future branching sites (HP. Helfer, personal communication).

Asynchrony in *A. gossypii* hyphae was shown to be based on the independent division of nuclei. Nuclei in living cells were followed through several generations of division showing that most nuclei were capable of division, yielding daughter nuclei that also divided (Gladfelter et al., 2006). The mean time between divisions of a nucleus was 112 minutes, but varied greatly from 46 to 250 minutes. Interestingly variability in cell cycle length was observed within daughter nuclei, produced from the same mitosis (Figure 3C). Thus most nuclei appear to be capable of division with variable timing, but surprisingly, they act independent of neighboring nuclei. The cell cycle stage of neighboring nuclei, have been determined by the visualization of the spindle pole bodies (Figure 4 A), and tubulin (Figure 4 B and D) in fixed mycelia. In general, $62 \pm 4.8\%$ of nuclei had 1 SPB, $18 \pm 2.6\%$ had duplicated, adjacent SPBs and $20 \pm 2.7\%$ showed a mitotic spindle, indicative for metaphase and anaphase nuclei (Gladfelter et al., 2006). Thus nuclei in *A. gossypii* appear to transit the different stages of the cell cycle regardless of the state of their neighbors.

In this thesis, initial molecular analysis of asynchronous nuclear division in the multinucleated fungus *A. gossypii* is presented. The completion of the genome sequencing project in *A. gossypii* revealed the most compact known eukaryotic genome, consisting of only 9 Mbp on 7 haploid

chromosomes, containing approximately 4'800 open reading frames (Dietrich et al., 2004). Interestingly, 95% of all genes identified in *A. gossypii* had an orthologue in the budding yeast *S. cerevisiae* and in particular, all cell cycle control genes described in budding yeast are present in *A. gossypii*. Despite this conservation of cell cycle genes, *A. gossypii* grows exclusively as hyphae containing many nuclei in linear arrays within the same cytoplasm. We wanted to analyze how periodic cell cycle proteins act in such a system in which nuclei are not dividing synchronously. A detailed characterization study of typical cell cycle regulated proteins, the five cyclins was performed in *A. gossypii*. The deletion analysis revealed reduced redundancy when compared to similar deletions in *S. cerevisiae*. Three of the five cyclins present in *A. gossypii* were essential. Most interestingly the S-phase cyclin *Agclb5/6 Δ* was essential, in contrast to the *Scclb5 Δ clb6 Δ* , implying its key involvement in the cell cycle. In addition, cyclin localization was followed during the cell cycle. Our experiments showed that both the G1 and the mitotic cyclins are present across all stages of the cell cycle. In addition, the mitotic cyclin *AgClb1/2p* was not degraded during mitosis and we speculate that in this case, CDK inhibitors such as *AgSic1p* provide the primary source of oscillation in mitotic cyclin activity instead of degradation. In contrast, the essential S-phase cyclin *AgClb5/6p* clearly disappears in anaphase nuclei, and we were able to show, that this disappearance was due to degradation.

The irreversible process of protein destruction is a way of driving the cell cycle onwards. However, in a multinucleated hyphae, where the continuous cytoplasmic streaming provides constant supply of proteins, controlling cell cycle progression on the basis of timely protein degradation, may be very wasteful. As a mean to decrease costs due to constant degradation of proteins entering a nucleus of a different nuclear stage, alternative regulation mechanisms through CDK inhibitors, regulated nuclear import, and cell cycle specific changes in the nuclear pore complex may have evolved. Some of these mechanisms have been investigated in more detail in *A. gossypii* and are discussed in the course of this thesis.

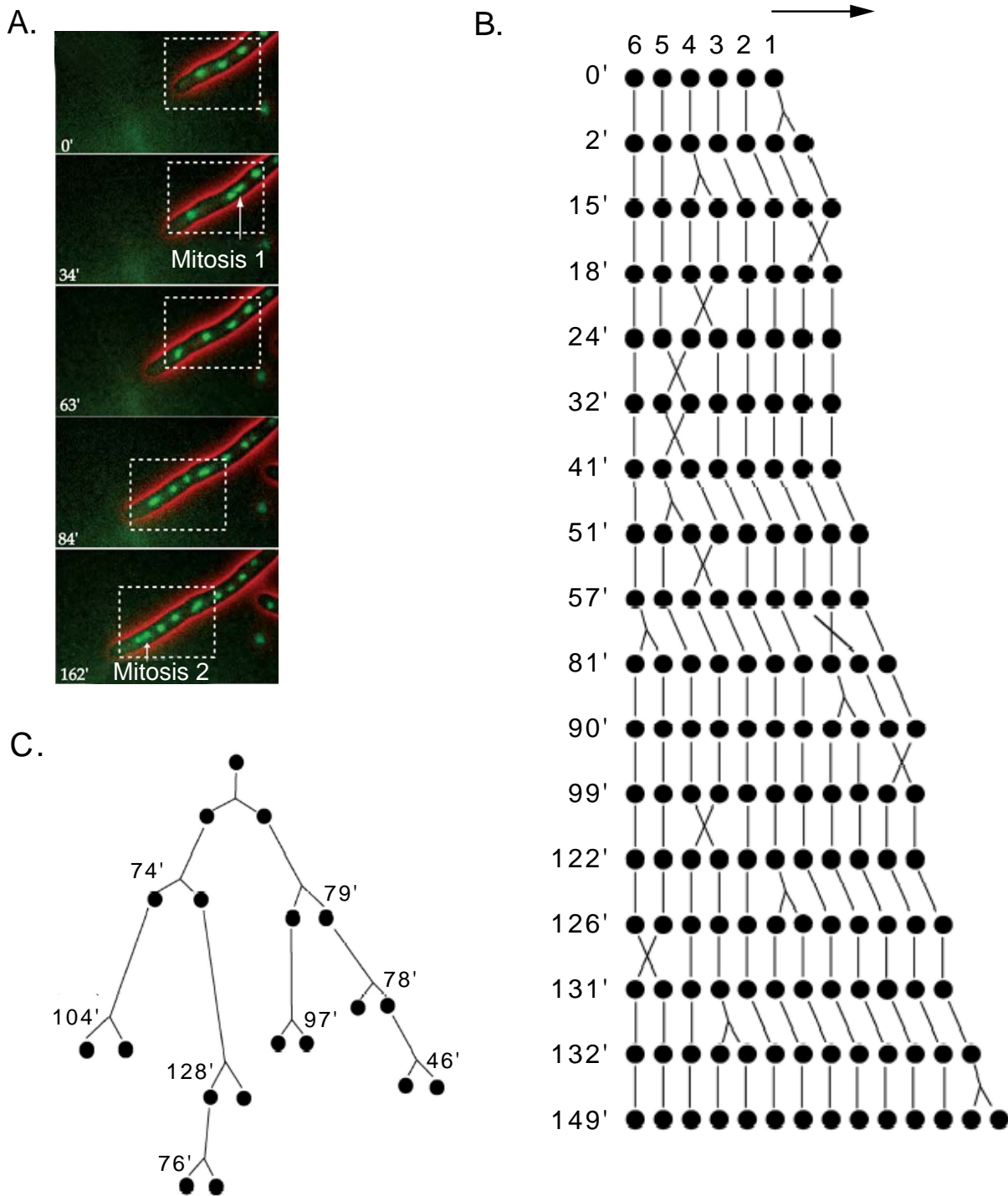


Figure 3
Mitoses are asynchronous in multinucleate *A. gossypii* cells.

A. Individual frames from a time-lapse video, recording the growth of a strain with GFP-labeled nuclei (kindly provided by C. Alberti-Segui). The nuclei indicated by the arrows divide independent from their neighbors.

B. Example of a nuclear pedigree demonstrating the capacity for all nuclei to divide. Six starting parent nuclei were followed through subsequent nuclear divisions. Numbers are time in minutes from start of time-lapse acquisition. In the pedigree diagram, X is a by-passing event, an upside-down Y a mitosis, and the arrow denotes the direction of growth.

C. Nuclear lineage demonstrating variability in nuclear division cycle length within related nuclei, where the time in minute represents the time between nuclear divisions.

(Figure B is kindly provided by A. Gladfelter, founded on a pedigree analysis of P. Philippsen which was based on a movie made by C. Alberti-Segui. Figure C is kindly provided by A. Gladfelter)

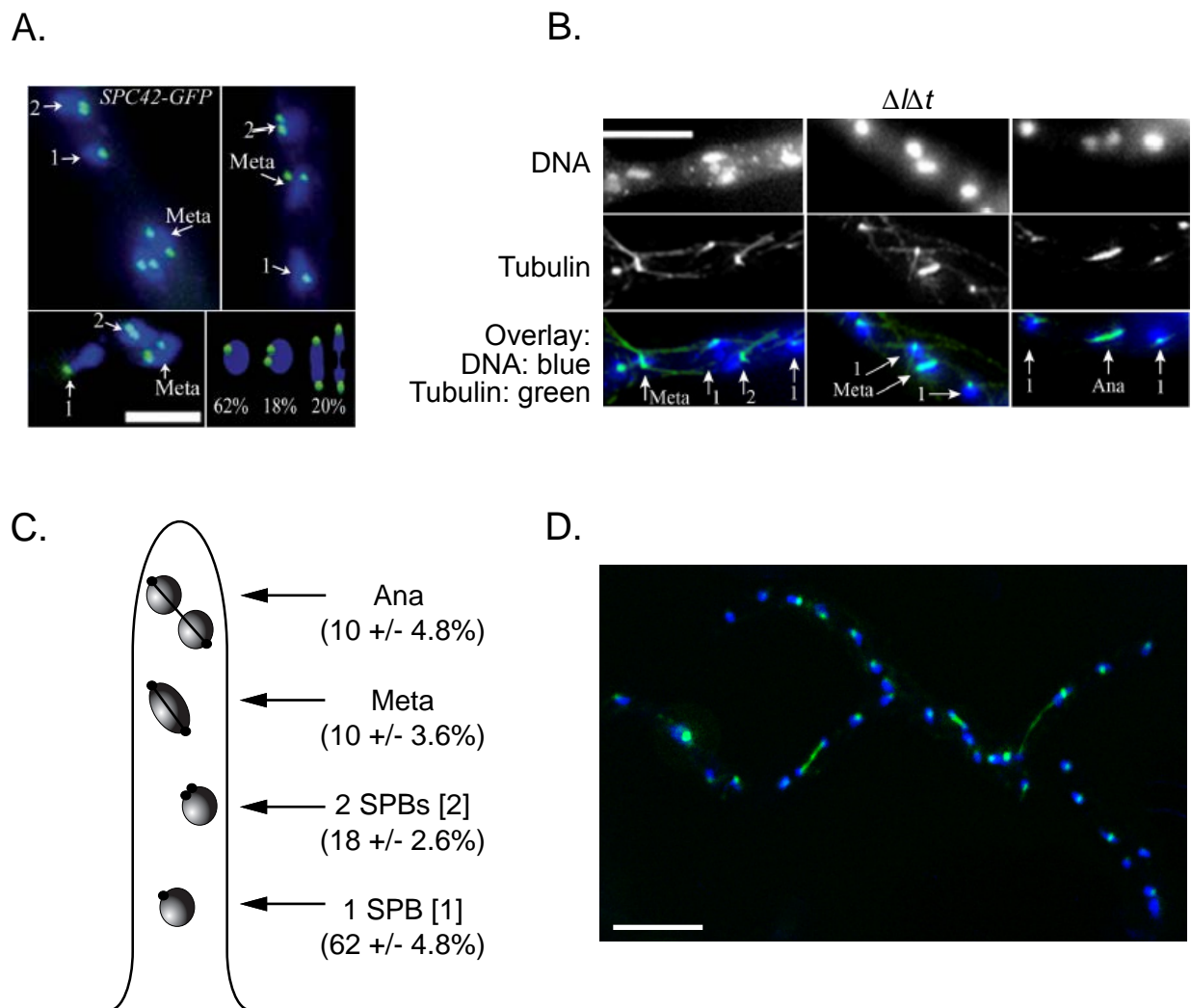


Figure 4
Neighboring nuclei are in different cell cycle stages.

A. *gossypii* spores were grown overnight at 30°C until young mycelium were formed that contained 75-100 nuclei. In all panels, arrows highlight neighboring nuclei in different spindle stages.

A. *SPC42-GFP* (ASG38) visualization for SPB observation.

B. Tubulin visualization in the reference strain by immunofluorescence using anti-tubulin antibody for spindle observation.

C. Schema on the scoring of the different nuclear stages. 1 indicates nuclei with a single SPB; 2 indicates nuclei with adjacent, duplicated SPBs or SPBs that are larger in diameter and >2x brighter than single SPBs; Meta indicates likely metaphase nuclei with a spindle aligned across the middle of the DNA; Ana indicates anaphase nuclei in which the spindle connects two separated DNA signals.

D. Example of the tubulin visualization in a small mycelium by immunofluorescence using anti-tubulin antibody for spindle observation.

In overlays, DNA is blue, and microtubules or SPBs are in green.

Bars, (A) 5 μm ; (B and D) 10 μm .

(The microscopy pictures in A and B were kindly provided by Amy Gladfelter)

CHAPTER I

Cyclin characterization in *A. gossypii*

The data presented here originate from close collaborative work of Amy Gladfelter and myself. These results were combined, to give an overview over the cyclins. Amy Gladfelter constructed and characterized the deletions of the G1 cyclins *AgCLN3* and *AgCLN1/2* and I investigated the B-type cyclins.

Abstract

The nuclear division cycle in multinucleated cells generally occurs synchronously, due to the free exchange of cell cycle regulators between nuclei sharing the same cytoplasm. The filamentous fungus, *Ashbya gossypii* however, undergoes asynchronous nuclear division in that neighboring nuclei are in different cell cycle stages despite close physical proximity. The behaviour of typically oscillating proteins such as cyclins was investigated in this model organism, where each nucleus has its own rhythm. As a first step towards a better understanding how such proteins function in a multinucleated cell, the deletion of the five cyclins was characterized in *A. gossypii*. Three of the five cyclins were essential and most interestingly the deletion of the S-phase cyclin *AgCLB5/6* revealed a lethal phenotype. This is in contrast to yeast, where the double deletion of *Scclb5Δclb6Δ* was viable with a delay in the timely initiation of DNA replication. Based on the lethality of the deletion of the S-phase cyclin, its key involvement in cell cycle regulation of *A. gossypii* is hypothesized.

A reduced amount of redundancy between the five cyclins of *A. gossypii* may explain the severe deletion phenotypes observed. This lack of redundancy may be the result of differences in substrate specificity, timing, levels of protein expression or localization between the different cyclins in *A. gossypii* and will be investigated in more detail in Chapter II and III.

Introduction

Progression through the eukaryotic cell cycle depends on sequential functions of the cyclin-dependent kinases (CDKs). Cdk activity oscillations are required for regulating cell cycle steps both positively and negatively. The catalytic

activity of the Cdk is dependent upon physical interaction with the cyclins. The concentration and activity of cyclins increases and decreases to ensure oscillation in the CDK activity and orderly progression through the cell cycle (Lodish, 2000). The cyclins are often recognized on a sequence level by the presence of a conserved domain, the cyclin box (Kobayashi et al., 1992).

In animals, multiple Cdks exist, which are activated by multiple cyclins. The many different complexes and tissue specific expression make analysis of cyclin function in animal cells complicated. Budding yeast possesses five CDKs (*Cdc28*, *Pho85*, *Kin28*, *Ssn3* and *Ctk1*), however passage through the cell cycle is based on a central Cdk, *Cdc28* which is the major oscillator of the yeast division cycle. It undergoes changes in activity by associating with distinct groups of cyclins that accumulate at different times and by stimulatory and inhibitory phosphorylation (Mendenhall and Hodge, 1998).

In *S. cerevisiae* three G1, or CLN cyclins (*ScCLN1*, *ScCLN2*, and *ScCLN3*), and six B-type cyclins (*ScCLB1-ScCLB6*) exist, which bind the central cyclin dependent kinase *Cdc28*. Whereas the main role of the G1 cyclins is the activation of the B-type cyclins and bud emergence, B-type cyclins are required for DNA replication and inhibiting re-replication (*ScClb5p*, *ScClb6p*), spindle formation (*ScClb3p*, *ScClb4p*) and initiation of mitosis (*ScClb1p*, *ScClb2p*, (Jacobson et al., 2000; Mendenhall and Hodge, 1998) . Each group of cyclins thus directs the *Cdc28* kinase for specific functions associated with various cell-cycle phases.

The multinucleate filamentous fungus *A. gossypii* and *S. cerevisiae* share similar gene sets and strikingly high synteny patterns, however the whole genome duplication in yeast resulted in many pairs of genes where only a single homologue is present in *A. gossypii*. In the case of cyclins *A. gossypii* contains two G1 cyclins (*AgCLN1/2* and *AgCLN3*) and three B-type cyclins (*AgCLB1/2*, *AgCLB3/4* and *AgCLB5/6*).

Mitosis in the multinucleate fungus *A. gossypii* occurs in an asynchronous manner, in that single nuclei divide independently in time and space from their neighbors. Each nucleus is in its own cell cycle rhythm and it was unclear how a typical oscillating protein such as the cyclins would behave in such a multinucleate cell. Cyclins are typically oscillating proteins and therefore we

wanted to study the behaviour of these cyclins in the multinucleate fungus *A. gossypii*. As a first step towards a better understanding how such proteins function in a multinucleate hyphae, the deletion phenotypes of the five cyclins were characterized.

The results presented here, show a higher sensitivity to changes in the cyclin abundance in *A. gossypii* compared to *S. cerevisiae*. Three of the five cyclins were essential, most interestingly the S-phase cyclin *AgCLB5/6*. In contrast to yeast where the double deletion of *Scclb5Δclb6Δ* prevented timely initiation of DNA replication and displayed elongated cells (Schwob and Nasmyth, 1993), *Agclb5/6Δ* cells died as bipolar germings with some branches and few, disintegrated nuclei. Therefore we speculate that *A. gossypii* has less redundancy buffering its cell cycle, making the cells more sensitive to perturbations of this cycle.

Results

Conserved gene set of cyclins found in *A. gossypii*

The cell cycle process has been conserved throughout eukaryotes and requires temporally regulated expression, localization and degradation of cyclins and regulatory proteins. Due to the high conservation of the core cell division cycle proteins

and the complete genome annotation of *A. gossypii* (Dietrich et al., 2004) sequence comparison using TFASTA with the *S. cerevisiae* cyclins as a template was successfully applied. For each of the cyclin pairs found in *S. cerevisiae* (*ScCLN1* and *ScCLN2*; *ScCLB1* and *ScCLB2*; *ScCLB3* and *ScCLB4*; *ScCLB5* and *ScCLB6*) one single homologue was identified in *A. gossypii*, named by combining both yeast homologues, separated by a slash (*AgCLN1/2*, *AgCLB1/2*, *AgCLB3/4* and *AgCLB5/6*, respectively). Only one homologue was found for the G1 cyclin *ScCLN3*, called *AgCLN3*. All cyclins identified in *A. gossypii* were present at syntenic positions with their homologues in *S. cerevisiae*, showing amino acid identity ranging from 34% for *ClN3p*, to 65% between *AgClb1/2p* and *ScClb2p* (Table 1, Figure 5). Thus *A. gossypii* and *S. cerevisiae* share a similar set of cyclins, despite their completely different growth forms. *S. cerevisiae* coordinates nuclear division with budding and cytokinesis to produce mononucleate cells, while *A. gossypii* duplicates nuclei without cytokinesis leading to multinucleate hyphae.

Cyclin function is conserved between *S. cerevisiae* and *A. gossypii*

To investigate whether cyclin function has been conserved between *S. cerevisiae* and *A. gossypii*, the *AgCLN1/2* and *AgCLB1/2* genes

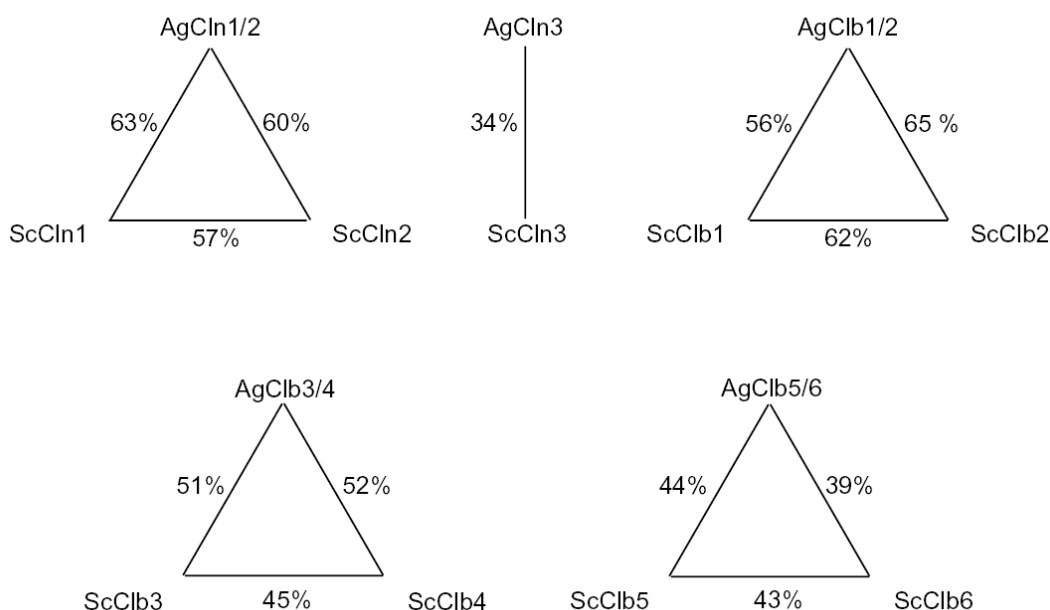


Figure 5
Percentage of amino acid sequence identity between *A. gossypii* and *S. cerevisiae* cyclins.

Table 1.
Overview over the *A. gossypii* cyclins and their homologues in *S. cerevisiae*.

A.g. cyclin	Homologue in S.c.		A.g. ORF size (aa)	Size of homologue in S.c. (aa)		Percentage Identity to S.c homologue		A.g. Deletion	Deletion in S.c. Homologues	
	1°	2°		1°	2°	1°	2°		1°	2°
AgCLN1/2 (AFL174C)	ScCLN1 (YMR199W)	ScCLN2 (YPL256C)	513	545	546	63	60	Lethal	Viable	Viable
AgCLN3 (ADR384W)	ScCLN3 (YAL040C)		459	580		34		Viable	Viable	
AgCLB1/2 (AAR099W)	ScCLB2 (YPR119W)	ScCLB1 (YGR108W)	556	491	471	65	56	Lethal	Viable	Viable
AgCLB3/4 (ADR068W)	ScCLB4 (YLR210W)	ScCLB3 (YDL155W)	376	460	427	52	51	Viable	Viable	Viable
AgCLB5/6 (AAR100C)	ScCLB5 (YPR120C)	ScCLB6 (YGR109C)	405	435	380	44	39	Lethal	Viable	Viable
									double Δ: Viable	double Δ: Viable

(under control of their *A. gossypii* promoters) were evaluated for their ability to complement mutant yeast strains deleted for the genes of the homologous cyclins. Both *A. gossypii* cyclins appeared functional in yeast, leading to growth of the otherwise inviable yeast deletions (Figure 6). This suggests that promoter regulation and cyclin substrate specificity have been functionally conserved between these two organisms. Since AgCln1/2p and AgClb1/2p appear to be functional cyclins in yeast, they very likely are key elements for nuclear cycle control in *A. gossypii*.

Deletion of the G1 cyclin *AgCLN3*

To characterize the function of the two G1 -and the three B-type cyclins in *A. gossypii* a deletion of each gene was performed. For each cyclin, the entire ORF was replaced via PCR based gene targeting with Gen3 or ClonNAT as a dominant selection marker (Wach et al., 1994;

Wendland et al., 2000). For each deletion at least three transformants were compared in a phenotype analysis to confirm that defects were due to the null mutation and not additional mutations. Every deletion constructed first went through a heterokaryotic stage, where wild-type and transformed nuclei coexisted. Only after clonal purification by isolating single, mononucleated spores, each nucleus contained the transformed DNA. However, for the evaluation of essential genes, spores were used, which originated from the heterokaryon containing wild-type protein. This protein leftover may allow growth until its disappearance. Therefore these deletion experiments may also be called depletion experiments in the case of essential genes, where spores had derived from the heterokaryon.

ScCLN3 is an integrator for signals that regulate the rate of G1 progression in *S. cerevisiae* (Laabs et al., 2003). By activating Start specific transcription of the other G1 cyclins and the B-type cyclin *ScCLB5* and *ScCLB6*, *ScCln3p* is

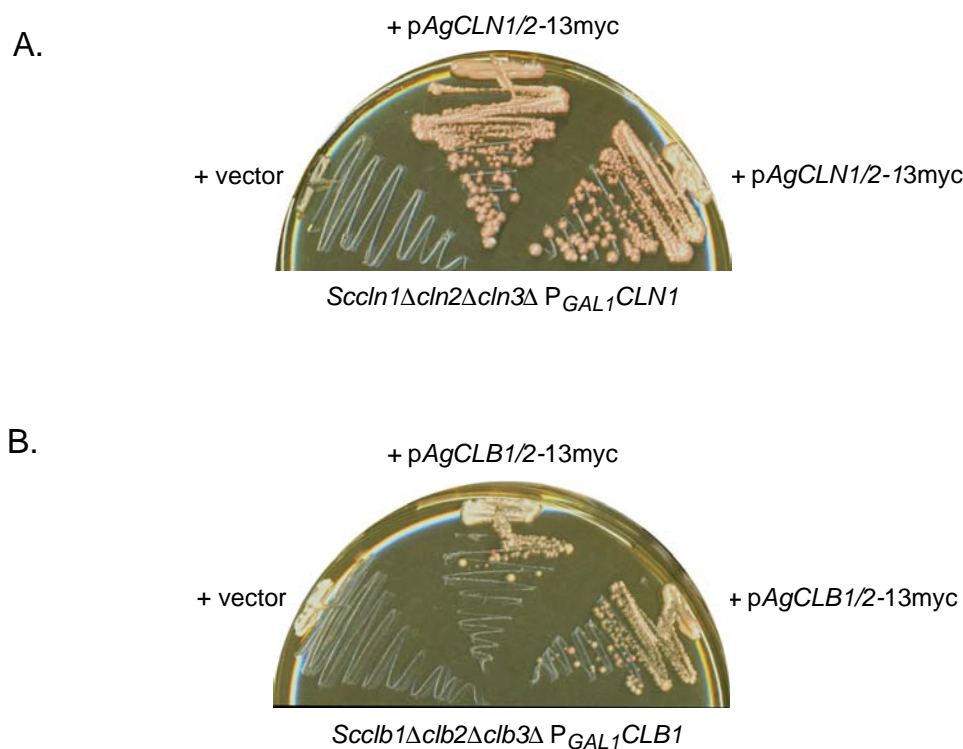


Figure 6

Conserved cyclin function between *A. gossypii* and *S. cerevisiae*

A. *S. cerevisiae* strain *Sccln1Δcln2Δcln3ΔP_{GAL1}CLN1* (AY52) was transformed with pCLN2-13myc containing the *AgCLN1/2-13myc* expressed from its own *A. gossypii* promoter.

B. *S. cerevisiae* strain *Scclb1Δclb2Δclb3ΔP_{GAL1}CLB1* (AY117) was transformed with pCLB2-13myc, containing the *AgCLB1/2-13myc* also expressed from its own *A. gossypii* promoter.

Both strains were transformed with control vectors containing the selectable marker but lacking a cyclin gene. The inducible yeast cyclins were repressed in glucose and complementation was evaluated at 30°C on YPD plates + 200 μg/ml G418.

substantially involved in the timing when a new cell cycle starts.

The G1 cyclin *AgcIn3Δ* mutants displayed the mildest phenotype, in that growth was comparable to the reference strain (Figure 7). No abnormalities were found in nuclear appearance, the actin cytoskeleton or chitin localization. A possible explanation for this phenotype may be the compensation by the other G1 cyclins due to their redundant functions.

The G1 cyclin deletion *AgcIn1/2Δ* shows hyphal morphology defects

The G1 cyclins ScCln1p and ScCln2p activate ScCdc28p to promote S-phase onset and restrict cortical actin to the site of polarized growth in *S. cerevisiae* (Lew and Reed, 1993). However, this polarization of the yeast cell is only transiently since the activation of ScCdc28p by mitotic cyclins causes depolarization of the cortical actin cytoskeleton in budded G2 cells. *A. gossypii* grows polarized during the whole cell cycle and changes in abundance of AgCln1/2p may therefore cause severe morphology defects. To test this hypothesis the G1 cyclin homologue *AgCLN1/2* was deleted.

The deletion of *AgCLN1/2* resulted in

inviable germlings which arrested growth as microcolonies with highly aberrant morphology (Figure 8 A). These cells displayed an enlargement of the hyphae, resulting in swollen branches. Actin distribution was investigated by Alexa488-Phalloidin staining, showing polarized actin in most tips, however only aberrant actin cables were observed (Figure 8 A, right). The enlargement of the hyphae observed in this deletion, may be the consequence of a diffuse zone of polarity. *AgcIn1/2Δ* cells were able to go through many rounds of nuclei division as shown by immunofluorescence, where small mycelia were stained with Hoechst, indicating nuclei, and tubulin antibody showing the different spindle stages (Figure 8 B). In contrast to *S. cerevisiae*, where the presence of one G1 cyclin is sufficient for the cells to survive, in *A. gossypii* the deletion of the G1 cyclin *AgCLN1/2* is lethal. Its deletion causes an enlargement of the hyphae, which may indicate its involvement in the maintenance of polarity.

Deletion of the mitotic cyclin *AgCLB1/2* results in growth arrest as unipolar germling containing two to four nuclei

In *S. cerevisiae* mitotic cyclins ScClb1p-ScClb4p are involved in processes during the

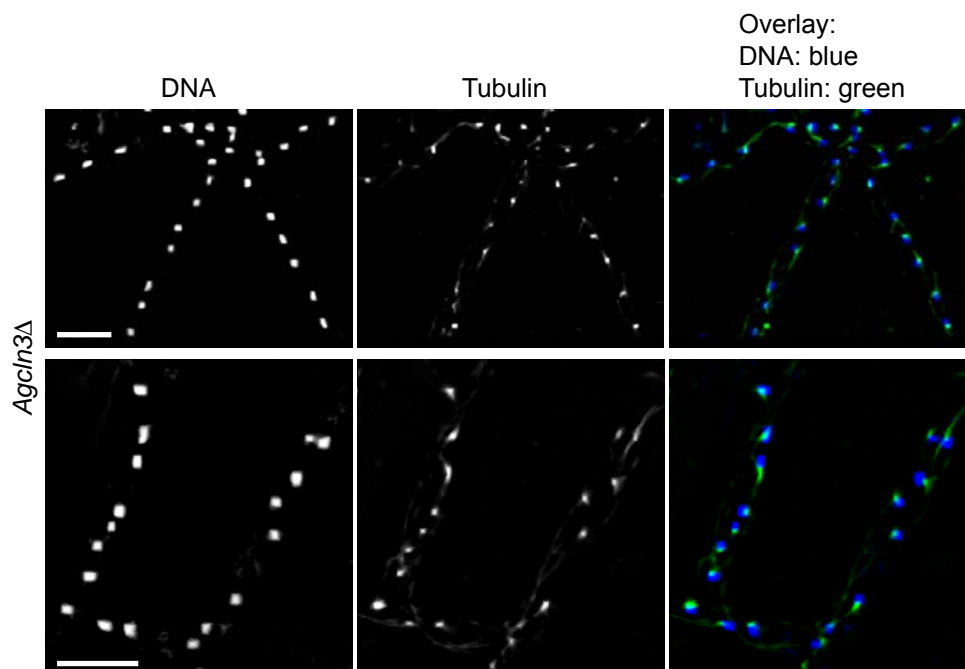


Figure 7

***AgcIn3Δ* mutants do not display any growth or nuclear division defect.**

Parts of a hyphae containing the G1 cyclin *AgcIn3Δ* mutation was stained with Hoechst (left) and tubulin antibody, showing different spindle stages by immunofluorescence (middle). In overlays, DNA is blue and tubulin is green. Bars, 10 μ m.

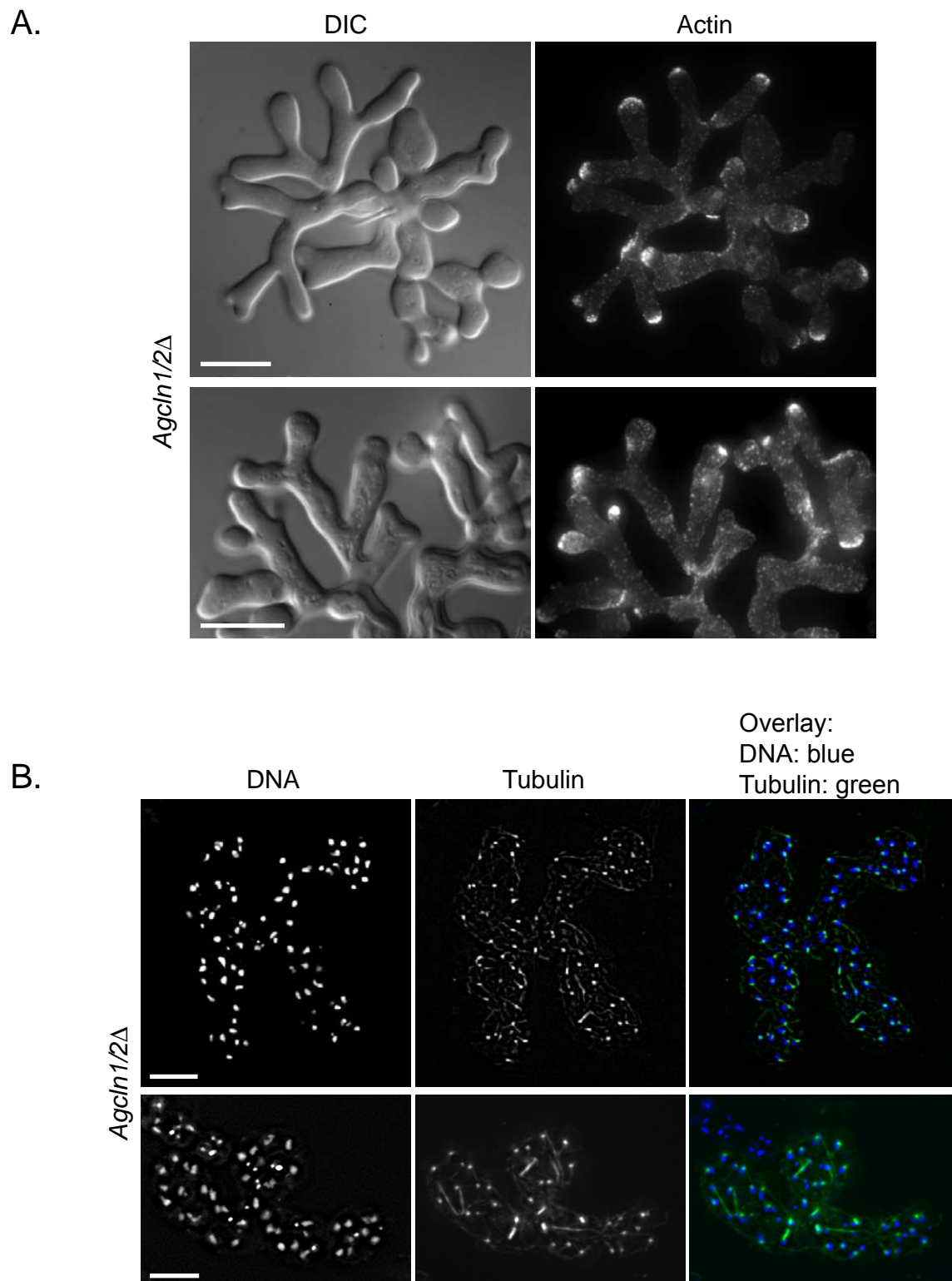


Figure 8
Phenotypic analysis of *AgcIn1/2Δ* by light microscopy showing the enlargement of hyphae in the arrest stage.

AgcIn1/2Δ mutants arrest growth as small mycelium with enlarged hyphae and highly aberrant morphology. A. Left: picture taken by differential-interference-contrast (DIC), right: actin staining by Alexa488- Phalloidin. B. Cells were processed for immunofluorescence and stained with Hoechst, showing nuclei (left) and with tubulin antibody showing different spindle stages (middle). In overlays, DNA is blue and tubulin is green. Bars, 10 μ m.

G2/M transition, which involve the transcriptional regulation of numerous genes such as the G1 cyclins (Amon et al., 1993), nuclear division (Richardson et al., 1992), formation of the mitotic spindle (Segal et al., 2000) and inhibition of polarized growth (Lew and Reed, 1993). Even though these cyclins are partially redundant, *ScCLB2* seems to be especially important, since it is the only B-type cyclin whose deletion shows a clear phenotype with a delay in G2 and elongated cells (Lew and Reed, 1993).

ScClb2p is involved in the apical-isotropic switch (Lew and Reed, 1993) and its activity promotes isotropic growth in *S. cerevisiae*. In *A. gossypii* isotropic growth is only observed briefly during germ bubble formation which is then followed by continuous polarized growth (Figure 2 A). Therefore, changes in abundance of the mitotic cyclin AgClb1/2p may cause severe morphology problems at an early growth stage in addition to difficulties expected for nuclear division. To test this hypothesis, a characterization of the mitotic cyclin *Agclb1/2Δ* mutant was performed.

Agclb1/2 deletion spores germinated, however they were not able to form a mycelium. Polar growth was limited to the primary germ tube, leading to a uniform growth arrest as unipolar germling (Figure 9 A). To characterize this arrest point, the germ tube length of the unipolar germlings was evaluated after various time points (16 h, 24 h, and 30 h). At each time point 70-100 germlings were measured, and the average germling size of each time point was very consistent around 60 μm (29.5 μm - 91.9 μm), implying only limited growth after 16 h. Different mitotic cyclin protein amounts may have been packed into spores in the heterokaryon, where only a subset of nuclei contains the cyclin gene deletion, leading to the observed variability in residual growth.

In yeast ScCdc28p associates with ScClb1p and ScClb2p to promote the transition from G2 to M-phase. Therefore *A. gossypii* cells lacking *AgCLB1/2* are predicted to be unable to go through mitosis. To check if there was any obvious nuclear distribution defect, Hoechst staining was done. Already at a very young growth stage, the signal detected by this staining was very “sparkly”, representing fragmented nuclei (Figure 9 B, left). We then looked in living cells by observing nuclei by H4-GFP (Figure 10). In the *Agclb1/2Δ* mutant, the signal often was diffuse, however, in some cells clearly more than one nucleus was identified (Figure 10 B). In most hyphae two to four individual nuclei were distinguishable, raising the question whether the mitotic cyclin in *A. gossypii* is not completely degraded at the end of its nuclear cycle. If complete degradation of AgClb1/2p happened, we

would expect to detect only two nuclei, due to the leftover protein concentration from the heterokaryon stage. However, eventually also other cyclins were able to partially complement. Possible explanations for this result are discussed in Chapter 2.

Actin distribution was evaluated by Alexa488-Phalloidin staining, a toxic cyclic peptide from *Amanita phalloides*, which interacts with F-actin. The actin rings which are thought to be precursors of septae looked normal (Figure 9 B). However, actin polarization was only seldom found at the tip, which may be due to the cells having stopped growth (Figure 9 B). The septum staining with Calcofluor showed that 40% of all germlings lacked a septum at the neck. These missing septae may be due to primary cell death, since the remaining 60% of cells, showed a septum (Figure 9 C).

Agclb1/2Δ mutants have a late lethal phenotype, meaning that the cells are still able to germinate and initiate a germ tube, but then stop growing. The presence of several nuclei in these cells implies limited ongoing mitosis. This observed nuclear division may be either due to incomplete mitotic cyclin degradation in the end of mitosis, or due to partial complementation by the other B-type cyclins as AgClb5/6p and AgClb3/4p.

***AgCLB3/4* functions as a sporulation cyclin**

The clonally purified homokaryotic *Agclb3/4Δ* transformants grew without observable difference to the reference strain, as shown in a growth comparison assay (Figure 11 A). All three independent transformants grew with the same radial growth speed as the reference strain (without selection). As expected, $\Delta\Delta t$ was not able to grow on plates containing GAFM. The only phenotype detected for *Agclb3/4Δ* cells was a clear sporulation defect. Spores could never be collected; therefore all phenotypic characterizations were done with the heterokaryotic spore preparation, grown under selective conditions.

The consistency of the *Agclb3/4Δ* mycelium seemed to be more “fluffy” than the host strain. Cells were checked by DIC microscopy whether this difference in consistency was the result from the sporulation defect, or from additional morphological changes. Some infrequent incidences of abnormalities were found such as increased branches, bulbs at the end of branches and uneven distribution of germ tubes around the germ bubble (Figure 11 B). However the majority of

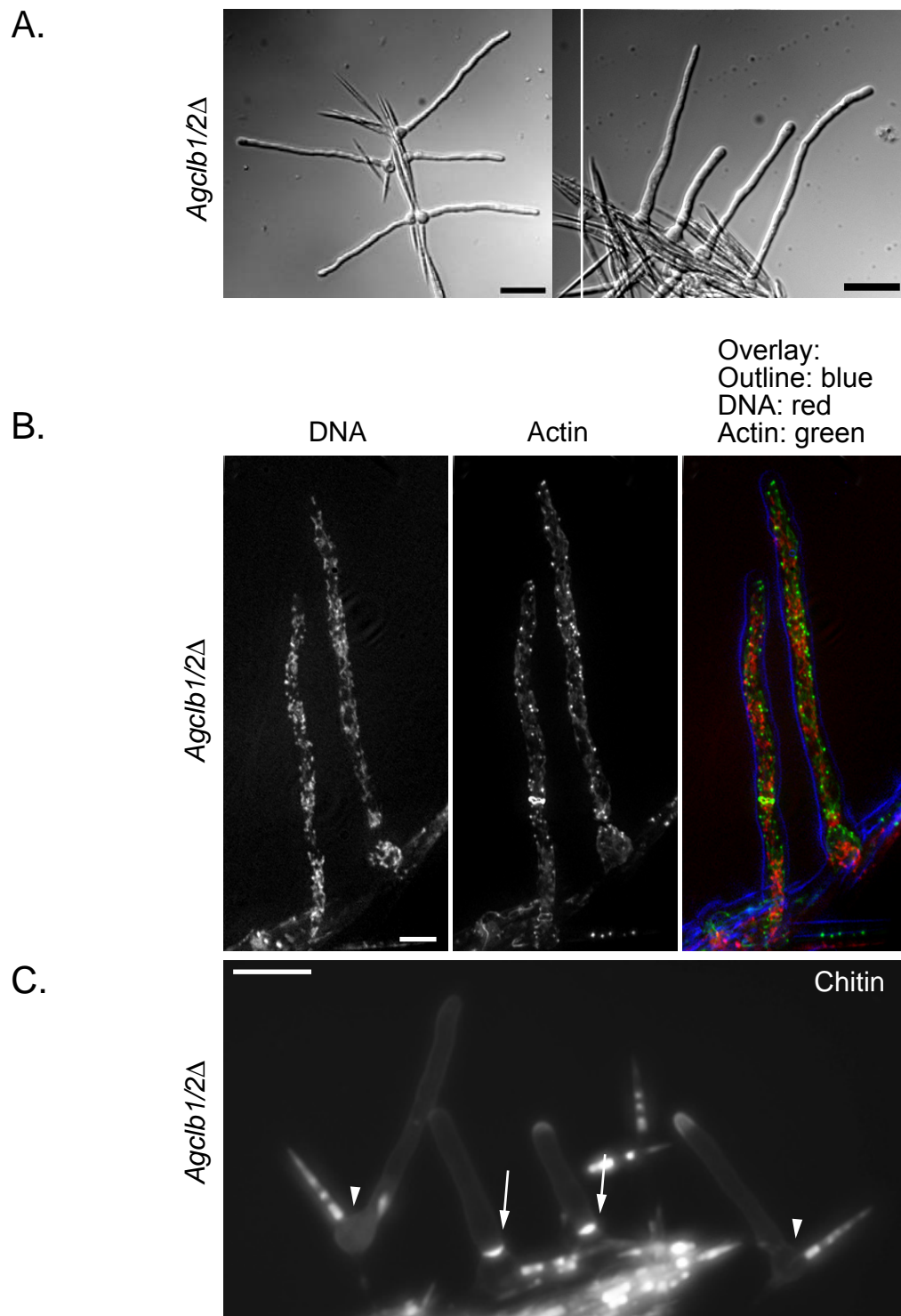


Figure 9
Phenotypic analysis of *Agclb1/2Δ* mutant by light microscopy showing the typical unipolar germling.

Cells were grown for 16 h in liquid media under Geneticin selection.

A. *Agclb1/2Δ* cells arrested as unipolar germlings. Pictures were taken by differential-interference-contrast (DIC).

B. Left: Nuclei staining done with Hoechst, showing fragmented nuclei, middle: actin staining by Alexa488-Phalloidin, right: overlay, showing nuclei in red, actin in green and brightfield in blue.

C. Chitin staining with Calcofluor. Arrows highlight “germ bubble necks” with a chitin ring and arrow heads highlight “germ bubble necks” without a chitin ring.

Bars, (A), 20 μm ; (B and C), 10 μm .

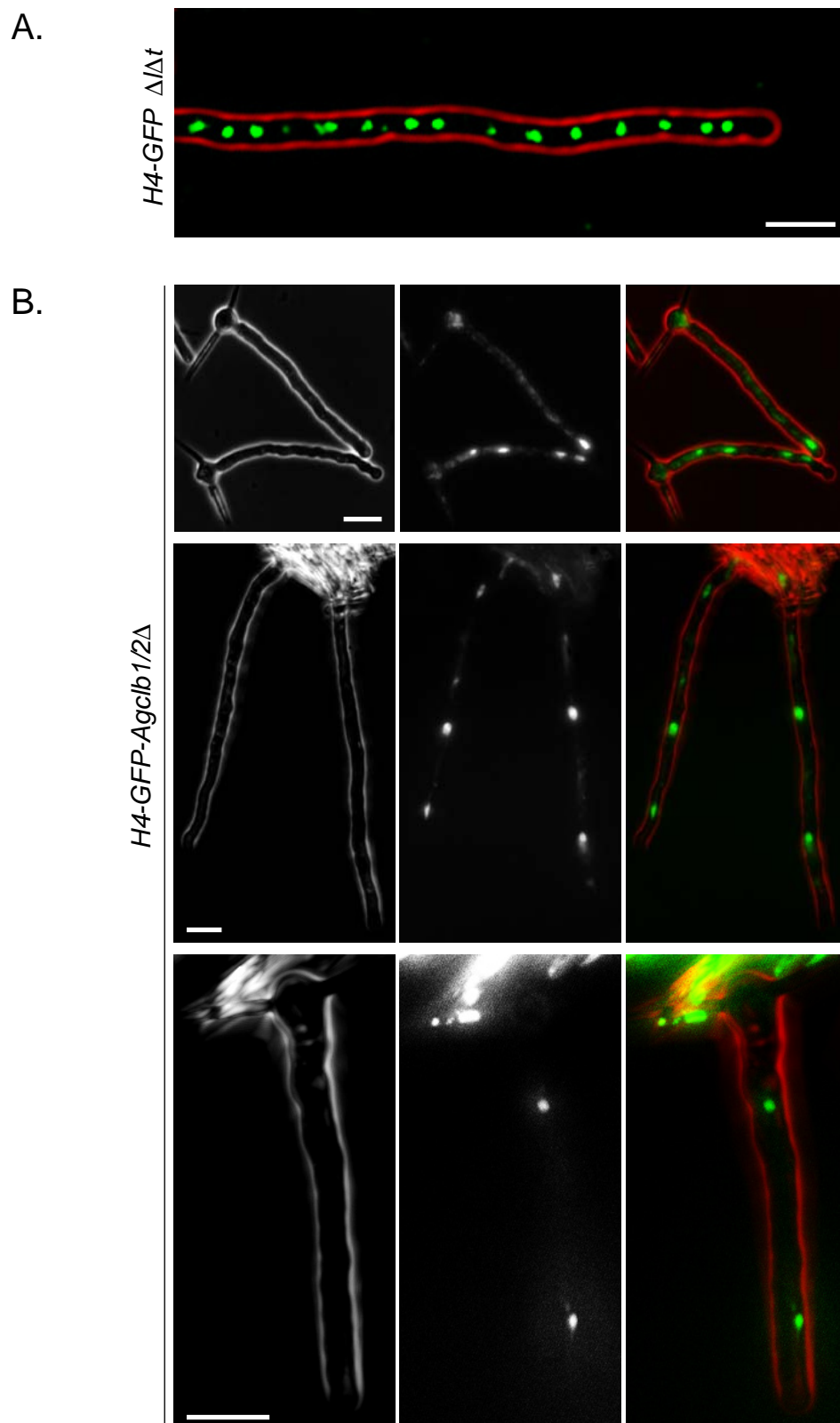


Figure 10

Nuclei are able to go through mitosis in *Agclb1/2*Δ cells.

A. *H4-GFP* strain, kindly provided by HP. Helper was used for the localization of nuclei in Δ/Δ .

B. *H4-GFP-*Agclb1/2*Δ* strain was used for the visualization of nuclei in *Agclb1/2*Δ. In overlays, Brightfield (left) is red and H4-GFP (middle) is green. Bars, 10 μ m.

cells did not show these abnormalities, suggesting the abnormal texture may be related to the sporulation defect.

To test whether there was any nuclear, actin or chitin distribution defect in these mutants, Hoechst, Alexa488-Phalloidin and Calcofluor staining was performed. Nuclei, actin cytoskeleton and septum formation appear without observable difference to the parental control strain (Figure 12).

In conclusion, the S-phase cyclin *Agclb3/4Δ* mutant revealed a very mild phenotype in that only sporulation was abolished. This let us hypothesize, whether the function of AgClb3/4p is primarily in controlling sporulation. There may be other functions as well; however, it seems as if the other cyclins are able to compensate them. We therefore hypothesize that *AgCLB3/4* may be a sporulation-specific cyclin.

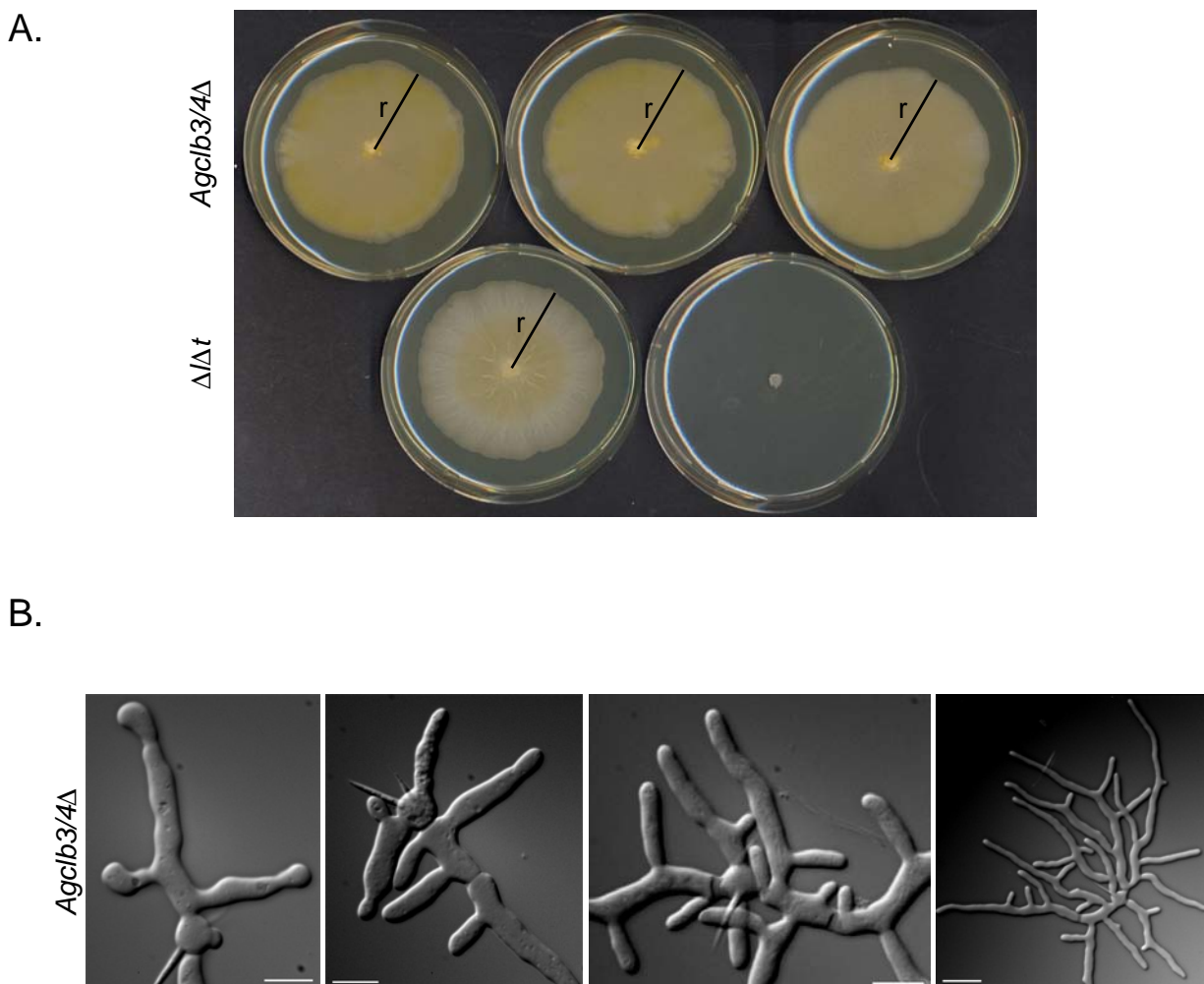
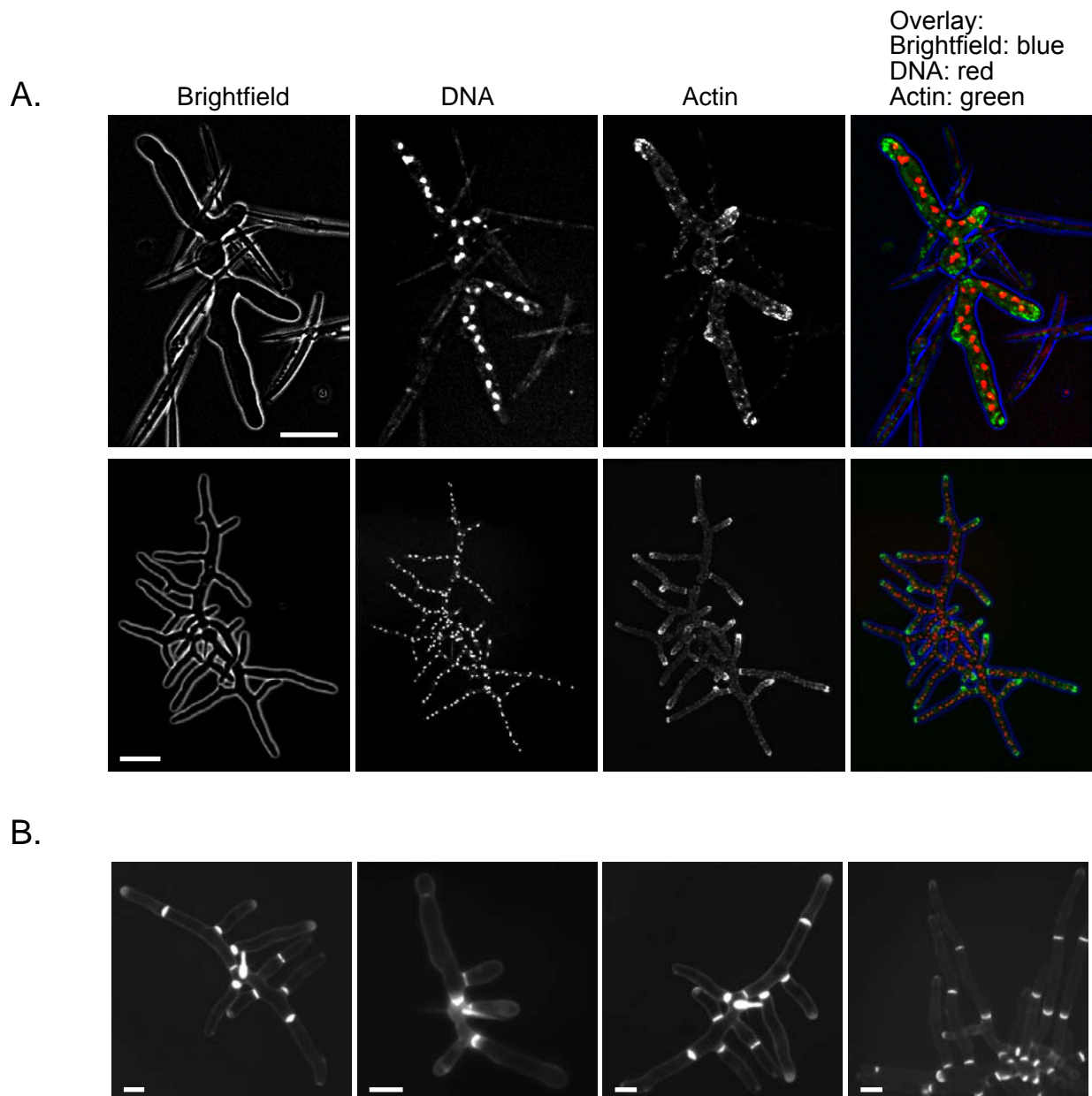


Figure 11

***Agclb3/4Δ* cells grow without observable difference to the reference strain ($\Delta\Delta t$).**

A. Top: Growth comparison assay showing the clonally purified homokaryotic *Agclb3/4Δ* strain after 7 days on selective media. All three independent transformants grew with the same radial growth speed (r) as the reference strain ($\Delta\Delta t$, without selection, bottom, left). Bottom: Comparison of $\Delta\Delta t$ cells on plates without G418 (left) and on plates containing G418 (right).

B. DIC pictures were taken after 15 h of growth under selection. Pictures represent infrequent incidences of abnormalities, such as bulbs at the end of branches, uneven distribution of germ tubes around the germ bubble and increased numbers of branches. Bars, 10 μm .

**Figure 12****Normal nuclear density, actin and chitin distribution in the S-phase cyclin *Agclb3/4*Δ.**

Spores were inoculated in liquid media, grown under selection for 13.5 h at 30°C until young mycelium was formed.

A. Nuclei were stained with Hoechst and actin with Alexa488-Phalloidin. Pictures were taken by light microscopy, showing on the left the brightfield picture, in the middle (left), the nuclei, in the middle (right) the actin staining and on the right the overlay with nuclei in red, actin in green and the outline in blue.

B. Calcofluor staining showing the chitin rings of the septae.

Bars, 10 μm.

The S-phase cyclin *AgCLB5/6* is essential in *A. gossypii*

Some of the crucial tasks which are controlled by the S-phase cyclin ScClb5p and ScClb6p in budding yeast are the timely initiation of S-phase (Schwob and Nasmyth, 1993), prevention of reinitiation on replication origins that have already “fired” (Dahmann et al., 1995) and negative regulation of Cln-Cdc28p activity (Basco et al., 1995). Despite their involvement in these various tasks in *S. cerevisiae*, the double deletion of *Scclb5Δclb6Δ* is not lethal, but causes a long S-phase initiation delay (Schwob and Nasmyth, 1993).

The deletion of the S-phase cyclin *AgCLB5/6* was performed with the dominant selection marker ClonNAT or Geneticin. In the *Agclb5/6Δ* strain containing the dominant ClonNAT marker, also wild-type spores derived from the heterokaryon were able to grow for several hours and build bipolar germlings. To avoid confusion which germlings contained the deletion and which were wild-type, we decided to focus the characterization of the *Agclb5/6Δ* on the strain, containing the *GEN3* selection marker. *Agclb5/6Δ* spores were able to germinate under selection in liquid as well as on plates. However, they were not able to form any mycelium; therefore clonal purification was not achieved. The germlings grew to different sizes and then arrested, mainly in the stage as a bipolar germling with few branches (Figure 13).

To gain some deeper insight into the cause of this late cell death and to determine if it is due to the aberrant nuclear, actin, or septum formation, germinating spores were stained with Hoechst, Alexa488-Phalloidin and Calcofluor. *Agclb5/6Δ* cells often contained nuclei which were fragmented and it was difficult to determine, whether these “sparkles” originated from one or more nuclei. Taking into account that the *A. gossypii* genome is based on seven chromosomes, which could potentially fall apart if the nucleus disintegrates, we may hypothesize that indeed, the signals detected had arisen from only one or two nuclei. AgClb5/6p leftover from the heterokaryon could have allowed one mitosis before the protein was depleted. However, immunofluorescence staining revealed that more than two nuclei had been present in *Agclb5/6Δ* cells. The stable structures of the SPBs and mitotic spindles were still intact, even though the nuclei already disintegrated. Tubulin staining in the *Agclb5/6Δ* strain showed a nuclear cycle arrest with mainly duplicated SPBs (Figure 14). In most

cases four to seven duplicated SPBs could be detected in one germling, indicating prior presence of up to seven nuclei in these hyphae. To further support these findings, this deletion should be repeated in the *H4-GFP* strain to investigate the exact amount of nuclei in living cells.

Actin and septum staining looked similar to wild-type in most cases. Often actin polarization at the branch tip or septae could not be observed, which may be due to these cells having ceased growth (Figure 13, 15).

Agclb5/6Δ mutants arrested after limited hyphal formation and fragmented nuclei. This is in contrast to the double deletion of *Scclb5Δclb6Δ* in *S. cerevisiae*, which is viable with a delay in the timely initiation of DNA replication (Schwob and Nasmyth, 1993). In multinucleated hyphae one would expect that such a DNA replication delay would not cause a severe phenotype, since other nuclei may be able to complement. However, this is not the case and *AgCLB5/6* is essential, strongly indicating its key involvement in cell cycle regulation of this multinucleated cell.

Cell cycle specific arrest phenotype in the cyclin deletion mutants in *A. gossypii*

When the five cyclin deletion strains were evaluated for cell cycle stage based on tubulin immunofluorescence, we were able to detect specific nuclear cycle arrest points (Figure 16). The G1 cyclin mutants arrested with mainly one or two SPBs, the strains lacking *AgCLB5/6* or *AgCLB3/4* with predominantly two SPBs and the strain lacking the mitotic cyclin *AgCLB1/2* displayed a clear arrest in mitosis. This cell cycle specific arrest of the various cyclin deletions further suggests that they function at specific time points in the nuclear division cycle.

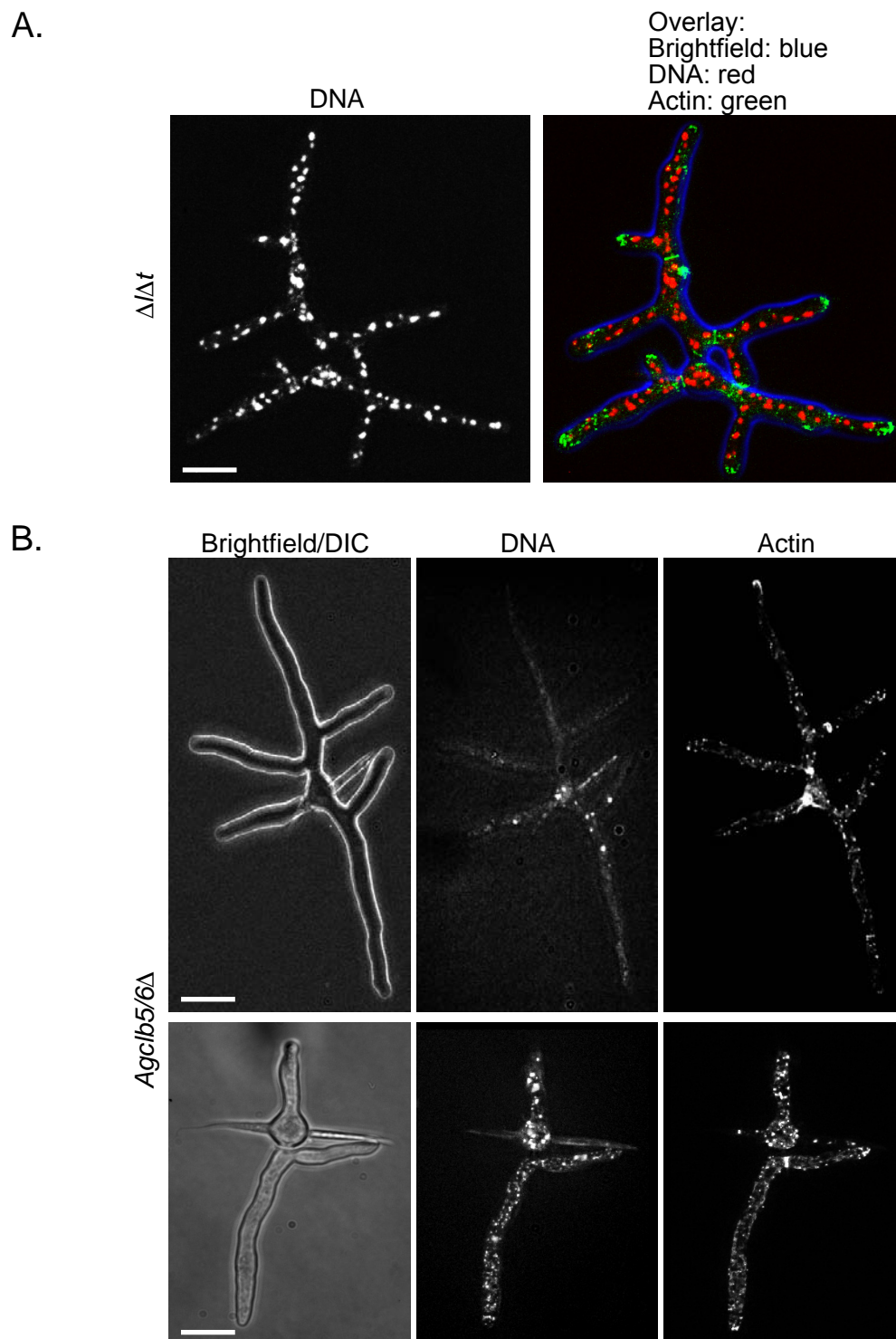


Figure 13
Phenotype analysis of the *Agc1b5/6Δ* strain by light microscopy showing bipolar germlings with some branches and disintegrated nuclei.

Cells were grown in liquid media under selection for 14 h at 30°C. Nuclei were stained with Hoechst and actin with Alexa488-Phalloidin. Pictures were taken by light microscopy.

A. $\Delta/\Delta t$ reference strain, showing nuclei in red, actin in green and the outline of the cell in blue.

B. *Agc1b5/6Δ* strain with the GEN3 cassette, showing fragmented nuclei. Bars, 10 μm .

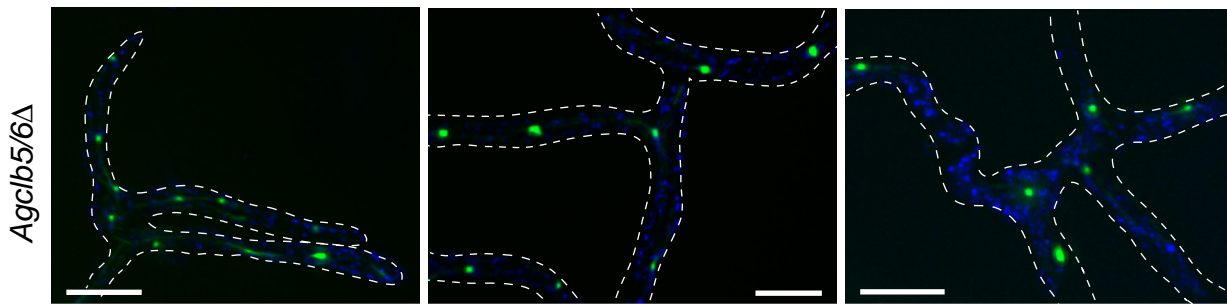


Figure 14

The S-phase cyclin *Agclb5/6* Δ mutant displays a cell cycle arrest with predominantly duplicated SPBs.

Agclb5/6 Δ cells were grown in liquid media under selection for 14 h at 30°C. Cells were processed for immunofluorescence and stained with Hoechst, showing disintegrated nuclei in blue and tubulin in green.

Bars, 10 μ m.

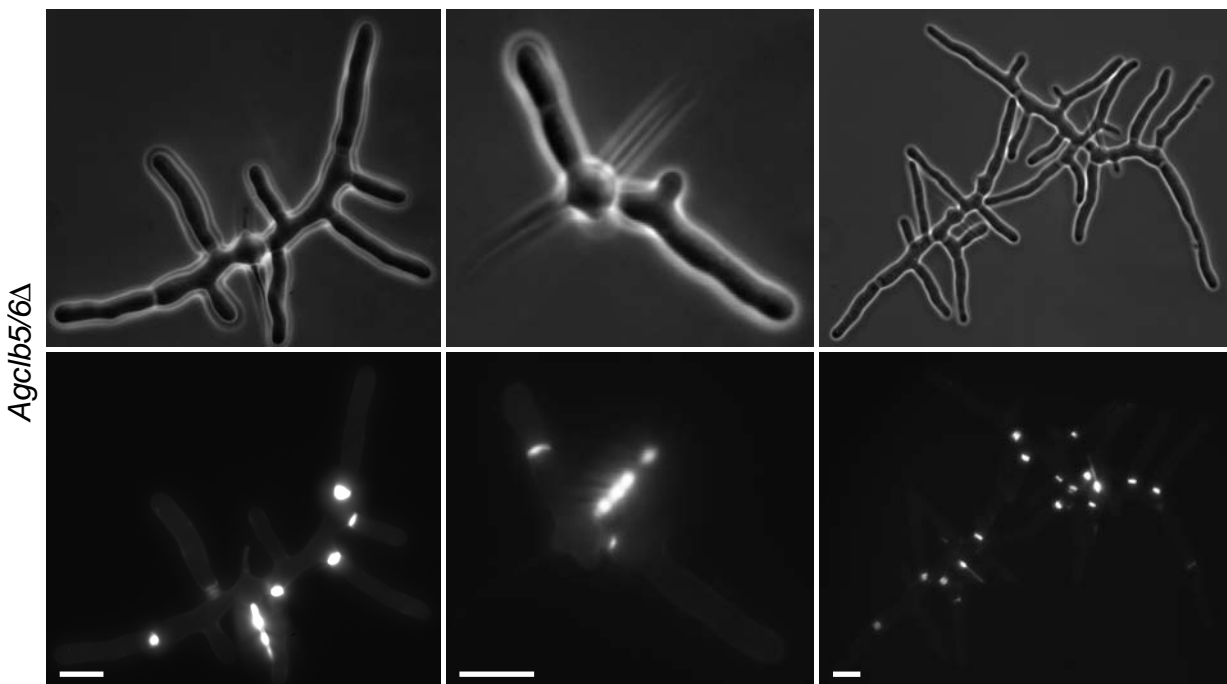


Figure 15

Normal septum formation in *Agclb5/6* Δ cells.

Agclb5/6 Δ cells were grown in liquid media under selection for 16 h at 30°C.

Top: Brightfield pictures showing the outline of the hyphae.

Bottom: Calcofluor staining showing the chitin rings of the septae. Bars, 10 μ m.

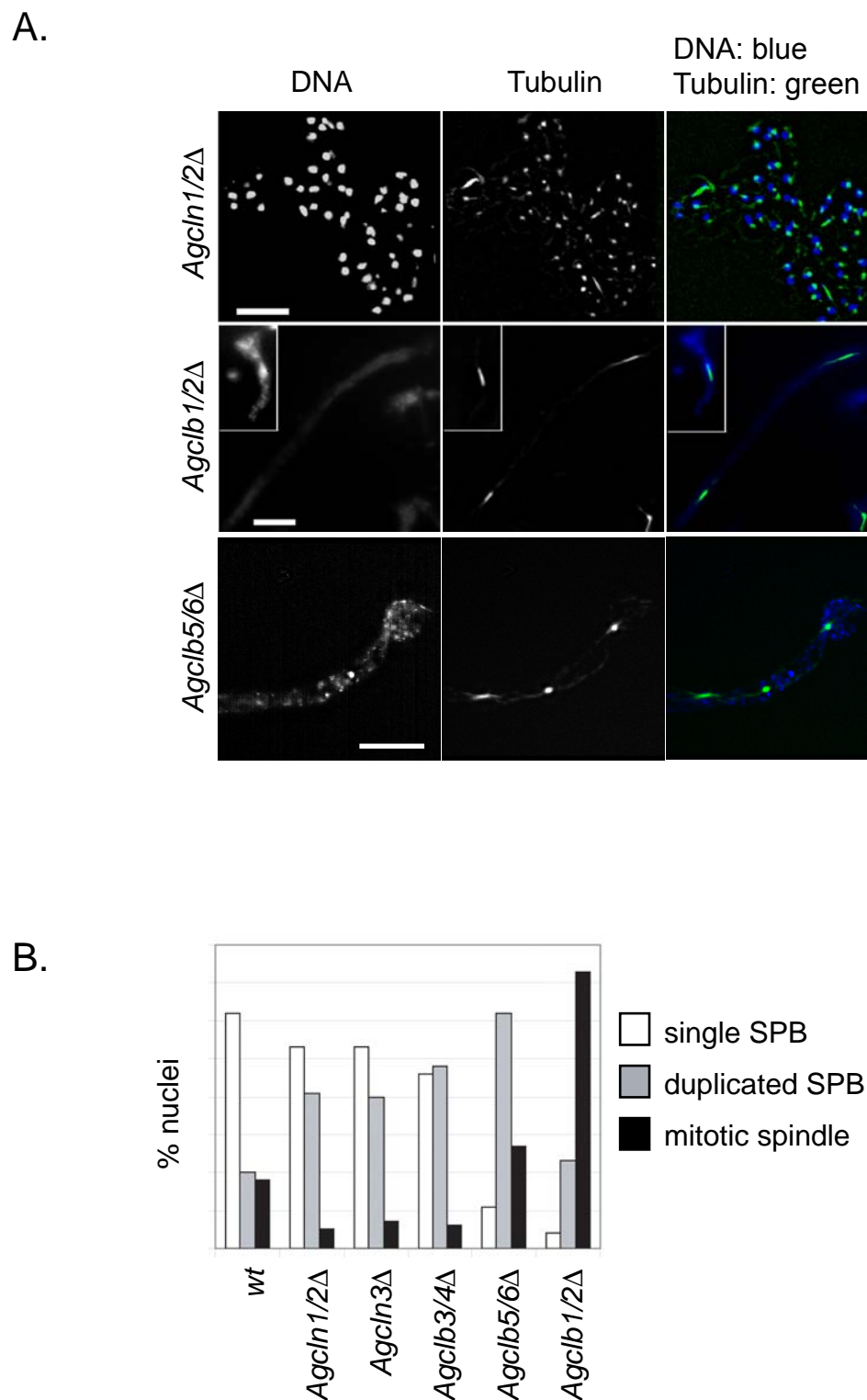


Figure 16
Cell cycle specific arrest in the cyclin deletions.

A. Cell cycle specific arrest of the three essential cyclins in *A. gossypii*. Top panel: *Agc1n1/2Δ* cells showing predominantly single and duplicated SPBs in aberrantly shaped hyphae, middle panel: *Agclb1/2Δ* strain showing arrest with mitotic spindles and one or two nuclei, and bottom panel: *Agclb5/6Δ* cells showing an arrest with predominantly duplicated SPBs and mitotic spindles. In overlays, DNA is blue, tubulin green. Bars, 10 μ m.

B. Cyclin deletion strains were evaluated for cell cycle stage based on tubulin immunofluorescence and categorized as having either a single SPB, a duplicated SPB or a mitotic spindle. N>200 nuclei were scored for each mutant.

Discussion

In *S. pombe* and *S. cerevisiae* activity changes of one central Cdk regulates the cell cycle. In higher eukaryotes, as in mammalian cells a small family of related Cdks are used to ensure progression through the cell cycle. Cdks in mammalian cells have been named Cdk1, 2, 4, and 6 in order of their discovery (Lodish, 2000). Like *S. cerevisiae*, mammalian cells express multiple cyclins. Cyclin D and E are expressed during G1, Cyclins A and B, function in S-phase, G2 and early mitosis. Their expression however does not only vary during the cell cycle, but their relative amount also differs in various cell types (ex. fibro-blasts and hematopoietic cells express different amounts of D-type cyclins, [Lodish, 2000]).

Multiple cyclins activate CDKs in eukaryotes, but it remains unclear whether multiple cyclins are really required for cell cycle progression. In *S. pombe*, oscillation of Cdc2p kinase activity provided by a single B-type cyclin (Cdc13p) can promote ordered progression through the cell cycle (Fisher and Nurse, 1996). Changes in levels of Cdc13/Cdc2 activity between low (G1), intermediate (S and G2) and high (M) act as master regulators, dictating whether cells undergo S-phase or mitosis (Stern and Nurse, 1996).

In *S. cerevisiae*, the existence of many duplicated genes, including the cyclin gene pairs, *ScCLN1/ScCLN2*, *ScCLB1/ScCLB2*, and *ScCLB5/ScCLB6* have arisen from a whole genome duplication event (Dietrich et al., 2004; Kellis et al., 2004). *A. gossypii* has diverged from the budding yeast before the whole genome duplication and therefore only contains two G1 cyclins (*AgCLN1/2* and *AgCLN3*) and three B-type cyclins (*AgCLB1/2*, *AgCLB3/4* and *AgCLB5/6*). It has been hypothesized that the B-type cyclin family of *S. cerevisiae* had gone through two duplication events since the last common ancestor preceding *Y. lipolytica* (Archambault et al., 2005). Before the whole genome duplication, the two B-type cyclins *CLB1/2* and *CLB5/6* may have been the result of an adjacent gene duplication of an ancestral *CLB1/2/5/6* (Figure 17). The whole genome duplication may have happened around 100 Mio. years ago, after *A. gossypii* had diverged from the common ancestor, therefore *A. gossypii* still has two instead of the four genes found in *S. cerevisiae*.

Despite the close evolutionary relationship between the *A. gossypii* and *S. cerevisiae* genomes, their lifestyles differ significantly from each other. Whereas *A. gossypii* is multinucleate and mitosis occurs in an asynchronous manner,

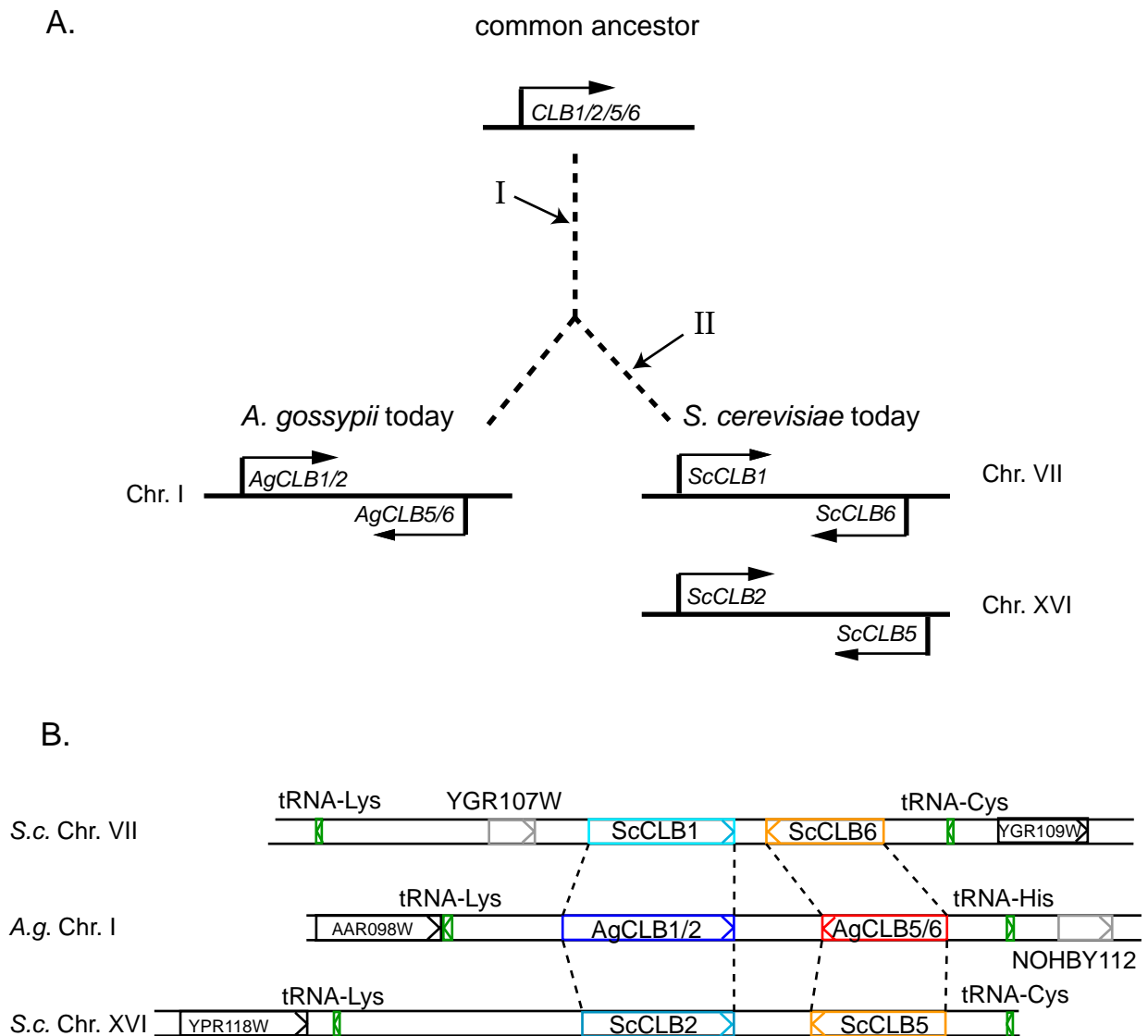
S. cerevisiae is a uninucleate model organism, which undergoes cytokinesis after each nuclear division. Therefore cyclins as typical cell cycle genes have been chosen to investigate, whether their role or behaviour during the cell cycle may have changed in multinucleate cells.

***Agcln3*Δ cells have no growth or nuclear division defects**

The deletion of the G1 cyclin *Agcln3*Δ did not have any obvious effect on the growth behaviour in *A. gossypii*. This may be surprising, since *Sccln3* disruption in *S. cerevisiae* results in a cell volume increase of at least 50% (Cross, 1988; Nash et al., 1988). When the cell has reached a critical size, *Cln3-Cdc28p* is activated and the expression of the SBF (*Swi4/Swi6*) and MBF (*Mbp1/Swi6*) transcription factors are induced, leading to the transcription of the SBF-regulated *CLN1* and *CLN2*, and the MBF-regulated B-type cyclins *CLB5* and *CLB6* (Koch and Nasmyth, 1994). In *S. cerevisiae*, *ScCln3p* is involved in measuring cell size, to start a new cell cycle at the right time. However, *A. gossypii* is multinucleated and ensures constant nuclei to cytoplasmic ratio by asynchronous nuclear division. How *A. gossypii* is able to maintain this constant nuclei to cytoplasmic ratio by coordinating when and which nucleus divides remains a mystery by now.

***Agcln1/2*Δ shows a severe polarization defect**

In *S. cerevisiae*, *ScCln1p* and *ScCln2p* are involved in polarized secretion and polarized growth by restricting cortical actin to an apical distribution (Lew and Reed, 1993). In contrast to *S. cerevisiae*, where the double deletion *Scln1Δcln2Δ* was viable, with effects such as elongated bud morphology, delayed times of bud emergence and DNA synthesis initiation (Hadwiger et al., 1989), in *A. gossypii* the deletion of the homologous gene resulted in inviable cells. *Agcln1/2*Δ cells were able to form microcolonies, however, possibly as a consequence of a diffuse zone of polarity, these hyphae enlarged significantly. Since *A. gossypii* grows as a filamentous fungus, thereby maintaining polarized growth during the entire nuclear cycle the cells may be more sensitive than yeast to disturbances of the apical actin distribution. In *S. cerevisiae* a single G1 cyclin is sufficient for survival. The remaining G1 cyclin *AgCln3p* however

**Figure 17****Evolutionary relationship between *AgCLB1/2*, *AgCLB5/6* and *ScCLB1*, *ScCLB2*, *ScCLB5* and *ScCLB6*.**

A. Evolutionary relationship of *AgCLB1/2* and *AgCLB5/6* with their homologues in *S. cerevisiae*.

I. Adjacent gene duplication of an ancient *CLB1/2/5/6* into *CLB1/2* and *CLB5/6* as found in *A. gossypii*.

II. Whole genome duplication of *CLB1/2* and *CLB5/6* into *CLB1*, *CLB2*, *CLB5* and *CLB6*, as found in *S. cerevisiae*. (adapted from Archambault, et al., 2005)

B. Gene order comparison of *AgCLB1/2* and *AgCLB5/6* and their homologues in *S. cerevisiae*. Green arrows represent tRNAs, black arrows indicate genes which have a homologous gene in *S. cerevisiae* and grey arrows show genes without homologues in the other species.

was not able to compensate for the missing G1 cyclin in *A. gossypii*, thereby leading to growth arrest.

AgCLB1/2, the essential mitotic cyclin

The deletion of the mitotic cyclin *AgCLB1/2* in *A. gossypii* resulted in a lethal phenotype. Spores lacking *AgCLB1/2* were able to germinate and build one unipolar germ tube, which contained in most cases between two and four nuclei. We hypothesize that the germ tube is able to grow until the leftover *AgClb1/2p* from the heterokaryon is depleted, leading to a mitotic arrest of the nuclei present. These 2-4 nuclei detected, are not able to provide enough supply for the unipolar germling to grow any further. The ability of these cells to go through one or two mitoses raises the question whether in *A. gossypii* other cyclins are able to partially complement and direct mitosis or, if *AgClb1/2p* in contrast to yeast is not degraded at the end of the nuclear cycle. Stable *AgClb1/2p* may allow progression through few mitosis before the complete depletion of the leftover protein. The double deletion of *Scclb1ΔScclb2Δ* is lethal in *S. cerevisiae*, resulting in an arrest prior to mitosis. The arrest observed in *Agclb1/2Δ* cells predominantly showed elongated spindles, representative of mitosis, suggesting its involvement in an essential task in the process of mitosis.

In *S. cerevisiae* *ScClb1p* and *ScClb2p* are not only essential for entry into mitosis but they also mediate the switch between polarized and isotropic growth (Lew and Reed, 1993). In *A. gossypii*, such a switch does not exist, since isotropic growth only occurs during germ bubble formation (Figure 2). However, *A. gossypii* has a “reverse switch”, from isotropic growth in the germ bubble to polarized growth in the hyphae. The *Scclb1ΔScclb2Δ* strain in *S. cerevisiae* is lethal, in that the cells arrest prior to mitosis. Those cells never undergo the switch between polarized and isotropic growth. In *A. gossypii* on the other hand, the “reverse switch” is still working in the mutant strain. *Agclb1/2Δ* strain is able to switch from the isotropically growing germ bubble to the apically growing germ tubes, which continue to grow apically. This difference that *S. cerevisiae* only grows apically during a short period of its cell cycle whereas *A. gossypii* is able to go through the entire nuclear division cycle while still growing polarized indicates a remarkable modulation in the *Clb1/2p* task. It could also be as in *Candida albicans* where two independent signals (growth signals and hyphal induction signal) are responsible for cell cycle and

hyphal elongation, thereby uncoupling the cell cycle from hyphal growth (Hazan et al., 2002). When *A. gossypii* cells were treated with Nocodazole, leading to an arrest of the nuclear cycle, polarized growth was still observed (Figure 18). Similarly, C. Alberti described the dynein heavy chain deletion (*Agdhc1Δ* mutant), which caused clustering of nuclei at the hyphal tips, but still maintained slow mycelium formation. Therefore we hypothesize that hyphal morphogenesis proceeded normally even when the nuclear cycle was blocked in *A. gossypii*.

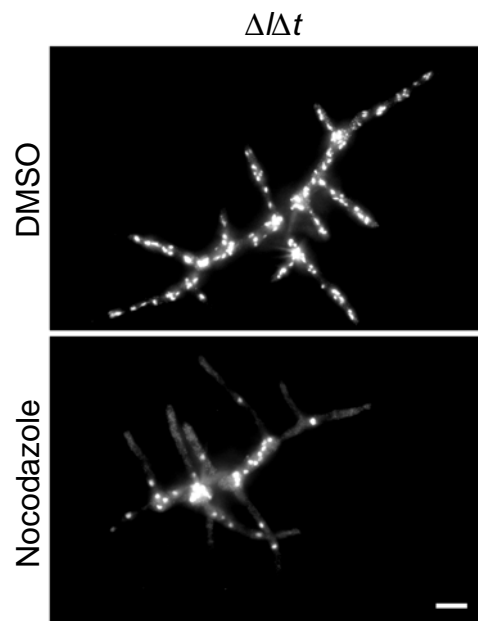


Figure 18
Polarized growth occurs despite arrest of nuclear cycle.

Nocodazole was added to $\Delta/\Delta t$ uni- or bipolar germlings (12 hour growth) and nuclei were observed after 4 hours incubation in drug or DMSO. Nuclei were visualized with Hoechst dye.

Bar, 10 μm .

(Microscopy pictures were kindly provided by A. Gladfelter)

AgCLB3/4, a potential sporulation cyclin

The deletion of *AgCLB3/4* did not produce any obviously altered morphology and radial growth speed was similar to the reference strain. The only phenotype observed was a sporulation defect, leading to the conclusion, that *AgCLB3/4* may be a sporulation-specific cyclin.

AgCLB5/6, the essential S-phase cyclin

In contrast to *S. cerevisiae*, where the double deletion of the S-phase cyclin *Scclb5Δclb6Δ* resulted in an S-phase initiation delay (Schwob and Nasmyth, 1993) the deletion of *AgCLB5/6* is lethal. Small mycelia are produced, with up to seven nuclei, which disintegrate, possibly due to the arrest of cell growth and subsequent cell death. If we hypothesize, that the S-phase cyclin protein levels oscillate, and AgClb5/6p is degraded in the end of mitosis (see Chapter III), what may be possible reasons for the existence of more than two nuclei? First of all, other cyclins may be able to partially complement and enable the cell to go through some mitoses, before the hyphae stop growing. Second, there may be protein leftover in the cytoplasm which was not ubiquitinated during the first mitosis, and therefore was not degraded, leading to few more mitoses.

The question arises, why is the phenotype of *Agclb5/6Δ* much more severe than *Scclb5Δclb6Δ* in yeast? One explanation to this question could be the amount of compensation which the other cyclins are able to provide. It may be that in yeast this compensation is more efficient, so that the other B-type cyclins can fulfil the job of ScClb5p and ScClb6p, as soon as they are expressed, resulting in a delay of S-phase. In *A. gossypii* this redundancy of the different B-type cyclins seems to be missing, since the few cyclins present are completely specialized, causing the lethal phenotype. This lack of redundancy could be due to differences in substrate specificity, timing, levels of expression or localization between the different B-type cyclins in *A. gossypii*.

Since the function of the Cdc28p protein kinase is determined by its association with different cyclins, absence of redundancy of cyclins, may explain the severe phenotype of their deletions in *A. gossypii*. Thus, three of the five cyclin deletions were lethal, and most surprisingly the S-phase cyclin *AgCLB5/6* is essential in *A. gossypii*. This is in contrast to yeast where the double deletion of *Scclb5Δclb6Δ* "only" showed S-phase prolongation and elongated cells. These data are especially striking because in both *S. cerevisiae* and *S. pombe* cells proliferate with only one single B-type cyclin (Fisher and Nurse, 1996; Haase and Reed, 1999). Haase and Reed described a strain in which *Scclb1,2,3,4,5,6* were deleted and replaced with *ScCLB1* under the control of the strong *GAL1* promoter. The viability of this strain strongly suggests, that multiple B-type cyclins are

not essential, provided that a single B-type cyclin is sufficiently overexpressed. The different B-type cyclins in *A. gossypii* may not have overlapping function, however also changes in protein expression levels may cause the severe deletion phenotypes observed. In Chapter III more details about AgClb5/6p and cyclin levels in *A. gossypii* will be discussed.

CHAPTER II

Regulation of cell cycle progression by noncycling cyclins in the multinucleated, filamentous fungus *A. gossypii*

The data presented here originate from close collaborative work of Amy Gladfelter and myself. Since her and my work complement one another and therefore give a more complete picture on cyclin behaviour our results were combined. In general, Amy Gladfelter constructed and characterized AgCln1/2-13myc, AgClb1/2-13myc, AgSic1-13myc and did the arrest-release experiments with Nocodazole. The other results, (including AgCln3-13myc/GFP, AgClb1/2-GFP, AgClb3/4-myc/GFP, diffusion studies with LacI/LacO, forced localization experiments with NESa/i and the D-box characterization) were done by myself.

Abstract

The cell cycle process has been conserved throughout eukaryotes and requires temporally regulated expression, localization and degradation of cyclins and other regulatory proteins. Cyclin localization and oscillation has been investigated in great detail in many uninucleated cells, however nearly no data existed on cyclin behaviour in multinucleated organisms. Characterization of cyclins in *A. gossypii* revealed that neighboring nuclei did not differ significantly in their patterns of cyclin protein localization such that both G1 and the mitotic cyclin AgClb1/2p were present regardless of cell cycle stage, suggesting that complete destruction of cyclins is not occurring in this system. Indeed, the expression of mitotic cyclin lacking N-terminal destruction box sequences did not block cell cycle progression. Nuclei remain independent in this system even though mitotic cyclin protein transcribed from one nucleus can diffuse to and enter neighboring nuclei. Furthermore, displacing a fraction of mitotic cyclin AgClb1/2p into the cytoplasm with two exogenous nuclear export signals (NESs) led to no change in asynchrony. Cells lacking AgSic1p, a predicted cyclin-dependent kinase (CDK) inhibitor, however, showed aberrant multipolar spindles and fragmented nuclei that are indicative of flawed mitoses. We hypothesize that the continuous cytoplasm in these cells promoted the evolution of nuclear division in which CDK

inhibitors primarily control CDK activity rather than oscillating mitotic cyclin proteins.

Introduction

Multinucleated cells are found in a variety of organisms and are integral to processes as diverse as the early development of the fruit fly, bone remodeling, placenta formation and cancer metastasis. However, information on how multinucleated cells regulate nuclear division is limited to relatively few systems. Fusion experiments with mammalian cells demonstrated that multiple nuclei in a shared cytoplasm synchronize their nuclear division cycles (Rao and Johnson, 1970). These experiments suggested that separate nuclei within a common cytoplasmic environment will alter their normal cell cycle kinetics and align temporally with other nuclei present. Synchronous mitosis has also been observed in binucleate yeast cells (Hoepfner et al., 2002). Furthermore, in naturally multinucleated cells, mitoses often occur either synchronously, as in the slime mold *Physarum polycephalum* (Nygaard et al., 1960), or parasynchronously, with a linear wave of nuclear division spreading across a cell, as in the filamentous fungus *Aspergillus nidulans* (Clutterbuck, 1970).

One hypothesis for the molecular basis for synchronous mitoses in multinucleated cells is that cell cycle regulators shuttle between nuclear and cytoplasmic compartments, allowing them to potentially diffuse in the cytoplasm and coordinate multiple nuclei in the same cytoplasm (Hagting et al., 1998; Hood et al., 2001). Thus, the dynamic localization of the cell cycle machinery may promote continual communication between individual nuclei and the cytoplasm and could explain synchronous nuclear division cycles although in no instance has this hypothesis been tested in multinucleated cells.

Synchronous mitosis is common in multinucleate cells. However, in a few cases, also asynchronous mitosis has been observed, where nuclei in different cell cycle stages share a common cytoplasm. The filamentous fungi *Neurospora crassa* and *Podospira anserina* are thought to

have asynchronous mitoses but in neither case has the phenomenon been studied in depth (Minke et al., 1999); Denise Zickler personal communication). Thus, it seems to be possible for the nucleus itself to control the decision to enter mitosis, although the molecular basis for such nuclear autonomy in any system remains unknown.

We present here initial molecular analysis of asynchronous nuclear division cycles in the multinucleated, filamentous fungus, *Ashbya gossypii*. *A. gossypii* cells grow exclusively as hyphae containing many nuclei in linear arrays within the same cytoplasm. Even though these nuclei are in very close physical proximity, each of them is dividing with variable timing, independently of neighboring nuclei (Gladfelter et al. 2006).

We analyzed asynchronous nuclear division in *A. gossypii* and evaluated how periodic cell cycle proteins act in such a system where nuclei are not in sync with each other. Our experiments show that both G1 and mitotic cyclins are present across all cell cycle stages. We present evidence that the continuous cytoplasm in these cells permits proteins to diffuse so that nuclei continually receive proteins from the cytosol, expressed from neighboring nuclei. In addition, nuclear autonomy is preserved even when mitotic cyclin are displaced to the cytoplasm with two exogenous NES. These data have led us to hypothesize that differences in cell architecture and spatial organization may have selected for alternative modes of cell cycle control during the evolution of *S. cerevisiae* and *A. gossypii*. When combined, our experiments suggest that CDK inhibitors rather than cycles of accumulation and complete destruction of the G1 and mitotic cyclins provide oscillation in the cell cycle machinery of *A. gossypii*.

Results

G1 cyclins are nuclear and present across all spindle stages

Are there clues in the *A. gossypii* genome to explain the molecular basis for nuclear asynchrony? The *A. gossypii* genome shows striking synteny patterns and similarity in gene set to *S. cerevisiae*, despite their different lifestyles and growth form. Whole genome comparisons between the two organisms strongly suggest that they diverged prior to the duplication of the budding yeast genome and thus the *A. gossypii* genome lacks many gene pairs retained in budding yeast after this duplication

(Dietrich et al., 2004). We examined homologues of the core cell cycle machinery in *A. gossypii* and found that the entire gene set is present at syntenic positions, with amino acid identity ranging from 31-86% (Table 2). Thus, *A. gossypii* and *S. cerevisiae* share similar cyclins, the CDK, transcription factors, inhibitors, activators and degradation machinery involved in cell cycle control.

How might this conserved network of cell cycle regulators be constructed to direct asynchronous mitosis in a multinucleated cell? Cyclin proteins are integral to the cell cycle clock in eukaryotic cells and when complexed to a cyclin dependent kinase (Cdk), drive cell cycle progression (Murray, 2004). Periodic transcription and degradation of cyclins is believed to be a central mode of oscillation, critical for orderly cell cycle progression. *A. gossypii* contains two G1 cyclins (*AgCLN1/2* and *AgCLN3*) and three B-type cyclins (*AgCLB1/2*, *AgCLB3/4* and *AgCLB5/6*), therefore of each cyclin pair in *S. cerevisiae*, only one cyclin homologue is present in *A. gossypii*.

AgCln1/2p is the essential G1 cyclin in *A. gossypii*. In *S. cerevisiae*, accumulation of *ScCLN1* and *ScCLN2* mRNA in late G1 is dependent on two transcription factor complexes, MBF (Swi6p-Mbp1p) and SBF (Swi6p-Swi4p), which bind to MCB and SCB promoter elements, respectively (Cross et al., 1994); (Stuart and Wittenberg, 1994). Upstream sequences of *AgCLN1/2* showed the conservation of these transcriptional regulatory elements (consensus sequences summarized in (Kellis et al., 2003). In contrast to *ScCLN1* and *ScCLN2* where transcription is cell cycle regulated, *ScCln3p* is regulated post-translationally (Cross and Blake, 1993; Tyers et al., 1992). *ScCln3p* is an unstable protein that contains PEST motifs (Cross and Blake, 1993; Tyers et al., 1992), which are sequences rich in proline, glutamic acid, serine, and threonine. PEST regions are thought to mark proteins for rapid turnover (Rechsteiner and Rogers, 1996; Rogers et al., 1986) and algorithms have been developed for finding and scoring such regions in proteins (www.at.embnet.org/embnet/tools/bio/PESTfind/). According to Rechsteiner and Rogers, scores greater than +5 are considered interesting (Rechsteiner and Rogers, 1996). All G1 cyclins in *S. cerevisiae* contain regions which meet this criteria (Figure 19). In contrast the *A. gossypii* G1 cyclins reach best scores of +3.96 and -2.21 for *AgCln1/2p* and *AgCln3p*, respectively. A homologous domain in *A. gossypii* G1 cyclins may have escaped the detection by this program; however, it could also be possible that the protein turnover of these cyclins in *A. gossypii* is regulated differently, in that these cyclins are more stable.

Table 2.
Amino acid sequence comparison of a subset of cell cycle control proteins

<i>S. cerevisiae</i> cell cycle protein	<i>A. gossypii</i> homologous protein	% identity (aa)
Cyclins and Cdk		
Cdc28	AgCdc28	86
Cln3	AgCln3	34
Cln1	AgCln1/2	63
Cln2	AgCln1/2	60
Clb5	AgClb5/6	44
Clb6	AgClb5/6	39
Clb3	AgClb3/4	51
Clb4	AgClb3/4	52
Clb1	AgClb1/2	56
Clb2	AgClb1/2	65
Degradation machinery		
Cdc4	AgCdc4	52
Cdc34	AgCdc34	82
Skp1	AgSkp1	87
Cdc53	AgCdc53	64
Grr1	AgGrr1	50
Cdh1	AgCdh1	66
Cdc20	AgCdc20	59
Cdc16	AgCdc16	53
Apc1	AgApc1	35
Cdk inhibitors and regulators		
Sic1	AgSic1	37
Far1	AgFar1	31
Hsl7	AgHsl7	45
Hsl1	AgHsl1	43
Mih1	AgMih1	34
Swe1	AgSwe1	52
Cdc5	AgCdc5	73
Transcription factors		
Swi6	AgSwi6	49
Swi4	AgSwi4	43
Mbp1	AgMbp1	53
Mcm1	AgMcm1	54
Swi5	AgSwi5/Ace2	35
Ace2	AgSwi5/Ace2	35
Fkh1	AgFkh1/2	46
Fkh2	AgFkh1/2	50

Genes that are duplicated in *S. cerevisiae* but present as a single copy in *A. gossypii* are named using both yeast names, separated by a slash (e.g., AgClb1/2p).
 (Taken from data published by Dietrich et al., 2004)

To investigate whether *A. gossypii* has developed different modes for the regulation of the G1 cyclins, a localization study has been performed.

The predicted G1 cyclins, *AgCLN1/2* and *AgCLN3* were epitope tagged at their endogenous loci with 13 copies of the c-myc epitope to evaluate cyclin protein distribution in the cell. These epitope tagged strains displayed normal growth and levels of nuclear asynchrony were similar to the reference strain ($\Delta\Delta t$). Cyclin protein localization in the cell was determined using indirect immunofluorescence. The myc antibody did not reveal any signal in untagged $\Delta\Delta t$ strains (Figure 20 A). *AgCln1/2p* was concentrated in nuclei with a single SPB and was diffusely present in the cytoplasm (Figure 20 B,

left panels). Surprisingly, this G1 cyclin homologue is also visible in nuclei with mitotic spindles (Figure 20 C, left panels). Additionally, *AgCln1/2p* was observed at many hyphal tips which are sites of polarized growth (Figure 20 B, left panels). Consistent with this observation, the *Agcln1/2* cells showed an enlargement of hyphae, which as we speculate may be a consequence of a diffuse zone of polarity (Chapter I). The other G1 cyclin *AgCln3p* was concentrated in nuclei of all cell cycle stages, similarly to its yeast homologue *ScCln3p* (Figure 20 B and C, right panels). The signal of *AgCln3p* was very weak and changes in abundance of protein in the nucleus could not be detected. To confirm this localization in living cells, we also

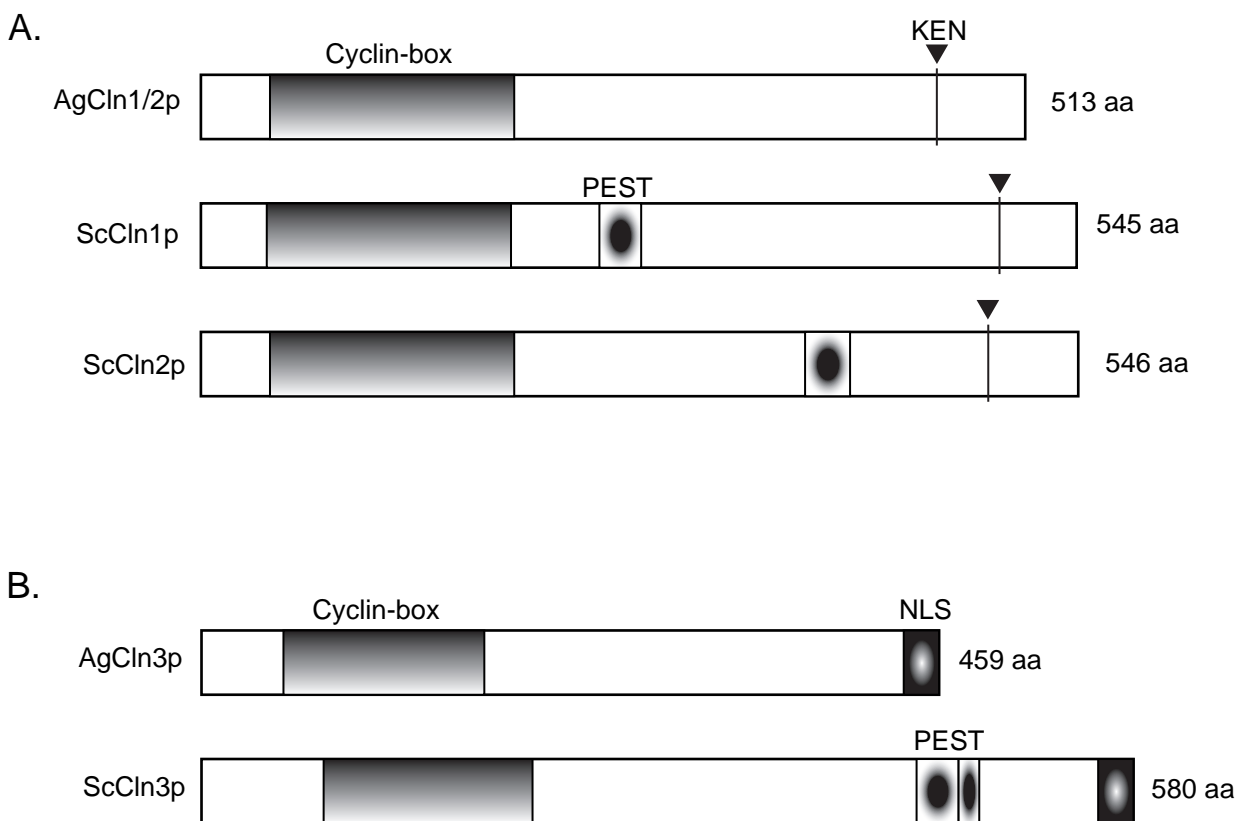
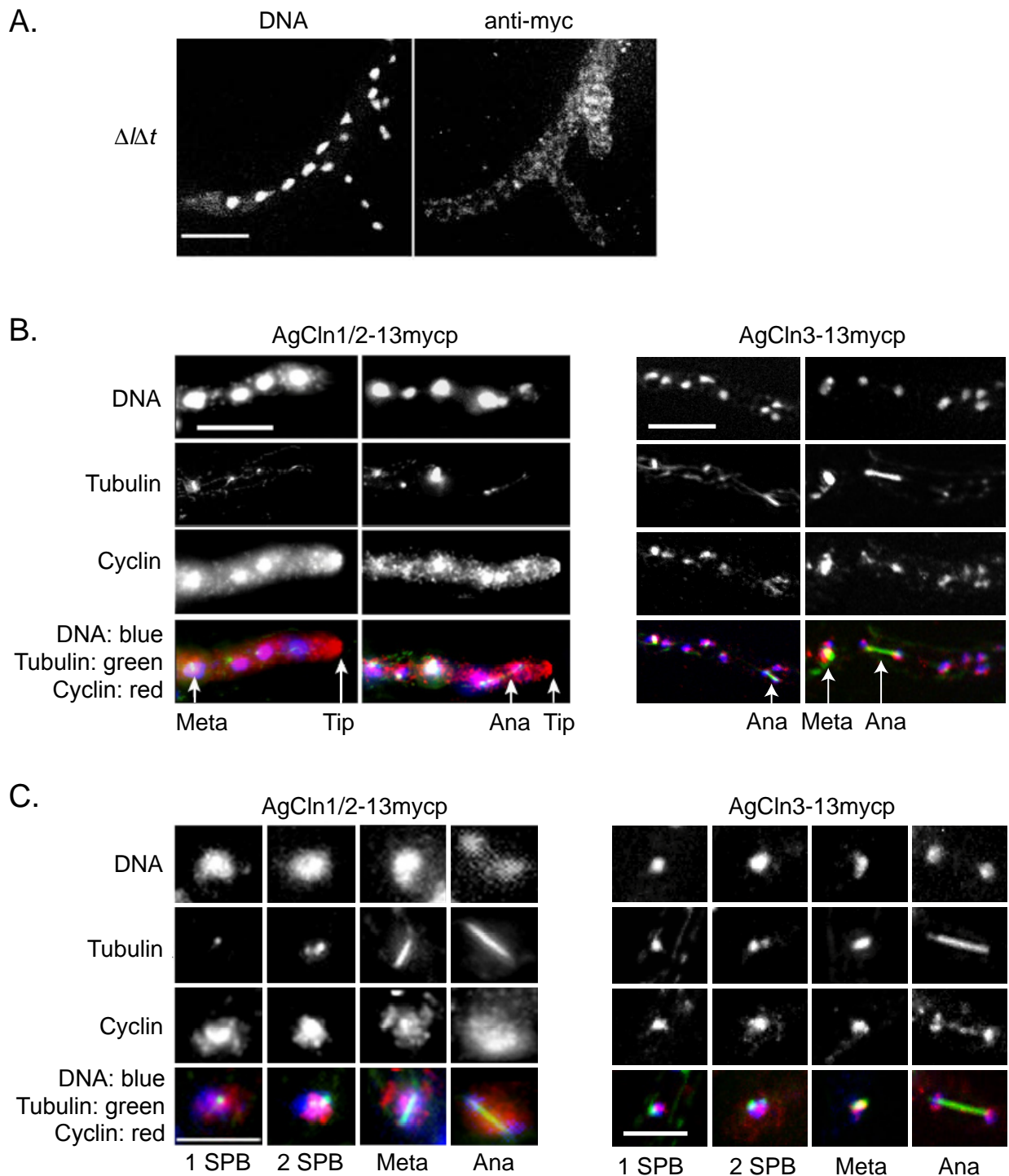


Figure 19
Comparison of *A. gossypii* and *S. cerevisiae* G1 cyclins.

A. Domain comparison between *AgCln1/2p*, *ScCln1p* and *ScCln2p*. The N-terminal cyclin domain was identified by a Pfam scan (*Ag* aa 43-195) and also a KEN-box was found in *AgCln1/2p* (*Ag* aa 458-460) and the homologous cyclins in *S. cerevisiae*. Potential PEST motifs (Rechsteiner and Rogers, 1996) have been detected by the PESTfind program (www.at.embnet.org/embnet/tools/bio/PESTfind/) for both *ScCln1p* and *ScCln2p*, giving scores of 14.12 and 6.99, respectively.

B. Domain comparison between *AgCln3p* and *ScCln3p*. These two proteins have a very low percentage identity (34%) and the only common domain found by Pfam was the N-terminal cyclin domain (*Ag* aa 51-176). In this domain, the percentage identity raises to 52%. In addition, a homologous potential bipartite NLS has been identified in *AgCln3p* (*Ag* aa 436-458), identified and described by Yaglom et al., 1995 and Miller and Cross, 2001. In *ScCln3p* two potential PEST domains were identified ([1], aa 445-471: 7.39; [2], aa 471-484: 10.65).

Scores were derived from the PESTfind program (www.at.embnet.org/embnet/tools/bio/PESTfind/).

**Figure 20****G1 cyclins are nuclear and present throughout all nuclear division stages.**

A. Reference strain, untagged *A. gossypii* cells were processed for immunofluorescence with the myc antibody to show the level of background fluorescence with this antibody.

B. Parts of a hyphae containing either the G1 cyclin AgCln1/2-13mycp or AgCln3-13mycp were visualized with tubulin by immunofluorescence. Arrows highlight nuclei of different nuclear stages.

C. G1 cyclin AgCln1/2-13mycp and AgCln3-13mycp were visualized along with tubulin by immunofluorescence. Individual nuclei are shown representing different spindle stages.

In overlays, DNA is blue, tubulin is green, and cyclins are red, leading to purple nuclei containing cyclins. Bars (A and B), 10 μ m; (C) 5 μ m.

epitope tagged the endogenous loci of *AgCLN3* with GFP. This strain grew normally, however, probably due to the low abundance of AgClb3p, a signal was never detected.

Both G1 cyclins seem to be present throughout all cell cycle stages (Figure 20 B, C). There was some variability in intensity of signals between nuclei but this did not correlate with cell cycle stage and we predict is due to variability inherent in immunofluorescence in fungal cells where there is irregularity in digestion of the cell wall. Thus, the G1 cyclins in *A. gossypii* do not display complete degradation in correlation with cell cycle progression but instead are found in most nuclei, regardless of their nuclear stage.

Mitotic cyclins are nuclear and present during the entire nuclear division cycle

Periodic transcription and degradation of cyclins ensures oscillation in CDK activity and orderly progression through the cell cycle. As a first step towards understanding the regulation of mitotic cyclins in *A. gossypii*, their sequences were studied and compared with their homologues in *S. cerevisiae*. Upstream sequences of *AgCLB1/2* showed conservation of transcriptional regulatory elements including Fkh1p, Fkh2p and Mcm1p sites in the *AgCLB1/2* promoter (consensus sequences summarized in (Kellis et al., 2003). Furthermore, protein sequences contain degradation motifs such as the destruction (D)-box and KEN-box motifs in AgClb1/2p (Figure 21 A, (Glotzer et al., 1991; Holloway et al., 1993; Pflieger and Kirschner, 2000; Yamano et al., 1996)). The AgClb1/2p sequence has one additional N-terminal -and another centrally located D-box, one of two nuclear export sequences (NES) compared to ScClb2p and one nuclear localization sequence (NLS, (Hood et al., 2001). The other mitotic cyclin AgClb3/4p contains a conserved D-box, however, other motifs (in addition to the conserved cyclin-box) have not been discovered.

Based on the homology and similar domain composition of the *A. gossypii* cyclins compared to those of budding yeast, we would predict that individual nuclei are expressing and degrading distinct cyclins depending upon their cell cycle stage. Given that protein translation occurs in a common cytoplasm, however, it is unclear how independent transcriptional programs and oscillating protein levels are achieved by neighboring nuclei that are out of phase with each other. In an effort to determine if such periodic expression patterns

could be locally established in a syncytial cell, the mitotic cyclins were localized in *A. gossypii*.

The predicted B-type cyclins, *AgCLB1/2* and *AgCLB3/4*, were epitope tagged at their endogenous loci with 13 copies of the c-myc epitope to localize these proteins in the cell. To confirm that epitope addition does not significantly effect function of the tagged protein, tagged strains were evaluated for growth and nuclear division. Unfortunately, *AgCLB3/4-13myc* did not display normal growth and failed to sporulate which is the behaviour of the *Agclb3/4Δ*. Therefore this strain was excluded from further studies. The localization of AgClb1/2-13mycp was determined using indirect immunofluorescence. AgClb1/2p was concentrated in nuclei with 2 SPBs and metaphase spindles as expected but remarkably was also clearly present in nuclei with a single SPB and in anaphase nuclei (Figure 22 A and B). Variability in intensity of signals detected between nuclei did not correlate with cell cycle stage and possibly is due to variability inherent in immunofluorescence in fungal cells where there is irregularity in digestion of the cell wall.

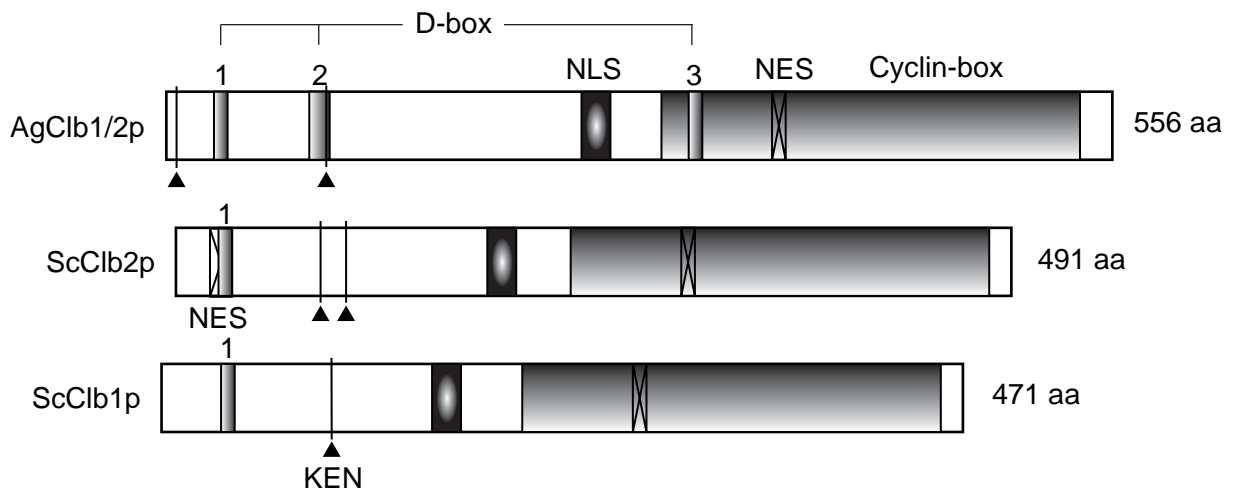
To confirm these localizations were not due to artefacts from fixation and immunofluorescence, we also epitope tagged the endogenous loci of *AgCLB3/4* and *AgCLB1/2* with GFP, to evaluate cyclin distribution in living cells. Unfortunately, AgClb3/4-GFP was not functional as observed for AgClb3/4-13myc (data not shown). The signal detected for AgClb1/2-GFP was vacuolar (Figure 22 C), which may be due to the degradation of the GFP.

Thus, also the mitotic cyclin AgClb1/2p in *A. gossypii* did not display degradation in sync with cell cycle progression. AgClb1/2p localized to nuclei of all cell cycle stages and changes in cyclin levels could not be correlated to any specific stage. Since G1 as mitotic cyclins seem to be nuclear during the entire cell cycle, many nuclei may contain different types of cyclins present at the same time.

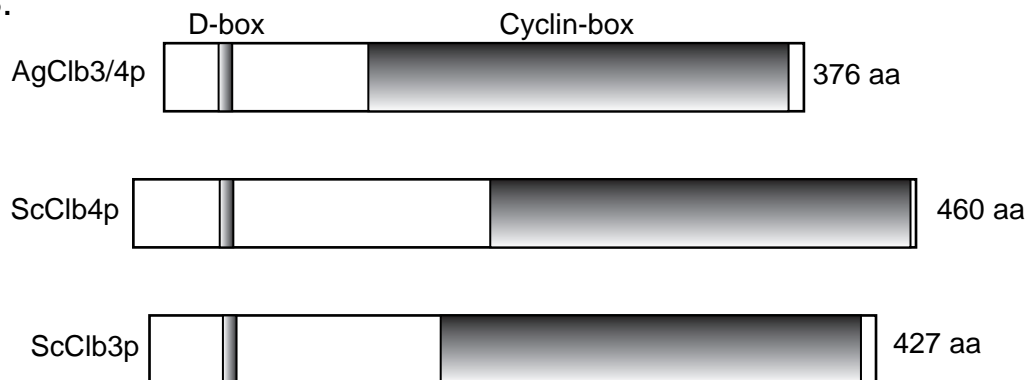
Mitotic cyclins are present in nuclei that are distinct from the site of expression

In most naturally multinucleated cells, mitosis tends to occur either synchronous, or parasynchronously with a wave of nuclear division rushing through a cell such as in the filamentous fungus *Aspergillus nidulans* (Clutterbuck, 1970). Also fusion experiments with mammalian cells demonstrated that multiple nuclei residing in a shared cytoplasm tend to synchronize their nuclear cycles (Rao and Johnson, 1970). These findings

A.

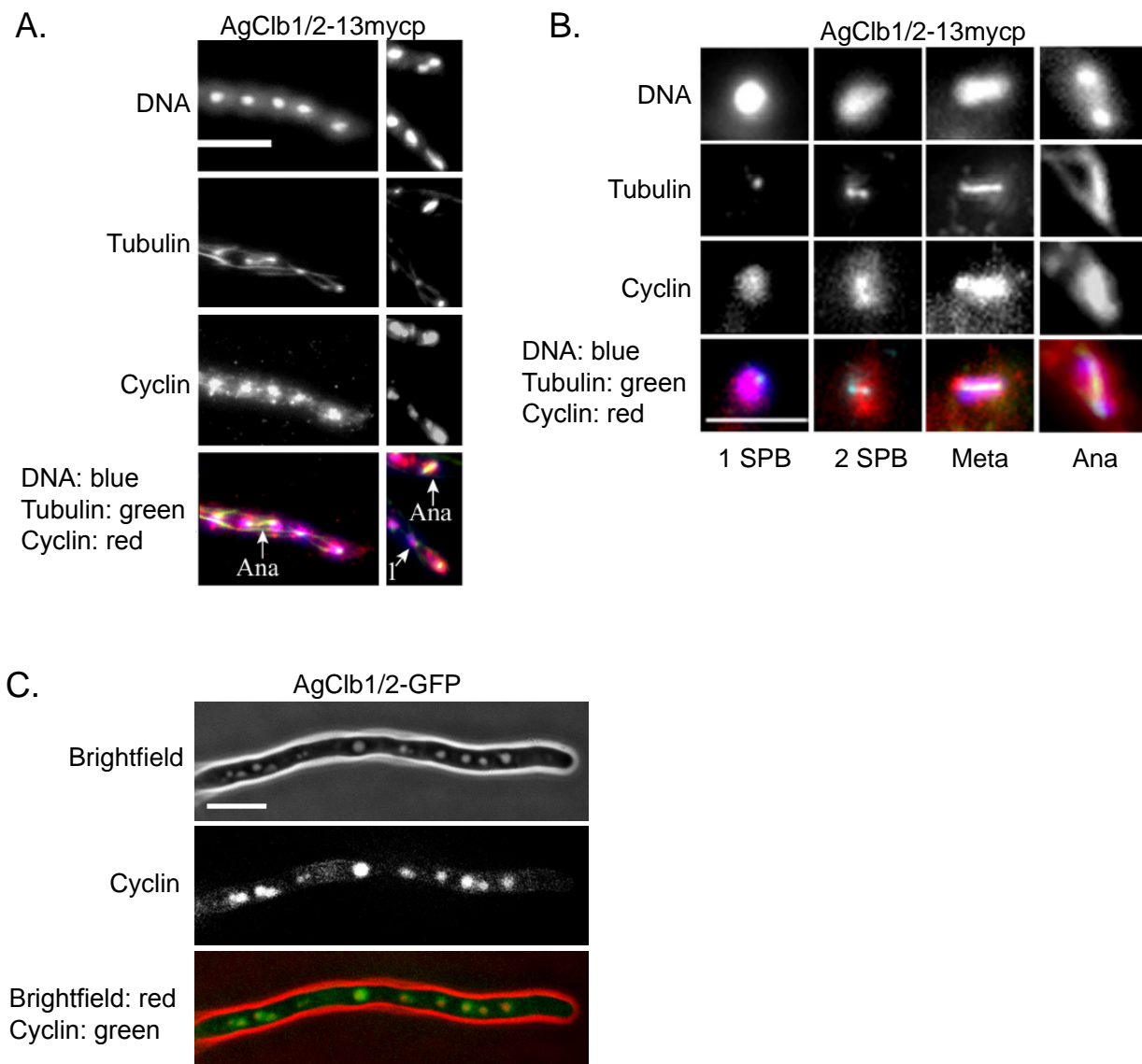


B.

**Figure 21****Comparison of *A. gossypii* and *S. cerevisiae* mitotic cyclins.**

A. Domain comparison between AgClb1/2p, ScClb2p and ScClb1p. The Cyclin-box was identified by a Pfam scan and is highly conserved (Ag aa 291-537). Three potential D-boxes, (db1 (homologous to the D-boxes in *S. cerevisiae*), [indicated by 1], Ag aa 28-36; db2, [indicated by 2], Ag aa 84-96; db3, [indicated by 3]; Ag aa 307-315, Glotzer et al., 1991), two KEN-boxes (indicated with an arrowhead [Ag aa 6-8 and aa 94-96, Pfleger and Kirschner, 2000; Hendrickson et al., 2001]), the NLS (Ag aa 244-261) and one of two NESs (Ag aa 356-364, Hood et al., 2001) were identified in the AgClb1/2p sequence.

B. Domain comparison between AgClb3/4p, ScClb4p and ScClb3p. The Cyclin-box was identified by Pfam scan (Ag aa 120-367) and a conserved D-box was found (Ag aa 32-40, Glotzer et al., 1991).

**Figure 22**

The mitotic cyclin AgClb1/2p is nuclear and present throughout all nuclear division stages.

A. Parts of a hypha of the *AgCLB1/2-13myc* strain, was visualized with tubulin by immunofluorescence.

B. *AgClb1/2-13myc* was visualized along with tubulin by immunofluorescence. Individual nuclei are shown representing different spindle stages.

In overlays, tubulin is green, cyclins are red and nuclei are blue, leading to purple nuclei containing mitotic cyclins.

C. *AgClb1/2-GFP* strain, showing the *AgClb1/2-GFP* signal in vacuoles.

In the overlay, *AgClb1/2-GFP* is green and brightfield is red.

Bars, (A and C) 10 μm ; (B) 5 μm .

suggested that distinct nuclei with a common cytoplasmic environment will accelerate or pause their normal cell cycle kinetics to align temporally with the other nuclei present. It has been hypothesized that synchrony in multinucleated systems depends upon the free diffusion of regulators in the cytoplasm.

However, *A. gossypii* is a multinucleated organism, which undergoes asynchronous mitosis with neighboring nuclei of different cell cycle stages. This leads to the question whether cell cycle specific proteins expressed from a single nucleus and translated in a common cytoplasm are able to freely diffuse and enter neighboring nuclei of different cell cycle stage? Basically there are two possible answers to this question. Either cell cycle specific proteins are selectively imported into the nuclei where they have been expressed, or these proteins are able to enter adjacent nuclei of different nuclear stage. However, if this was the case, proper cell cycle progression can only be ensured, if proteins from a different cell cycle stage are either inhibited or degraded (Figure 23 A).

To evaluate the basis of ubiquitous nuclear cyclin localization, we generated heterokaryon cells in which only a subset of nuclei express a tagged version of the mitotic cyclin *AgCLB1/2*. This cyclin was chosen, due to its known nuclear localization in *A. gossypii* and its cell cycle specific involvement in mitosis. We then asked whether the nuclei that do not themselves contain an epitope tagged cyclin gene have detectable levels of tagged cyclin proteins expressed from neighboring nuclei. To find out which nucleus was expressing the tagged cyclin we made use of the LacI-LacO system (Pearson et al., 2001; Straight et al., 1996). This system was discovered in *E. coli* and is based on the interaction of a DNA binding protein (Lac repressor) to the LacO array. Each Lac repressor dimer binds to a single operator sequence, and this interaction can be recognized based on the amino terminal GFP fusion to the Lac repressor (32-mer of AAATTGTTATCCGCTCACAATTCCACATGTGGC CAC). GFP-LacI-NLS was stably integrated into the genome at the *AgADE2* locus, using the pAIC module, kindly provided by P. Knechtle. This locus has been chosen, so that no selection marker had to be used. A strong GFP signal was detected in all nuclei (Figure 23 B).

In a second round, *A. gossypii* was transformed with autonomously replicating plasmids. This plasmid contained the epitope tagged mitotic cyclin (*AgCLB1/2-13myc*), which can be localized by immunofluorescence, the LacO array, the dominant Geneticin selection marker, the Ampicillin resistance gene and a CEN/ARS

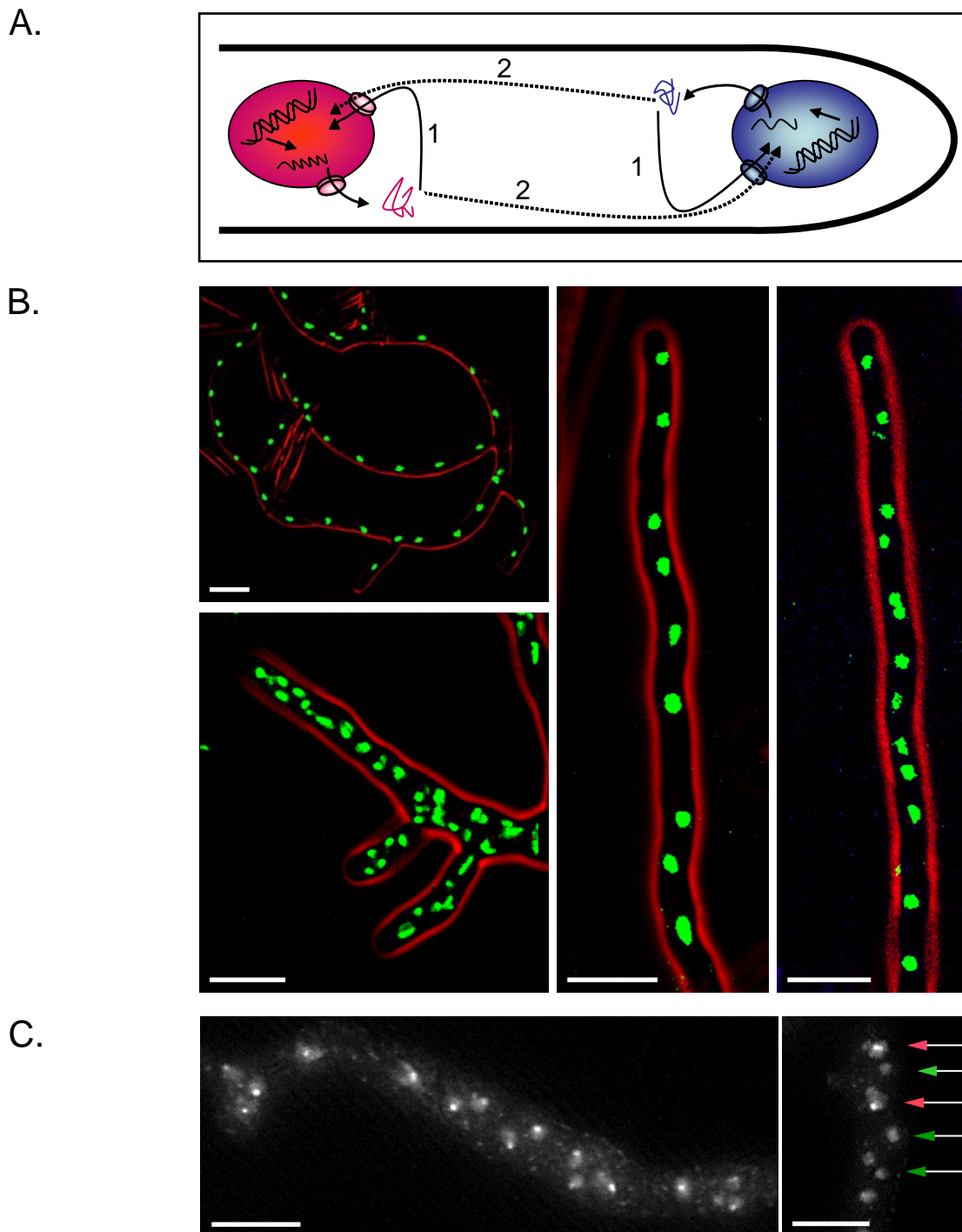
site (Figure 24 A, top). Already by looking at the GFP signal, it became clear which nuclei contain the plasmid, since there the whole GFP-LacI was accumulated at a specific spot, representing the binding of the Lac repressor to the Lac operator (the plasmid, Figure 23 C).

When those transformed cells were grown under strong selection, nearly all nuclei revealed the GFP signal (Figure 24 B, left). However, when selection for the plasmid was removed, the bright dots of GFP signal were lost from many nuclei, so that only a fraction of nuclei (28%, n = 300) retained a plasmid (5 h after release from selection; Figure 24 B, right). We then asked whether the *AgClb1/2-13myc* was visible in nuclei that did not appear to contain a plasmid. Tagged cyclin proteins were detected in nearly all nuclei regardless of whether they obtained the plasmid expressing the epitope tagged gene. In hyphae in which very few GFP dots were visible, *AgClb1/2-13myc* protein was still apparent in many nuclei.

Thus, nuclei that clearly lacked the plasmid containing the tagged gene had tagged protein product. These proteins most likely derived from neighboring nuclei that still possessed a plasmid. This experiment suggests that mitotic cyclins are freely diffusing, taken up by, and maintained in neighboring nuclei. However, we also cannot exclude that nuclei lacking the plasmid, still contain a reservoir of stable protein. Since *AgClb1/2p* was detected in all stages of the nuclear division cycle, cell cycle specific degradation of this mitotic cyclin has never been detected and therefore the cyclin may be stable for more than one cell cycle.

Asynchrony persists when cyclins are displaced from nuclei with two exogenous NESs

To further address how mitotic cyclin nuclear localization contributes to asynchrony, we shifted a proportion of the cyclin protein out of the nucleus with the addition of two Nuclear Export Sequences (NESs) to the *AgClb1/2-13myc* protein (Edgington and Futcher, 2001). If nuclear sequestration of newly made cyclin protein is important for nuclear autonomy then we would predict that displacement of mitotic cyclin into the cytoplasm, where it could potentially more freely diffuse, would lead to an increase in synchrony of nuclear division. The two additional NESs led to an increase in the cytoplasmic levels of *AgClb1/2-13myc* protein as visible by immunofluorescence but still left sufficient protein in the nucleus to promote normal growth

**Figure 23**

Strategy to distinguish which nuclei contain a plasmid by the specific binding of the Lac repressor to the Lac operator sequence.

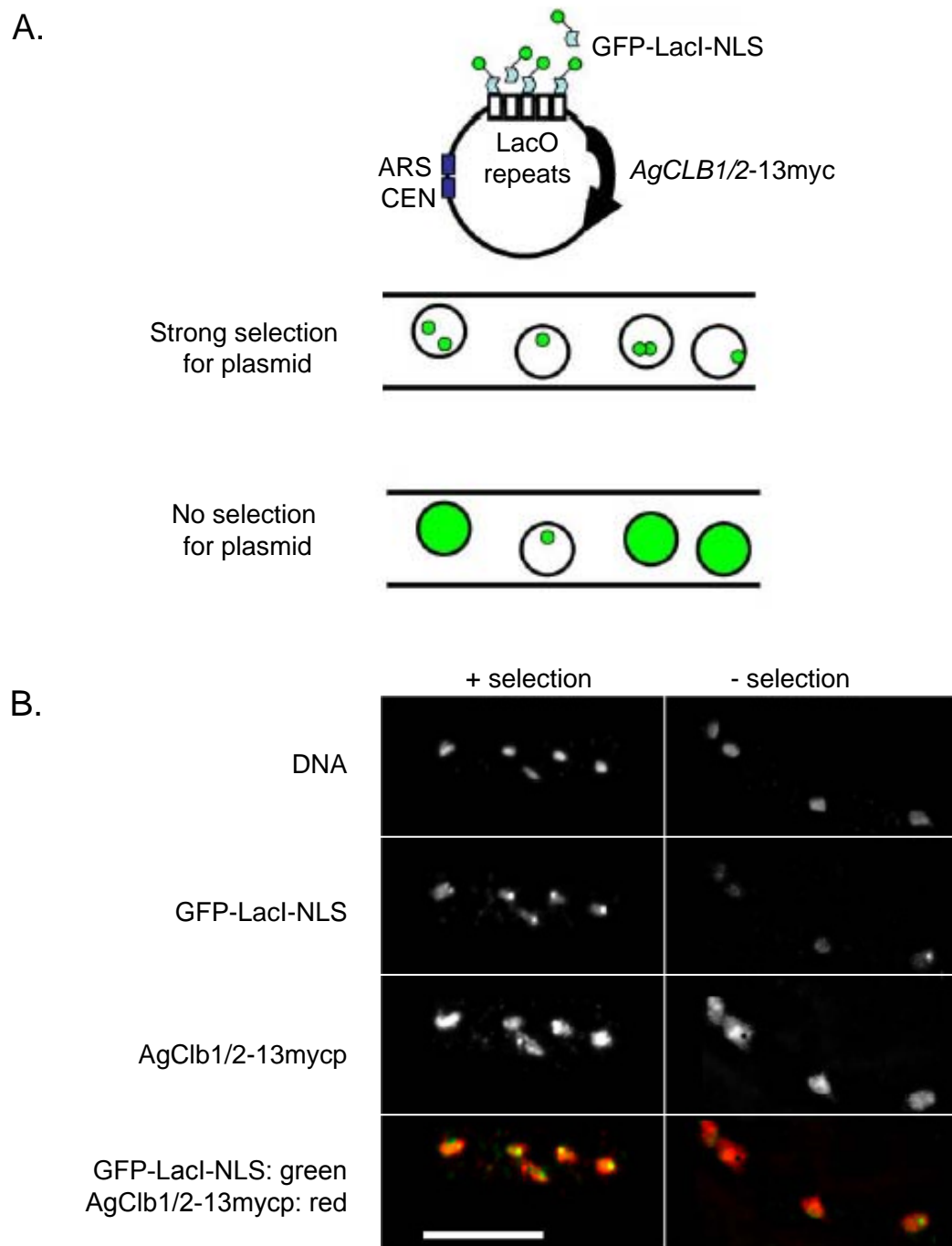
A. Two hypotheses how *A. gossypii* may maintain asynchronous mitosis.

1: Each nucleus is insulated, expressing and containing its own cell cycle specific proteins.

2: Cell cycle specific proteins are able to get into neighboring nuclei. Therefore all nuclei contain the same repertoire of proteins. Proteins which are not needed, are either inactivated by inhibitors or degraded.

B. Integration of LacI-NLS-GFP into the genome at the ADE2 locus gave a bright GFP signal in every nucleus.

C. The Lac repressor bound to the Lac operator repeats, showing an accumulation of the GFP signal as a very bright dot in the nucleus, representative for the existence of the plasmid. Arrows in red, contain the plasmid, arrows in green, do not contain a plasmid. Bars, 10 μm .

**Figure 24****Mitotic cyclins are present in nuclei that are distinct from their site of expression.**

A. Top: Centromere-based plasmid containing an epitope-tagged *AgCLB1/2-13myc*, 32-LacO repeats and a GEN3 resistance marker, able to replicate and segregate in *A. gossypii* nuclei.

Bottom: *A. gossypii* GFP-LacI-NLS cell strains were transformed with the plasmid containing the *AgCLB1/2-13myc* and the LacO repeats. In presence of G418, many nuclei show one or two dots of GFP, indicative of a plasmid. When the selection was removed, within 5 h, the GFP signal was lost in the majority of nuclei and GFP-LacI appeared as diffuse signal in the nucleoplasm, indicative of the absence of the plasmid.

B. GFP-LacI-NLS + pLacO-*AgCLB1/2-13myc* were grown overnight for 16 h under selection. Half of the cells were fixed before washing out G418 (left), the other half of the cells were resuspended in fresh media lacking the selective drug and grown for 5 h before fixation (right). Cells were processed for immunofluorescence to visualize GFP-LacI-NLS and AgClb1/2-13mycp. Bar, 10 μ m.

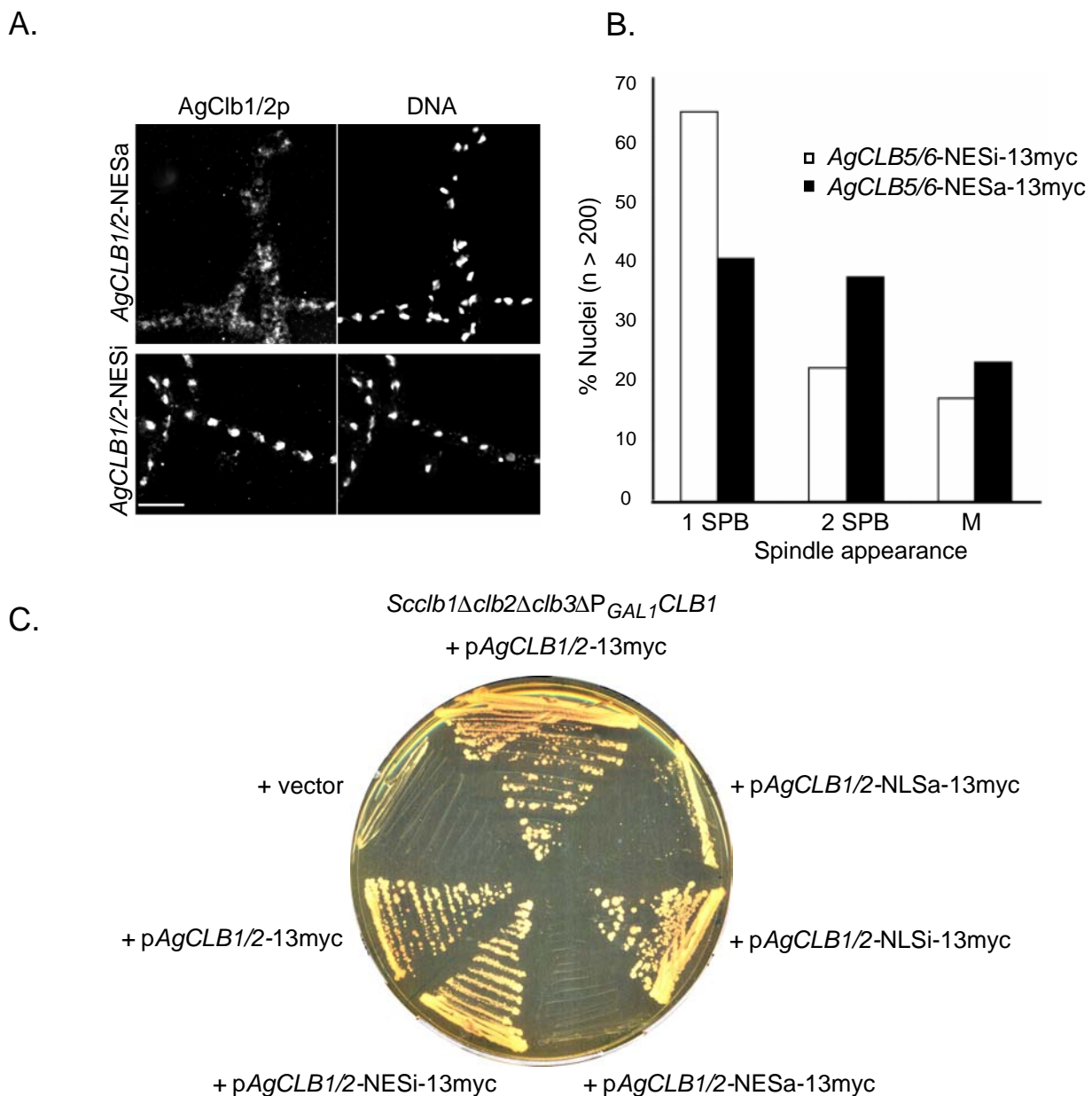


Figure 25
Displacement of AgClb1/2p to the cytoplasm with two exogenous NESs

A. *AgCLB1/2-NESa-13myc* (active NES) and *AgCLB1/2-NESi-13myc* (inactive NES control) were grown for 16 h and processed for anti-tubulin and anti-myc immunofluorescence. Images were captured and processed identically to compare protein intensities within the figure. Bar, 10 μ m.

B. Percentage of nuclei in each spindle stage based on tubulin immunostaining. $n > 200$ nuclei scored for each strain.

C. *S. cerevisiae* strain *clb1Δclb2Δclb3ΔP_{GAL1}CLB1* (AY117) was transformed with pCLB2-13myc, and the forced localization plasmids, pAgCLB1/2-NLSa-13myc (active NLS, pAKH23), pAgCLB1/2-NLSi-13myc (inactive NLS control, pAKH24), pAgCLB1/2-NESa-13myc (active NES, pAKH25) and pAgCLB1/2-NESi-13myc (inactive NES control, pAKH26). In all these plasmids, *AgCLB1/2* was expressed from its own *A. gossypii* promoter. The control vector contained the selectable marker but lacked the cyclin gene. The inducible yeast cyclins were repressed in glucose and complementation was evaluated at 30°C on YPD plates + 200 μ g/ml G418.

and nuclear division (Figure 25 A). There was no increase in cell cycle synchrony observed, despite the increase in cytoplasmic levels of cyclin proteins between cells with an inactive NES or active NES fusion protein. Interestingly, however, these cells did show a higher proportion of nuclei with duplicated SPBs or mitotic spindles suggesting that cyclin protein concentration gradients were altered by this displacement leading to an increase in the frequency of mitosis (Figure 25 B). Thus, nuclear asynchrony or autonomy seems to be established independent of the origins, levels and localization of the mitotic cyclin AgClb1/2p.

Localization studies of the mitotic cyclin ScClb2p have revealed, that in addition to its major localization in the nucleus, a subpopulation of ScClb2p is present at the bud neck (Hood et al., 2001), where it possibly is involved in the induction of the switch from apical to isotropic growth (Amon et al., 1993; Lew and Reed, 1993; Richardson et al., 1992). Since *A. gossypii* does not undergo such an apical-isotropic switch and in addition did not greatly respond to changes in AgClb1/2p localization, we wanted to test, whether *S. cerevisiae* is more sensitive to such changes in local protein concentrations. Plasmids containing the mitotic cyclin *AgCLB1/2* gene, or mislocalized *AgCLB1/2*, (containing C-terminally fused NES or NLS sequences) were evaluated for their ability to complement mutant yeast strains deficient for the homologous cyclin. As previously shown in Chapter I, wild-type AgClb1/2p is functional in yeast leading to growth of the otherwise inviable yeast cells (Figure 25 C, 6 B). However, unlike *A. gossypii*, mislocalized AgClb1/2p did not complement yeast, leading to inviability. Possibly, *S. cerevisiae* responds more sensitive to destabilization of the protein equilibrium between cytoplasm and nucleus than *A. gossypii* due to its task in the apical-isotropic switch. In addition, *A. gossypii* may have adapted some kind of “resistance” to proteins floating in the common cytoplasm, since nuclei of different nuclear stage are constantly in close proximity.

Mitotic cyclin degradation does not correlate with mitotic exit

Cyclin proteins appear to be present in all cell cycle stages which raises the question of how nuclei are able to progress through the cell cycle with accuracy. To further examine the possible persistence of a pool of mitotic cyclin protein across all cell cycle stages, the mitotic cyclin AgClb1/2p was evaluated during a Nocodazole

arrest and release experiment. This allowed AgClb1/2p localization and protein levels to be followed through a synchronous mitotic exit, the time period when mitotic cyclins are predicted to be degraded. Mitotic cyclins were observed both by immunofluorescence and by Western blots on whole cell extracts even in cells where the majority (73%) of nuclei had extended spindles and separated DNA indicative of late anaphase/telophase (Figure 26 A, B). Since the Nocodazole arrest and release experiment synchronizes at best 75% of nuclei in *A. gossypii*, degradation and subsequent absence of proteins during a short time-frame, may not be visible by Western blots due to the presence of protein in non-synchronized nuclei. However, by immunofluorescence we were able to clearly detect AgClb1/2p in all phases of the cell cycle, including anaphase. This suggests that mitotic cyclin degradation does not correlate with mitotic exit and that any regulative degradation, if present, must occur on only a small fraction of the total protein. Thus, mitotic cyclins seem to persist across the M-G1 transition and potentially may be inactivated for G1 by direct inhibition rather than degradation.

In *S. cerevisiae*, the APC-dependent proteolysis of the mitotic cyclin ScClb2p is essential for mitotic exit (Wasch and Cross, 2002). If, indeed, AgClb1/2p is not degraded in late mitosis, we might expect to see a clear cell cycle arrest, when the *A. gossypii* cyclin is expressed in yeast. Therefore, *AgCLB1/2* was expressed in yeast cells, either from its own promoter or from the *GAL1* promoter. Interestingly, yeast cells showed a delay in telophase, suggesting that the *A. gossypii* mitotic cyclin may be intrinsically stable compared to the yeast homologue (Figure 26 C).

Mitotic cyclin destruction box mutants do not show altered cell cycle progression

These localization and protein level data suggest that cyclin levels do not dramatically fluctuate in a cell cycle dependent manner in these syncytial cells. The essential mitotic cyclin AgClb1/2p, contains two N-terminal D-box sequences which in other systems have been shown to lead to APC-mediated degradation by the proteasome (Glotzer et al., 1991). In *Xenopus laevis*, *S. cerevisiae* and *Drosophila melanogaster* cells, expression of cyclins lacking the D-boxes leads to cell cycle arrest as a result of an inability to exit mitosis (Holloway et al., 1993; Sigrist et al., 1995; Surana et al., 1993; Yamano et al., 1996).

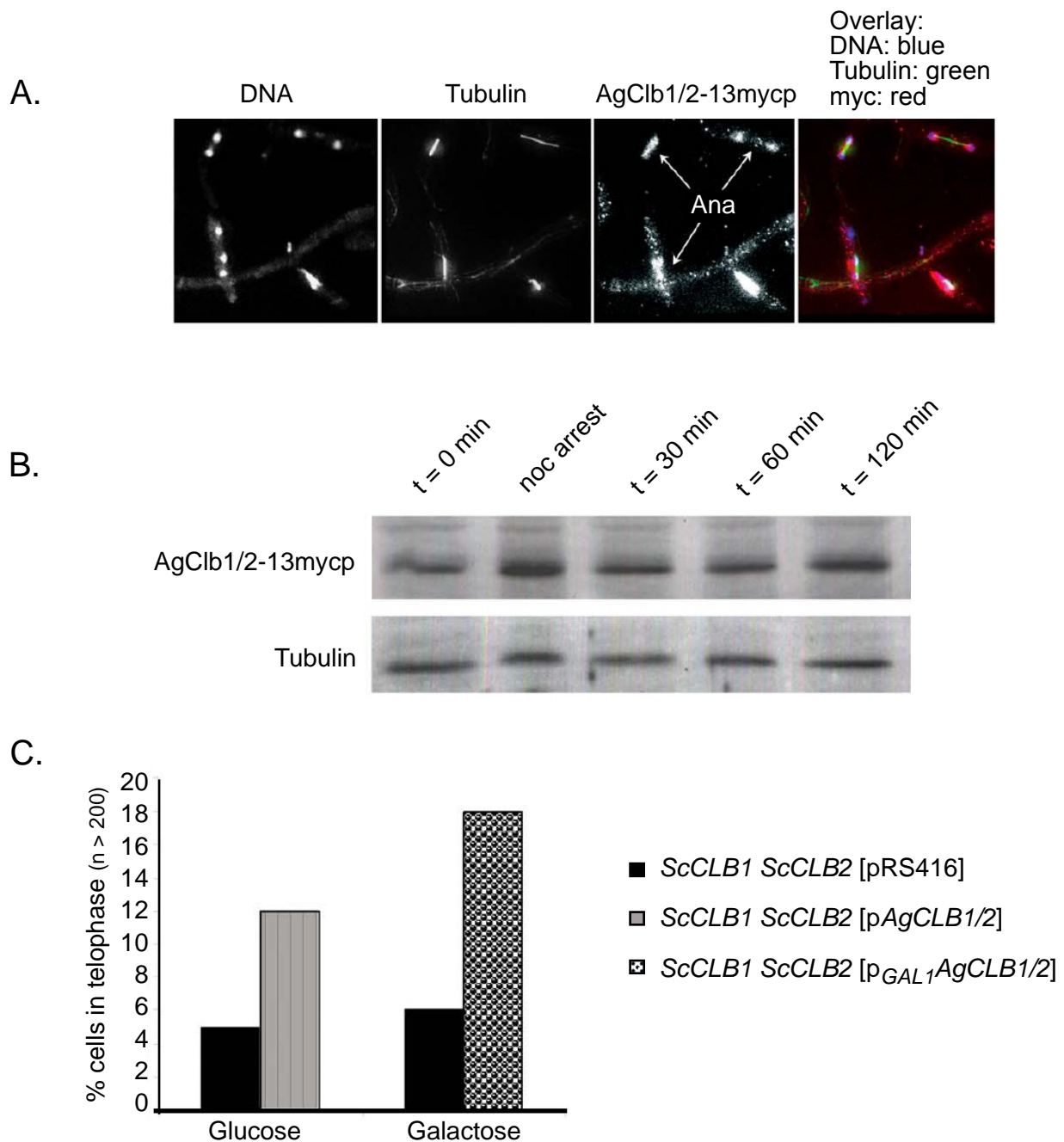


Figure 26
AgClb1/2p levels do not diminish at mitotic exit.

A. Mitotic AgClb1/2-13mycp was visualized in young germling cells that were arrested and released from Nocodazole. AgClb1/2-13mycp was evaluated by immunofluorescence. Arrows highlight anaphase/telophase nuclei with mitotic cyclin. In overlays, DNA is blue, tubulin is green, and cyclins are red, leading to purple nuclei containing cyclins.

B. AgClb1/2-13mycp cells before and after Nocodazole arrest (as in [A]), were evaluated on a Western blot, where tubulin was used as a loading control.

C. AgClb1/2p causes a transient delay in the budding yeast cell cycle. *S. cerevisiae* cells were transformed with pAgCLB1/2, p_{GAL1}AgCLB1/2 or the vector (pRS416). Asynchronously growing (on either glucose or galactose) yeast transformants were fixed and processed for tubulin immunofluorescence. Cells were categorized for cell cycle stage by observing spindle morphology. Telophase cells had an extended mitotic spindle that connected two completely separated nuclei that were at opposite ends of the mother and the bud. N > 200 cells were scored for each strain.

If some amount of cyclin destruction is required in vegetatively growing *A. gossypii* cells, then *AgCLB1/2* D-box mutants should display a clear cell cycle block or delay.

Several parallel attempts have been chosen to investigate the effect on the D-box deletions in the mitotic cyclin in *A. gossypii*. Expression of mutants in which either D-box was deleted individually (*AgCLB1/2Δdb1* and *AgCLB1/2Δdb2*) or both were deleted (*AgCLB1/2Δdb1Δdb2*) by direct replacement at the endogenous locus (Figure 27 A), at the *ADE2* locus (Figure 27 B) or as an additional plasmidic version (Figure 27 C) led to no growth defect. In addition, no alterations in nuclear division based on the proportion of nuclei in different cell cycle stages or levels of asynchrony (Figure 27 D, top, $n > 200$ cells scored for each strain) were determined in the strains containing the *AgCLB1/2* D-box plasmids. To determine if these mutant strains were delayed in exiting mitosis, cells were synchronized with Nocodazole and released to observe a synchronous mitosis in the population (during the first hour after release from Nocodazole, cells rebuild cytoplasmic microtubules prior to restoring nuclear microtubules). When compared to cells with wild-type *AgCLB1/2*, both the single and double D-box mutants showed similar rates of return to asynchrony and similar proportions of nuclei in mitosis after 120 minutes suggesting no significant delay in mitotic exit (Figure 27 D, bottom). Surprisingly, protein levels of *AgClb1/2Δdb1p*, *AgClb1/2Δdb2p* and *AgClb1/2Δdb1Δdb2p* were comparable to wild-type *AgClb1/2p* (Figure 27 E). We predict that the D-box sequences may be required in a different growth stage but are dispensable for normal nuclear division during vegetative growth.

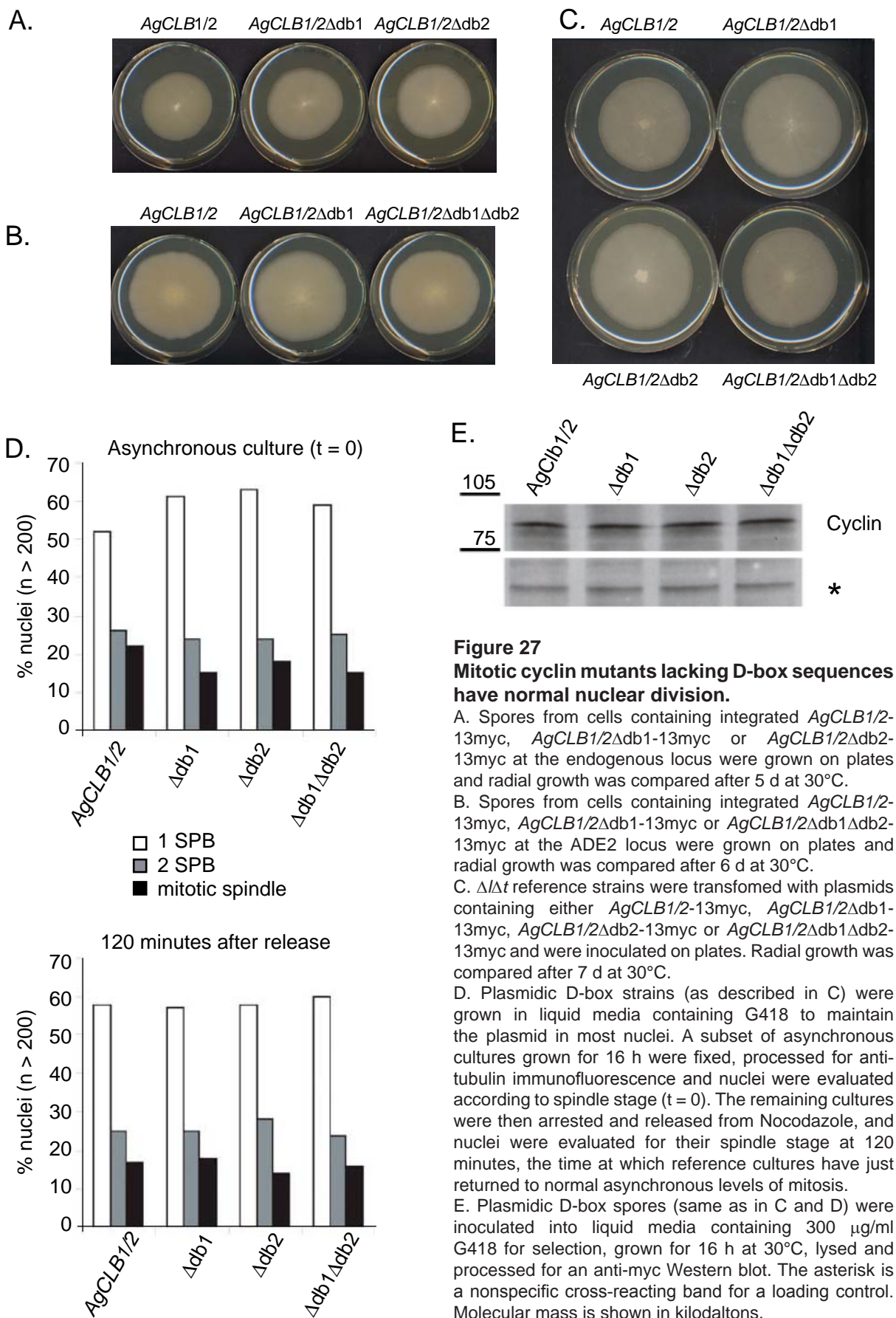
AgSic1p contributes to accurate nuclear division

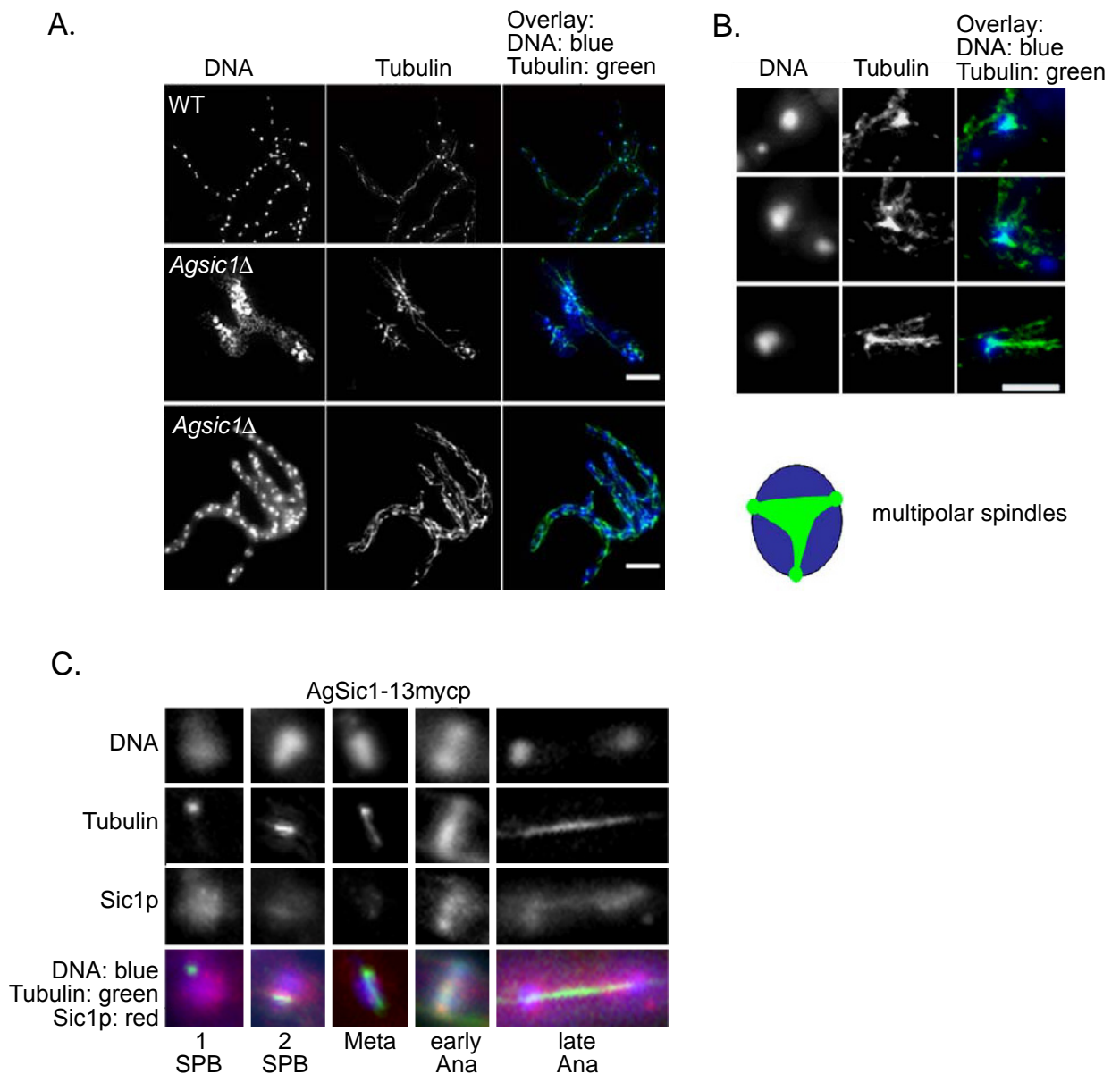
Normal mitotic progression does not appear to require sharp degradation of the mitotic cyclin pools yet nuclear division is apparently accurate and faithful in *A. gossypii*. What prevents premature entry into mitosis given the presence of M-phase promoting cyclin early in the cell cycle? One possibility is that mitotic CDK inhibitors such as *AgSwe1p* and *AgSic1p* are acting in a nuclear autonomous fashion and repress any CDK/*AgClb1/2p* complexes present in G1 nuclei. While mutants lacking *AgSWE1* showed minimal mitotic defects (A. Gladfelter, personal communication), 35% of *Agsic1Δ* cells stopped growth with 10-20 nuclei,

aberrant multipolar spindles and irregular nuclear distribution and density (Figure 28 A, middle panel and 28 B). A proportion of *Agsic1Δ* cells (55%) formed a developed mycelium but of these, the majority ultimately arrested growth with up to a 100 densely packed nuclei (Figure 28 A, bottom panel). Around 10% of mutant spores produced viable and sporulating mycelia, potentially due to the acquisition of a suppressing mutation or the production of multinucleated spores during sporulation that contain a wild-type nucleus. Many cells in an *Agsic1Δ* mutant population show defects in nuclear division suggesting that *AgSic1p* may help limit the premature activity of mitotic CDK complexes.

AgSic1p localization changes across the nuclear division cycle

If *AgSic1p* is a source of *AgCDK/AgClb1/2p* activity oscillation, the protein may vary in localization and /or abundance across different stages of the cell cycle. We localized *AgSic1p* protein by immunofluorescence and evaluated its behavior during different nuclear division cycle stages to examine whether this predicted CDK inhibitor may oscillate in any way. *AgSic1p* undergoes notable changes to its sub-nuclear localization correlating with distinct stages of nuclear division (Figure 28 C). In nuclei with a single SPB and nuclei that are in late anaphase, *AgSic1p* was present throughout the nucleoplasm. Interestingly, the signal was not uniformly distributed; rather, there were foci of intense staining in addition to a more diffuse signal across the nucleus. In nuclei with duplicated SPBs, the nucleoplasm signal weakened, and some protein accumulated on short spindles. When metaphase spindles were present, *AgSic1p* was barely detectable in the nucleoplasm, and, occasionally, a low level of *AgSic1p* was apparent on spindles. In anaphase, as soon as any separation was detectable between the DNA signals, *AgSic1p* reappeared on elongating spindles as an intense signal. *AgSic1p* was observed on spindles throughout anaphase/telophase as well as in the nucleoplasm of the daughter nuclei. These dynamics would suggest that *AgSic1p*'s sub-nuclear localization is regulated to alter either its own activity or its contact with interacting proteins through different stages of the nuclear cycle.



**Figure 28****The essential B-type cyclin inhibitor AgSic1p undergoes changes in localization according to the nuclear division cycle stage.**

A. *Agsic1Δ* mutants were germinated in the presence of 50 $\mu\text{g/ml}$ CloNAT to select for cells with the gene disrupted, fixed, processed for anti-tubulin immunofluorescence and compared with wild-type cells. The middle panel shows typical arrest phenotype of bipolar germlings and the bottom panel shows cells which arrest as a small mycelia and high nuclear density.

B. Higher magnification of nuclei showing multipolar spindle defects observed in *Agsic1Δ* cells.

Bars, (A) 10 μm ; (B) 5 μm .

C. AgSic1-13mycp cells were grown for 18 hours and then processed for anti-tubulin and anti-myc immunofluorescence. All images in the AgSic1p panel were taken with identical exposure times and processed in parallel with identical processing conditions. 82% of 1 SPB nuclei, 76% of 2 SPB nuclei, 75% of metaphase nuclei, 80% of early anaphase and 79% of late anaphase nuclei showed signal as depicted by these representative nuclei ($n = 400$ nuclei). In overlays, DNA is blue, microtubules are green and Sic1p is red, leading to purple nuclei containing the Sic1p.

Discussion

In this study we provide first insight into the regulation of mitosis in multinucleate fungal cells. G1 and mitotic cyclin proteins appear to be highly enriched in nuclei but are able to diffuse in the cytoplasm without disturbing asynchrony. Remarkably, G1 cyclins and the mitotic cyclin protein AgClb1/2p are present in all stages of the nuclear division cycle suggesting that oscillation of CDK activity is not primarily generated by periodic expression and complete degradation of G1 and mitotic cyclins (Figure 29). From our experiments, we propose that the syncytial nature of these cells has favored the evolution of a cell cycle oscillator built upon the action of CDK inhibitors rather than G1 or mitotic cyclin protein abundance. These data raise two unique problems for these cells: How does cell cycle progression occur accurately given the apparent lack of coordinated oscillation in cyclin proteins and how do nuclei behave independently in the same cytoplasm?

Current models of cell cycle control are rooted in the principle of a biochemical oscillator built through the intertwined regulation of synthesis and destruction of many proteins (Murray, 2004). In yeast, about 800 genes display periodic expression over the cell cycle including the cyclins, CDK inhibitors, degradation machinery, and transcription factors and many of these proteins similarly have periodic destruction patterns (Spellman et al., 1998). Extensive experimental data combined with recent mathematical models have shown that this choreographed synthesis and destruction program enables the cell cycle to function as a bistable system that alternates between two stable but mutually exclusive and irreversible states, G1 and S/G2/M phases (Chen et al., 2000; Cross et al., 2002). In yeast, the basis of this bistability is thought to originate from essentially two redundant, though distinct biochemical oscillators: one rooted in a negative feedback loop that triggers mitotic cyclin (ScClb2p) degradation and the other a "relaxation oscillator" that ensures alternating states of high ScClb2p/low ScSic1p and low ScClb2p/high ScSic1 activity (Cross, 2003). Only one of the two oscillators needs to be present for yeast to divide. Importantly, however, both oscillators require fluctuating protein levels of either Clb2p or Sic1p to properly function and maintain the bistable nature of the system (Cross, 2003).

All homologues of the core regulators of the *S. cerevisiae* cell cycle are present in the *A. gossypii* genome suggesting that in principle mitosis could be built with similar circuitry to

yeast (Dietrich et al., 2004). The syncytial nature of *A. gossypii* cells, however, complicates the maintenance of an oscillating transcriptional and degradation program which is fundamental to bistability in the yeast system. In multinucleated cells, translation occurs in a common cytoplasm and it is unclear how individual nuclei could have independent transcriptional programs which would then generate local differences in protein levels between neighboring nuclei. Indeed, the behavior of the G1 and mitotic cyclins suggest that these multinucleated cells are not tightly controlling the levels of such proteins in a cell cycle regulated manner. Another multinucleated cell, *Physarum polycephalum*, which undergoes synchronized mitoses, also appears to maintain constant levels of mitotic cyclins across all cell cycle stages (Cho and Sauer, 1994). Does the different spatial organization of a syncytial cell dictate a fundamentally different mode of cell cycle oscillation?

It appears as if the cell cycle oscillator in *A. gossypii* may not require temporally regulated synthesis and complete degradation of at least some key cell cycle control proteins. Conceivably, there is highly localized degradation of a small but functionally significant fraction of cyclin proteins that has escaped our detection in these studies. Lack of a dominant phenotype however in cells expressing cyclin D-box mutants suggests that regulated proteolysis of mitotic cyclins is not critical for regulating mitosis during normal vegetative growth. The continuous cytoplasmic streaming of a syncytial cell complicates the establishment of an oscillating protein gradient through degradation alone because new proteins are always supplied by the cytoplasm. Thus, multinucleated cells like *A. gossypii* may have evolved to favor the modulation of CDK activity by inhibitors instead of cyclin abundance to generate bistability in the cell cycle circuit. While the G1 and mitotic cyclins are consistently present in nuclei throughout the cell cycle, we predict they can not be simultaneously active. In these cells, the feedback loops that run the cell cycle oscillator would lead to changes in activity instead of changes in protein synthesis and degradation. In fact, a bistable cell cycle oscillator has been shown to function with constant levels of mitotic cyclins in *Xenopus* egg extracts simply through modulating the activity of Cdc2 (CDK, (Pomerening et al., 2003). Our data suggest that Sic1p acts in *A. gossypii* cells to ensure alternating states of CDK activity even in the presence of relatively constant cyclin protein levels.

Nuclear autonomous regulation of a single factor such as the inhibitor AgSic1p could be sufficient to provide necessary oscillation in

CDK activity needed for DNA synthesis, spindle construction and chromosome segregation without great changes in cyclin levels. The requirement for ScClb2p degradation during mitosis was dispensable when ScSIC1 was overexpressed with the GAL1 promoter in ScCLB2 Δ db strains (Wasch and Cross, 2002). Thornton and Toczyski also recently presented evidence in *S. cerevisiae* that oscillation in CDK activity could be generated without degradation of mitotic cyclins simply by overexpression of ScSic1p (Thornton et al., 2004; Thornton and Toczyski, 2003). In these cells, ScClb2p was modified to be present in G1 phase, as is observed in the normal *A. gossypii* cycle, but was held inactive by an over-abundance of ScSic1p. Furthermore, ScSic1p became essential in yeast cells overexpressing ScClb2p (Cross et al., 2005). In *S. cerevisiae*, the action of ScSic1p may be redundant to cyclin degradation; however, in *A. gossypii* it has an essential task. Clearly, AgSic1p makes a vital contribution to accurate division in these multinucleated cells and may prevent G1 nuclei with AgClb1/2p from entering mitosis before the completion of S-phase. The AgSic1p homologue shows relatively low identity to the yeast homologue (37% amino acid identity) suggesting it could have diverged to be more stable and active and may act as a more potent CDK inhibitor. Additionally, AgSic1p sub-nuclear localization dynamics present the possibility that it is tightly regulated in the nuclear cycle. In the middle of mitosis, when CDK/Clb activity is at a peak, AgSic1p levels diminish in the nucleus potentially due to either nuclear autonomous degradation or transient nuclear export. The rapid accumulation of AgSic1p shortly thereafter in early anaphase, however, argues that nuclear import rather than new synthesis would replenish the nuclear protein pool. Thus we hypothesize that multinucleated cells such as *A. gossypii* may generate oscillation in CDK activity through post-translational regulation of inhibitor and cyclin protein activity rather than through tightly controlled abundance of G1 and mitotic cyclins.

How does each nucleus cycle independently? One simple possibility is that asynchrony or nuclear autonomy could be generated due to the nature of the cell cycle circuits in *A. gossypii* which, as discussed above, may be subtly different than those used in uninucleated cells. Interestingly, recent modeling and experimental work by Pomering et al. (2005) in *Xenopus* egg extracts in which a positive feedback loop in the Cdc2/APC circuit is blocked (producing damped oscillations in CDK activity) led to asynchrony among nuclei in the extracts. In *A. gossypii*, the

core circuit regulating CDK oscillations may be wired in such a way that transitions between division stages are gradual (which happens when positive feedback loops are repressed in the *Xenopus* model) making nuclei divide out of sync. Alternatively, cell cycle stage identity is given by a periodically transcribed gene(s) that may produce proteins that are translated in a common cytoplasm but, unlike the mitotic cyclins, could be directed back to their transcriptional “mother” nucleus. With the help of the LacI-LacO system other proteins than AgClb1/2p should be tested for their ability to freely diffuse in the common cytoplasm. So far, a corresponding strain has been constructed, where the behaviour of the G1 cyclin AgCln1/2p can be investigated, however, it would even be more interesting to follow a direct regulator of Sic1p that ensures temporal regulation of the localization and potentially then activity of the CDK inhibitor.

What are possible mechanisms to limit the presence of such an “identity” factor to a specific stagenucleus? Potentially, mRNAs could be targeted to a domain of the ER adjacent to nuclear pores to facilitate rapid uptake into nuclei after translation or the newly translated proteins could be immediately complexed with nuclear import factors (in Chapter IV more details about specialized cyclin import into the nucleus will be discussed). Conceivably such a protein could actually be translated within the nuclei thereby avoiding post-translational diffusion within the cytoplasm (Iborra et al., 2001). Alternatively, perhaps such a factor is constitutively transcribed but would be selectively blocked in certain cell cycle stages by small regulatory RNA molecules that exist only within the nucleus. The nuclear pore complex itself could be remodeled in a cell cycle dependent manner such that certain proteins are only “allowed” to enter nuclei of a particular cell cycle phase (De Souza et al., 2004; Makhnevych et al., 2003), in Chapter IV this possibility will be closely investigated). Finally, this “factor” could be associated with some cell cycle event -such as DNA replication-and be activated in a nuclear autonomous manner only upon completion of the event in an individual nucleus. Thus, there are many ways to conceive of how the nuclei could maintain independent cell cycle stage identity within the same space.

When combined these experiments demonstrate that the basic eukaryotic cell cycle control network may have evolved in diverse ways to accommodate the unique geometry of a multinucleated cell. Given the evolutionary relationship between budding yeast and *A. gossypii*, it is clear that dramatic differences in cell behavior can be achieved through modulating a very similar

set of proteins. Variability in the cell cycle between these systems arises not simply due to the presence and absence of a particular gene in the genome but rather through differences in regulation and relations between conserved factors. Future work will determine how nuclei retain autonomy and cell cycle stage identity despite sharing a common cytoplasm in *A. gossypii* cells. It is not clear how such a cell cycle is constructed with an oscillator that uses alternative mechanisms to periodic synthesis and degradation of AgCln1/2p but possibilities include post-translational modifications of a central

regulator like AgSic1p such as phosphorylation, methylation, ubiquitination and sumoylation. Fluctuations in such modifications could impact activity, protein-protein interactions, or localization to ensure oscillation in the cell cycle and with that, order in the cycle. Future studies in this system will broaden our understanding of alternative modes of cell cycle control and how large, multinucleated cells can spatially compartmentalize signaling.

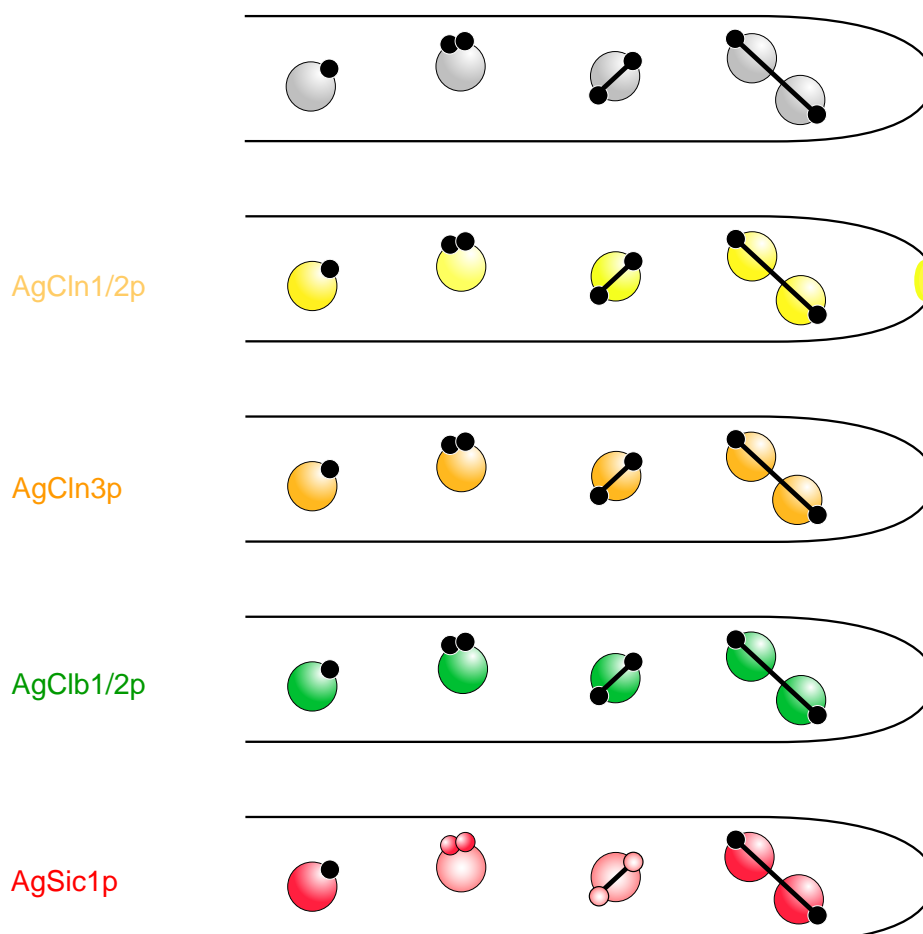


Figure 29

Summary of *A. gossypii* nuclear division cycle

Summary of asynchronous nuclear division and localization of cell cycle regulators.

CHAPTER III

The S-phase cyclin as a major cell cycle regulator in *A. gossypii*

Abstract

Progression through the eukaryotic cell cycle is mediated by the action of different cyclins which bind and activate a cyclin-dependent kinase to control distinct events in each stage of the cell cycle. We wanted to understand how asynchronous mitosis is controlled in the multinucleate fungus *A. gossypii*. Despite sharing a common cytoplasm, each nucleus seems to be independent of its neighbors and has its own cell cycle rhythm. Therefore we wanted to know, whether each nucleus contains different proteins according to its nuclear stage. Both G1 -and the mitotic cyclin AgClb1/2p had been shown to be present and nuclear during the entire division cycle. The essential S-phase cyclin AgClb5/6p was an alternative candidate for nuclear cycle dependent protein oscillation and was therefore chosen to investigate.

AgClb5/6p was localized in the nucleus of G1, S, G2 and metaphase nuclei, however during anaphase, no AgClb5/6p could be detected. Changes in protein abundance due to coordinated nuclear export could have been an explanation for its absence during anaphase. The addition of two exogenous NLSs did not reveal any effect on cell cycle progression and therefore regulation through changes in localization of the S-phase cyclin seems unlikely. However, the addition of two exogenous NESs raised the levels of synchrony in these nuclei, suggesting more diffusion and thereby interaction between nuclei.

The absence of nuclear AgClb5/6p in anaphase is likely based on cyclin degradation. Two potential degradation motifs have been identified in the N-terminus of AgClb5/6p, and one of them has been shown to cause S-phase cyclin degradation during metaphase. Therefore we hypothesize that *A. gossypii* has evolved a mechanism to ensure proper cell cycle progression where only few key cell cycle proteins are oscillating and others are rather regulated by their activity through Cdk-inhibitors such as AgSic1p.

Introduction

It is generally accepted that progression through the eukaryotic cell cycle is mediated by G1, S -and mitotic cyclins which bind and activate a cyclin-dependent kinase (Cdk, (De Bondt et al., 1993; Jeffrey et al., 1995)). These cyclins are thought to confer substrate specificity to the kinase complex by their temporal expression, protein association and subcellular localization (Baldin et al., 1993; Hood et al., 2001; Miller and Cross, 2001; Pines and Hunter, 1991). Thus, expression of different cyclin subgroups at different times followed by their degradation is thought to control distinct events in each stage of the cycle.

Accurate cell division is based on the precise order of cell cycle events. Therefore chromosome segregation has to follow DNA replication and precede cell division. Segregation of unreplicated chromosomes would lead to aneuploidy, repeated DNA replications in the absence of chromosome segregation would cause polyploidy. Both cases may finally result in cell death and therefore the coordination of cell cycle events is strictly controlled by redundant mechanisms.

Sustained polarized growth in addition to alternating DNA replication and chromosome segregation in absence of cell separation (cytokinesis) causes *A. gossypii* to grow with long hyphae, filled with many nuclei in one common cytoplasm. However, despite the continuous cytoplasmic diffusion of cell cycle specific proteins from different cell cycle stages, each nucleus has to independently control timing of DNA replication and mitosis. If a nucleus, which is in the process of going through DNA replication, expresses S-phase specific proteins which are able to enter and influence neighboring nuclei, not in S-phase, then premature DNA replication or rereplication before DNA segregation may be the consequence. To guarantee proper order in the progression through the cell cycle, cell cycle specific proteins from neighboring nuclei need to be inactivated, destroyed or excluded to avoid their influence on the order of cell cycle events.

Initiation of DNA replication in proliferating cells is linked in *S. cerevisiae* to specific thresholds in the nuclei to cytoplasmic ratio (under normal growth conditions). When this threshold is passed,

elevated levels of the S-phase cyclin/Cdk complex initiate replication at various origins, some early, others later during S-phase; however, every sequence in the genome is replicated once and only once during the cell cycle. Therefore, redundant pathways exist, to prevent reinitiation on origins that have already “fired”. ScClb5/Cdk has been shown to inhibit rereplication by phosphorylation of ScCdc6p (thereby targeted for degradation), inhibiting phosphorylation of the origin of replication complex (ORC) and by causing nuclear exclusion of the Mcm proteins (Archambault et al., 2005; Wilmes et al., 2004). Overlapping mechanisms strictly control that DNA replication occurs once and only once in each cycle. To maintain constant ploidy, replication depends on the completion of previous mitosis. Mitotic exit is controlled by mitotic cyclin inactivation by inhibitors or their degradation and only then cytokinesis and cell separation proceed.

We wanted to understand how asynchronous nuclear division is controlled in the multinucleated fungus, *A. gossypii*. How does it control the proper order of nuclear cycle events with respect to each other? Are cell cycle specific protein concentrations oscillating in asynchronously dividing nuclei? The continuous cytoplasmic streaming in a syncytial cell may complicate the establishment of an oscillating protein gradient through degradation alone, because new proteins are always supplied by the cytoplasm. Their exclusion, inhibition or degradation in nuclei of different cell cycle stages to ensure proper oscillation, would potentially require a sophisticated network in addition to high expenses.

In contrast to most eukaryotic cells, G1 and mitotic cyclins were present across all nuclear cycle stages in *A. gossypii*. These cyclins were constantly present in nuclei and changes in abundance have not been detected (Chapter II). The presence and activity of these cyclin proteins in the nucleus may activate the Cdk and trigger cell cycle events at improper time. Therefore, it was hypothesized, that Cdk inhibitors rather than cycles of accumulation and complete destruction of the cyclins provide the primary source of oscillation in the cell cycle machinery of *A. gossypii*. Due to the noncycling nature of the G1 and mitotic cyclins in *A. gossypii* and the previously shown significance of proper timing and unique progression through DNA replication during each division cycle, we decided to investigate the S-phase AgClb5/6p.

Data presented in this chapter, describe the first oscillating protein in *A. gossypii*, the S-phase cyclin AgClb5/6p which changes its

protein abundance in respect to progression through the cell cycle. AgClb5/6p was localized in the nucleus of G1, S, G2 and metaphase nuclei, however during anaphase, no AgClb5/6p could be detected. The disappearance of AgClb5/6p in anaphase is likely due to cyclin degradation. Two potential degradation motifs have been identified in the N-terminus of *AgCLB5/6* and one of them is likely to cause S-phase cyclin degradation during metaphase, as concluded from in frame deletions. Therefore we hypothesize that *A. gossypii* has evolved a mechanism to ensure proper cell cycle progression where only few key cell cycle proteins are oscillating and others are kept inactive by Cdk-inhibitors such as AgSic1p.

Results

The S-phase cyclin AgClb5/6p levels oscillate during the cell cycle

In *S. cerevisiae* cyclin degradation as well as cell cycle control obtained by Cdk inhibitors are involved in maintaining faithful cell cycle progression. Even though *A. gossypii* and *S. cerevisiae* share similar cyclins, CDK inhibitors, activators, transcription factors and the degradation machinery involved in nuclear cycle regulation, (Table 2) there are striking differences in their cell cycle control. It was shown that weakly expressed G1 and mitotic cyclins were present in every nucleus, independent of their division status (Chapter II). Since cell cycle specific degradation of these cyclins could not be detected, it was hypothesized that their activity may be regulated by direct inhibition rather than degradation.

We wanted to find out, whether all proteins that were expected to oscillate behave like AgCln1/2p and AgClb1/2p and display a more or less constant protein level, or whether protein abundance of some proteins is fluctuating, coordinated with the nuclear cycle in the multinucleated fungus *A. gossypii*? Therefore we decided to characterize the so far not localized essential S-phase cyclin, AgClb5/6p in *A. gossypii*. The S-phase cyclin gene, *AgCLB5/6* was epitope tagged like the other cyclin genes previously, at its endogenous locus with 13 copies of the c-myc epitope to evaluate cyclin distribution in the cell. To confirm that epitope addition does not significantly effect function of the tagged protein, the tagged strain was evaluated for growth and nuclear division, because lack of AgClb5/6p causes a growth arrest. *AgCLB5/6-13myc* displayed normal

growth and the cyclin localization was investigated by indirect immunofluorescence. AgClb5/6-13mycp displayed a diffuse, but intense nuclear signal, which was visible in all nuclear cycle stages except anaphase (Figure 30 A and B). The protein started to disappear as early as metaphase, since 29% of all metaphase nuclei did not contain any observable AgClb5/6-13mycp signal. During anaphase nuclei did not show any detectable AgClb5/6p, however the protein returned quickly, since around 94% of all nuclei with 1 SPB had visible AgClb5/6p levels (Figure 30 D, n = 328).

To confirm that this localization was not due to artefacts from fixation and immunofluorescence, we also epitope tagged the endogenous locus with GFP, to evaluate cyclin distribution in living cells. AgClb5/6-GFP could be observed in nuclei (Figure 30 C), however the signal was too weak to be followed over time by in vivo time-lapse microscopy. Therefore, the disappearance of the GFP signal in anaphase nuclei could not be followed.

Thus, even though G1 -and mitotic cyclins did not display detectable changes in protein abundance during the nuclear cycle (Chapter II), the essential S-phase cyclin AgClb5/6p clearly disappeared from the nucleus during metaphase and did not reappear until G1-phase. This localization data shows that at least one cyclin can oscillate during the nuclear division cycle, demonstrating that a multinucleated organism such as *A. gossypii* can control AgClb5/6p abundance in individual nuclei. G1 -and mitotic cyclins may be regulated on the level of activity rather than abundance, however, it seems possible that control of cell cycle progression is also obtained by the regulation of protein levels, as shown for the S-phase cyclin AgClb5/6p.

Comparison of the S-phase cyclin AgClb5/6p with its homologues in *S. cerevisiae*

The sequence comparison of AgClb5/6p with the homologous cyclins ScClb5p and ScClb6p revealed an identity of 44% to ScClb5p and 39% to ScClb6p (Figure 31 B). Most of the domains found in *S. cerevisiae* are conserved in *A. gossypii* (Figure 31 A). The cyclin-box is present in *A. gossypii* (with a length of 254 aa), sharing 51% identity to ScClb5p and 47% to ScClb6p, compared to the N-terminal region which only shares 20% identity for both genes (Figure 31 B, right). This significantly higher degree of identity in the cyclin-box, may display its conserved function in

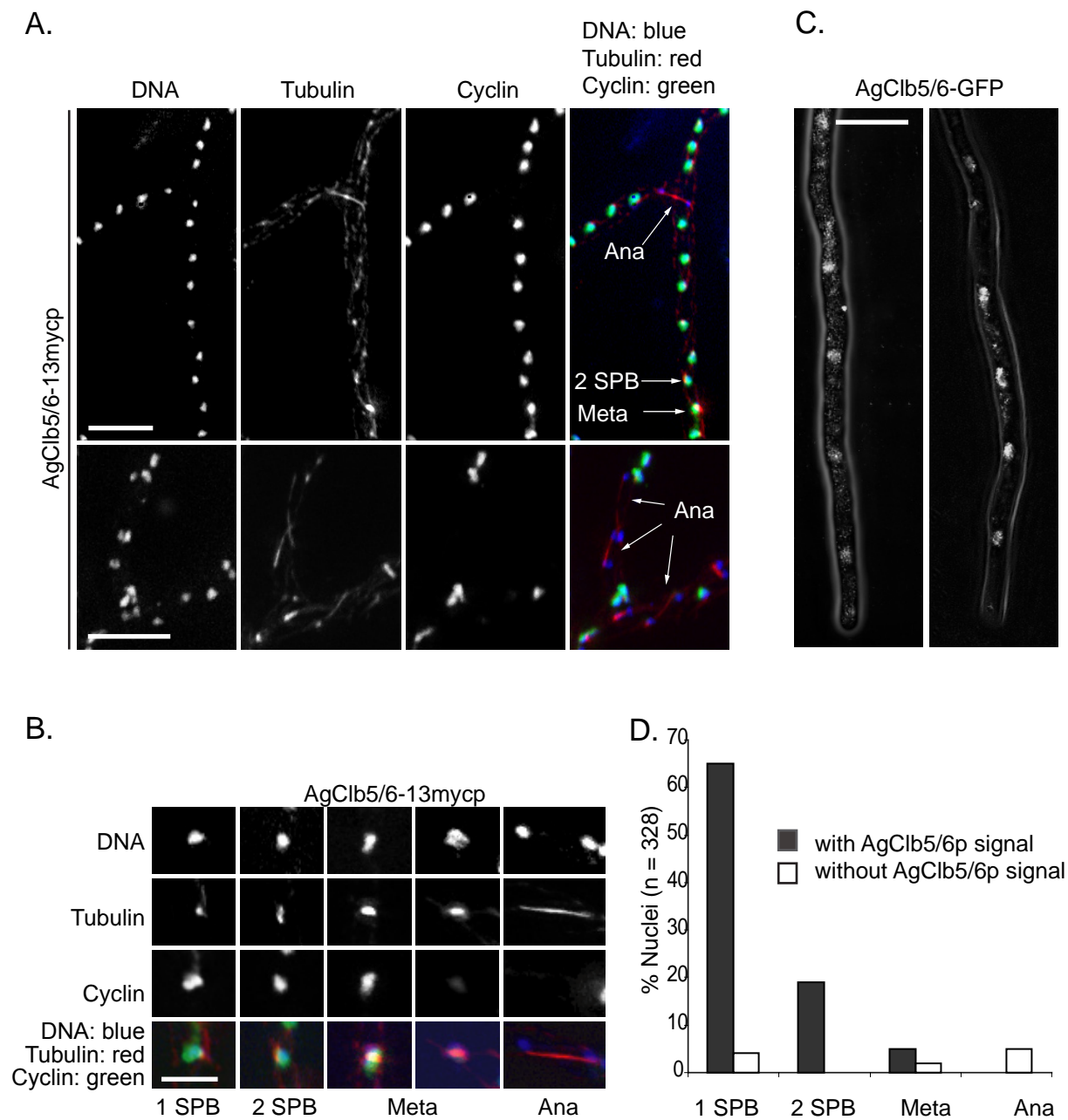
its interaction with the Cdk or potential substrates. Most of the domains found in *S. cerevisiae* Clb5p are also conserved in *A. gossypii* (Figure 31). A potential leucine rich Nuclear Export Signal (NES), the Potential Substrate-Binding Domains (PSBD, (Cross and Jacobson, 2000)) and a D-box (Glotzer et al., 1991) are present in *A. gossypii*. However, the *A. gossypii* homologue revealed in addition a second, more N-terminal D-box (db1) and a bipartite Nuclear Localisation Signal (NLS).

Based on the domains identified in the protein sequence of AgClb5/6p, the disappearance of AgClb5/6p during metaphase could be explained in either of two ways. First AgClb5/6p may be specifically degraded, as it has been shown to be the case for many cyclins in other systems. Or AgClb5/6p might be sequestered to the cytoplasm, to keep it separate from its targets in the nucleus. The second possibility is appealing because the loss and reappearance of the signal in the nucleus could be achieved very fast through its dilution in the cytoplasm. In support of this, the localization of AgClb5/6p suggests that the recovery of AgClb5/6p in the nucleus in G1 is very efficient after its absence in anaphase (Figure 30 D). Based on the protein domains, degradation as well as nuclear export may be possible explanations for the loss of AgClb5/6-13mycp signal.

Forcing AgClb5/6p into the nucleus by the addition of two exogenous NLSs does not have an effect on cell cycle progression

To test if nuclear export is important we forced the AgClb5/6p cyclin protein to enter the nucleus by the addition of two NLSs (Edgington and Futcher, 2001). If nuclear export is needed for efficient mitosis, we would predict that forcing the S-phase cyclin into the nucleus during anaphase may result in an increased amount of nuclei being arrested or delayed in mitosis. Since AgClb5/6p also contains an endogenous NES, a portion of AgClb5/6p may always be present in the cytoplasm and we are only able to change the ratio between nuclear and cytoplasmic protein toward nuclei.

AgClb5/6-NLSa-13mycp grew comparably to the reference strain and did not display any kind of growth impairment. The additional NLSs did not lead to any detectable levels of AgClb5/6-13mycp in anaphase nuclei (Figure 32 A) and as in the AgClb5/6-13mycp strain the signal already disappeared during metaphase (30% without signal). In addition, no significant change in the number of nuclei in each nuclear cycle stage

**Figure 30****The nuclear signal of the S-phase cyclin AgClb5/6p disappears during the nuclear cycle.**

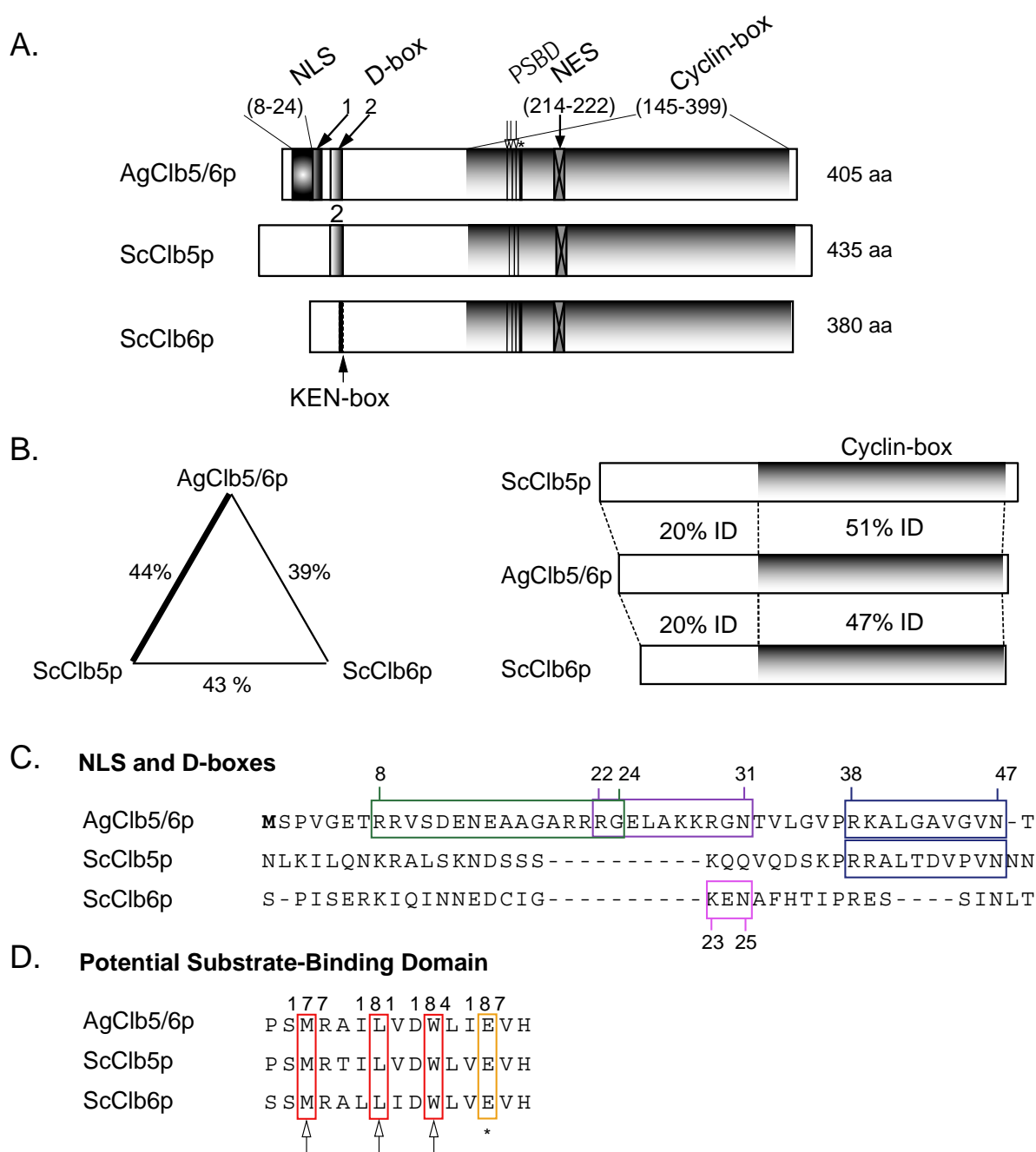
A. Parts of a hypha containing the S-phase cyclin AgClb5/6-13mycp was visualized with tubulin by immunofluorescence. Arrows highlight nuclei of different nuclear stages.

B. AgClb5/6-13mycp was visualized along with tubulin by immunofluorescence. Individual nuclei are shown representing different spindle stages.

C. Nuclear localization of AgClb5/6-GFP expressed from the genome under the control of the endogenous *AgCLB5/6* promoter, in living cells. The signal was too dim to see except with the camera.

D. Percentage of nuclei in each spindle stage with and without AgClb5/6-13mycp, based on tubulin and myc immunostaining. $n > 300$ nuclei scored.

In overlays, tubulin is red, cyclins are green and nuclei are blue, leading to turquoise nuclei containing cyclins. Bars (A and D), 10 μm ; (B) 5 μm .

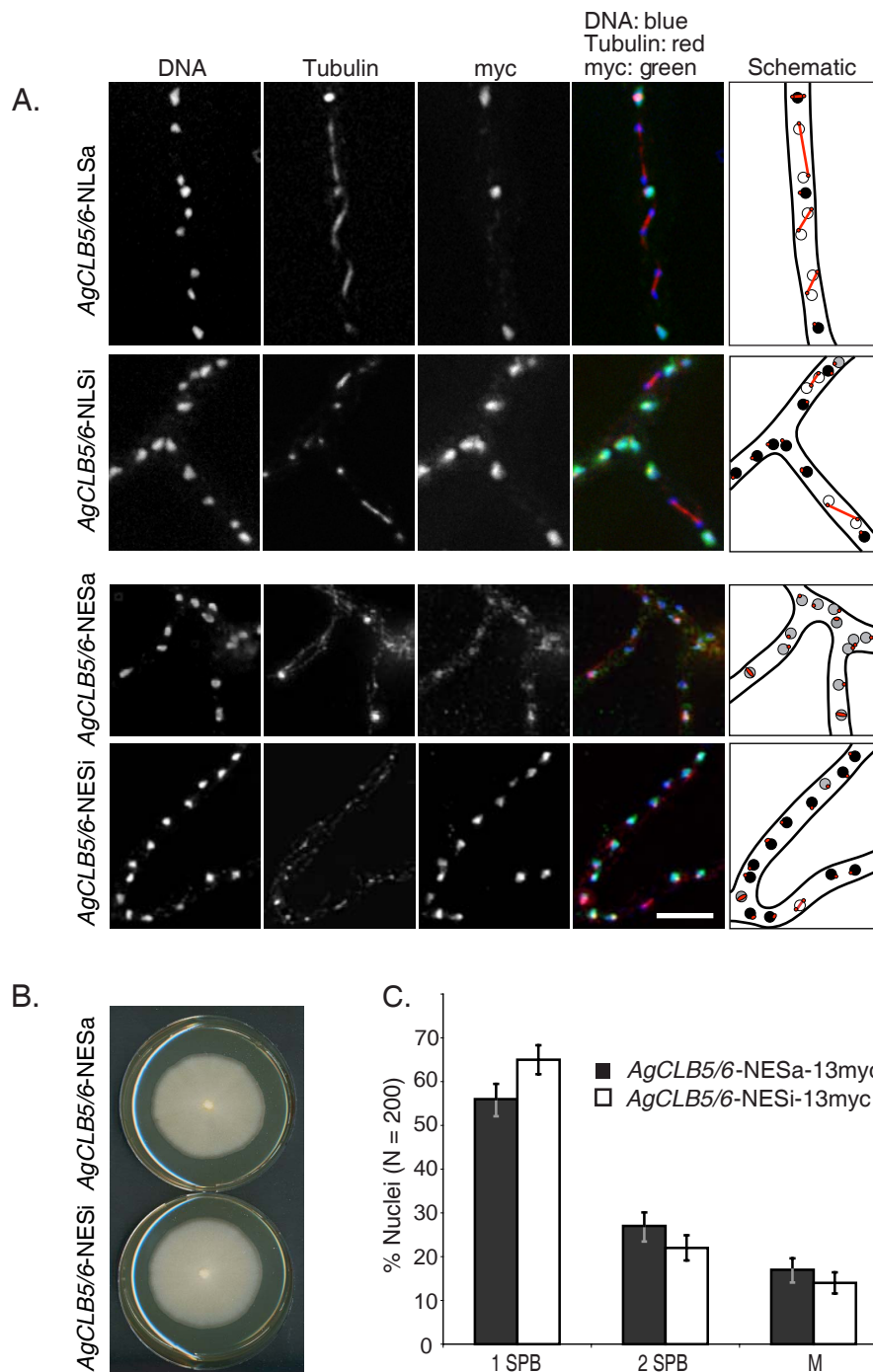
**Figure 31****Comparison of the S-phase cyclin in *A. gossypii* and *S. cerevisiae*.**

A. Domain comparison between AgClb5/6p, ScClb5p and ScClb6p. The D-box (db2 [indicated by 2], Ag aa 38-47), the Cyclin-box (Pfam scan [Ag aa 145-399]), the potential NES ([Ag aa 214-222] Hood et al., 2001) and the Potential Substrate-Binding Domain (PSBD, Cross and Jacobson, 2000) as the Hydrophobic Patch (highlighted by arrows [Ag aa 177, 181, 184]) and the Salt bridge (marked by asterisk [Ag aa 187]) are conserved in *A. gossypii*. AgClb5/6p appears to have an additional putative D-Box sequence at aa 22-31 (db1, [indicated by 1]) and an additional putative bipartite NLS at aa 8-24 (ProSite scan).

B. Amino acid identity between AgClb5/6p, ScClb5p and ScClb6p (left) and their Cyclin-box (right).

C. Sequence comparison of the NLS and D-boxes of AgClb5/6p, ScClb5p and ScClb6p. The putative bipartite NLS in green, the putative D-box1 in lila, D-box2 in blue, and the KEN-box in pink.

D. Sequence comparison of the Potential Substrate-Binding Domain (Cross and Jacobson, 2000). Arrows show the conserved Hydrophobic patch, asterisk the conserved salt-bridge.

**Figure 32****Displacement of AgClb5/6p from the nucleus disturbs nuclear cycle progression .**

A. *AgCLB5/6-NLSa*-13myc (active NLS), *AgCLB5/6-NLSi*-13myc (inactive NLS control), *AgCLB5/6-NESa*-13myc (active NES) and *AgCLB5/6-NESi*-13myc (inactive NES control) were grown for 14-16 hours in liquid, selective medium and then processed for anti-tubulin and anti-myc immunofluorescence. False coloring: DNA is blue, tubulin is red, and cyclins are green, therefore nuclei containing cyclins appear turquoise. Bars, 10 μ m.

B. Radial growth assay. A small patch of mycelium from *AgCLB5/6-NESa*-13myc or *AgCLB5/6-NESi*-13myc was transferred to the center of plates containing complete medium (+ G418). The diameter of the radially expanded colonies were determined after seven days of growth at 30°C.

C. Percentage of nuclei in different spindle stages based on tubulin staining. 200 nuclei were scored for each strain.

could be detected (data not shown). Levels of synchrony, scored by comparing the spindle stage of neighboring nuclei, did not significantly alter (*AgCLB5/6-NLSa*-13myc: 56% compared to *AgCLB5/6-NLSi*-13myc: 55%). The fusion of two additional C-terminal NLSs to the S-phase cyclin *AgClb5/6p* did not result in observable protein levels during anaphase, suggesting that *A. gossypii* has evolved a very efficient way to ensure its absence in these nuclei (most probably by degradation).

To test, whether the displacement of S-phase cyclin into the cytoplasm, may increase its concentration in the cytoplasm and therefore result in an increase of synchrony, two exogenous NESs were fused to *AgCLB5/6*. The additional NESs led to an increase in the cytoplasmic levels of *AgClb5/6-13myc*, shown by immunofluorescence. Sufficient protein may have been left in the nucleus to allow normal nuclear division, however, spore formation was severely impaired by this partial shift of *AgClb5/6p* out of the nucleus (Figure 32 A and B). The shift of subcellular cyclin protein distribution was tolerated for normal vegetative cell growth, but sporulation seemed to be more sensitive to these alterations and therefore abolished. The comparison of nuclei in different spindle stages did show a slightly higher proportion with duplicated SPBs or mitotic spindles, compared to the inactive NES fusion, suggesting a faster nuclear cycle progression into S, G2 and M-phase (Figure 32 C). Interestingly, increased levels of synchrony were observed (*AgCLB5/6-NESa*-13myc: 63% compared to *AgCLB5/6-NESi*-13myc: 54%), suggesting that nuclear sequestration of *AgClb5/6p* may be important for asynchrony. This higher amount of synchrony may have resulted from an increased diffusion due to the elevated levels of *AgClb5/6p* in the cytoplasm.

The functionality of the forced localization cassettes in the case of NES addition was directly observed by microscopy in that signal intensities were clearly altered. However, since no changes in *AgClb5/6-NLSa*-13myc localization could be detected by immunofluorescence, functionality of NLS cassettes has only been indirectly approved by complementation experiments shown in Figure 25 C in Chapter II. To directly test NES and NLS effect on protein localization, a C-terminal GFP fusion should be constructed. Unfortunately, attempts into this direction have failed so far due to point mutations in the oligonucleotides.

A nondegradable form of *AgClb5/6p* causes severe growth defects in *A. gossypii*

As already pointed out, the essential S-phase cyclin *AgClb5/6p* disappears during metaphase and reappears early in G1. We wanted to know whether the S-phase cyclin *AgClb5/6p* is degraded in *A. gossypii* or whether the loss of signal during anaphase is due to nuclear export. Degradation of S-phase cyclins would have to be very tightly organized, taking place only in meta- and anaphase nuclei.

The *AgClb5/6p* homologue does contain N-terminal D-box sequences, which are conserved from the sea urchin *Arbacia punctulata*, to frog, starfish up to human cyclin B and have been shown to lead to anaphase-promoting complex (APC) mediated degradation by the proteasome (Glotzer et al., 1991). Two destruction box elements were found in *A. gossypii*, one at a site homologous to the D-box in *S. cerevisiae* (*db2*), and a second one which lays more N-terminal from *db2* (*db1*, Figure 31 C). To test if degradation is essential for normal cell cycle progression, plasmids were constructed which contained *AgCLB5/6-13myc* with $\Delta db1$, $\Delta db2$, $\Delta db1\Delta db2$ or $\Delta (db1-db2)$.

Since D-box deletion from endogenous *ScCLB5* in *S. cerevisiae* had little cell cycle phenotype (Wasch and Cross, 2002), we decided to construct these D-box plasmids, by overlap PCR approach in combination with co-transformation in yeast (details in Materials and Methods and Figure 45 and 46). However, despite numerous attempts, we were never able to obtain correct $\Delta db1$, $\Delta db2$, $\Delta db1\Delta db2$ or $\Delta (db1-db2)$ plasmids. Based on these findings we decided to construct the various D-box mutants under the inducible *GAL1* promoter, to mask a potential dominant negative effect. Transformed yeast cells were normally grown on YP-Glucose and repicked on YP-Galactose. Interestingly growth on Galactose (*GAL1* promoter on) was completely abolished with $P_{GAL1}AgCLB5/6-13myc$ as well as with the various D-box mutants (Figure 33). This is in contrast to integrated overexpressed $P_{GAL1}ScCLB5$ in *S. cerevisiae*, which has been shown to be not lethal (Jacobson et al., 2000). On the other hand, $P_{GAL1}Scclb5\Delta db$ was lethal (Wasch and Cross, 2002), suggesting that there may be a defined threshold of *ScClb5p*, which if exceeded, causes incomplete degradation or incomplete inactivation of *ScClb5p*.

After the exchange of the *GAL1* promoter with the endogenous *A. gossypii AgCLB5/6* promoter, these D-box plasmids were transformed again into *S. cerevisiae* cells (600 ng). As described

before, we were not able to obtain $\Delta db1$, $\Delta db2$ or $\Delta db1\Delta db2$ transformants (Figure 34 A, bottom). This may suggest that AgClb5/6p degradation is either not efficient in yeast, that it may be an overall more stable protein or that its basic levels are elevated in comparison to ScClb5p.

A. gossypii reference strain ($\Delta/\Delta t$) was transformed with the D-box plasmids, where *AgCLB5/6* was under its endogenous promoter. Interestingly, we were able to see a minor dominant phenotype of the strains containing a deletion of the D-box1 ($\Delta db1$) and a major dominant phenotype in the strains with the deletion of the D-box2 or both D-boxes ($\Delta db2$, $\Delta db1\Delta db2$, and $\Delta (db1-db2)$). Two days after *A. gossypii* transformation with 6 μ g plasmid, the plates containing *pAgCLB5/6-13myc* or *pAgCLB5/6 $\Delta db1$ -13myc* were covered with primary transformants (5-10 mm in size), whereas the plates containing *pAgCLB5/6 $\Delta db2$ -13myc*, or *pAgCLB5/6 $\Delta db1\Delta db2$ -13myc* had transformants growing, which were hardly visible (Figure 33 A, top). The deletion of D-box2 (homologous to the D-box found in yeast *ScCLB5*) and of both D-boxes revealed a very severe growth defect by growth speed reduction of around 70% (Figure 34 B).

To test, whether AgClb5/6p is not degraded and therefore is stabilized during anaphase in the D-box mutants, immunofluorescence staining was performed. In *AgCLB5/6 $\Delta db1$ -13myc*, the myc signal was detected in all stages of the nuclear cycle except in meta- and anaphase nuclei (Figure 35 B). There the signal was in most cases completely abolished and only in very few

anaphase nuclei low AgClb5/6-13mycp could be observed. However, signal intensity was reduced by at least 64% compared to the signals detected of neighboring nuclei. This suggests that the D-box1 only plays a minor role if at all for the degradation of AgClb5/6p. In contrast 13mycp was visualized in anaphase nuclei, in strains lacking D-box2 and/or both D-boxes (Figure 35 C and 36), suggesting impairment of cyclin degradation. The degradation of the S-phase cyclin AgClb5/6p is caused primarily by the D-box2, which is at a homologous position to the D-box found in *S. cerevisiae*.

Strains which displayed stabilized AgClb5/6p, displayed the previously described slow growth phenotype with low density of hyphal network. In addition to normal apical tip splitting, these cells also made lateral branches after 24 h of growth (Figure 37 A). This is in contrast to wild-type cells, which exclusively grow by tip splitting. Since not all nuclei in these cells contain a plasmid, it could be that AgClb5/6p protein concentration varies in these cells, allowing growth in some regions, where protein is less abundant, but not in others. This hypothesis has been supported by nuclei localization in which regions of nearly normal nuclear distribution alternate with other regions containing mainly fragmented nuclei (Figure 37 B). This data suggests that cell cycle dependent AgClb5/6p disappearance in anaphase nuclei was due to degradation, mediated by the D-box2 domain.

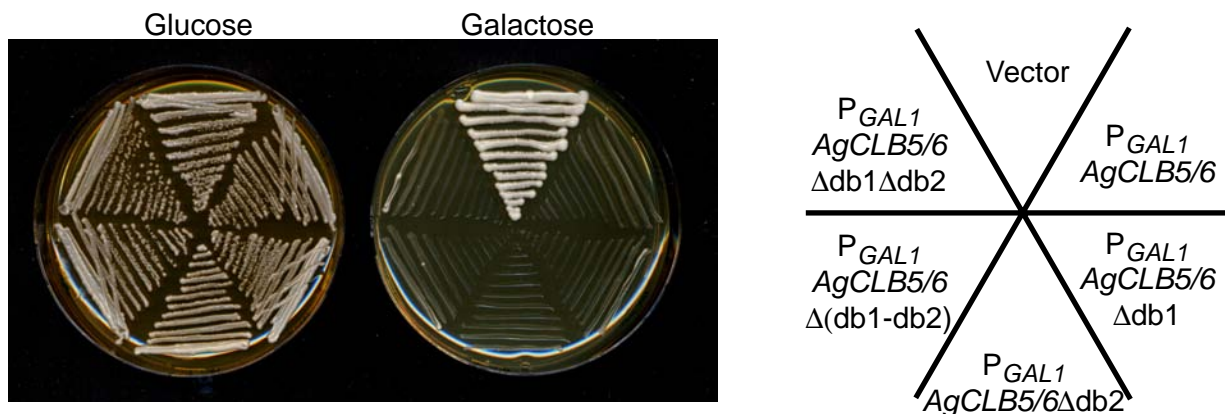
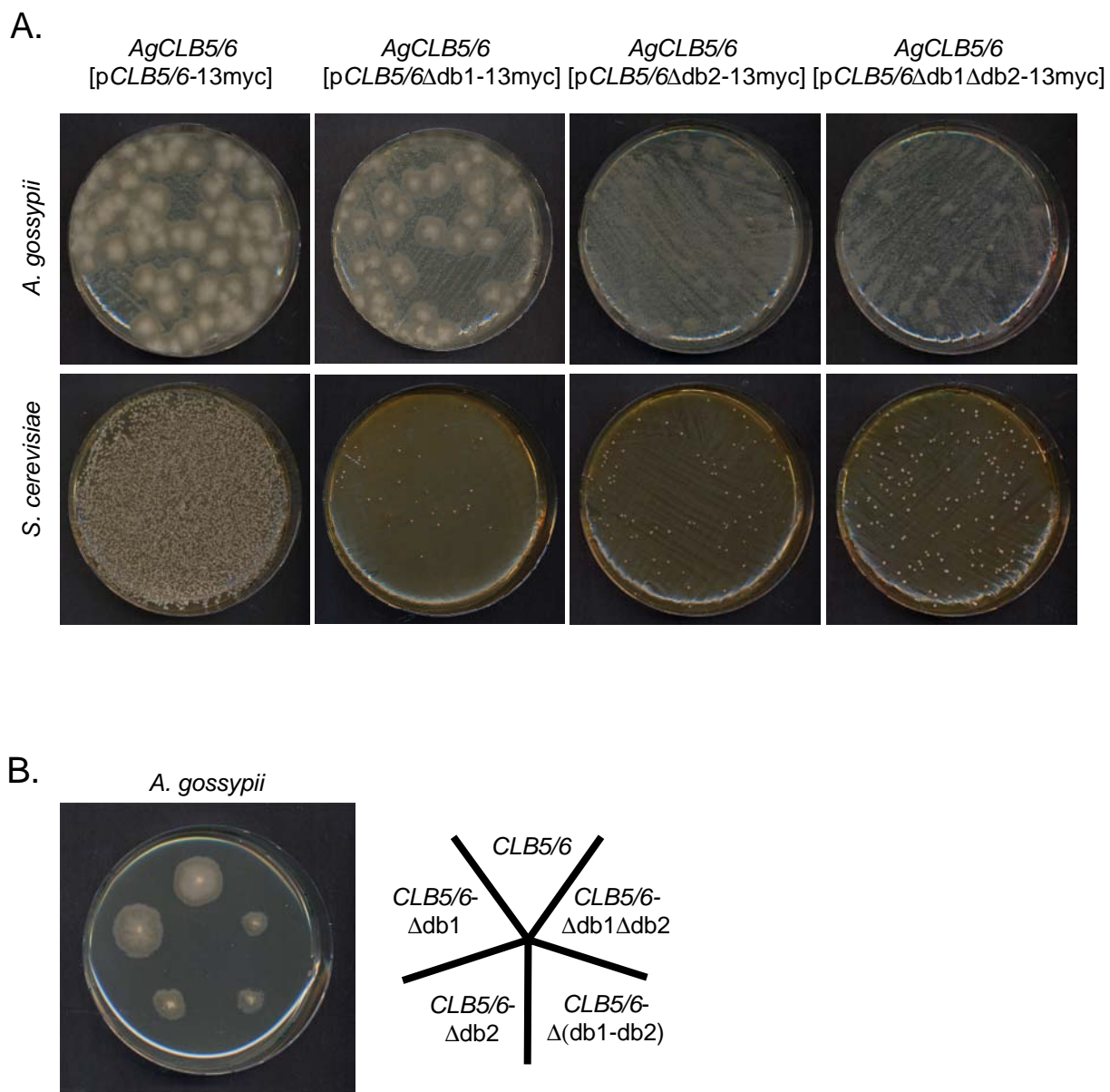


Figure 33
Overexpression of the *AgCLB5/6-13myc* or the D-box constructs by the *GAL1* promoter caused lethality in *S. cerevisiae*.

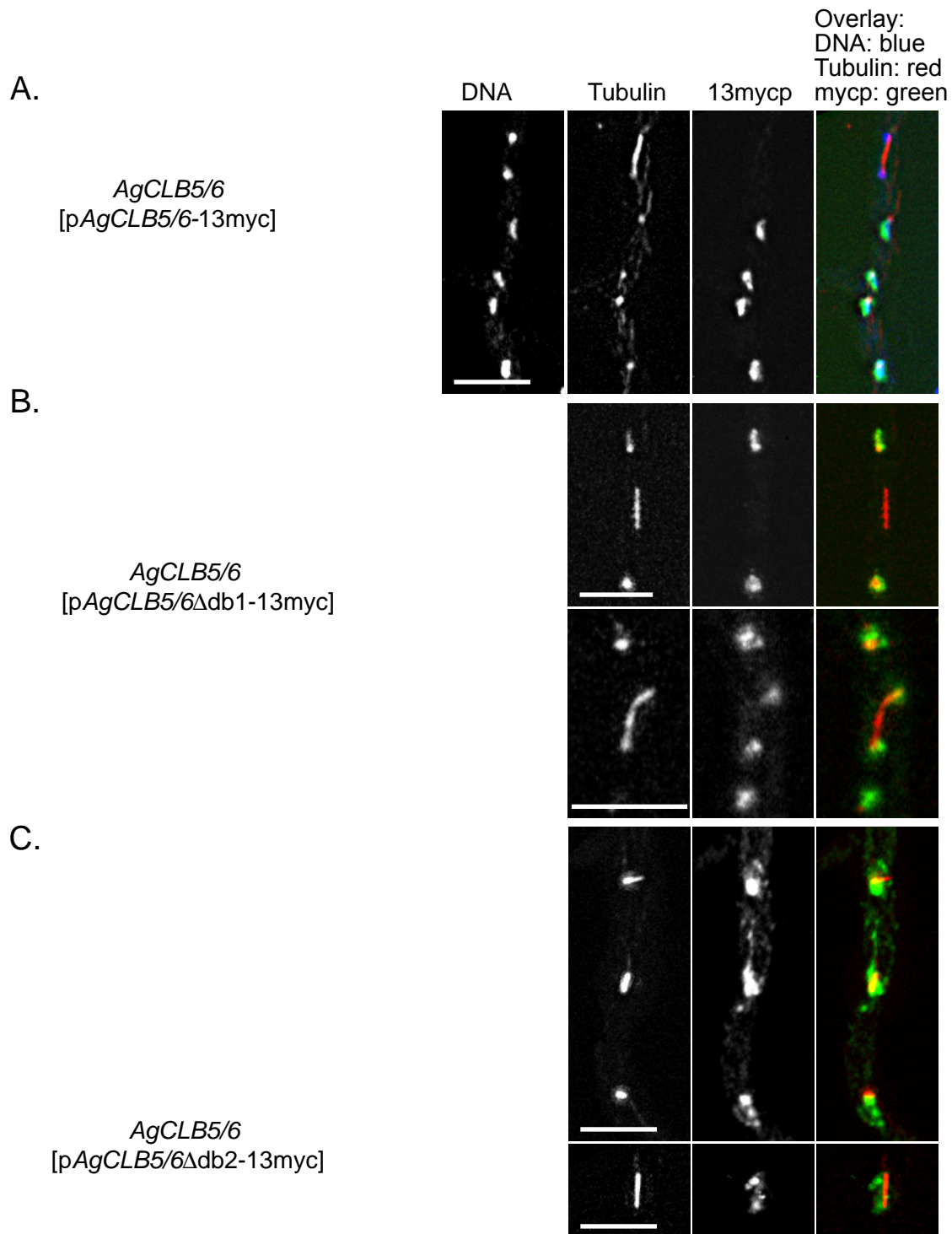
S. cerevisiae cells were transformed with 600 ng of either $P_{GAL1}AgCLB5/6-13mycp$, $P_{GAL1}AgCLB5/6\Delta db1-13mycp$, $P_{GAL1}AgCLB5/6\Delta db2-13mycp$, $P_{GAL1}AgCLB5/6\Delta db1\Delta db2-13mycp$, $P_{GAL1}AgCLB5/6\Delta (db1-db2)-13mycp$ or the vector (as a positive control). Cells were grown on YP-Glucose plates under Geneticin selection and then regrown on YP-Galactose plates containing Geneticin, where the *GAL1* promoter was on.

**Figure 34****Influence on cell growth of S-phase cyclin mutants lacking D-box sequences.**

A. Top. Young *A. gossypii* mycelia were transformed with 6 mg plasmids containing either *AgCLB5/6-13myc*, *AgCLB5/6Δdb1-13myc*, *AgCLB5/6Δdb2-13myc* or *AgCLB5/6Δdb1Δdb2-13myc* and growth under selection was evaluated after 2 days on plates.

Bottom. *S. cerevisiae* was transformed with 6 ng plasmids (same as mentioned above) and growth under selection was evaluated after 2 days on plates.

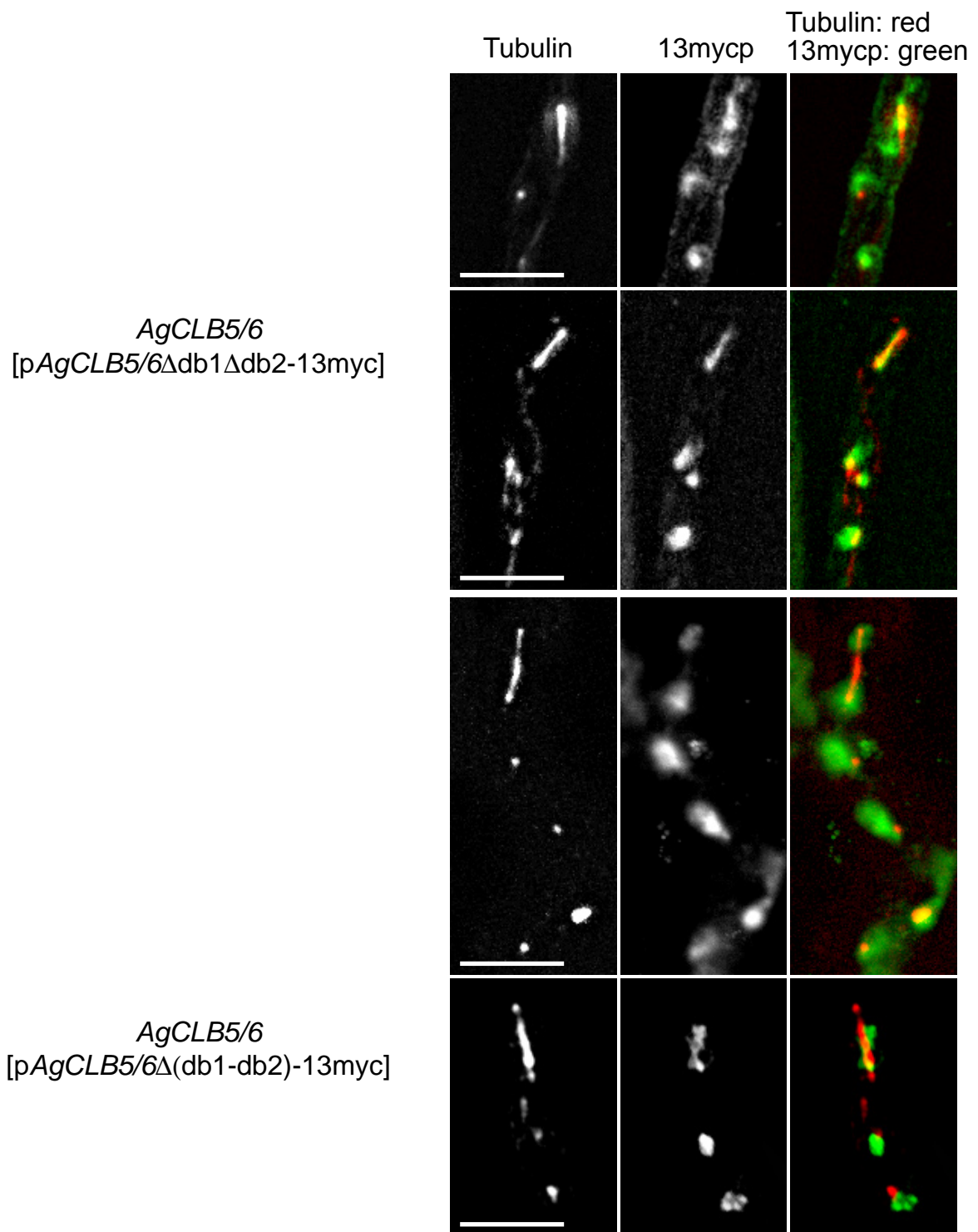
B. A piece of mycelium from cells containing *AgCLB5/6* [p*AgCLB5/6-13myc*], *AgCLB5/6* [p*AgCLB5/6Δdb1-13myc*], *AgCLB5/6* [p*AgCLB5/6Δdb2-13myc*], *AgCLB5/6* [p*AgCLB5/6Δ(db1-db2)-13myc*] and *AgCLB5/6* [p*AgCLB5/6Δdb1Δdb2-13myc*] was inoculated on plates containing G418 and radial growth was evaluated after 3 days at 30°C.

**Figure 35****The second D-box of *AgCLB5/6* is responsible for its degradation during anaphase.**

A. *AgCLB5/6* [p*AgCLB5/6*-13myc] spores were incubated in liquid AFM + G418 for 16 h at 30°C before immunofluorescence treatment. Clear loss of nuclear signal during anaphase can be observed.

B. *AgCLB5/6* [p*AgCLB5/6*Δ*db1*-13myc] mycelium was grown on AFM + G418 plates for 4 days, scraped off and grown in liquid AFM + G418 for 16 h at 30°C, prior to immunofluorescence staining. Complete loss of nuclear signal during anaphase in the majority of hyphae.

C. *AgCLB5/6* [p*AgCLB5/6*Δ*db2*-13myc] was grown as described for B. Presence of *AgClb5/6p* signal in all cell cycle stages. In overlays, tubulin is shown in red, myc in green and DNA in blue. Bars, 10 μm.

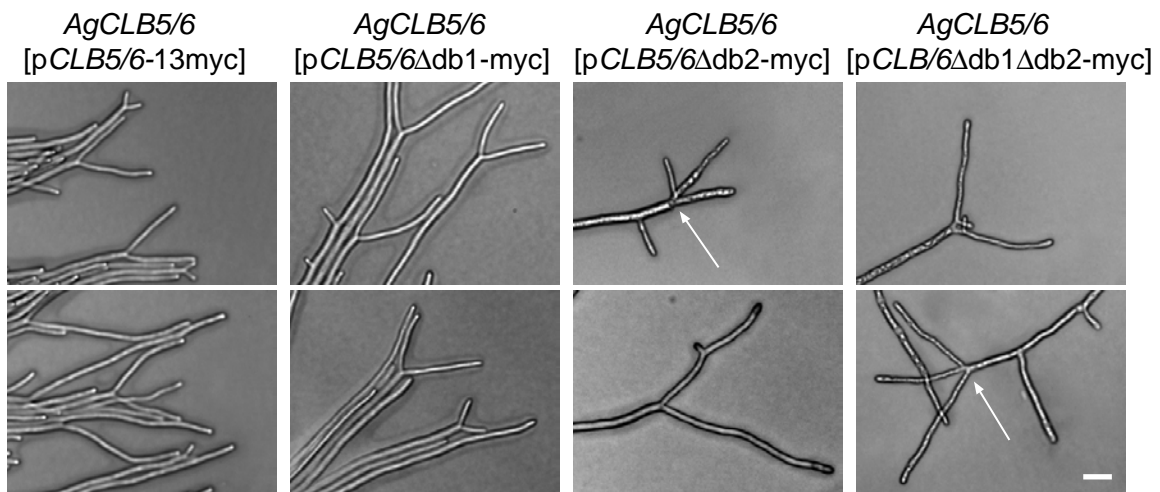
**Figure 36**

***A. gossypii* strains lacking both D-boxes in *AgCLB5/6* showed a clear signal of *AgCLB5/6*-13mycp during anaphase.**

AgCLB5/6 [p*AgCLB5/6*Δ*db1*Δ*db2*-13myc] and *AgCLB5/6* [p*AgCLB5/6*Δ(*db1*-*db2*)-13myc] were grown on plates for 4 days under selection, scraped off and grown in liquid AFM + Geneticin for 16 hours, prior to immunofluorescence staining. In overlays, tubulin is shown in red, myc in green.

Bars, 10 μm.

A.



B.

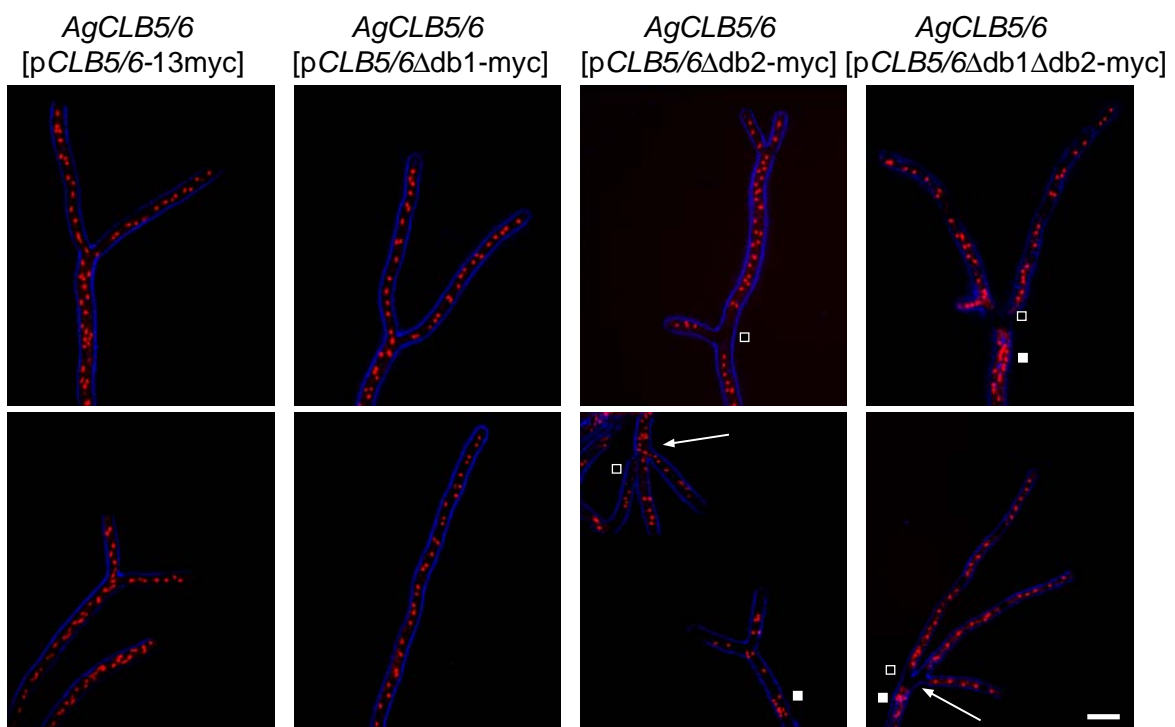


Figure 37
Phenotypic analysis of the D-box mutants

Mycelium of the *AgCLB5/6* D-box deletion strains was grown under selection for two days.

A. Brightfield pictures show major growth defects in *db2Δ* and *db1Δdb2Δ* strains. In these strains, tip splitting often was accompanied with lateral branching or triple tip splitting.

B. Nuclei staining of the D-box deletion strains done with Hoechst. Arrows indicate triple tip splitting, white squares show sites with clustered nuclei and open squares show regions without nuclei. Brightfield in blue, nuclei in red. Bars (A), 20 μ m; (B), 10 μ m.

Discussion

Data presented in this Chapter tried to answer the question, whether asynchronously dividing nuclei are containing different proteins according to their nuclear stage. Experiments presented in Chapter II showed, that the mitotic cyclin AgClb1/2p as well as the G1 cyclins AgCln1/2p and AgCln3p were present during the entire nuclear cycle, indicating no major oscillation of protein abundance during the cell cycle. The continuous cytoplasmic streaming of a syncytial cell complicates the establishment of an oscillating protein gradient since new proteins are always supplied by the cytoplasm. Therefore we hypothesized that *A. gossypii* has favoured mechanisms to control protein activity rather than control of protein abundance by degradation.

However, is accurate cell cycle progression possible in the absence of oscillation in protein concentrations? If cyclin inhibitors have overtaken control of cyclin activity instead of cyclin abundance by degradation, then at least these proteins would have to be cyclically active. Ways to bypass the huge protein pool of the cytoplasm filled with proteins specific for each cell cycle stage include nuclear translation (Iborra et al., 2001) and protein inhibition by regulatory RNA molecules. In these cases, transcription could occur at a specific cell cycle stage, and due to constant nuclear localization, these molecules could avoid diffusion in the common cytoplasm, thereby guaranteeing cell cycle specificity.

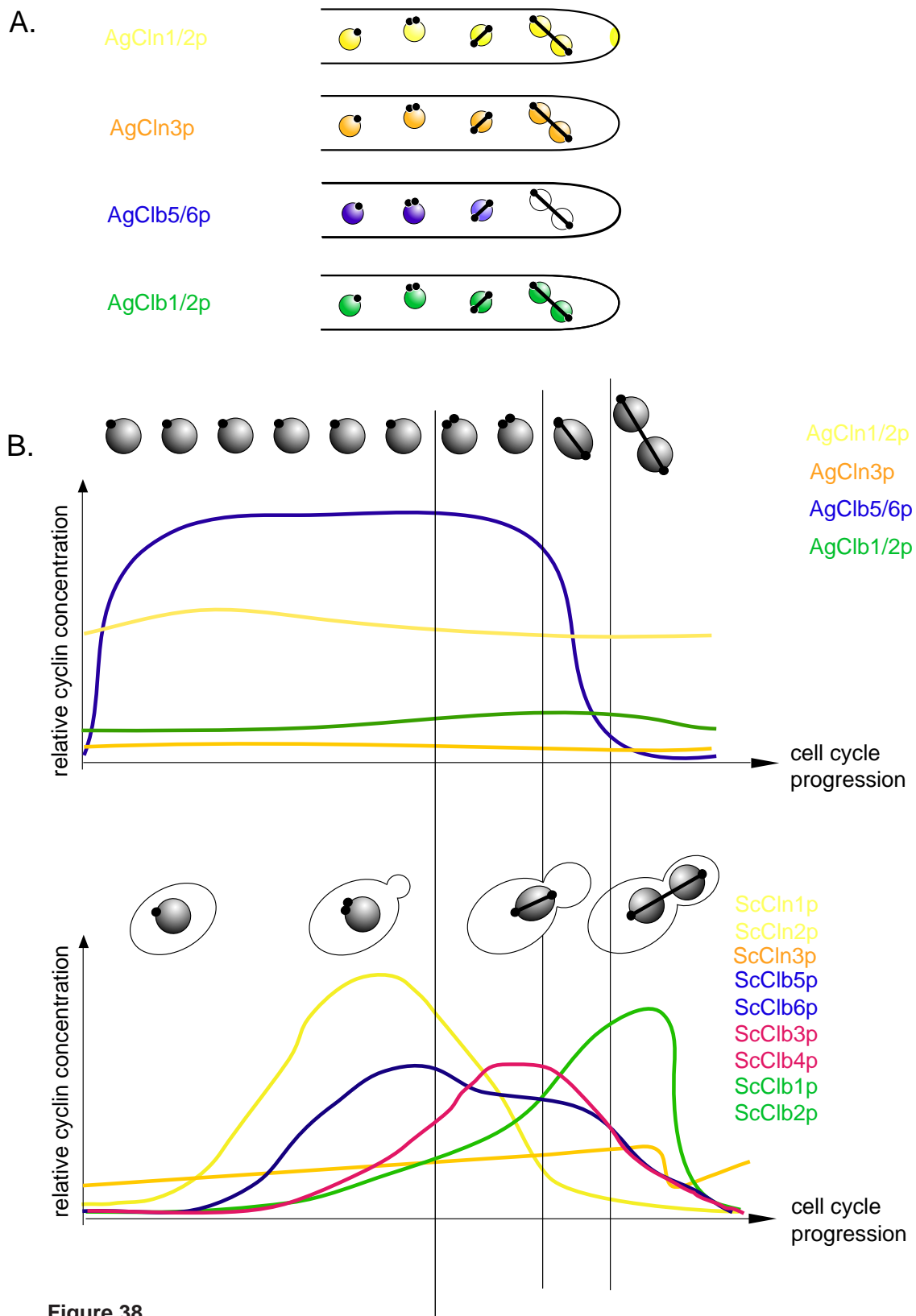
In *S. cerevisiae* around 800 genes have been found to be expressed in a cell cycle specific manner (Spellman et al., 1998). It does not seem likely that a close relative like *A. gossypii* has created completely new ways to control activity instead of abundance of all these proteins. Since G1 and mitotic cyclins did not reveal any oscillation in protein levels during the cell cycle, we decided to investigate also the S-phase cyclin AgClb5/6p. AgClb5/6p was shown to be a major oscillator during the nuclear division cycle. We were able to show by immunofluorescence that the 13myc-tagged version of the S-phase cyclin is nuclear during all cell cycle stages but during anaphase. AgClb5/6p disappears during progression through metaphase and reappears early during G1 phase. In contrast to the two other essential cyclins, AgCln1/2p and AgClb1/2p, the S-phase cyclin AgClb5/6p clearly shows changes in protein abundance in the nucleus, where its potential substrates are localized (Figure 38 A). Changes in protein abundance due to coordinated nuclear export could have been an

explanation for the disappearance of AgClb5/6p in anaphase. However, the addition of two exogenous NLSs did not reveal any effects on cell cycle progression and therefore it seems unlikely that localization changes of the S-phase cyclin control cell cycle progression. However, the addition of two exogenous NESs raised the levels of synchrony in these nuclei, suggesting more diffusion and thereby interaction between nuclei.

In *S. cerevisiae* the transition from G1 to S phase is triggered by the S-phase cyclins ScClb5p and ScClb6p. Although *ScCLB5* and *ScCLB6* are transcribed in G1, complexes of these S-phase cyclins and Cdc28p remain inactive until the G1/S border. During that time, the B-type cyclin inhibitor ScSic1p, is degraded by the action of the ubiquitin ligase complex, SCF^{Cdc4} (Skp1/Cullin/F-box, (Schneider et al., 1996; Schwob et al., 1994; Verma et al., 1997)). ScClb5p and ScClb6p appear to play partially redundant roles, since either of them can promote timely entry into S-phase (Basco et al., 1995; Epstein and Cross, 1992; Schwob and Nasmyth, 1993). However, only ScClb5p but not ScClb6p is required for timely progression through S-phase. ScClb5p has been shown to persist throughout S-phase and is marked for destruction (via its D-box) in mitosis by the action of the ubiquitin ligase complex APC^{Cdc20} (Irniger and Nasmyth, 1997; Jacobson et al., 2000). ScClb6p is targeted for destruction at the G1/S border by the activity of a functionally distinct ubiquitin ligase complex SCF^{Cdc4} (Jackson et al., 2006). Despite their redundancy in timely initiation of S-phase, clear differences in their regulation in turnover have been observed. Possibly these differences may account for the distinct ability of ScClb5p and ScClb6p to promote timely progression through S-phase.

A. gossypii in contrast to yeast only has one S-phase cyclin homologue, *AgCLB5/6*. AgClb5/6p is nuclear during all stages of the cell cycle but anaphase. During metaphase AgClb5/6p disappears and only early in G1 the signal reappears. Two different D-box elements have been found in *A. gossypii*, a very N-terminal one, and a second one, which is homologous to the D-box found in ScClb5p. The deletion of the primary D-box in *A. gossypii* resulted in a minor growth defect with slightly reduced density in the hyphal network. Due to the absence of AgClb5/6p in anaphase nuclei, we conclude, that this D-box only has a minor role in the degradation of AgClb5/6p.

The deletion of the D-box homologous to the one in ScClb5p caused a major growth defect in that growth was reduced by 70%, in addition

**Figure 38****Summary of the asynchronous nuclear division cycle in *A. gossypii***A. Localization of cyclins during the nuclear division cycle in *A. gossypii*B. Top: Relative cyclin protein concentrations during the nuclear division cycle in *A. gossypii*Bottom: Relative cyclin protein concentrations during the cell cycle in *S. cerevisiae*(relative cyclin concentration in *S. cerevisiae* adapted from Nasmyth et al., 1996 and Cross et al., 2002)

to a low density in hyphal network. In the D-box2 deletion mutant, AgClb5/6p was clearly identified in anaphase nuclei, suggesting that its destruction at the end of mitosis is greatly abolished.

The degradation of the AgClb5/6p seems to be more similar to ScClb5p homologue, than to ScClb6p, in that degradation occurs prior to mitosis. If there is AgClb5/6p destruction by SCF^{Cdc4} at G1/S border, it may only account for a very small fraction of the total protein concentration, since no decrease in AgClb5/6p levels have been detected in nuclei with duplicated SPBs. Even though three putative (S/T-P) phosphorylation sites are present in the N-terminus of *A. gossypii* (Appendix 1, Sequence Alignment), these phosphorylation sites are not embedded in consensus SCF^{Cdc4} degron sequences (Jackson et al., 2006), suggesting that the degradation at the G1/S border is not very likely.

The major growth defect in the *A. gossypii* D-box deletion is in contrast to the D-box deletion in *S. cerevisiae* from endogenous *ScCLB5*, which had little cell cycle phenotype, although its abundance was significantly deregulated (Wasch and Cross, 2002). D-box dependent degradation of ScClb5p was not required for exit from mitosis and viability. In contrast to ScClb5p, where only strong overexpression with the *GAL1* promoter in combination with the D-box deletion caused lethality (Jacobson et al., 2000), P_{GAL1}AgCLB5/6-13mycp transformed into yeast was sufficient to cause the same lethal phenotype when grown on Galactose. This may suggest that the degradation of AgClb5/6p is either not efficient in yeast, that it may be an overall more stable protein or that its basic levels are elevated in comparison to ScClb5p. Comparisons of protein levels by signal comparison by microscopy and Western of asynchronously growing cells, clearly showed that the S-phase cyclin is much more abundant than the constantly present the G1 and the mitotic cyclins in *A. gossypii*. Therefore its high abundance may be the reason, why P_{GAL1}AgClb5/6-13mycp causes lethality in contrast to P_{GAL1}ScClb5-HA.

The presence of high levels of AgClb5/6p compared to the other cyclins is very interesting (Figure 38 B), since from yeast, it had been shown that in log-phase of diploid cultures, ScCln1p, ScCln2p, ScClb2p and ScClb3p clearly showed higher levels than ScClb5p and ScClb6p (ScClb6p is the cyclin with the lowest number of copies per diploid cell (Cross et al., 2002). This tendency, which we are able to observe, should be investigated in more detail (by Western and/or RT-PCR), to be able to precisely state how strong this effect may be. However, independent of the exact levels of the

different cyclins, we clearly demonstrated that even though most of the cyclins in *A. gossypii* are present during the entire nuclear cycle the protein levels of the S-phase cyclin AgClb5/6p are oscillating.

Degradation of AgClb5/6p is crucial for normal growth, since deletion of the D-box2 resulted in very severe morphology problems. Whereas growth in mature hyphae of the reference strain occurs exclusively by apical tip splitting, the *AgCLB5/6Δdb2* mutant strain had obvious difficulties with this task. In addition to apical tip splitting, triple tip splitting and lateral branches were observed, suggesting major growth problems. This effect may be traced back to the dominant negative effect of the plasmids, where sites with more normal growth, indicative of low plasmid concentration and sites with severe morphology problems, indicative of high plasmid concentration alternate. When we looked at the nuclei distribution this effect became even more obvious, since regions with normal nuclei distribution alternated with regions where nuclei were disintegrated. It may be hypothesized, that these morphological problems arose due to premature S-phase initiation, before mitosis was completed, thereby resulting in partial polyploidy. Potentially, the presence of AgClb5/6p in anaphase may also result in the interaction with new substrates or with “known” substrates, but new timing, thereby causing this phenotype.

During the past years several substrates of ScClb5p have been identified in budding yeast. Many of these substrates include proteins involved in DNA replication, including ScOrc6p, a subunit of the origin of replication complex (ORC) and ScCdc6p (involved in the formation of the pre-replicative complex, (Archambault et al., 2005; Wilmes et al., 2004)). Due to the high conservation of the process of replication, we might expect that these interactions are conserved in *A. gossypii*. The interaction of ScClb5p with ScOrc6p has been shown to be dependent on the hydrophobic patch of ScClb5p and an “RXL” motif in ScOrc6p (Wilmes et al., 2004). Sequence comparison of the homologous proteins in *A. gossypii* clearly demonstrated, that these sites are also conserved in AgClb5/6p and AgOrc6p (Appendix 1, sequence alignment), suggesting the preservation of AgOrc6p as a substrate of AgClb5/6p. Based on the role of ScClb5p, interaction with these proteins may be expected, however also substrates as the microtubule-associated protein ScFin1p and ScFar1p (a G1 cyclin-Cdc28 inhibitor) have been identified (Archambault et al., 2005).

The early reappearance of AgClb5/6p in G1-phase raises the question, whether AcClb5/6p

is active at that time. Previous localization studies (Chapter II), had shown, that one of the potential inhibitors of AgClb5/6p, AgSic1p is present and nuclear during G1 phase. Therefore it seems likely that as in yeast, AgClb5/6p is inhibited, until high protein levels in combination with other factors, allow it to proceed into S-phase. During progression through the nuclear cycle, AgSic1p signal disappears slowly from its nuclear localization in G1 phase until complete loss of signal during metaphase. These changes in AgSic1p levels may correlate with a contrariwise activity of the S-phase cyclins in *A. gossypii*. In *S. cerevisiae* it had been shown, that ScSic1p is involved in preventing premature S-phase initiation by inhibiting ScClb5-Cdc28p and ScClb6-Cdc28p complexes. When Cln-Cdc28 levels have risen sufficiently, ScSic1p is phosphorylated, causing its SCF-dependent degradation (Schwob et al., 1994). Since all G1 cyclins were constantly present in *A. gossypii* the question raises how constant AgSic1p degradation could be avoided. A potential inhibitor, which had been shown in *S. cerevisiae* to control G1-cyclin activity is ScFar1p. Potentially AgFar1p may be involved in a similar task, to inactivate the G1 cyclins and only after this inhibition is loosened, the B-type cyclin inhibitor ScSic1p is being degraded and AgClb5/6p are able to initiate replication. Whether such a concept is possible localization studies of AgFar1p may show.

Another cyclin inhibitor is Cdh1p. Its levels stay constant throughout the cell cycle, however it only binds and activates the APC during G1. During the rest of the cell cycle, its association with the APC is blocked, by the phosphorylation of the Cdc28p (Prinz et al., 1998; Zachariae et al., 1996). It had been suggested, that ScClb5p binds via its hydrophobic patch the conserved "RXL" motif of ScCdh1p and inactivates it by phosphorylation (Archambault et al., 2005). As in *S. cerevisiae*, AgCdh1p is nuclear and present during the entire nuclear cycle in *A. gossypii* (N. Sustreanu, personal communication). This "RXL" is also conserved in the AgCdh1p, additionally supporting the hypothesis, that the inactive pool of AgClb5/6p is able to switch into an active pool, as soon as it has reached a certain concentration, thereby prolongating G1 phase.

Neighboring nuclei of different cell cycle stages are in very close proximity ($< 1 \mu\text{m}$ when nuclei by-pass each other, and $7 \mu\text{m}$ with a mean of $3.6 \mu\text{m} \pm 0.1 \mu\text{m}$, (Gladfelter et al., 2006)) in *A. gossypii*. Therefore, cell cycle specific proteins may enter nuclei of a different cell cycle stage. These proteins have to be inhibited, degraded or

exported to ensure, that the cell cycle rhythm of the nucleus is not affected. As an alternative possibility cell cycle progression may be linked to changes in the nuclear pore structure (De Souza et al., 2004; Makhnevych et al., 2003), thereby prohibiting entry of proteins of a different cell cycle stage. From our experiments we propose, that asynchrony in multinucleate cells is based on the action of few key cell cycle oscillators in combination with CDK inhibitors. The exclusion of these cell cycle specific oscillating proteins from nuclei with different cell cycle stage may be an efficient mechanism to ensure controlled progression through the cell cycle. The potential role of the nuclear pore complex in combination with import factors in monitoring the regulation of protein import will be discussed in more detail in Chapter IV.

CHAPTER IV

Characterization of Karyopherins and Nucleoporins in *A. gossypii*

Abstract

Nuclear division in the multinucleate ascomycete *A. gossypii* is asynchronous meaning that nuclei of different spindle stages co-exist and proceed independently of each other through the nuclear cycle. Although proteins from every nuclear stage are translated in the common cytoplasm, they do not seem to interfere with nuclear progression of nuclei in a different stage. Therefore we speculate that nuclear autonomy may be based on cyclic alterations in the uptake of proteins from this common cytoplasm.

Nuclear proteins translated in the common cytoplasm need to be guided by transport factors called karyopherins into the nucleus. Bidirectional exchange of macromolecules between the nucleus and the cytoplasm takes place through the nuclear pore, which is built by nucleoporins. As a first step to find out whether asynchrony is maintained by controlling the uptake of protein, various karyopherins and nucleoporins have been investigated. *A. gossypii* and *S. cerevisiae* sequences were compared by applying bioinformatics, gene deletions and GFP fusions of several candidate karyopherins and nucleoporins were constructed in *A. gossypii* and a complementation assay between *A. gossypii* and *S. cerevisiae* was made to get fundamental knowledge on the control of cell cycle progression in the multinucleate fungus *A. gossypii*.

Introduction

The first three chapters of this PhD-thesis focussed on the potential role of cyclins and the CDK inhibitor AgSic1p to explain asynchronous division of nuclei in *A. gossypii*. The average distances between nuclei in the multinucleated hyphae are only two to three times longer than the nuclear diameter, but adjacent nuclei are in different nuclear cycle stages pointing to a high level of regulatory autonomy. How can such autonomy be achieved assuming, like in other eukaryotes, an intense uptake of proteins from a common cytoplasm? As a first step to answer this question I screened the *A. gossypii* genome for nuclear import and export genes and began studying, as a side project, the

phenotypes of several *A. gossypii* strains deleted for these genes.

The bidirectional exchange of macromolecules between the nucleus and the cytoplasm takes place through the nuclear pore complex (NPC), which forms a gateway across the nuclear envelope. The active transport of large molecules requires carrier proteins that shuttle rapidly between these compartments. Soluble transport factors called karyopherins (importins/exportins) recognize the bipartite Nuclear Localization Signal (NLS) of the cargo protein. Most eukaryotic genomes encode 20 or more karyopherins and each karyopherin recognizes a distinct set of cargos based on the sequence or the structure of the NLS or NES on the cargo molecules, providing some specificity in nuclear import. However, the cargo sets recognized by individual karyopherins contain overlapping members, establishing functional redundancy between certain karyopherins (Jans et al., 2000). Translocation from the cytoplasm into the nucleus is mediated through the NPC which forms a channel across the nuclear membrane, composed of over 30 different nucleoporins (Rout et al., 2000). Specific binding of the karyopherin-cargo complex to the FG-nucleoporins (nucleoporins characterized by the presence of phenylalanine-glycine repetitive peptide motifs) facilitates their translocation through the NPC (reviewed in [Ryan and Wentze, 2000]).

An essential factor for directed nucleocytoplasmic transport is Ran, a small nuclear Ras-related GTP binding protein (called Gsp1p and Gsp2p in *S. cerevisiae*). This nuclear G-protein undergoes cycles of GTP binding, hydrolysis and GDP release (Belhumeur et al., 1993). The directional movement through the NPC is based on the unequal distribution of the two Ran nucleotide states (Ran-GTP predominantly in the nucleus and Ran-GDP in the cytoplasm). In the nucleoplasm, Ran-GTP interacts with importin β , causing the dissociation of the cargo, thereby delivering free cargo protein to the nucleoplasm. To support another cycle of import, importin α and the importin β -Ran-GTP complex are transported back to the cytoplasm. The cytoplasmic Ran binding protein (ScYrb1p, (Becker et al., 1995)) binds Ran and collaborates with the Ran GTPase-activating protein (Ran-GAP, ScRna1p) to stimulate conversion of Ran-GTP to Ran-GDP resulting in a conformational change in Ran that causes it to dissociate from importin β .

After Ran-GDP is imported back into the nucleus and through the action of the Ran-GEF (ScSrm1p), which causes it to release GDP and rebind GTP, the Ran-GTP/GDP cycle is reset.

We wanted to find out, whether asynchrony in nuclear cycles is controlled by cyclic alternations in the uptake mechanism? Progression through the cell cycle involves the presence and activity of the sequential action of cell cycle proteins in the nucleus. Therefore nuclei in distinct cell cycle stages may contain different sets of active proteins. Few proteins have so far been identified in *A. gossypii*, which are not present during the entire nuclear cycle, and therefore exist in only a fraction of all nuclei (AgCib5/6p, Chapter III, AgPds1p, N. Sustainu, personal communication). What are possible mechanisms to limit the presence of such a protein to a specific stage nucleus? One possible mechanism is the nuclear cycle dependent regulated transport into the nucleus, through its gate, the NPC. Possible mechanisms of the selective import of proteins into the nucleus in *A. gossypii* include immediate complex building of newly translated proteins with import factors, which specifically enter nuclei of a certain cell cycle stage. Or the nuclear pore complex itself could be remodelled in a cell cycle dependent manner such that certain proteins are only “allowed” to enter nuclei of a particular cell cycle phase (De Souza et al., 2004; Makhnevych et al., 2003).

The comparison of the *S. cerevisiae* and *A. gossypii* gene sets revealed a high sequence conservation of all known proteins involved in nucleo-cytoplasmic exchange. Deletions of candidate genes revealed that, like in *S. cerevisiae*, the karyopherin genes *AgSRP1*, *AgKAP95*, *AgPSE1*, *AgRNA1* and *AgYRB1* are essential with the exception of *AgKAP123*. In contrast to yeast, the deletion of the nucleoporin gene *AgNUP53/59* is not viable but the deletions of *AgNUP116/100* and *AgNUP145* revealed, like in yeast, a lethal phenotype. A localization study of the nucleoporin (AgNup116/100p) showed asymmetric distribution in the nuclear membrane.

Results

Deletion of the importin α , *AgSRP1*

The karyopherin α is thought to form a dimer with karyopherin β , ScKap95p to mediate import of nuclear proteins in *S. cerevisiae*. Karyopherin α is

involved in the binding of the nuclear localization signal (NLS) of the substrate during import into the nucleus. Even though six isoforms of the karyopherin α exist in mammalian cells, only a single karyopherin α homologue has been detected in *S. cerevisiae* and *A. gossypii*. A homologue to the *S. cerevisiae* importin α , ScSrp1p has been identified in *A. gossypii*, AgSrp1p. Interestingly these proteins share 84% identity and therefore are highly conserved (Table 3).

As in *S. cerevisiae*, the deletion of *AgSRP1* resulted in a lethal phenotype. Germinating spores were able to form a germ bubble, often a primary germ tube and in some cases a secondary germ tube with or without a first branch. They stopped growth with depolarized actin and degraded nuclei (Figure 39). These nuclei seem to go through an “empty sphere” stage, where most DNA is localized at the periphery of the nucleus, before they disintegrate. Srp1p is involved in binding NLS sequences in target proteins. Even though this process is essential for the cell, neither *A. gossypii* nor *S. cerevisiae* seem to have other redundant pathways, which could compensate and rescue these cells.

Deletion of importin β , *AgKAP95*, *AgPSE1* and *AgKAP123*

In the cytoplasm, importin α and β interact cooperatively with the cargo protein to provide its transport into the nucleus. The importin β subunit of the resulting trimeric cargo complex interacts with components of the NPC, translocating the complex into the nucleoplasm (Aitchison et al., 1996; Gilchrist and Rexach, 2003).

For each of the importin β present in *S. cerevisiae*, one homologue has been identified in *A. gossypii* (Table 3), which display strict length conservation. The entire ORFs of three of these homologous importin β genes, *AgKAP95*, *AgPSE1*, and *AgKAP123* have been deleted in *A. gossypii*. Similarly to *S. cerevisiae* *Agkap95 Δ* and *Agpse1 Δ* showed a lethal phenotype and only *Agkap123 Δ* was viable.

Agpse1 Δ mutant was able to form up to four germ tubes with or without a branch before the lethal arrest. Data presented in yeast, showed defects in mating and in the transition from the normal yeast form to the pseudohyphal, invasive form in ScPSE1-ts cells (Leslie et al., 2002). Interestingly, also *A. gossypii* revealed abnormalities in morphology. Their hyphae were constricted and apical branches could be observed

Table 3.
Overview over the *A. gossypii* karyopherin α and karyopherin β and their homologues in *S. cerevisiae*.

A.g. protein	Homologue in S.c.	SH	A.g. ORF size (aa)	Size of S.c. Homologue (aa)	% identity	A.g. Deletion	Deletion in S.c.	Description
AgSRP1 ABL150W	ScSRP1 (ScKAP60) YNL189W	+	544	542	84	Lethal	Lethal	Importin α
AgKAP95 ACL187W	ScKAP95 (ScRSL1) YLR347C	+	862	861	73	Lethal	Lethal	Importin β
AgPSE1 AGL349C	ScPSE1 (ScKAP121) YMR308C	+	1093	1089	68	Lethal	Lethal	Importin β
AgKAP123 AGL298C	ScKAP123 (ScYRB4) YER110C	+	1116	1113	74	Viable	Viable	Importin β
AgKAP104 AER219C	ScKAP104 YBR017C	+	910	918	55	n.d.	Viable (but ts!)	Importin β
AgSXM1 AFR396W	ScSXM1 (ScKAP108) YDR395W	+	950	944	57	n.d.	Viable	Importin β
AgMTR10 AAR115C	ScMTR10 (ScKAP111) YOR160W	+	965	972	55	n.d.	Lethal	Importin β
AgCSE1 AFR273W	ScCSE1 (ScKAP109) YGL238W	+	970	960	67	n.d.	Lethal	Importin β
AgNMD5 ABL068C	ScNMD5 (ScKAP119) YJR132W	+	1042	1048	56	n.d.	Viable	Importin β
AgLOS1 AFR424C	ScLOS1 YKL205W	+	1052	1100	47	n.d.	Viable	Importin β
AgMSN5 AEL094C	ScMSN5 (ScKAP142) YDR335W	+	1222	1224	67	n.d.	Viable	Importin β
AgCRM1 ADL128C	ScCRM1 (ScKAP124) YGR218W	+	1083	1084	80	n.d.	Lethal	Importin β
AgKAP122 AGR166W	ScKAP122 (PDR6) YGL016W	+	1014	1081	36	n.d.	Viable	Importin β
AgKAP114 AFR269W	ScKAP114 YGL241W	+	1019	1004	41	n.d.	Viable	Importin β
AgKAP120 ACR159C	ScKAP120 YPL125W	+	1026	1032	56	n.d.	Viable	Importin β

already after 15 h (Figure 40 A). However, no abnormalities in nuclei and actin distribution could be detected (Figure 40 B, top panel), as expected for a secretion enhancer. Since AgPse1p is needed for efficient secretion, it would be interesting to study its overexpression and test whether increased secretion may cause an increase in growth speed.

Agkap95 Δ cells stopped growth as a germ bubble with or without a primary germ tube containing one to four nuclei. Since physiological protein concentrations of the deleted gene may be present in spores, produced by the heterokaryon, this arrest stage containing few nuclei, may represent the depletion of this karyopherin β . In

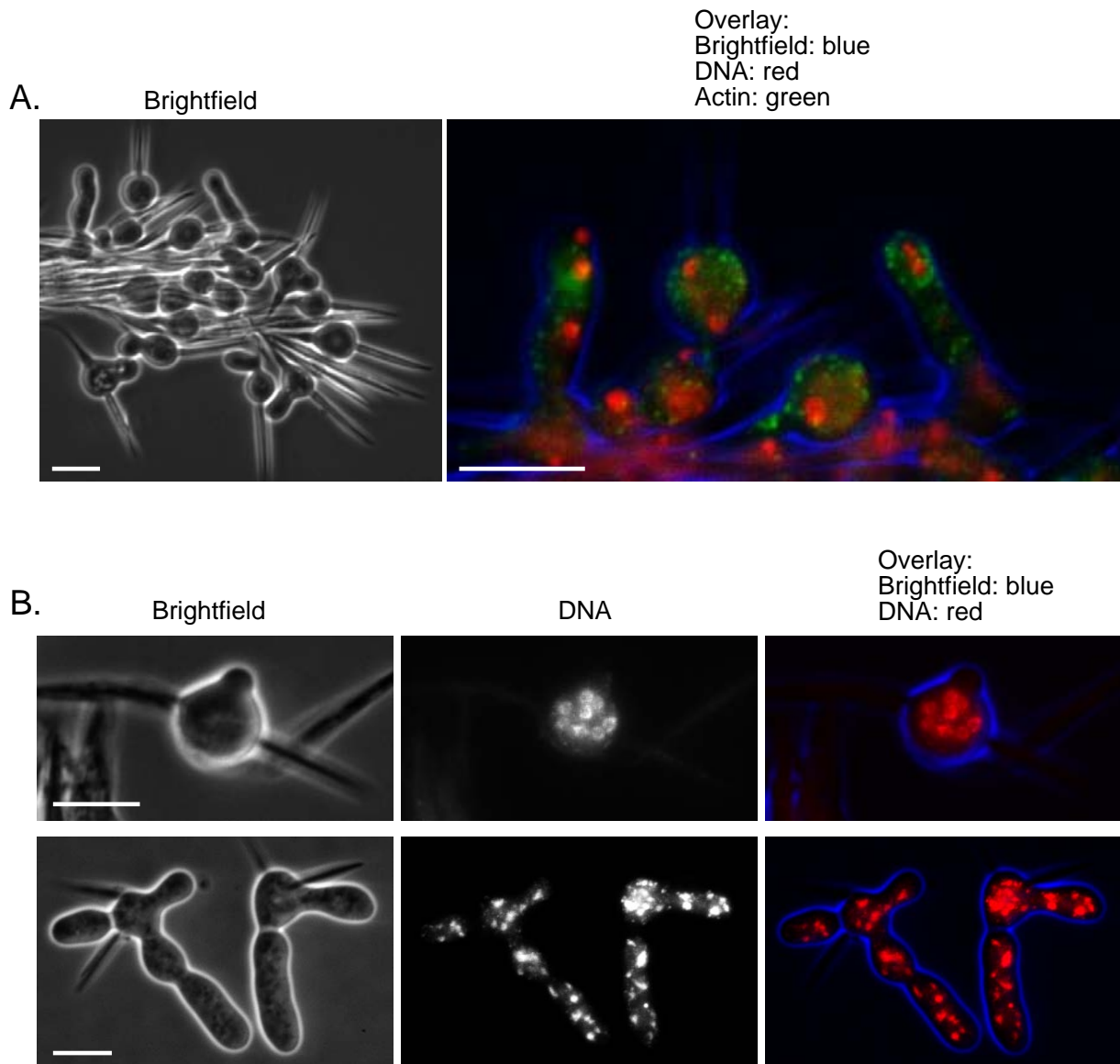
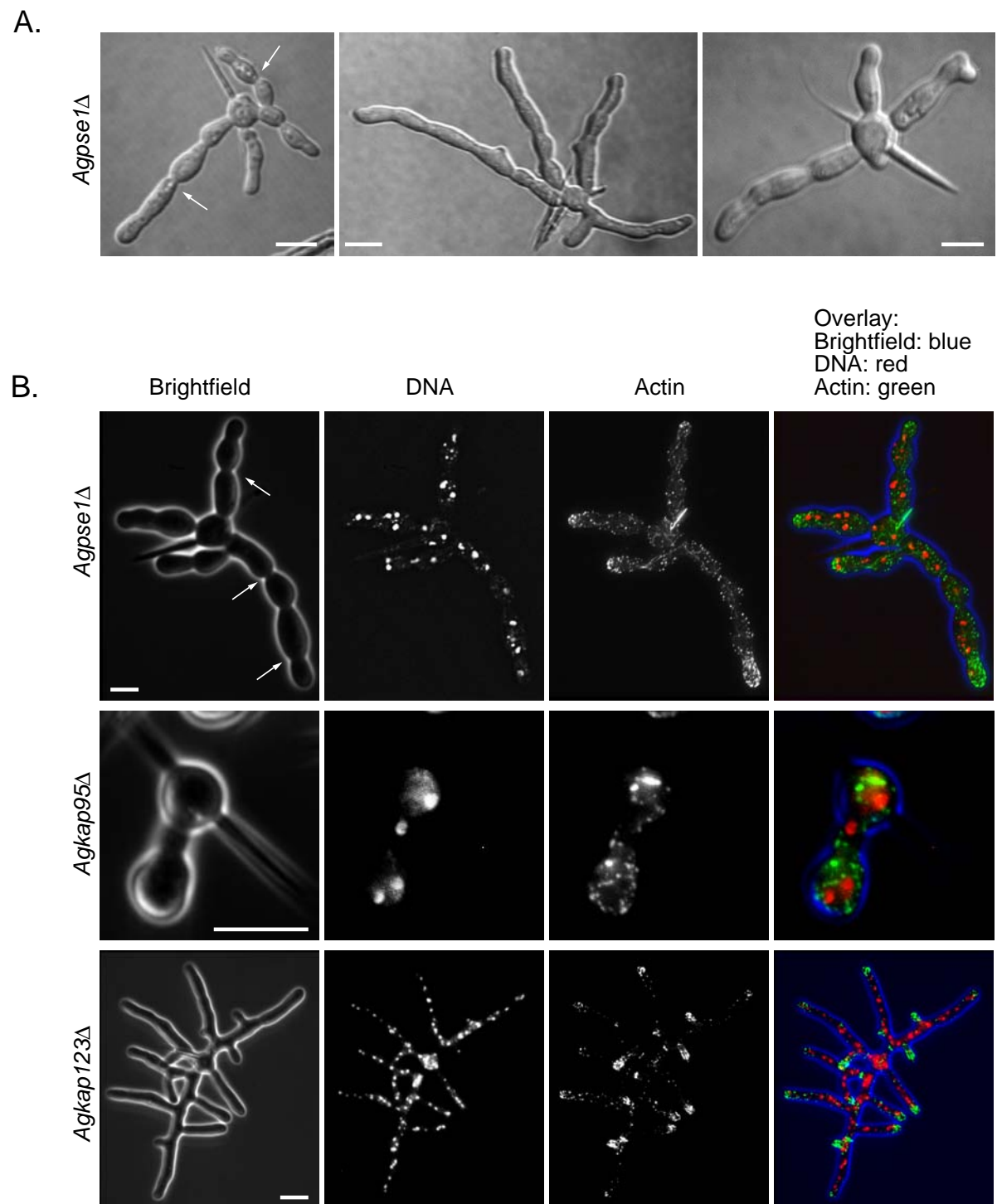


Figure 39
Phenotypic characterization of the importin α *Agsrp1* Δ .

Agsrp1 Δ mutants arrest growth as germlings. Spores isolated from heterokaryotic mycelium were incubated in liquid AFM + G418 for 15 h and nuclei were stained with Hoechst and actin with Alexa488-Phalloidin.

A. Arrest phenotype of *Agsrp1* Δ mutants as small germlings.

B. Detailed view on single cells, representative of the whole population. Top panel showing nuclei with typical “empty sphere” phenotype and bottom panel showing disintegrated nuclei, with “sparkly” phenotype. Pictures were taken by Brightfield on the left, nuclei in the middle and the overlay on the right with nuclei in red and Brightfield in blue. Bars, 10 μ m.

**Figure 40**

Phenotypic analysis of the deletions of the three importin β , *Agpse1Δ*, *Agkap95Δ* and *Agkap123Δ*.

Importin β mutant strains were grown in liquid AFM + G418 for 16 h at 30°C.

A. *Agpse1Δ* cells arrested with up to four germ tubes with or without a branch. Pictures were taken by DIC.

B. *Agpse1Δ*, *Agkap95Δ* and *Agkap123Δ* were stained with Hoechst, showing nuclei and Alexa488-Phalloidin, showing the actin cytoskeleton. In overlays, Brightfield is blue, nuclei are red and actin is green. Bars, 10 μ m.

addition, actin polarity at the tip of the germ tube seems to get lost when the cell ceases to grow (Figure 40 B).

Agkap123Δ was viable and grew wild-type like. No incidences of abnormal nuclei or actin distribution were detected (Figure 40 B). In contrast to *A. gossypii*, which grew without observable difference to the reference strain, the homologous deletion in *S. cerevisiae* caused 10-20% reduction of growth rate in rich media and an increase in cell size, compared to *wt* (Schlenstedt et al., 1997).

Phenotypic analysis of the deletion of the Ran binding protein (*AgYRB1*) and the Ran GTPase activating protein (*AgRNA1*)

In addition to the importin α and importin β characterization, also the Ran binding protein (AgYrb1p) and the Ran GTPase activating protein (Ran-GAP, AgRna1p) have been investigated. All identified components of the Ran-GTP/GDP cycle from *S. cerevisiae* are present in *A. gossypii* and show a high degree on conservation (with Gsp1, the Ran homologue sharing 97% identity, Table 4). The *AgRNA1* and *AgYRB1* deletions resulted in a lethal phenotype. *Agyrb1Δ* strain stopped growth with either a germ bubble with or without one germ tube, containing several nuclei (Figure 41 A), whereas *Agrna1Δ* mutant already arrested as a germ bubble with predominantly one to four nuclei (Figure 41 B). In the *Agyrb1Δ* strain, actin polarization is lost, probably due growth arrest, whereas in the *Agrna1Δ* mutant, germling never proceed through the isotropic-polarized switch, therefore always showing random distribution of actin (Figure 41 A and B).

To more closely investigate the directed movement through the NPC based on the unequal distribution of the two Ran nucleotide states, the two locked states, AgRan1p-GDP and AgRan1p-GTP should be constructed and characterized for their ability to maintain directed transport.

Heterologous complementation assay with RNA1

The conservation between *A. gossypii* and *S. cerevisiae* karyopherins varies from 36% identity (Kap122p) to 84% identity (Srp1p, Table 3). Despite the differences in the environment in which they act, some of the karyopherins are highly conserved. Whereas in yeast cells only one nucleus expresses proteins which are translated

in the cytoplasm, in *A. gossypii* the cytoplasm is filled with nuclei of various cell cycle stages, expressing different cell cycle specific proteins. How does an import factor know to which nucleus it has to transport its cargo? Have the tasks of the karyopherins changed between *A. gossypii* and *S. cerevisiae*? To answer these questions a complementation assay was performed. We intended to use *ts*-mutants of various *S. cerevisiae* karyopherins to test, whether the *A. gossypii* homologues could rescue the lethal phenotype at nonpermissive temperature. Unfortunately, due to limitations in *S. cerevisiae* karyopherin-*ts* strains, as well as suitable *A. gossypii* plasmids, only one complementation assay with the GTPase activating protein (*AgRNA1*) was performed. The *ScRNA1-ts* mutant (PSY714, kindly provided by P. Silver) was transformed with plasmids containing the *AgRNA1* gene. Despite the relatively high conservation between these proteins in *A. gossypii* and *S. cerevisiae* (58%), no complementation was observed at the restrictive temperatures, 34°C and at 37°C (Figure 41 C). Reasons for this could be the non-functional *A. gossypii* promoter, differences due to protein concentrations or differences in modifications. Another reason may have been lack of recognition of the Ran GTPase activating protein *AgRNA1* and the *S. cerevisiae* Ranp (ScGsp1p and ScGsp2p). However, this does not seem very likely since the AgGsp1/2p shares 97% and 96% identity with its homologue in *S. cerevisiae*. Further comparative system analysis may be substantial to provide insight into the evolutionary conservation between these two species, which despite their differences in constitution, share closely related genomes.

Domain comparison of three *S. cerevisiae* and *A. gossypii* nucleoporins

Bidirectional exchange of molecules between the cytoplasm and the nucleus is mediated through the NPC. This highly organized structure is composed of nucleoporins, of which some directly interact with translocating proteins (Table 5 and 6). ScNup116p and ScNup100p are highly related nucleoporins, called twins ORFs, which may have arisen by gene duplication (Wente et al., 1992). Both of them belong to a group of five nucleoporins containing multiple repeats of the amino acids GLFG (ScNup49p, ScNup57p, ScNup100p, ScNup116p and ScNup145p) which are also detected in the homologous AgNup116/100p (Figure 42 B). ScNup116p is stoichiometrically

Table 4.
Overview over the *A. gossypii* Ran homologues, Ran binding protein, Ran-GAP and Ran-GEF

A.g. protein	Homologue in S.c.		SH	A.g. ORF size (aa)	Size of S.c. Homologue (aa)	% identity	A.g. Deletion	Deletion in S.c.		Description
	1°	2°						Viability	Viability ?	
AgYRB1 AER002W	ScYRB1 YDR002W		+	211	201	72	Lethal	Lethal		Ran binding protein
AgRNA1 AFR525C	ScRNA1 YMR235C		+	398	407	58	Lethal	Lethal		Ran-GAP
AgSRM1 AFL045C	ScSRM1 (ScPRP20) YGL097W		+	487	482	71	n.d.	Lethal		Ran-GEF
AgGSP1/2 AGR294C	ScGSP2 YOR185C	ScGSP1 YLR293C	+/+ Twin	215	220	219	n.d.	Viability	Viability ?	Ran homologue

SH = Syntenic Homologue

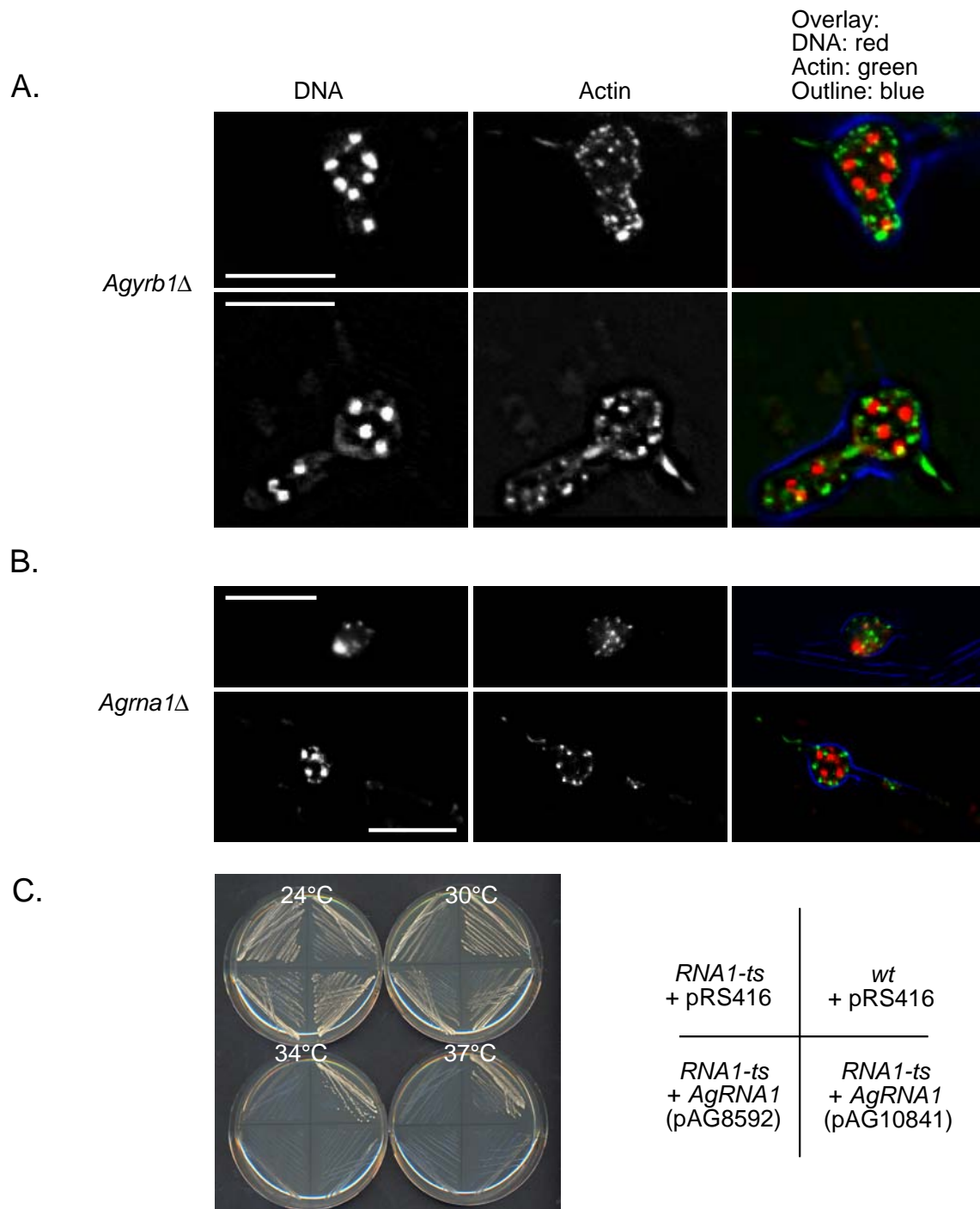


Figure 41
Phenotypic analysis of *Agyrb1*Δ and *Agrna1*Δ mutant strains.

Spores were grown in liquid medium under selection for 15 h at 30°C until arrest stage.

A. *Agyrb1*Δ mutant stops growth with either a germ bubble or one short germ tube. Several *wt*-size nuclei can be observed.

B. Growth stops predominantly as a germ bubble, containing one to four nuclei in the *Agrna1*Δ strain.

In overlays, outline is blue, DNA is red and actin is green. Bars, 10 μm.

C. Complementation assay. *ScRNA1-ts* (kindly provided by P. Silver) grows normally at 24°C, but arrests growth with temperatures higher than 30°C. *ScRNA1-ts* strain was transformed with pAG8592 and pAG10841 (both plasmids containing the *AgRNA1* homologue). In addition *ScRNA1-ts* was also transformed with the control vector pRS416. Complementation was evaluated at restrictive temperatures 34°C and 37°C on selective plates.

Table 5.
Amino acid sequence comparison of the nucleoporins.

<i>S. cerevisiae</i> nucleoporin		<i>A. gossypii</i> homologue		% identity (aa)
Nup53	(YMR153W)	AgNup53/59	(ADR272W)	} Twin 40
Nup59	(YDL088C)	AgNup53/59	(ADR272W)	
Nup145	(YGL092W)	AgNup145	(AFL059C)	} Twin 42
Nup116	(YMR047C)	AgNup116/100	(ABR099C)	
Nup100	(YKL068W)	AgNup116/100	(ABR099C)	48
Nic96	(YFR002W)	AgNic96	(AGR004W)	46
Nsp1	(YJL041W)	AgNsp1	(ACR060W)	59
Nup57	(YGR119C)	AgNup57	(AAR105W)	49
Nup49	(YGL172W)	AgNup49	(ADL045W)	56
Nup1	(YOR098C)	AgNup1	(ACL075C)	54
Nup2	(YLR335W)	AgNup2	(ABR034W)	31
Nup42	(YDR192C)	AgNup42	(AGL116C)	48
Nup159	(YIL115C)	AgNup159	(ADL248C)	35
Nup60	(YAR002W)	AgNup60	(AFL004C)	31
Nup82	(YJL061W)	AgNup82	(AEL168C)	31
Nup84	(YDL116W)	AgNup84	(ADL289C)	47
Nup85	(YJR042W)	AgNup85	(AEL073C)	49
Nup120	(YKL057C)	AgNup120	(ABR073C)	40
Nup133	(YKR082W)	AgNup133	(ADR272W)	37
Nup170	(YBL079W)	AgNup170/157	(AER397C)	} Twin 61
Nup157	(YER105C)	AgNup170/157	(AER397C)	
Nup188	(YML103C)	AgNup188	(AER284W)	46
Nup192	(YJL039C)	AgNup192	(ACR061C)	43
Pom34	(YLR018C)	AgPom34	(AAL159C)	53
Gle1	(YDL207W)	AgGle1	(ABL110W)	32
Gle2	(YER107C)	AgGle2	(AGL301C)	47
Seh1	(YGL100W)	AgSeh1	(AFL038C)	74
Ndc1	(YML031W)	AgNdc1	(AER307W)	73
Pom152	(YMR129W)	AgPom152	(AFR225W)	41
Cdc31	(YOR257W)	AgCdc31	(AAL110C)	54
				77

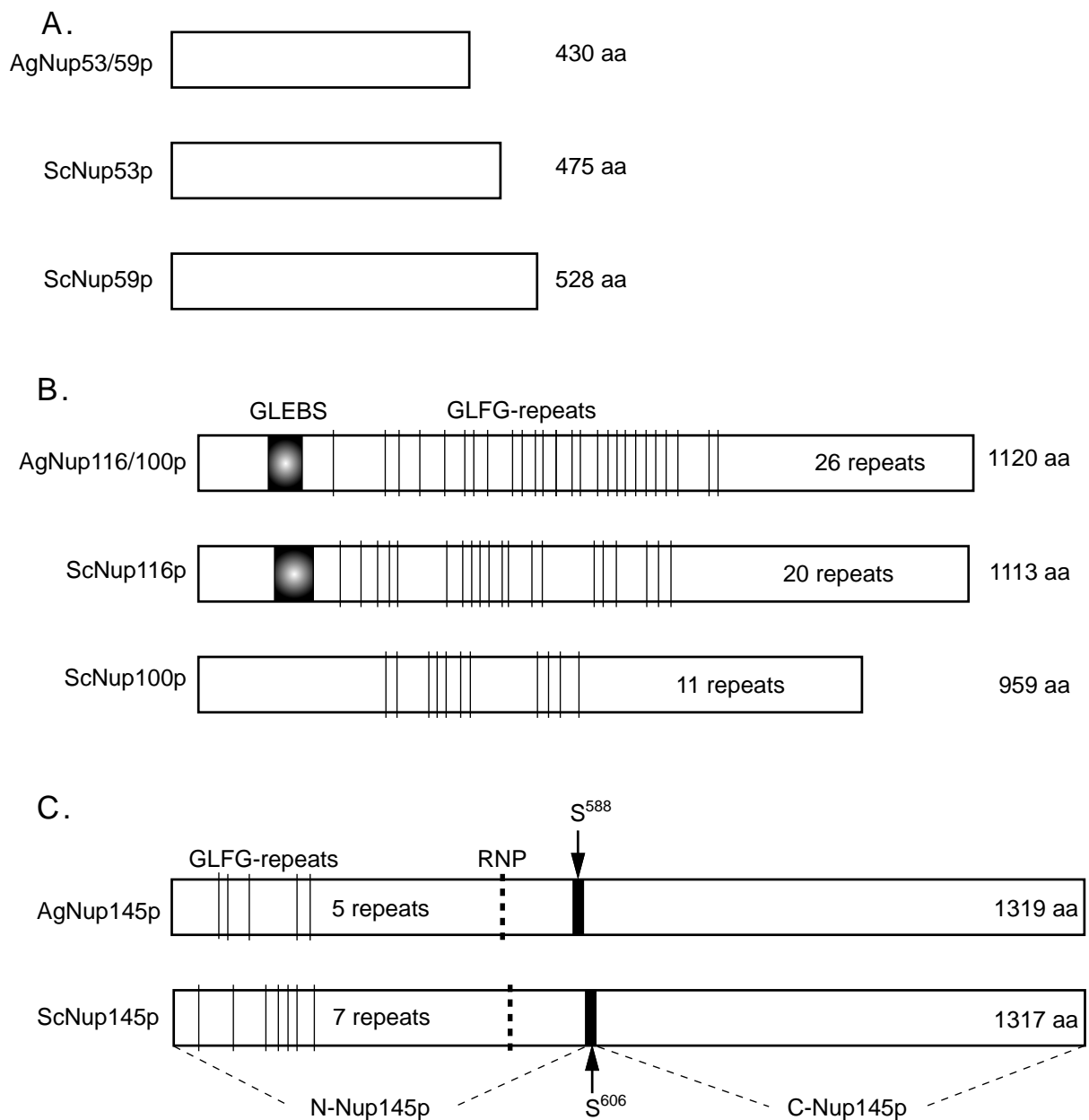
Genes that are duplicated in *S. cerevisiae* but present as a single copy in *A. gossypii* are named using both yeast homologues, separated by a slash (e.g., AgNup53/59p). (Taken from data published by Dietrich et al., 2004)

% identity > 70% is shown in bold

Table 6.
Overview over the *A. gossypii* nucleoporins and their homologues in *S. cerevisiae*.

A.g. protein	Homologue in S.c.		SH 1°/2°	A.g. ORF size (aa)	Size of Homologue in S.c. (aa)		% Identity to S.c Homologue		A.g. Deletion	Deletion in S.c. Homologues	
	1°	2°			1°	2°	1°	2°		1°	2°
AgNUP53/59 ADR272W	ScNUP53 YMR153W	ScNUP59 YDL088C	+/+	430	475	528	40	41	Lethal	Viable	Viable
	ScNUP145 YGL092W		+	1319	1317		42		Lethal	Lethal	
AgNUP145 AFL059C	ScNUP116 YKL068W	ScNUP100 YMR047C	+/+	1120	1113	959	48	46	Lethal	Viable	Viable
AgNUP116/100 ABR099C										Viable	Viable

Genes that are duplicated in *S. cerevisiae* but present as a single copy in *A. gossypii* are named using both yeast homologues, separated by a slash (e.g., AgNUP53/59).

**Figure 42****Domain Comparison of *A. gossypii* and *S. cerevisiae* nucleoporins**

A. Domain comparison between AgNup53/59p and ScNup53p and ScNup59p.

B. Domain comparison between AgNup116/100p and ScNup116p and ScNup100p. In all three proteins several GLFG-repeats (also only called FG-repeats) have been identified. In addition, in the ScNup116p a Gle2p-binding sequence (GLEBS, Bailer et al., 1998) was found, which is 68% identical to a potential GLEBS in the *A. gossypii* homologue.

C. Domain comparison between AgNup145p and ScNup145p. Five GLFG-repeats have been identified in AgNup145p (Ag aa 68-71; 81-84; 112-115; 191-194 and 200-203) compared to seven, found in ScNup145p. The highly conserved NRM-domain (Ag aa 580-595) containing the evolutionary conserved cleavage site ser (Ag aa 588) has been identified. Therefore AgNup145 as ScNup145 may be cleaved into an N- and a C-Nup145p. In addition a potential RNP-like motif was found (Ag aa 471-478), which may be responsible for its RNA affinity (Fabre et al., 1994).

bound to the mRNA export factor ScGle2p, forming a stable complex. A short, 56 aa ScGle2p-binding sequence within ScNup116p (GLEBS) is sufficient and necessary to anchor Gle2p at the nuclear pore (Bailer et al., 1998). This Gle2p-binding sequence is also present in the homologue in *A. gossypii* with an identity of 68%, indicating conserved interaction of these proteins in *A. gossypii*.

ScNup116p and ScNup100p are similar to a stretch of 140 amino acids within N-terminus of Nup145p (Wente and Blobel, 1994). ScNup145p and its apparent vertebrate homologue are the only known nucleoporins to be composed of two functionally independent peptide moieties resulting from the post-translational cleavage of a large precursor molecule. This cleavage site has been mapped to directly upstream of an evolutionary conserved serine⁶⁰⁶ in *S. cerevisiae* (Teixeira et al., 1999). In the *A. gossypii* homologue, this NRM-domain, containing the cleavage site is highly conserved, including this serine (Figure 42 C), indicating that most likely also the AgNup145p is cleaved into an N-terminal and a C-terminal part. ScNup145p has been shown to be essential for mRNA export in *S. cerevisiae* (Fabre et al., 1994) and a RNP-like motif was also detected in *A. gossypii*. In addition we were able to identify four GLFG-repeats in AgNup145p, however only one of them at a homologous site to its *S. cerevisiae* homologue, suggesting no strict positional control.

Characterization of three nucleoporin deletions in *A. gossypii*

To characterize the function of the NPC, the gate between cytoplasm and nucleus, we decided to delete three Nups, *AgNUP53/59*, *AgNUP116/100* and *AgNUP145*. The entire ORF was replaced via PCR based gene targeting with the dominant selection marker Gen3 (Wach et al., 1994; Wendland et al., 2000). All three deletions showed the same lethal phenotype. These cells were able to grow to small germlings with a primary germ tube and produce 3-9 nuclei in most cases, but then stopped growth with randomly distributed actin (Figure 43).

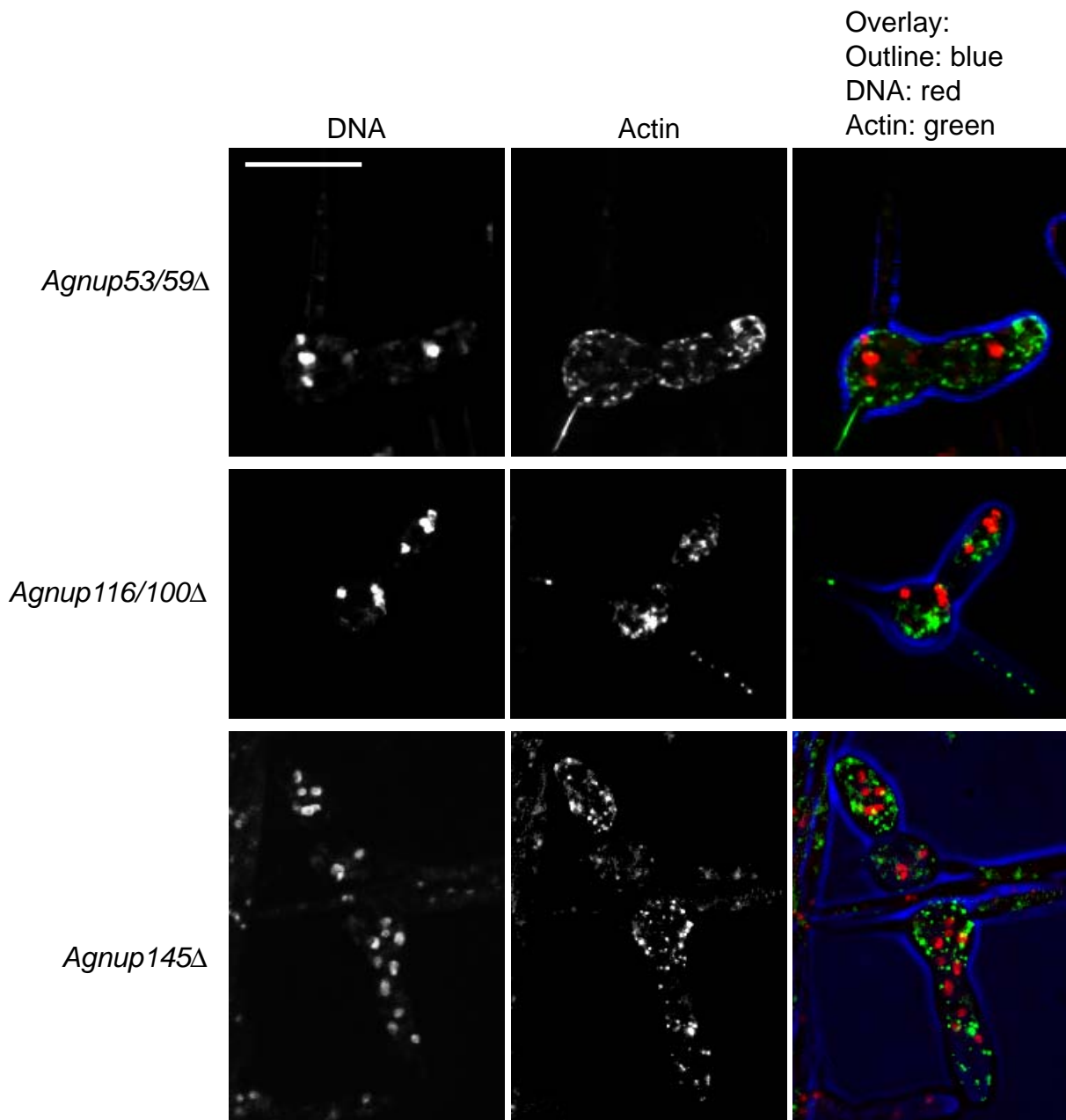
Asymmetric localization of the nucleoporin *AgNUP116/100*

The amino terminal region of the repetitive tetrapeptide "GLFG" motifs of ScNup116p and ScNup100p in *S. cerevisiae* have been shown

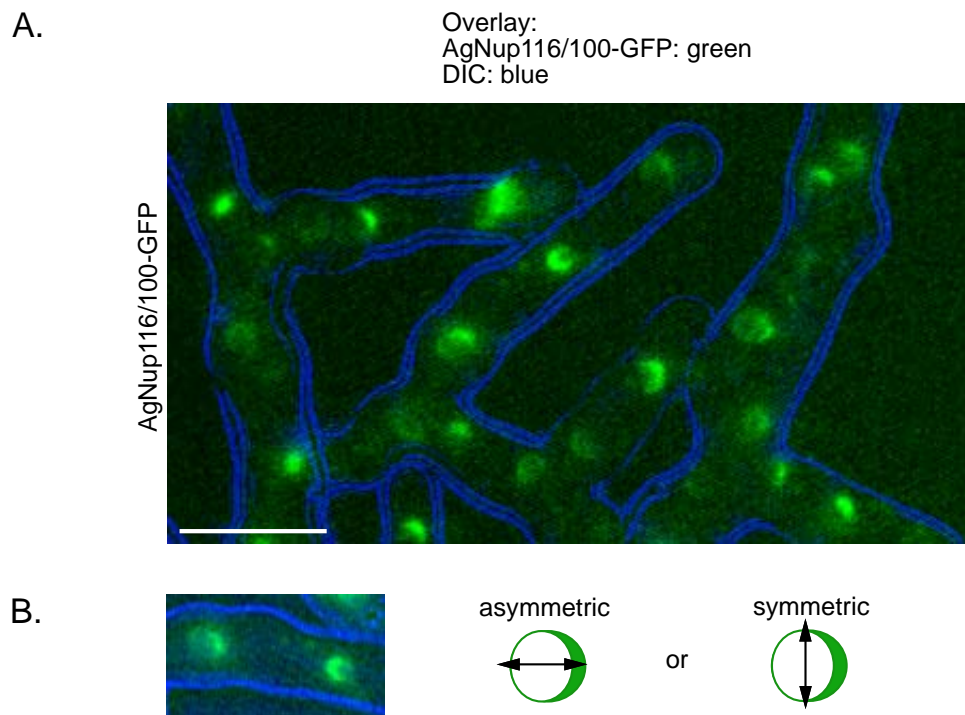
to bind directly to ScKap95p (Iovine et al., 1995; Iovine and Wente, 1997) and other karyopherins (Hodge et al., 1999). These specific interactions supports the idea, that import into the nucleus may be strictly controlled, first by the specific interaction of the karyopherin with its cargo and then by the interaction of the karyopherin with the nucleoporins. In addition, there has been evidence of changes in the NPC during the cell cycle (Makhnevych et al., 2003). We wanted to investigate, whether such changes could eventually be detected by localization and/or intensity changes of nucleoporin-GFP fusions on nuclear membranes of nuclei in different cell cycle stages in *A. gossypii*. A gene fusion of GFP to *AgNUP116/100* at its endogenous locus was performed and a clear GFP signal was detected on the nuclear membrane, possibly NPCs. Interestingly, the signal was not evenly distributed around the nucleus, but often one site revealed a much stronger signal. Therefore the question arises, whether this asymmetric distribution of AgNup116/100-GFP is due to artefacts based on the GFP fusion or whether nuclei are in fact asymmetric in respect to their NPC composition. If nuclei are asymmetric, it would be interesting to find out, whether they divide in a way, so that one daughter nucleus gets the majority of the protein, or whether division occurs symmetrically. To test these two hypotheses, further analysis by time-laps video microscopy should be performed in combination with immunofluorescence microscopy using anti-nucleoporin antibodies in wild-type cells.

Discussion

This dataset on the characterization of karyopherins and nucleoporins is one of several experimental approaches to search for proteins helping to maintain nuclear autonomy. The deletion of the karyopherins *Agsrp1Δ*, *Agkap95Δ*, *Agpse1Δ*, *Agyrb1Δ* and *Agrna1Δ* were lethal, indicating their importance in regulating nuclear import/export. Interestingly, several yeast strains that were mutated in essential components of the nucleocytoplasmic transport machinery including mutations in *ScSRP1* and *ScYRB1* showed a distinct cell cycle arrest phenotype at G2/M phase, indicating an important role for cell cycle progression (Loeb et al., 1995; Ouspenski, 1998). In the case of the yeast Ran-binding protein ScYrb1p it was shown, that its activity is crucial for efficient APC- and SCF-mediated proteolysis of important cell cycle regulatory proteins such as ScPds1p, and ScSic1p (Baumer et al., 2000). As a means to gain some

**Figure 43****Phenotypic analysis of the deletion of the three nucleoporins *AgNUP53/59*, *AgNUP116/100* and *AgNUP145***

Spores were isolated from heterokaryotic nucleoporin deletion strains and grown for 16 h at 30°C under G418 selection. *Agnup53/59* Δ , *Agnup116/100* Δ and *Agnup145* Δ strains arrested as germlings. When stained with Hoechst three to nine nuclei were detected in most cases. The actin cytoskeleton was shown by Alexa488-Phalloidin. In overlays, the outline is blue, DNA is red and actin is green. Bar, 10 μ m.

**Figure 44****Asymmetric distribution of AgNup116/100-GFP in the nuclear envelope.**

A. Spores from homokaryotic mycelium of AgNup116/100-GFP were incubated in liquid AFM + G418 for 16 h at 30°C. The GFP signal was detected on the nuclear membranes. Bar, 10 μ m.

B. Asymmetry of the AgNup116/100p signal raises the question whether how this asymmetric localization of AgNup116/100p is divided. Indeed nuclear division may occur in an asymmetric way, so that one daughter nucleus gets the majority of pores containing AgNup116/100p or in a symmetric way, so that both daughter nuclei contain a similar NPC composition.

insight into the involvement of karyopherins during the nuclear cycle in *A. gossypii*, the arrest stage of these deletions should be analyzed by tubulin immunofluorescence.

The lethality observed in these karyopherin deletions, may have one cause in the deficiency of nuclear import of cargoes, which exert their roles in the nucleus. One example of such an important cargo is the mitotic cyclin ScClb2p in *S. cerevisiae*, which has been shown to be dependent upon ScSrp1p, ScKap95p, ScYrb1p and ScRna1p for correct localization (Hood et al., 2001). In *A. gossypii*, the homologous mitotic cyclin AgClb1/2p is essential and effects due to blocked nuclear import may be strong.

However, in addition also the *AgKAP123* Δ was deleted, showing a viable, wild-type like behaviour. In *S. cerevisiae* this karyopherin β mediates nuclear import of ribosomal proteins prior to assembly into ribosomes and import of histones H3 and H4 (Mosammaparast et al., 2002; Schlenstedt et al., 1997). Despite these crucial

tasks that ScKap123p fulfils, this protein is not essential. Therefore it is thought that in its absence ScPse1p, ScSxm1p and ScNmd5p are able to substitute Kap123p in its role in import (Sydorsky et al., 2003). Due to the rather high identity (74%) which ScKap123p and AgKap123p share and the observed viability in their deletions, it seems likely that also in *A. gossypii* other karyopherins are able to complement.

Due to the severity of most of the karyopherin mutants, localization of cell cycle specific proteins in these strains could not be achieved. In the absence of *ts*-alleles, it is only possible to work with heterokaryon strains, where only some nuclei contain the deleted karyopherin. One possible attempt could be, to use as an epitope tagged cyclin strain (*AgCLB5/6-13myc*, which has been shown of being degraded and therefore absent in anaphase nuclei, Chapter III) in the integrated Ade2-LacI strain as a background. In this strain, the deletion of a specific karyopherin could be performed using a disruption cassette,

containing a dominant selection marker and the LacO repeats. With this, nuclei containing the karyopherin deletion could be identified due to the discrete GFP spot based on the specific interaction of the NLS-LacI-GFP and the 32-mer of LacO. In this strain the tagged protein could be followed and its requirement for nuclear localization based on specific karyopherin import could be tested.

Another approach may be the construction of temperature sensitive karyopherin mutants, similar to those used in *S. cerevisiae*, or the use of *S. cerevisiae* *ts*-alleles in *A. gossypii*. Karyopherins sharing high identity in *A. gossypii* and *S. cerevisiae* (as Srp1p with 84% identity) may be functional with similar point mutations as karyopherin-*ts* strains already used in *S. cerevisiae*. However, so far any attempts working with *ts*-mutants in *A. gossypii* failed due to lethality of these strains already at permissive temperature.

The NPC is a highly organized structure and the deletion of single components seem to either disrupt the structure as a whole, or may interfere with the transport of essential proteins, which thereby may be mislocalized. The second possibility seems appealing, since direct interactions between karyopherins and nucleoporins have been presented and many single deletions of nucleoporins did not cause lethality, therefore suggesting that the NPC structure as a whole was still intact. A direct interaction of the ScNup53p, ScNup59 and ScNup170 with the karyopherin β ScPse1p has been identified (Marelli et al., 1998). The double deletion of ScNUP53/59 was viable in *S. cerevisiae*, indicating no general misaggregation of the nucleoporins to build the NPC, however ScPse1p displayed an altered subcellular distribution. If ScPse1p is mislocalized, also import and proper localization of several cargo proteins of ScPse1p (as shown for the ribosomal L25 reporter protein) may be effected and their mislocalization may have very broad and indirect effects. The karyopherin ScPse1p is not only bound by ScNup53p, but also by ScNup116p. In addition to ScPse1p, ScNup116p also interacts with ScKap95p, requiring its GLFG repeats.

M-phasespecificmolecularrangements in the NPC causes changes in nuclear import (Makhnevych et al., 2003; Marelli et al., 1998). In particular, it was shown, that ScNup53p acts as a transport inhibitory nucleoporin, slowing nuclear transport mediated by ScPse1p during mitosis. During interphase, most ScNup53p is associated with ScNup170p, thereby allowing active Pse1p transport. In contrast, during mitosis ScNup53p is tightly associated with Pse1p, thereby blocking

its transport through the NPC. While it is generally accepted, that the regulation of nucleocytoplasmic transport can be controlled by modifications of a cargo, which alters binding to its cognate karyopherin, it was also shown, that cell cycle changes in the NPC itself can regulate specific transport pathways (Makhnevych et al., 2003).

It seems likely that similar changes in the NPC composition may be involved to regulate cell cycle specific transport in the various nuclei in *A. gossypii*. Preliminary studies on the localization of AgNup116/100p indicate that they may be asymmetrically distributed across the nuclear membrane. However, this may be due to artefacts of epitope-tagging or limitations in imaging. In the case, that there in fact is asymmetry it may be very interesting to determine whether this is a way for nuclei to be insulated from neighbours of different cell cycle stage. As first attempt towards understanding this process in more detail, immunostaining using nucleoporin-antibodies on wild-type cells should be done. With this, artefacts due to the epitope-tag could be excluded. In addition time-laps movies of the AgNup116/100-GFP should be performed to find out, whether the unequal localization of AgNup116/100p on the nuclear envelope is divided in an asymmetric way.

AgCib5/6p and AgPds1p (N. Sustreanu, personal communication) are both essential proteins, which are present in certain cell cycle stages, but not in others. Their absence in anaphase nuclei, directly leads to the question, how is oscillation of cell cycle specific proteins regulated in a syncytial cell. Changes in nuclear import due to changes in the NPC during the cell cycle may be a means to exclude proteins specific for different cell cycle stages, thereby providing nuclear independency. Whether or not such a mechanism accounts for the regulation of autonomous nuclear division in an asynchronous multinucleate cell, as in *A. gossypii*, we do not know by now. However, progression through the cell cycle is accurate and maintenance of asynchrony is very strong, suggesting a sophisticated regulatory network that excludes, inactivates or destroys proteins of different cell cycle stage to provide order in cell cycle progression.

MATERIALS AND METHODS

Materials and Methods

A. gossypii strains and growth conditions

A. gossypii media, culturing, and transformation protocols are described in (Wendland et al., 2000) and (Ayad-Durieux et al., 2000). The genotype $\Delta leu2 \Delta thr4$ of the *A. gossypii* strain ATCC10895 (reference strain) was used for the generation of all *A. gossypii* strains. Either pGEN3 (Wendland et al., 2000), pUC19-NATPS (D. Hoepfner, personal communication) or pGUG (Knechtle, 2002) were used as templates to generate gene-targeting cassettes encoding Geneticin-resistance, ClonNAT resistance or GFP plus Geneticin-resistance, respectively. The strains were verified by PCR and are listed in Table 7. Nocodazole stocks for the arrest-release experiments were 3 mg/ml in DMSO and used at a final concentration of 15 μ g/ml (Sigma).

DNA manipulations

All DNA manipulations were carried out according to (Sambrook and Russell, 2001) using DH5 α F' as host (Hanahan, 1983). Plasmids generated and used here are listed in Table 9. PCR was performed using standard methods with Taq polymerase, Expand High Fidelity PCR system and GC-Rich PCR system from Roche (Basel, Switzerland). Oligonucleotides were synthesized at MWG (Ebersberg, Germany) or Microsynth (Balgach, Switzerland) for PAGE purified oligonucleotides. Oligonucleotide primers are listed in Table 10. All restriction enzymes came from New England Biolabs or Roche.

Plasmid isolation from yeast was performed as described in (Schmitz et al., 2006), using DHD5 as yeast reference strain (Arvanitidis and Heinisch, 1994). All sequencing to verify plasmids was done at MWG (Ebersberg, Germany).

Generation of deletions

A. gossypii deletion mutants were generated using the PCR based one-step gene targeting approach (Baudin et al., 1993; Wach et al., 1994; Wendland et al., 2000). *A. gossypii* deletion mutants were made in *Ag $leu2\Delta$ thr4 Δ* using pairs of „gene name“-S1/S2 oligonucleotides (for *GEN3*, which consists of the open reading frame of the kan^R gene under the control of promoter and terminator sequences of the *ScTEF2* gene) or -NS1/NS2 oligonucleotides (for ClonNAT resistance) for each locus, which contained at least 45 bp homology upstream and downstream of the ORFs. *Ag Δ Δ t* young mycelia were transformed with PCR products amplified off the pGEN3 or the pUC19NATPS template with the S1/S2 or NS1/NS2 oligonucleotide pairs. The primary transformation produced heterokaryon mycelia which contained a mixture of wild-type and transformed nuclei, thus even mutations in essential genes produce viable transformants. Heterokaryon and homokaryon transformants were verified by analytical PCR with oligonucleotides „gene name“-G1 and G2 (Geneticin marker) or V2*NAT1 (ClonNAT marker) and „gene name“-G4 with G3 (Geneticin marker) or V3*NAT1 (ClonNAT marker). For each deletion three independent transformants were characterized, excluding phenotypes by random mutations. To evaluate phenotypes of lethal mutants, the heterokaryon was sporulated to produce uninucleated spores which were then germinated under selective conditions. Since these spores were products of hyphae which contain a mixture of wild-type and transformed nuclei, protein leftover of the deleted gene has to be depleted, before the deletion phenotype is completely represented.

To generate the AKHAg9 strain, *Ag $clb1/2\Delta$* was constructed in the background of *AgHPH04* (H. Helfer, PhD Thesis, 2006), which contains HH1-GFP (histone H4-GFP), stably integrated at the ADE2 locus.

Agarose gels of the verification PCRs of the deletions are presented in Appendix 2.

pAG plasmid construction

The tagging of the cyclins was performed via co-transformation in yeast using a PCR fragment containing 45 bp homology to the cyclin gene cloned in pRS416. This plasmid was either taken from the *Ashbya gossypii* pAG clone collection (pAG7578 containing *AgCLB1/2*, pAG9687 for *AgCLB5/6*, pAG10848 for *AgNUP116/100*, (Dietrich et al., 2004)) or the plasmid was constructed by amplifying the gene from genomic DNA. To construct pAKH53 (containing *AgCLN3*), genomic DNA was amplified with the oligonucleotides CLN3-P1 and CLN3-P2, containing at the 5' ends restriction sites for BamH1 and Xba1, respectively. The PCR fragment obtained (2296 bp) was cut with these enzymes resulting in a 2273 bp fragment and ligated into cut and column purified pRS416 vector. The resulting pAKH53 was sequenced to avoid mutations due to random PCR errors. pAKH54 (containing *AgCLB3/4*) was constructed by amplifying the gene from genomic DNA with the oligonucleotides CLB3/4-P1 and CLB3/4-P2, containing at the 5' ends restriction sites for HindIII and Xba1, respectively. The PCR product (2148 bp) was cut with HindIII and Xba1, resulting in a fragment of 2125 bp, which was ligated into a HindIII and Xba1 cleaved and column purified pRS416 plasmid and transformed into *E. coli*. This gave rise to pAKH54, which was also verified by sequencing.

AgCLB5/6 was subcloned from pAG9687 by digestion with Not1 and Xho1, resulting in a fragment of 2120 bp. This fragment was gel purified and ligated into the Not1 and Xho1 cut pRS415, leading to pAKH1, which was verified by restriction digests. pAKH2 was constructed in a similar manner, in that pAG9687 was digested with Xho1, resulting in a 2519 bp fragment, which was ligated into the Xho1 cleaved pRS415. The resulting plasmid pAKH2, was verified by restriction digest.

Generation of GFP-Fusions

To C-terminally GFP-tag genes, the pGUG cassette (Knechtle, 2002) was amplified with pairs of „gene name“-GS1/GS2 oligonucleotides containing 45 bp homology to the C-terminus of the gene. The resulting PCR product (~2850 bp, containing the *Aequorea victoria* green fluorescent protein [GFP] with the *ScURA3* terminator and the *GEN3*) was co-transformed in yeast with the plasmid pAG9687 (for *AgCLB5/6*), pAG7578 (for *AgCLB1/2*), pAKH53 (for *AgCLN3*), pAKH54 (for *AgCLB3/4*) or pAG10848 (for *AgNUP116/100*) to produce pAKH40, pAKH7,

pAKH58, pAKH55 and pAKH51, respectively. pAKH40 was digested with Sal1 and Stu1, pAKH7 with Fsp1 and Spe1, pAKH58 with Pst1, pAKH55 with Nhe1 and Aat2 and pAKH51 with BamH1 and Sph1 before transformation into *A. gossypii* mycelia. This produced AKHAg31, AKHAg7, AKHAg54, AKHAg47 and AKHAg36, which were verified by PCR using oligonucleotides CLB5-I1, CLB1/2-I1, CLN3-I1, CLB3/4-I1 and GG2/Green2 and CLB5-G4, CLB1/2-G4, CLN3-G4, CLB3/4-G4 and G3.

To construct *AgCLB1/2*-GFP in the nonreplicating plasmid pUC19, pAKH7 was digested with Sph1 and EcoR1, the 3734 bp fragment was purified and ligated into Sph1 and EcoR1 cut pUC19, resulting in pAKH9. Prior to transformation into *A. gossypii*, pAKH9 was digested with Fsp1 and Aat2. This produced the integrated *AgCLB1/2*-GFP strain, AKHAg57.

Agarose gels of verification PCR of the GFP-tagged genes are shown in Appendix 2.

Epitope tagging with 13myc

The pAg-13myc-GEN3 cassette for *A. gossypii* was generated by digesting pFA6-13myc (Longtine et al., 1998) with BglII and ligating the gel purified 3.2 kb fragment containing the 13myc with the *ScADH1* terminator and the amp^R to the 1.7 kb fragment generated from digesting pGEN3 (Wendland et al., 2000) with EcoRV/BamHI.

To C-terminally myc-tag the cyclin genes and *AgSic1p* the pAg-13myc cassette was amplified with oligonucleotides Clb2-MycF and Clb2-MycR for *AgCLB1/2*; Cln2-MycF and Cln2-MycR for *AgCLN1/2*; CLB5mycF and CLB5mycR for *AgCLB5/6*, CLN3-M1 and CLN3-M2 for *AgCLN3*, CLB3/4-myc-P1 and CLB3/4-myc-P2 for *AgCLB3/4* and Sic1-MycF and Sic1-MycR for *AgSIC1*. The resulting PCR products (~2650 bp) were co-transformed in yeast with the plasmid pAG7578 (for *AgCLB1/2*), pAG5016 (for *AgCLN1/2*), pAG9687 (for *AgCLB5/6*), pAKH53 (for *AgCLN3*), pAKH54 (for *AgCLB3/4*) to produce pCLB2-13myc, pCLN2-13myc, pCLB5/6-13myc (pAKH52), pCLN3-13myc (pAKH59) or pCLB3/4-13myc (pAKH56). *AgSIC1* was tagged at its endogenous locus by direct transformation with the PCR fragment, leading to the ASG61 strain. pCLB2-13myc was digested with BglII and NcoI, pCLN2-13myc with ApaI, pAKH52 with Nhe1, Kpn1 and Nde1, pAKH59 with Aat2 and PpuM1 and pAKH56 with Nhe1 and Aat2 before transformation of young *A. gossypii* mycelia to tag the endogenous cyclin genes. After clonal purification,

the homokaryotic ASG43, ASG60, AKHAg46, AKHAg55, and AKHAg48 strains were obtained, which were verified with the oligonucleotides Clb1-Myc-I, Cln2-Myc-I, CLB5MycI, CLN3-I1, CLB3/4-I1 and MycI and CLB5-G4, CLB1/2-G4, CLN3-G4, CLB3/4-G4 and G2.

The plasmid pAKH52 (containing the 13myc tagged *AgCLB5/6*) was digested with Not1 and Xho1, due to its big size (12'324 bp) and the presence of the entire *AgCLB1/2*. The gel purified fragment (4'676 bp) was ligated into the Not1 and Xho1 digested pRS416, resulting in pAKH63. This plasmid was later used for the construction of the *GAL1* overexpressed *AgCLB5/6* and the D-box mutations.

LacI-LacO constructs

The GFP-LacI-NLS integration cassette for *A. gossypii* was generated with pLKL55Y, kindly provided by C. Pearson and K. Bloom. pLKL55Y was digested with Sap1 and HindIII to generate a 2 kb fragment, containing the P_{ScHIS3} GFP-LacI-NLS, blunt ends were generated with Vent polymerase and ligated into the Sca1 site of the pAIC (Knechtle, 2002) plasmid. This produced two plasmids, pAKH35 and pAKH36, which were verified by sequencing and differ only in the orientation of LacI-NLS-GFP. pAKH35 and pAKH36 were digested with HindIII/Not1 and transformed into the *Agade2Δ1 A. gossypii* strain (Knechtle, 2002), to generate AKHAg26 and AKHAg27, which contain the LacI-NLS-GFP integrated at the *AgADE2* locus. These strains were verified by PCR and showed a strong, nuclear GFP signal.

To generate the plasmid containing the LacO-repeats and *AgCLB1/2*-13myc (pAKH38), pLKL60Y (kindly provided by C. Pearson and K. Bloom) was cut with Pac1 and BamHI to generate a 1.5 kb fragment containing 32-LacO repeats and blunt ends were generated using Vent polymerase. pUC21 was linearized with the blunt end cutter HincII and ligated with the LacO-fragment, resulting in pAKH37. pAKH38 was generated by digesting pAKH37 with KpnI and Nde1 and ligating this 1.6 kb fragment to the 9535 bp fragment generated from digesting pCLB2-13myc with KpnI/Nde1. pAKH38 was sequenced and transformed as plasmid into AKHAg26 and AKHAg27, resulting in AKHAg28 and AKHAg29, respectively.

To generate the plasmid containing the LacO-repeats and *AgCLN1/2*-13myc (pAKH57), pAKH37 was digested with Xho1, EcoRV and Not1, resulting in a 1.5 kb fragment (containing the LacO-

32mer), which was gel purified and ligated with the purified and dephosphorylated 10 kb fragment from the pCLN2-13myc, which had been digested with Xho1 and Stu1. This gave rise to pAKH57, which was verified by sequencing and transformed as a plasmid into AKHAg26, resulting in AKHAg49.

Construction of the D-box mutants (*AgCLB1/2*)

The *Agclb1/2Δdb* mutants were made using an overlap PCR approach which deleted amino acids 27-36 ($\Delta db1$) and/or amino acids 84-96 ($\Delta db2$) in *AgClb1/2p*. To generate pAKH47 ($\Delta db1$), pCLB2-13myc was used as a template for a PCR reaction with the primer pair clb2dbA and clb2db1B to produce a 643 bp product and a second reaction with the primer pair clb2db1C and clb2dbD to create a 537 bp product. Oligonucleotide clb2dbA was homologous to a region 500 bp upstream of the D-box1 and clb2dbD was homologous to a region 600 bp downstream of the D-box1. Oligonucleotide clb2db1B contained homology to *AgCLB1/2* immediately upstream of the D-box but lacking the D-box sequences between nt 81-108. Additionally, the 3' end of this oligonucleotide has homology to the region immediately downstream of the D-box. This sequence is also present in the 5' half of oligonucleotide clb2db1C. This overlapping homology was then used in a second PCR reaction involving the two products of A+B and C+D and additional clb2dbA and clb2dbD primers to create a 1.1 kb fragment containing an in-frame deletion of the D-box1 ($\Delta db1$) and part of the *AgCLB1/2* ORF. To generate a full length D-box1 mutant, this 1.1 kb fragment was co-transformed into yeast strains with pCLB2-13myc, which had been digested with Nhe1 which is located just upstream of the D-box1. The gap-repaired plasmid containing the deleted D-box1 was confirmed by sequencing and called pAKH47 (*pAgCLB1/2Δdb1*-13myc-*GEN3*).

Similarly, to generate pAKH45 ($\Delta db2$), oligonucleotides clb2dbA and clb2db2B were used with pCLB2-13myc as a template in the first reaction and clb2db2C and clb2dbD were used in the second reaction. Clb2db2B contains sequence homology just upstream of D-box2, lacking the sequence from nt 248-287 corresponding to $\Delta db2$. Additionally, at the 3' end, clb2db2B has homology to the region immediately downstream of the D-box2, which is also present in the 5' half of oligonucleotide clb2db2C. The full length mutant lacking $\Delta db2$ was generated via co-transformation in yeast, as $\Delta db1$, but the pCLB2-13myc plasmid

was digested with Aar1 for co-transformation in yeast. To delete both D-boxes (pAKH46), a similar attempt was chosen, but pAKH45 was used as template for both PCR reactions, using clb2dbA and clb2db1B for the first, and clb2db1C and clb2dbD as primers for the second PCR reaction, as described for constructing the $\Delta db1$ mutant. pAKH45 (pAgCLB1/2 $\Delta db2$ -13myc-GEN3) and pAKH46 (pAgCLB1/2 $\Delta db1\Delta db2$ -13myc-GEN3) were also both confirmed by sequencing. The plasmids pAKH47, pAKH45 and pAKH46 were transformed into *A. gossypii*, resulting in AKHAg39, AKHAg40 and AKHAg41, in which the plasmid was maintained due to constant selection with G418.

In addition, pAKH47 ($\Delta db1$) and pAKH45 ($\Delta db2$) were digested with Eag1 prior to transformation, for stable integration into the genome replacing the endogenous *AgCLB1/2*. The resulting AKHAg37 (*AgCLB1/2* $\Delta db1$ -13myc-GEN3) and AKHAg38 (*AgCLB1/2* $\Delta db2$ -13myc-GEN3) strains, were verified by PCR and subsequent verification digest.

In addition, the various D-box plasmids were integrated at the ADE2 locus. pCLN2-13myc, pAKH47, pAKH45 and pAKH46 were digested with Nae1 to generate a blunt end, 4.9 kb fragment which was ligated into the Sca1 cut and dephosphorylated pAIC (Knechtle, 2002). The resulting plasmids (pAKH78, pAKH79, pAKH80 and pAKH81) were digested with Not1 and Msc1 and transformed into the *Agade2* $\Delta 1$ *A. gossypii* strain (Knechtle, 2002), generating ASG70 (*AgCLB1/2*-13myc-GEN3), ASG71 (*AgCLB1/2* $\Delta db1$ -13myc-GEN3) and ASG73 (*AgCLB1/2* $\Delta db1\Delta db2$ -13myc-GEN3).

Construction of the overexpressed *AgCLB1/2*

The inducible *GAL1* promoter was placed in front of *AgCLB1/2* (pAKH2) and *AgCLB1/2*-13myc (pCLB2-13myc) to overexpress the mitotic cyclin. The pFA6a-His3MX6-P_{GAL1} cassette (Longtine et al., 1998) was amplified with the oligonucleotides GALClb2F and GALCLB2R, resulting in a PCR fragment of 1929 bp. This PCR fragment was co-transformed into yeast together with pAKH2 or pCLB2-13myc to generate pAKH41 (P_{GAL1}*AgCLB1/2*) and pAKH42 (P_{GAL1}*AgCLB1/2*-13myc) via homologous recombination. Both plasmids were verified with various digestions.

Construction of D-box mutants (*AgCLB5/6*) under their endogenous promoter or the *GAL1* promoter

The *AgCLB5/6* Δdb -13myc mutants were made using an overlap PCR approach, which deleted amino acids 22-31 ($\Delta db1$) or amino acids 38-47 ($\Delta db2$) or amino acids 22-31 and 38-47 ($\Delta db1\Delta db2$) or amino acids 22-47 ($\Delta [db1-db2]$) in *AgClb5/6p*. Since *AgCLB5/6* $\Delta db2$, *AgCLB5/6* $\Delta db1\Delta db2$ and *AgCLB5/6* $\Delta (db1-db2)$ caused lethality in *S. cerevisiae*, the inducible *GAL1* promoter was placed in front of *AgCLB5/6*-13myc (pAKH63). The pFA6a-His3MX6-P_{GAL1} cassette (Longtine et al., 1998) was amplified with the oligonucleotides GAL_CLB5/6-F and GAL_CLB5/6-R, resulting in a PCR fragment of 1996 bp containing the *GAL1* promoter and the *Schizosaccharomyces pombe HIS5* gene. This PCR fragment was co-transformed into yeast together with pAKH63 (pAgCLB5/6-13myc) to generate pAKH67, which was verified by sequencing. To generate pAKH68, pAKH67 was used as a template for a PCR reaction with the primer pair GAL_CLB5-dbA and CLB5db1B to produce a 470 bp product and a second reaction with the primer pair CLB5db1C and CLB5dbD to create a 428 bp product. Oligonucleotide GAL_CLB5-dbA was homologous to a region 400 bp upstream and CLB5dbD was homologous to a region 400 bp downstream of the D-box1. Oligonucleotide CLB5db1B contained homology to *AgCLB5/6* immediately upstream of the D-box1, but lacked the D-box1 sequences between nt 64-93. Additionally the 3' end of CLB5db1B had homology to the region immediately downstream of the D-box1, which was also present in the 5' half of oligonucleotide CLB5db1C. This overlapping homology was then used in a second PCR reaction involving the two products of A+B and C+D and additional GAL_CLB5-dbA and CLB5dbD primers to create a 845 bp fragment containing an in-frame deletion of the D-box1. To generate a full-length *AgCLB5/6* $\Delta db1$ mutant, this fragment was co-transformed into yeast with previously Nhe1 cut, dephosphorylated and gel purified pAKH67. The gap-repaired plasmid containing the deleted D-box1 was confirmed by sequencing and was called pAKH68 (P_{GAL1}*AgCLB5/6* $\Delta db1$ -13myc).

Similarly, to generate pAKH70 (P_{GAL1}*AgCLB5/6* $\Delta db2$ -13myc), oligonucleotides GAL_CLB5-dbA and CLB5db2B were used with pAKH67 as a template in the first reaction and CLB5db2C and CLB5dbD in the second reaction, resulting in two PCR fragments of 485 bp and 380 bp, respectively. CLB5db2B contained

sequences just upstream of D-box2 and lacked the sequences from nt 112-141 corresponding to db2. Additionally the 3' end of CLB5db2B had homology to the region immediately downstream of the D-box2, which was also present in the 5' half of oligonucleotide CLB5db2C. This overlapping homology was again used in a second PCR reaction involving the two products of A+B and C+D and additional GAL_CLB5-dbA and CLB5dbD primers to create a 845 bp fragment containing an in-frame deletion of the D-box2. The full-length mutant (pAKH70) lacking db2 was generated as for db1 via co-transformation in *S. cerevisiae* and verification by sequencing.

For the construction of pAKH69 ($P_{GAL1}AgCLB5/6\Delta db1\Delta db2$ -13myc), a similar attempt was chosen as for the $\Delta db2$. The only minor changes have been the template pAKH68 which was used instead of pAKH67 and the oligonucleotide "CLB5db2B_in_db1" instead of CLB5db2B.

To delete both D-boxes ($\Delta[db1-db2]$), a similar attempt was chosen with pAKH67 as template and the primer pair GAL-CLB5dbA and CLB5dbdB in the first, and CLB5db2C and CLB5dbD in the second PCR reaction. CLB5dbdB contained sequences just upstream of D-box1 and lacked the sequence from nt 64-141 corresponding to $\Delta(db1-db2)$. Additionally the 3' end of CLB5dbdB had homology to the region immediately downstream of the D-box2, which was also present in the 5' half of oligonucleotide CLB5db2C. The full-length mutant lacking both D-boxes was generated as db1, resulting in pAKH71, which was verified by sequencing.

Since these D-box mutants were all expressed from the inducible *GAL1* promoter which is not functional in *A. gossypii*, the *GAL1* was removed by digestion with Aat2. A 1900 bp fragment was excised from pAKH68 ($\Delta db1$), pAKH70 ($\Delta db2$), pAKH71 ($\Delta[db1-db2]$) and pAKH69 ($\Delta db1\Delta db2$) and each plasmid was self-religated, resulting in pAKH72, pAKH73, pAKH74 and pAKH75 which are expressed from their endogenous *A. gossypii* promoter.

Forced Localization cassettes (*AgCLB1/2* and *AgCLB5/6*)

The forced localization cassettes were built using p306-NLSa, p306-NLSi, p306-NESa and p306-NESi, kindly provided by N.P. Edgington and B. Futcher. In a first step the NLSa, NLSi, NESa and NESi were fused to 13myc. The NLSa and NLSi of the plasmids p306-NLSa and p306-NLSi

were PCR amplified with primers NLS-P1-Nde1 and NLS-P2-Sma1, containing at the 5' ends restriction sites for Nde1 and Sma1, respectively. The 158 bp PCR-product was cut with Nde1 and Sma1, resulting in a 132 bp fragment, ligated into the Nde1 and Sma1 cut and purified pAg-13myc vector. The resulting plasmids were called pAKH18 (containing NLSa) and pAKH19 (containing NLSi), which were both verified by sequencing.

The NESa and NESi of the plasmids p306-NESa and p306-NESi were PCR amplified with the primers NES-P1-Nde1 and NES-a-P2-Sma1 or NES-i-P2-Sma1, containing at their 5' ends restriction sites for Nde1 and Sma1, respectively. The 156 bp PCR-product was cut with Nde1 and Sma1, resulting in a 130 bp fragment, ligated into the Nde1 and Sma1 cut and purified pAg-13myc. This gave rise to pAKH20 (containing NESa) and pAKH21 (containing NESi), which were both verified by sequencing.

For the construction of the forced localization cassettes of the mitotic cyclin *AgCLB1/2*, the pAKH20 and pAKH21 cassettes were amplified with the oligonucleotides Clb1/2-NES-P1 and Clb1/2-Myc-P2, each giving rise to a 2800 bp fragment. These PCR fragments were co-transformed into yeast cells together with pAG7578 to generate pAKH25 (*AgCLB1/2*-NESa-13myc) and pAKH26 (*AgCLB1/2*-NESi-13myc). pAKH18 and pAKH19 were amplified with the oligonucleotides Clb1/2-NLS-P1 and Clb1/2-Myc-P2, giving rise to 2808 bp fragments, which were co-transformed into yeast together with pAG7578, generating pAKH23 (*AgCLB1/2*-NLSa-13myc) and pAKH24 (*AgCLB1/2*-NLSi-13myc). pAKH23, pAKH24, pAKH25 and pAKH26 were digested with Stu1, Nco1 and BsrG1 and the resulting DNA was transformed into *A. gossypii* mycelia, giving rise to the strains AKHAg21 (*AgCLB1/2*-NLSa-13myc), AKHAg20 (*AgCLB1/2*-NLSi-13myc) AKHAg19 (*AgCLB1/2*-NESa-13myc) and AKHAg22 (*AgCLB1/2*-NESi-13myc). These new strains were verified using oligonucleotides CLB1/2-I1 with G3 and CLB1/2-G4 with G2.

To force the S-phase cyclin *AgClb5/6p* into nuclei during the entire nuclear cycle two exogenous NLS sequences were C-terminally fused to *AgCLB5/6*. Forced localization cassettes were built with pAKH18 (containing NLSa-13myc) and pAKH19 (containing NLSi-13myc) cassettes, which were amplified with the oligonucleotides CLB5/6-NLS-A-P1 (for NLSa) or CLB5/6-NLS-I-P1 (for NLSi) and CLB5/6-NES-Myc-P2, each giving rise to a 2800 bp fragment. These PCR

fragments were co-transformed into yeast cells together with pAG9687, to generate pAKH76 (*AgCLB5/6-NLSa-13myc-GEN3*) and pAKH77 (*AgCLB5/6-NLSi-13myc-GEN3*), both verified by sequencing. About 30 μ g of pAKH76 and pAKH77 was digested with Apa1 and BsrG1 and the cut DNA was transformed into *A. gossypii* mycelia, giving rise to the strains AKHAg72 and AKHAg73, which were controlled by verification PCR with the primers CLB5-I1 with Mycl, and CLB5-G4 with G2.

To force *AgClb5/6p* out of the nuclei two exogenous NES sequences were C-terminally fused to *AgCLB5/6*. The pAKH20 (containing NESa-13myc) and pAKH21 (containing NESi-13myc) cassettes were amplified with the oligonucleotides CLB5/6-NES-P1 and CLB5/6-NES-Myc-P2, each giving rise to a 2800 bp fragment. These PCR fragments were co-transformed into yeast cells together with pAG9687, to generate pAKH61 and pAKH62 (verified by sequencing). pAKH61 and pAKH62 were digested with Apa1 and BsrG1 and the resulting DNA was transformed into *A. gossypii* mycelia. This gave rise to the strains AKHAg64 (*AgCLB5/6-NESa-13myc-GEN3*) and AKHAg65 (*AgCLB5/6-NESi-13myc-GEN3*), which were controlled by verification PCR with the primers CLB5-I1 and Mycl, and CLB5-G4 with G2.

Immunofluorescence, Hoechst/Actin and Calcofluor staining

Young *A. gossypii* mycelia were processed for immunofluorescence as described for yeast cells (Pringle et al., 1991) with slight modifications. Young mycelium containing approximately 75-100 nuclei were fixed for 1 hour in 3.7% formaldehyde (Fluka) in growth media at 30°C. Cells were incubated with 1.0 mg/ml Zymolyase (Seikagaku corporation) and 1% β -mercaptoethanol (Sigma) for 30-45 minutes to digest away the cell wall. Mycelia are washed twice with 1xPBS, resuspended in 1xPBS, allowed to settle on the immunofluorescence slide and blocked for 30 minutes with PBS + 1.0 mg/ml BSA (Sigma). Anti-myc and tubulin stainings were done sequentially so as to limit cross reactivity beginning with mouse anti-myc (Santa Cruz Biotech) at 1/100, then Alexa488-anti-Mouse (Molecular Probes) at 1/200, then Rat anti-tubulin (YOL34, Serotec) at 1/50 and finally Alexa 568-anti-Rat (Molecular Probes) at 1/200 with Hoechst (Molecular Probes) dye to visualize nuclei at 5 μ g/ml. Rabbit anti-GFP (Molecular Probes) was used to detect GFP-LacI-NLS at 1/100 dilution and Alexa488-anti-rabbit was used at 1/200 dilution

(Molecular Probes). Antibody dilutions and washes were made with PBS + 1.0 mg/ml BSA.

When nuclei were visualized in combination with actin, *A. gossypii* was grown to the desired stage, fixed for 1 hour in 3.7% formaldehyde in growth media at growth temperature and washed twice in 1xPBS. 100 μ l cells were mixed with 100 μ l Hoechst (1 μ g/ml, Molecular Probes) and 10 μ l Alexa488-Phalloidin (6.6 μ M in MeOH, Molecular Probes). Mycelia were incubated for at least 1 hour in the dark, at room temperature, then washed three times in 1xPBS and resuspended in a drop of mounting medium (100 mg-phenylenediamine in 10 ml 1xPBS, adjusted to pH 8.0 with 0.5 M Na₂CO₃ (pH 9.0) and brought to 100 ml final volume with glycerol), stored at -70°C.

Calcofluor, a fluorescent dye that interacts with chitin was used to stain the septa. 800 μ l of cell culture were mixed with 200 μ l of 1 mg/ml Calcofluor and incubated for 10 minutes in the dark. Mycelia were washed three times with ddH₂O and finally resuspended in a drop of mounting medium.

Protein extraction and Western blotting

A. gossypii was grown under desired conditions, collected, washed once with ice-cold 1xPBS and suspended in ice-cold lysis buffer (50 mM Tris-HCl [pH 7.5], 150 mM NaCl, 5 mM EDTA, 1% NP-40, 2 mM sodium pyrophosphate, 1 mM Na₃VO₄, 1 mM β -Glycerolphosphate and Roche complete protease inhibitor cocktail). An equal volume of 0.5 mm glass beads was added to this suspension, and cells were broken by vigorous vortexing during 6 x 30 sec. intervals in a bead beater at 4°C. A total of 150 μ g protein was separated on a 12% SDS-PAGE, transferred to nitrocellulose membranes (Amersham Biosciences), using standard conditions (Sambrook, 2001). Blocking was performed with 5% milk in PBS-Tween-20 (0.1%). Mouse anti-myc was used at 1/2000 and HRP-anti-mouse (Jackson Immunoresearch) was used at 1/10'000. ECL chemiluminescence solution (Amersham Biosciences) was used to develop the Western blots.

Microscopy

The microscope used for all fixed cell images (immunofluorescence and Hoechst stainings with cells mounted in standard fluorescent mounting medium was essentially as described in (Hoepfner et al., 2000).

Microscopy pictures were taken with an Axioplan 2 imaging microscope (Carl Zeiss, Feldbach, Switzerland) with a Plan Neofluar 100X Ph3 N.A. 1.3 objective. It was equipped with a 75 WXBO and a 100 WHBO illumination source controlled by a MAC2000 shutter and filter wheel system (Ludl Electronics, Hawthorne, NY). The camera was a TE/CCD-1000PB back-illuminated cooled charge-coupled device (CCD) camera (Princeton Instruments, Trenton NJ). The following filter sets for different fluophores were used: #02 for Hoechst, #15 for Rhodamine 568 and #09 for GFP (Carl Zeiss). The excitation intensity was controlled with different neutral density filters (Chroma Technology). MetaMorph 6.2r6 software (Universal Imaging Corporation) controlled the microscope, camera, and Ludl shutter controller (Ludl Electronics, Hawthorne, USA) and was used for processing images.

Stacks of tubulin, nuclei or actin images were processed using the "no-neighbors" deconvolution within MetaMorph 6.2r6. The Z-stacks were compressed using stack arithmetic "Maximize", brightness and contrast were adjusted, and images were overlayed using "color align".

Table 7. A. gossypii strains

Strain	relevant Genotype	Source
Δ/Δ	leu2Δ thr4Δ	
HHEF1-GFP	pHHEF1-GFP::GEN3 leu2Δ thr4Δ	C. Mohr PhD Thesis, (Altmann-Johl et al., 1996)
ASG38	AgSSPC42-GFP-GEN3, leu2Δ thr4Δ	(Alberti-Segui et al., 2001)
AKHAg1	Agclb1/2Δ::GEN3, leu2Δ thr4Δ / AgCLB1/2 leu2Δ thr4Δ	(Gladfelter et al., 2006)
AKHAg3	Agclb3/4Δ::GEN3, leu2Δ thr4Δ	This study
AKHAg4	Agclb5/6Δ::NAT1, leu2Δ thr4Δ / AgCLB5/6 leu2Δ thr4Δ	This study
AKHAg5	Agc1c1Δ::GEN3, leu2Δ thr4Δ	This study
ASG65	Agc1c1Δ::NAT1, leu2Δ thr4Δ	(Gladfelter et al., 2006)
ASG7	Agc1h1/2Δ::GEN3, leu2Δ thr4Δ / AgCLN1/2 leu2Δ thr4Δ	(Gladfelter et al., 2006)
ASG29	Agc1h3Δ::GEN3, leu2Δ thr4Δ	(Gladfelter et al., 2006)
AKHAg7	AgCLB1/2-GFP-GEN3, leu2Δ thr4Δ	This study
AKHAg8	Agclb5/6Δ::GEN3, leu2Δ thr4Δ / AgCLB5/6 leu2Δ thr4Δ	This study
AghPH04	leu2Δ thr4Δ ade2::ADE2-H4-GFP	H. Helfer
AKHAg9	Agclb1/2Δ::GEN3, leu2Δ thr4Δ ade2::ADE2-H4-GFP / AgCLB1/2 leu2Δ thr4Δ	This study
AKHAg11	Agyrb1Δ::GEN3, leu2Δ thr4Δ / AgYRB1 leu2Δ thr4Δ	This study
AKHAg12	Agstp1Δ::GEN3, leu2Δ thr4Δ / AgSRP1 leu2Δ thr4Δ	This study
AKHAg13	Agkap95Δ::GEN3, leu2Δ thr4Δ / AgKAP95 leu2Δ thr4Δ	This study
AKHAg14	Agmat1Δ::GEN3, leu2Δ thr4Δ / AgRNA1 leu2Δ thr4Δ	This study
AKHAg15	Agpse1Δ::GEN3, leu2Δ thr4Δ / AgPSE1 leu2Δ thr4Δ	This study
AKHAg17	Agkap123Δ::GEN3, leu2Δ thr4Δ	This study
AKHAg19	AgCLB1/2-NESa-13myc-GEN3, leu2Δ thr4Δ	This study (Gladfelter et al., 2006)
AKHAg20	AgCLB1/2-NLSi-13myc-GEN3, leu2Δ thr4Δ	This study
AKHAg21	AgCLB1/2-NLSa-13myc-GEN3, leu2Δ thr4Δ	This study
AKHAg22	AgCLB1/2-NESI-13myc-GEN3, leu2Δ thr4Δ	This study (Gladfelter et al., 2006)
Agade2Δ1	Agade2Δ310-566::GEN3, leu2Δ thr4Δ	This study (Knechtle, 2002)
AKHAg26	ade2::GFP-LacI-NLS::ADE2	This study (Gladfelter et al., 2006)
AKHAg27	ade2::GFP-LacI-NLS::ADE2	This study (Gladfelter et al., 2006)
AKHAg28	ade2::GFP-LacI-NLS::ADE2 + pAKH38 [pLacO-AgCLB1/2-13myc]	This study (Gladfelter et al., 2006)
AKHAg29	ade2::GFP-LacI-NLS::ADE2 + pAKH38 [pLacO-AgCLB1/2-13myc]	This study (Gladfelter et al., 2006)
AKHAg31	AgCLB5/6-GFP-GEN3, leu2Δ thr4Δ	This study
AKHAg32	Agnup1/6/100Δ::GEN3, leu2Δ thr4Δ / AgNUP1/6/100 leu2Δ thr4Δ	This study
AKHAg33	Agnup53/59Δ::GEN3, leu2Δ thr4Δ / AgNUP53/59 leu2Δ thr4Δ	This study
AKHAg34	Agnup145Δ::GEN3, leu2Δ thr4Δ / AgNUP145 leu2Δ thr4Δ	This study

AKHAg36	AgNUP116/100-GFP-GEN3, <i>leu2Δ thr4Δ</i>	This study
AKHAg37	AgCLB1/2Δdb1-13myc-GEN3, <i>leu2Δ thr4Δ</i>	This study
AKHAg38	AgCLB1/2Δdb2-13myc-GEN3, <i>leu2Δ thr4Δ</i>	This study
AKHAg39	pAKH47 [AgCLB1/2Δdb1-13myc-GEN3] <i>leu2Δ thr4Δ</i>	This study (Gladfelter et al., 2006)
AKHAg40	pAKH45 [AgCLB1/2Δdb2-13myc-GEN3] <i>leu2Δ thr4Δ</i>	This study (Gladfelter et al., 2006)
AKHAg41	pAKH46 [AgCLB1/2Δdb1Δdb2-13myc-GEN3] <i>leu2Δ thr4Δ</i>	This study (Gladfelter et al., 2006)
AKHAg42	pAKH52 [AgCLB5/6-13myc-GEN3] <i>leu2Δ thr4Δ</i>	This study
AKHAg46	AgCLB5/6-13myc-GEN3, <i>leu2Δ thr4Δ</i>	This study
AKHAg47	AgCLB3/4-GFP-GEN3, <i>leu2Δ thr4Δ</i>	This study
AKHAg48	AgCLB3/4-13myc-GEN3, <i>leu2Δ thr4Δ</i>	This study
AKHAg49	<i>ade2::GFP-LacI-NLS::ADE2</i> + pAKH57 [pLacO-AgCLN1/2-13myc]	This study
AKHAg54	AgCLN3-GFP-GEN3, <i>leu2Δ thr4Δ</i>	This study
AKHAg55	AgCLN3-13myc-GEN3, <i>leu2Δ thr4Δ</i>	This study
AKHAg57	AgCLB1/2-GFP-GEN3, <i>leu2Δ thr4Δ</i>	This study
AKHAg58	pAKH63 [AgCLB5/6-13myc-GEN3] <i>leu2Δ thr4Δ</i>	This study
AKHAg64	AgCLB5/6-NESa-13myc-GEN3, <i>leu2Δ thr4Δ</i>	This study
AKHAg65	AgCLB5/6-NESi-13myc-GEN3, <i>leu2Δ thr4Δ</i>	This study
AKHAg66	pAKH72 [CLB5/6Δdb1-13myc-GEN3] <i>leu2Δ thr4Δ</i>	This study
AKHAg67	pAKH73 [CLB5/6Δdb2-13myc-GEN3] <i>leu2Δ thr4Δ</i>	This study
AKHAg68	pAKH74 [CLB5/6Δ(db1-db2)-13myc-GEN3] <i>leu2Δ thr4Δ</i>	This study
AKHAg69	pAKH75 [CLB5/6Δdb1Δdb2-13myc-GEN3] <i>leu2Δ thr4Δ</i>	This study
AKHAg72	AgCLB5/6-NLSa-13myc-GEN3, <i>leu2Δ thr4Δ</i>	This study
AKHAg73	AgCLB5/6-NLSi-13myc-GEN3, <i>leu2Δ thr4Δ</i>	This study
ASG43	AgCLB1/2-13myc-GEN3, <i>leu2Δ thr4Δ</i>	(Gladfelter et al., 2006)
ASG60	AgCLN1/2-13myc-GEN3, <i>leu2Δ thr4Δ</i>	(Gladfelter et al., 2006)
ASG61	AgSIC1-13myc-GEN3, <i>leu2Δ thr4Δ</i>	(Gladfelter et al., 2006)
ASG70	<i>ade2::AgCLB1/2-13myc-GEN3::ADE2</i>	This study (Gladfelter unpublished)
ASG71	<i>ade2::AgCLB1/2Δdb1-13myc-GEN3::ADE2</i>	This study (Gladfelter unpublished)
ASG73	<i>ade2::AgCLB1/2Δdb1Δdb2-13myc-GEN3::ADE2</i>	This study (Gladfelter unpublished)

All AKHAg and ASG strains are *A. gossypii* derived from our reference strain ($\Delta/1f$) strain. Individual nuclei are haploid and in homokaryotic strains, all nuclei have the same genotype. In cases of heterokaryons, where different nuclei have different genotypes, the two different types are written, separated by a slash (/).

Table 8.
***S. cerevisiae* strains**

Strain	relevant Genotype	Source
AY52	<i>cln1Δcln2Δcln3Δ P_{GAL1}CLN1</i>	D. Lew
AY117	<i>clb1Δclb2Δclb3Δ P_{GAL1}CLB1</i>	D. Lew
AKHSc1	PAKH67 [P _{GAL1} AgCLB5/6-13myc]	This study
AKHSc2	PAKH68 [P _{GAL1} AgCLB5/6Δdb1-13myc]	This study
AKHSc3	PAKH69 [P _{GAL1} AgCLB5/6Δdb1Δdb2-13myc]	This study
AKHSc4	PAKH70 [P _{GAL1} AgCLB5/6Δdb2-13myc]	This study
AKHSc5	PAKH71 [P _{GAL1} AgCLB5/6Δ(db1-db2)-13myc]	This study
AKHSc6	AY52 + pCLB2-13myc	This study
AKHSc7	AY52 + PAKH23 [AgCLB1/2-NLSa-13myc]	This study
AKHSc8	AY52 + PAKH24 [AgCLB1/2-NLSi-13myc]	This study
AKHSc9	AY52 + PAKH25 [AgCLB1/2-NESa-13myc]	This study
AKHSc10	AY52 + PAKH26 [AgCLB1/2-NESi-13myc]	This study
PSY714	<i>MAT a, rna1-1 ura3-52 leu2Δ1 trp1</i>	P. Silver

**Table 9.
Plasmids**

Plasmids	Vector	Insert	Source
pGEN3		GEN3	(Wendland et al., 2000)
pUC19		NAT1	(Yanisch-Perron et al., 1985)
pUC19NATPS			(D. Hoepfner, personal communication)
pFA-13myc			(Longtine et al., 1998)
pAg-13myc	pGEN3	13myc-GEN3	(Gladfelter et al., 2006)
pCLB2-13myc	pAG7578	AgCLB1/2-13myc-GEN3	(Gladfelter et al., 2006)
pCLN2-13myc	pAG5016	AgCLN1/2-13myc-GEN3	(Gladfelter et al., 2006)
pGUG	pGEN3	GFP	(Knechtle, 2002)
pAIC	pBSIISK(+) ^{ScaI}	Ade2Δ1	(Knechtle, 2002)
pFA6a-His3MX6-P _{GAL1}	pBM272	P _{GAL1/10}	(Longtine et al., 1998)
pAG7578	PRS416	AgCLB1/2	C. Mohr (Dietrich et al., 2004, Suppl. Material)
pAG5016	PRS416	AgCLN1/2	C. Mohr (Dietrich et al., 2004, Suppl. Material)
pAG9687	PRS416	AgCLB5/6, AgCLB1/2	C. Mohr (Dietrich et al., 2004, Suppl. Material)
pAG8592	PRS416	AgRNA1	C. Mohr (Dietrich et al., 2004, Suppl. Material)
pAG10841	PRS416	AgRNA1	C. Mohr (Dietrich et al., 2004, Suppl. Material)
pAG10848	PRS416	AgNUP116/100	C. Mohr (Dietrich et al., 2004, Suppl. Material)
pAKH1	PRS415	AgCLB5/6	This study
pAKH2	PRS415	AgCLB1/2	This study (Gladfelter et al., 2006)
pAKH7	pAG7578	AgCLB1/2-GFP	This study
pAKH9	pUC19	AgCLB1/2-GFP	This study
pAKH12	PRS306	NLSa	(Edgington and Futcher, 2001)
pAKH13	PRS306	NLSi	(Edgington and Futcher, 2001)
pAKH14	PRS306	NESa	(Edgington and Futcher, 2001)
pAKH15	PRS306	NESi	(Edgington and Futcher, 2001)
pAKH18	pAg-13myc	NLSa	This study
pAKH19	pAg-13myc	NLSi	This study
pAKH20	pAg-13myc	NESa	This study (Gladfelter et al., 2006)
pAKH21	pAg-13myc	NESi	This study (Gladfelter et al., 2006)
pAKH23	pAG7578	AgCLB1/2-NLSa-13myc	This study
pAKH24	pAG7578	AgCLB1/2-NLSi-13myc	This study
pAKH25	pAG7578	AgCLB1/2-NESa-13myc	This study (Gladfelter et al., 2006)
pAKH26	pAG7578	AgCLB1/2-NESI-13myc	This study (Gladfelter et al., 2006)
pLKL55Y	PRS303	P _{Sch153} GFP-LacI-NLS	(Pearson et al., 2001)

PLKL60Y	pFA6MX	LacO-32mer	(Pearson et al., 2001)
PAKH35	PAIC	P _{S^{CH}/S³} GFP-LacI-NLS (6)	This study (Gladfelter et al., 2006)
PAKH36	PAIC	P _{S^{CH}/S³} GFP-LacI-NLS (12)	This study (Gladfelter et al., 2006)
PAKH37	pUC21	LacO-32mer	This study (Gladfelter et al., 2006)
PAKH38	pCLB2-13myc	LacO-32mer	This study (Gladfelter et al., 2006)
PAKH40	PAG9687	AgCLB5/6-GFP	This study
PAKH41	PAKH2	P _{GAL} ¹ AgCLB1/2	This study (Gladfelter et al., 2006)
PAKH42	pCLB2-13myc	P _{GAL} ¹ AgCLB1/2-13myc	This study (Gladfelter et al., 2006)
PAKH45	pCLB2-13myc	AgCLB1/2Δdb2-13myc-GEN3	This study (Gladfelter et al., 2006)
PAKH46	pCLB2-13myc	AgCLB1/2Δdb1Δdb2-13myc-GEN3	This study (Gladfelter et al., 2006)
PAKH47	pCLB2-13myc	AgCLB1/2Δdb1-13myc-GEN3	This study (Gladfelter et al., 2006)
PAKH51	PAG10848	AgNUP116/100-GFP	This study
PAKH52	PAG9687	AgCLB5/6-13myc	This study
PAKH53	PRS416	AgCLN3	This study
PAKH54	PRS416	AgCLB3/4	This study
PAKH55	PAKH54	AgCLB3/4-GFP	This study
PAKH56	PAKH54	AgCLB3/4-13myc	This study
PAKH57	pCLN2-13myc	LacO-32mer	This study
PAKH58	PAKH53	AgCLN3-GFP	This study
PAKH59	PAKH53	AgCLN3-13myc	This study
PAKH61	PAKH52	AgCLB5/6-NESa-13myc	This study
PAKH62	PAKH52	AgCLB5/6-NESi-13myc	This study
PAKH63	PRS416	AgCLB5/6-13myc	This study
PAKH67	PAKH63	P _{GAL} ¹ AgCLB5/6-13myc	This study
PAKH68	PAKH67	P _{GAL} ¹ AgCLB5/6Δdb1-13myc	This study
PAKH69	PAKH68	P _{GAL} ¹ AgCLB5/6Δdb1Δdb2-13myc	This study
PAKH70	PAKH67	P _{GAL} ¹ AgCLB5/6Δdb2-13myc	This study
PAKH71	PAKH67	P _{GAL} ¹ AgCLB5/6Δdb1-13myc	This study
PAKH72	PAKH68	P _{GAL} ¹ AgCLB5/6Δ(db1-db2)-13myc	This study
PAKH73	PAKH70	AgCLB5/6Δdb1-13myc	This study
PAKH74	PAKH71	AgCLB5/6Δdb2-13myc	This study
PAKH75	PAKH69	AgCLB5/6Δdb1Δdb2-13myc	This study
PAKH76	PAKH52	AgCLB5/6-NLSa-13myc	This study
PAKH77	PAKH52	AgCLB5/6-NLSi-13myc	This study
PAKH78	PAIC	AgCLB1/2-13myc-GEN3	This study
PAKH79	PAIC	AgCLB1/2Δdb1-13myc-GEN3	This study
PAKH80	PAIC	AgCLB1/2Δdb2-13myc-GEN3	This study
PAKH81	PAIC	AgCLB1/2Δdb1Δdb2-13myc-GEN3	This study

Table 10.
Oligonucleotide primers

Primer	Sequence 5'-3'
CLB5S1	CTTCGGTTGAGAGCAACTGTGAGGGCACGGAACTGGAGCCgctagggataacagggtaaat
CLB5S2	CAGCACGTAATTCATAATCTTGATATTTTTCTATATAGgcatgcaagcttagatct
CLB5-NS1	CTTCGGTTGAGAGCAACTGTGAGGGCACGGAACTGGAGCCccagtgaaatcagctcgg
CLB5-NS2	CAGCACGTAATTCATAATCTTGATATTTTTCTATATAcgccaagcttgcagcct
CLB5-G4	CAAGGGTGC GTGCGTAGAGC
CLB5-I1	GGTCCCGAGGGTTTCGAGTG
CLB5-G1	GC CGTCCACCCAGCCCTGG
CLB5/6-GS1	GGGCTTTGGTTGCCGTGAAAACCTGGTGTGATGAACAAAAGATTGTGAGAggtcagggcgtggagctg
CLB5/6-GS2	GTGCAAGGATGTGCTATGGTTACGGTCTCGCCATTTGGCCAGTCagggaccctggcacggagc
CLB5mycF	GGGTTGCCGTGAAAACCTGGTGTGATGAACAAAAGATTGTGAGAcggtaccctggggttaataacggtgaa
CLB5mycR	CGGTCCTCGCCATTTGGCCAGTCAACGCCATGTTCATGAACCAATACcactagtggtatcagatcagctg
CLB5MycI	CTGCGCCATGATGCTCAACTACGGTG
CLB3-S1	GCAACGGTAGCAGCTTCAGCAGCAAGAGCGGAGAGCAGCGAAACCTGGAGGCGctagggataacagggtaaat
CLB3-S2	CATATCCTATCCACAGACGCCAGCCCTATCCGGCTGCCCCGATGCATaggcatgcaagcttagatct
CLB3/4-G1	CGTCGCTGGGGCCAGCCGCCG
CLB3/4-I1	GC CGTGAGCAAGGCCGACAAC
CLB3/4-G4	CAATGCTATCCGGCTGTATTGCC
CLB3/4-P1	CGTCTGAGGTC TAGAGACTCGCCCCGAGCAGATCATCGAC
CLB3/4-P2	GAGCGAGTAAGCTTCATTCACATATAGCCGGCCG
CLB3/4-GS1	CAGGTGGTTGCTCGGTGGATCGCGATGGCGGAGGAGAACTCCAGCCGGCTgggicagggcgtggagctg
CLB3/4-GS2	CTTGTTGGCGGCTCTTGTTCCGCCAACACATGCTTATTAGTTTCATATCCTATCCagggaccctggcacggagc
CLB3/4-myc-P1	CAGGTGGTTGCTCGGTGGATCGCGATGGCGGAGGAGAACTCCAGCCGGCTcggatccccgggtaattaa
CLB3/4-myc-P2	CTTGTTGGCGGCTCTTGTTCCGCCAACACATGCTTATTAGTTTCATATCCTATTCcgtggatcgtatcagatcgtg
CLB1/2-S1	GCAGGACAAACGACCCGGGACCGCAGCAGACTGCCGGTGGGCAGCCGGTACGAAGCCCTGAGcctagggataacagggtaaat
CLB1/2-S2	GCAATTAGTTATTACTGTCATGATTAATGCTGTATGAGTGCCGCTGGATCTATCCGaggtcagcttagatct
CLB1/2-G1	CGAGGCACCAACGGGCTACTAC
CLB1/2-I1	CCAACCCGGTGGTCCACGACG
CLB1/2-I1*	GGGATTCTGCCCTCCTTATGTG
CLB1/2-G4	CAGCTCTACGCCACGCCACCCTTGTGCC
CLB1/2-GS1	GTTATGACCAGAAAGTTACGATATTATGACTTTACATGAGACACAAAACCTGAATATgggicagggcgtggagctg
CLB1/2-GS2	GAATGCAATTAGTTACTGTCATGATTAATGCTGTATGAGTGCCCGTGGagggaccctggcacggagc

CLB2-MycF	CCAGAAGTTACGATATTATGACTTTACATGAGACACAACCTGAATATcggatccccgggthaata
CLB2-MycR	CTGTCAITGATTAATGCTGTATGAGTGCCTGGATCTATCCGTTTCCAglygatcigatatacagatcig
CLB2-Myc-I	GGGATGGGAACCTTGATACATTACAGTg
GALC1b2F	GACATTTGGACACACGAAACGACCAAGCCACCAAGTGCCTTCTTcgaattcgaagctcgtttaaac
GALCLB2R	CTTGTTCAACGCTCGACATCTCAGGCTTCGTACCCTGCCCCcaithttagatccgggtttt
CLN1/2S1G	GGCCGGGTTTTGGCCGACCCGGTGAAGATCAGACGCACAGAGCCCAACCCGAGgctaggatatacaggytaat
CLN1/2S2G	GCTCGGAATGAAAAAAGACAGCCGCGGGAATAAATTACCCTCAGGAAAAGCCGagycatcyaagcttagatct
CLN1/2-I1	CCGTAGCACCACCGCGCTTCGAGCAGTAACGG
CLN1/2-G1	CCGCTCCAGCAGCACACAAGATGGGAAGACC
CLN1/2-G4	GGGCTAAGCGCGGATTCGCCGAACCCCGATGC
CLN2-MycF	GATCATCCCTTGATATCACTGGCAATTTGGAAATGCCAACTCAITTTGGTAacggtatccccgggthaata
CLN2-MycR	CTATTATTACGATGAACCTTAAATGAAAAACGGTAATGAAGATGCTCggtlygatcigatatacagatcig
CLN2-Myc-I	GTGAGCGTCAATAGCATATCTCAGAAG
CLN3S1G	GGGCTGTTAATATCTCATACCCCGAACAACCTTTGCATATTATACACATATTCGTcgtaggatatacaggytaat
CLN3S2G	GCAGTAGACCGGATAGATAGACAGCCGGATAGTGGGGCCGGTATGCTAGagycatcyaagcttagatct
CLN3-I1	GGCTCTGTCCCGCTCCGCTC
CLN3-G1	CCAGGATCTGCATAACCGATTc
CLN3-G4	GATCCGTTCCGACTAGCGTcGAG
CLN3-P1	CGTCTGATGCTAGACCTGCCGTGGAATGTCATGTCCC
CLN3-P2	GATCTAGTGGATCCGTTCCGACTAGCGTCGAGAATGCC
CLN3-GS1	CATGGACCTTGAGTTCTTCGACATGGATCATGCCCTGTTCAAGAAACTACCGcgttcagcctcgtgagctg
CLN3-GS2	CTGCATTTAATGGCCGACTGTGCCATATGGCCCTAGAGAGCAGTAGAGCCaggyactcgtcagcagc
CLN3-M1	CATGGACCTTGAGTTCTTCGACATGGATCATGCCCTGTTCAAGAAACTACCGcggatccccgggthaata
CLN3-M2	CTGCATTTAATGGCCGACTGTGCCATATGGCCCTAGAGAGCAGTAGAGCCgltlygatcigatatacagatcig
Sic1-S1	TACACGGAGCAGCGCGGAACCTAGTGGGCGCCGAGAAAGGGAAAGCCGAGgctaggatatacaggytaat
Sic1-S2	CCCCGACTGGTTATGCCAAGCCCTCCGCCAGTTTCGAACTCACCAGagycatcyaagcttagatct
Sic1-NS1	CACGGAGCAGGCGGAACCTAGTGGGCGCCGAGAAAGGGAAAGCCGACcaglygaattcgaagctcgtg
Sic1-NS2	CGCGGCTTGAAACAGCTCCTCCTCTCCGGCGGTGAGCTCCCGCTGgtaagccaagcttgcagctcct
Sic1-G1	CCTGCCCCCTGCCGCCACTGTC
Sic1I	CGGATCGTGACGTTCCGAACCTGGCCGG
Sic1-I1	GTTCTGCTCCGGCGACCCGCAC
Sic1-G4	CGCGGCGTAAGACCAAGCCGGGCACC
Sic1-MycF	GTTGTTTGGCCCGGAGCTGGAGGACCGGGCCCTGGCCGATGGCATGcggatccccgggthaata
Sic1-MycR	CCAAGTTTCCCTACGTACAGATAGTTATTGACCATACTAAAGTCCCGGcgtlygatcigatatacagatcig
G2	GTTTAGTCTGACCATCTC
G2.1	TGCCCTCCAGCATAGTCGAAG

G3
V2*NAT1
V3*NAT1
GG2
Green2
MycI

TCCGAGACCGGATACCAGGATC
GTGGTGAAGGACCCCATCCAG
ACATGAGCATGCCCTGCCCC
CATCACCTTCAACCCTCTCCAC
GTCCTGTAGTCCCGTTCATC
CGAGTCCGTTCAAGTCTTCTTCTGAG

NLS-P1-Nde1
NLS-P2-Sma1
NES-P1-Nde1
NES-a-P2-Sma1
NES-i-P2-Sma1
Cib1/2-NES-P1
Cib1/2-NLS-P1
Cib1/2-Myc-P2
CLB5/6-NES-P1
CLB5/6-NES-Myc-P2
CLB5/6-NLS-A-P1
CLB5/6-NLS-I-P1

GATGGCATAGCATATGAATTCGAGCTCTGCGGCCGCGGTCC
GTCAAAGATATGCCCGGATGACTAGTGGCCCGTACTACCTACC
GATGGCATAGCATATGGCCCGGTTTAGCACTTAAATTAGC
GTC AAGCTAGGCCCGGGCTACTACCGATATCTAAACCTGCC
GTC AAGATATGCCCGGGCTACTACCGATATCTGCACCTGCC
CCAGAAGTTACGATATTAATGACTTTACATGAGACACAAACTGAATA Tggtttagcacttaaatagc
CCAGAAGTTACGATATTAATGACTTTACATGAGACACAAACTGAATA Tatttcgagctcgcgcccgggtcc
CTGTCAATGATTAATGCTGTATGAGTGCCGTGGATCTCCGTTCCAgactcactataggagaccg
GGTTGCCGTGAAAACCTGGTGTGATGAACAAAAGATTGTGAGAGgttttagcacttaaatagc
CGGTCCCTGCCATTTGGCCAGTCAACGCCATGTCATGAA CCAATACcgcactactataggagaccg
GGTTGCCGTGAAAACCTGGTGTGATGAACAAAAGATTGTGAGAGgtccaaaagaaagcgaag
GGTTGCCGTGAAAACCTGGTGTGATGAACAAAAGATTGTGAGAGgtccaaaagaaagcgaag

clb2dbA
clb2db1B
clb2db1C
clb2dbD
clb2db2B
clb2db2C

CGAGGTCGACGGTATCGATAAGCTTGATATCGAATTCCTGCAGCCCGGGGATCATCAAGCCAAAC
GCCTCTTGAGACAAAGTAGTCTTCGGCCAGCTAGCAGTGGTCTTTCATCCCGCAGCCACTCGG
CTACTTTGTCTCAAGAGGCTGCGAATCCAAATGCGACTCTGTTCCGGCTACACGAACCTCGTTCCG
CAGTGCTCGTAGTCAATCGCTGCTACTCGGACTGACCCCTGTAAGCGTTGATTTAATGTCTGC
GCGACCCAGTGGGCACAACCTTCAATTTGCGGGATCAATGAGCCAGCCACCTCGCCGACTG
GTTGTGCCCACTGGGTCCACCTGTCTGCCGTTGCGGCAGCAGCAGCGGCTCAAATGGC

GAL_CLB5/6-F
GAL_CLB5/6-R
GAL_CLB5-dbA

CCTCGCTGACGAGCGGCTTCTGGTTGAGAGCAACTGTGAGGCGACGGACGTcgaattcgagctgttaaac
GTCCGACACTCTTCTGGTTCCCTACCAGGACTCATGGCTCCAGTTCGACGTccttcgtagctgcaggtcgac
GGCAGTAACTGGCCCCACAAAACCTTCAAATGAACGAATCAAATTAACAACCATAGGATG

CLB5dbD
CLB5db1B
CLB5db1C
CLB5db2B
CLB5db2C
CLB5dbdB
CLB5db2B_in_db1
AgKAP95-S1
AgKAP95-S2

CCGGATGTAACCGGCACTGCCGTTCTGCACGTAGTTCACCACGCACCGTTGTCTCCTG
CTTGCCGGCACCCCAAGCACCCTCCCGCCGCCCCGGCTGCTTCGTTCTCGTCCGACACTCTTCTG
ACGGTGTGGGGTCCCGCGCAAGCGCTCGGAGCAGTGGCGTGAACACCGCGGAAGCAGGAGCG
GTCGCCCTCCCTGCTCCCGCTCGCACCCCAACCGTGTGCGCCGCTTCCGCTAGCTCCCC
ACCGGAAGCAGGAGCGCGACGGGCGGCGACGGGAGCGCGCGGCTGCTCGTCCGACACTCTTCTGTTTC
GTCGCCCTCCCTGCTCCCGCTCCCGCCGCCCCGGCTGCTTCGTTCTCGTCCGACACTCTTCTGTTTC
GTCGCCCTCCCTGCTCCCGCTGGCACCCCAACCGTCCCGCCGCCCCGGCTGCTTCGTTCTCGTCC
GCGTACCAGGTTGTGCGGCGAACCCAGAGTGGTACAAAGAGCGAAAgctagggataaacagggtaac
CGCAGAAAGAAAATGAGTAATAAGATAAAATTTCTGGAGTGTAAGGaggtcatgcagcttagatct

AgKap95-G1 GCCCCGGATCTTCAACATGAAGG
 AgKap95-I1 GGAGGGCTCGAGATCTGCGCCC
 AgKap95-G4 CGCAGAAAGTGTCCAATGGACGTTAC
 AgSRP1-S1 GCAGTAGTGAGCCGATCGCAAGAGTCTCAGAGCGTATTGCAgctaggataaccaggytaat
 AgSRP1-S2 GGTTCATGTTGGAACCAAAAGGTTACCAGGCGTGGCCGgagycatgcaagcttagatct
 AgSRP1-G1 GGCAAGCCAAATCGCAGGAATCCCG
 AgSRP1-I1 GCATTTCCGGCTGGTCTCGTTCA
 AgSRP1-G4 CTGCACATCCTCATCAACCCGG
 AgYRB1-S1 GTTTACTCCTGGCGTAGGTTCCGGGTCCACAGTACAGATCAACGAGGAATCgctaggataaccaggytaat
 AgYRB1-S2 CTTAATATACTCGCCTATCTCCTACATAACTTCCCGGATCAGCGagycatgcaagcttagatct
 AgYRB1-G1 CCTGTGATCTCGCTACCGAAACACC
 AgYRB1-I1 CAGGAACCTCACGTCCTCCCGTGC
 AgYRB1-G4 CTCCCATCACAGAAAGCAGATTTGG
 AgKAP123-S1 GATACCAATAGCACCCCGCACACGATTTACCCTAGACCCTAGCATAAGCCGAGCgctaggataaccaggytaat
 AgKAP123-S2 CAGGCGATAACGGGAGCCAGAACAGCAGCATTCTGGGCCACAATGCCATTTAG agycatgcaagcttagatct
 AgKAP123-G1 CCATAATCCTCGCAGCTGAGAAGC
 AgKAP123-I1 CCTCGTCTCCAAGGACCGCGGAATCG
 AgKAP123-G4 GACGCCCTCCGGCTGAAGATGAC
 AgPSE1-S1 GCAGCGGAAGAGACCTTGAATAACCAATGGATCACCGGAGGAAACATCgctaggataaccaggytaat
 AgPSE1-S2 GTCGTAATGTCCTTGCAATATAGAGGATGGATATCTCTGGAAGTATCGTAGGGCagycatgcaagcttagatct
 AgPSE1-G1 GGATGTCGGCTTATCTAGCGACG
 AgPSE1-I1 GCCTGACGTGCGTTGTGTAAG
 AgPSE1-G4 GGTCCTAGTAGCTGCCAACCCCATG
 AgRNA1-S1 TTACTTTGAGCCCAAGGGCCAGGACGCAAAAGCAGGACGAGGACAGGACAAAgctaggataaccaggytaat
 AgRNA1-S2 TGATGAGGTATACTCCAGCAGATACAGTGACGAAACCAGAGGTTACCAGgagycatgcaagcttagatct
 AgRNA1-G1 GTAAGGTTATGTGAGCCCGCGTCCG
 AgRNA1-I1 CTGATGCCGTTCTGTACAGGGCCGAC
 AgRNA1-G4 CATGCTGTCCGGATAAAGGACC
 AgNUP53-S1 CTGTAAGTCGACTGGCGCTTGTCCGTTAGATTGTGCTCAGGAAACAagctaggataaccaggytaat
 AgNUP53-S2 GGCGCGGATTTGTCAAITCACAAITTCGTTCCAGGCCAAAAAGCCAAITTGagycatgcaagcttagatct
 AgNUP53-G1 CAAAAGCACTGCGACAGCCGGCCCTGG
 AgNUP53-I1 GGAGGCCGTTAATTTACGCGTCCG
 AgNUP53-G4 CATAACTTCCTCAGCAGGTCGGGAGG
 AgNUP116-S1 CCGTAAACAACGTAAGCAGCGAAAGGATTGATCCGTAACACTCCAGCTCAgctaggataaccaggytaat
 AgNUP116-S2 CGCACGTGACAAGCACGTTAGATTAGGCGACCGCGGTGTCTACGATGagycatgcaagcttagatct
 AgNUP116-G1 GGCAACGAGCCTTGAAGACATGG
 AgNUP116-I1 CCACCTCCACCGGCCGATCGAGTTCC
 AgNUP116-G4 CCACCCGAGGGTGTCTCGGCTATTCC
 AgNUP145-S1 CGATACAGGCACTTGAAGCTTGGATACATATAATCTGCCCATGTTTGgctaggataaccaggytaat
 AgNUP145-S2 GACCGTTAGTGTACGTGATGCGAGCGCCGTTTCAAGGTAGATAGagycatgcaagcttagatct

AgNUP145-G1	CAATGACGCTGCATGTAGCTCCAGC
AgNUP145-I1	GCTGCTAACTTGCAGACACTGCCG
AgNUP145-G4	GGTTACGACACCCGACGGAGGTTG
AgNUP116-GS1	GTC AAGACGGGCACCTACACCTTCATCGTAGACACGCCCGGTCCCGgtgcaggcctggagctg
AgNUP116-GS2	GGAGTACAAAACAAGTTAAACATCCACCGCTCATTGCTCCAACAGGaggaccctggcacgggagc

Lower case letters are regions of homology to the cassette containing a selectable marker.

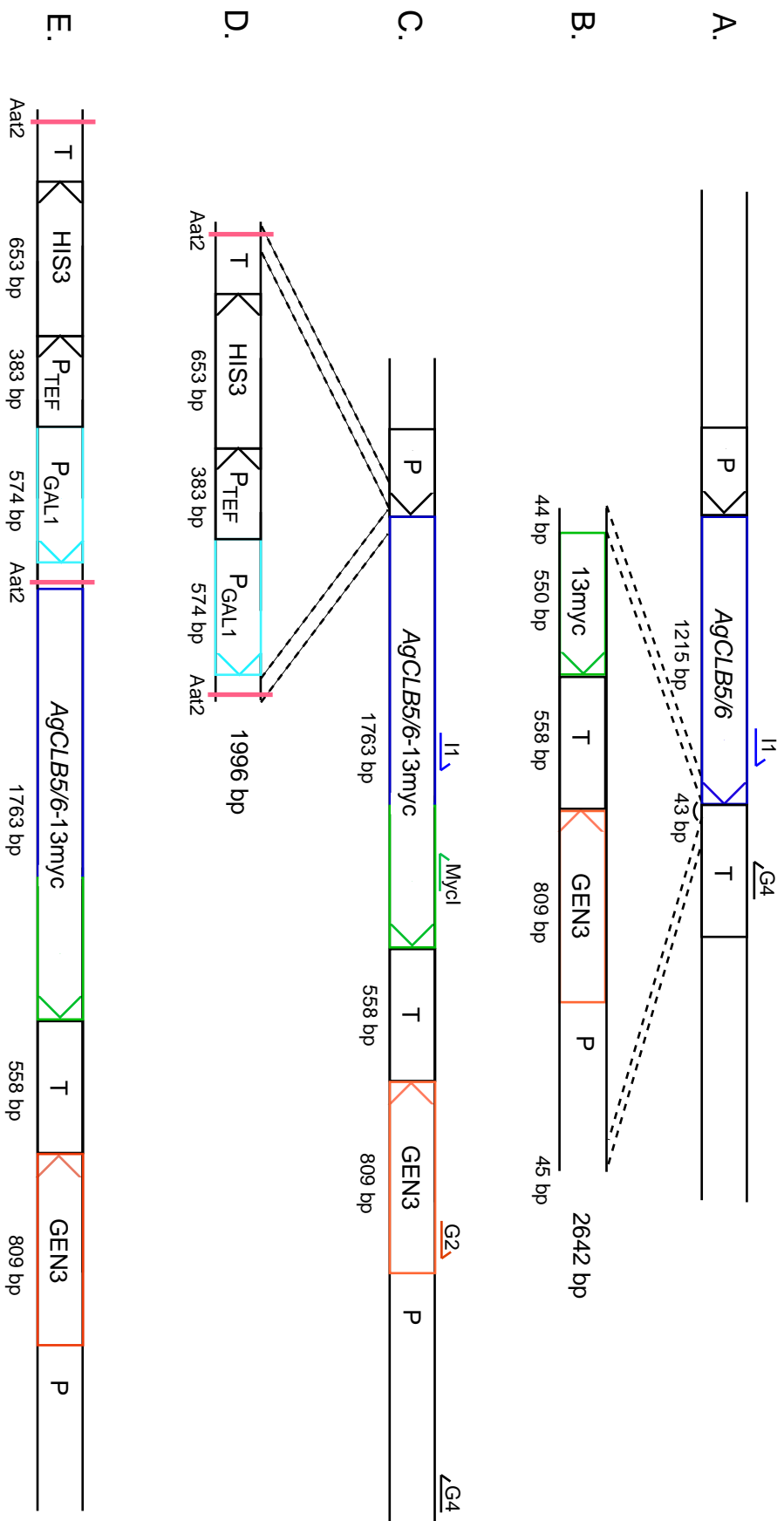


Figure 45

Construction of pGAL1AgCLB5/6-13myc

A. pAG9687 containing *AgCLB5/6*. B. pAg-13myc amplified with the oligonucleotides for C-terminal *AgCLB5/6*-13myc fusion resulting in a PCR fragment of 2642 bp. 43 bp of the terminator region of *AgCLB5/6* are deleted, as indicated. Dashed lines represent the homology region of pAG9687 and the PCR cassette. C. Homologous recombination in *S. cerevisiae* during co-transformation. The plasmid (pAKH52) was sequenced, completely digested with *Nhe*I, *Kpn*I and *Nde*I and transformed into *A. gossypii* resulting in AKHAg46. Verification oligonucleotides are indicated by arrows. D. pFA6a-His3MX6-P_{GAL1} was amplified by PCR with the oligonucleotides for GAL1 overexpression, containing *Aat2* restriction sites on both ends, resulting in a 1996 bp fragment. E. Homologous recombination in *S. cerevisiae* during co-transformation of the PCR fragment and pAKH63 (pAKH52 digested with *Not*I and *Xho*I and ligated in the previously cut and purified pRS416), resulting in the overexpression of *AgCLB5/6*-13myc if grown on Galactose (pAKH67). This construct was the basis for the construction of all *AgCLB5/6*-D-box mutants.

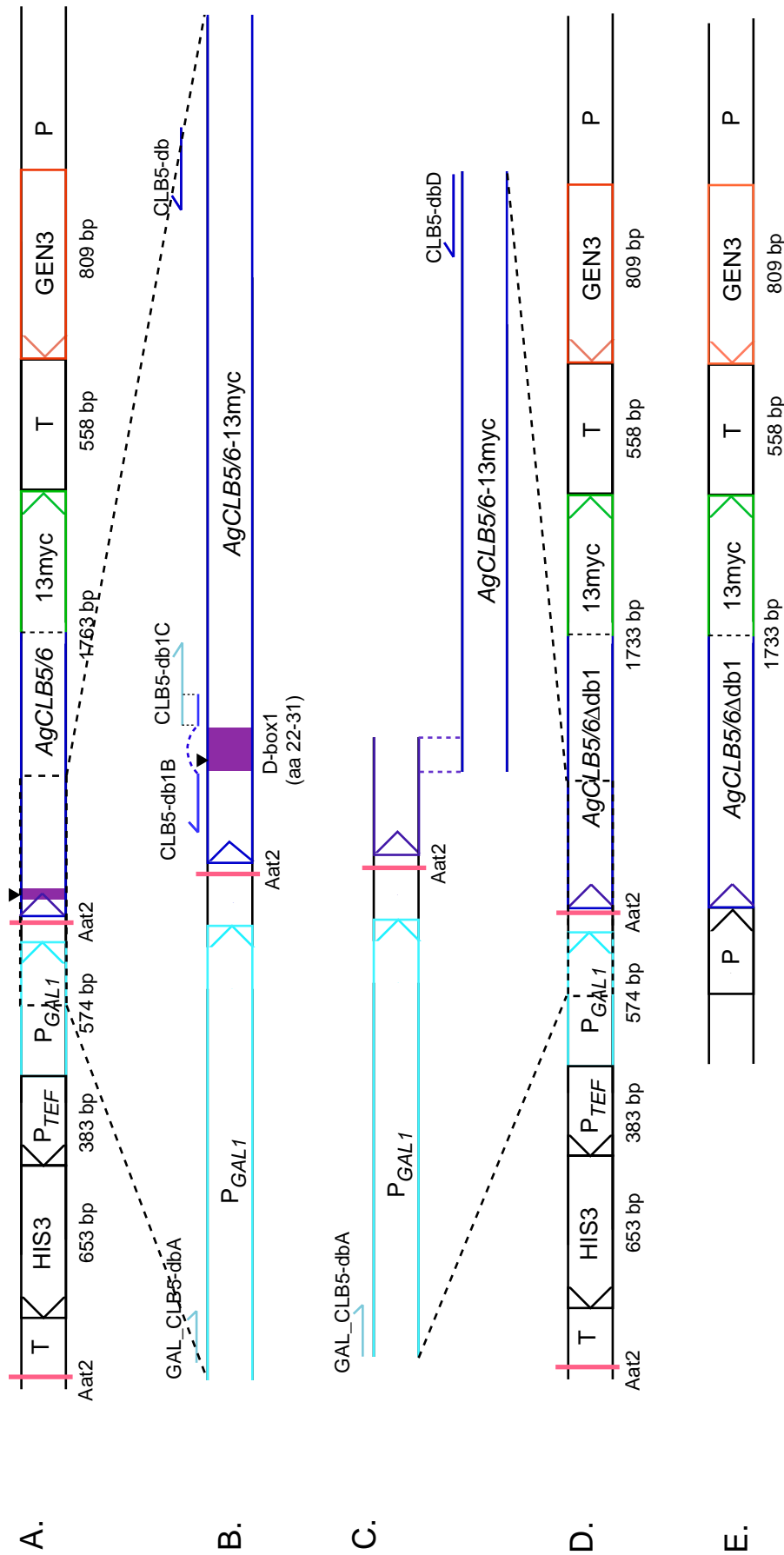


Figure 46
Construction of the *AgCLB5/6*-D-box1 mutant

A. The *AgCLB5/6Δdb1* mutants were made using an overlap PCR approach with P_{GAL1}*CLB5/6-13myc* (pAKH67) as a template. B. 6x magnification of the involved region in A, marked by a square. P_{GAL1}*CLB5/6-13myc* was used as a template for two PCR reactions, using the oligonucleotides GAL_CLB5-dbA and CLB5db1B to produce a 470 bp product and CLB5db1C and CLB5dbD to create a 428 bp product in a second reaction. C. PCR reaction with the two former PCR products as template and GAL_CLB5-dbA and CLB5/6-dbD as oligonucleotides, creating a 845 bp fragment containing an in-frame deletion of D-box1. D. Co-transformation into yeast with the previously Nhe1 cut, pAKH67 (Nhe1 restriction site, indicated as black arrow head in D-box1), resulted in pAKH68. E. The GAL1 promoter was excised by restriction digest with Aat2, to express the D-box1 mutant under its endogenous *A. gossypii* promoter, resulting in pAKH72.

REFERENCES

References

- Aitchison, J.D., G. Blobel, and M.P. Rout. 1996. Kap104p: a karyopherin involved in the nuclear transport of messenger RNA binding proteins. *Science*. 274:624-7.
- Alberti-Segui, C., F. Dietrich, R. Altmann-Johl, D. Hoepfner, and P. Philippsen. 2001. Cytoplasmic dynein is required to oppose the force that moves nuclei towards the hyphal tip in the filamentous ascomycete *Ashbya gossypii*. *J Cell Sci*. 114:975-86.
- Altmann-Johl, R., and P. Philippsen. 1996. AgTHR4, a new selection marker for transformation of the filamentous fungus *Ashbya gossypii*, maps in a four-gene cluster that is conserved between *A. gossypii* and *Saccharomyces cerevisiae*. *Mol Gen Genet*. 250:69-80.
- Amon, A., M. Tyers, B. Futcher, and K. Nasmyth. 1993. Mechanisms that help the yeast cell cycle clock tick: G2 cyclins transcriptionally activate G2 cyclins and repress G1 cyclins. *Cell*. 74:993-1007.
- Archambault, V., N.E. Buchler, G.M. Wilmes, M.D. Jacobson, and F.R. Cross. 2005. Two-faced cyclins with eyes on the targets. *Cell Cycle*. 4:125-30.
- Arvanitidis, A., and J.J. Heinisch. 1994. Studies on the function of yeast phosphofructokinase subunits by in vitro mutagenesis. *J Biol Chem*. 269:8911-8.
- Ashby, S.F., and W. Nowell. 1926. *Annals of Botany*. XL No. CLX.
- Ayad-Durieux, Y., P. Knechtle, S. Goff, F. Dietrich, and P. Philippsen. 2000. A PAK-like protein kinase is required for maturation of young hyphae and septation in the filamentous ascomycete *Ashbya gossypii*. *J Cell Sci*. 113 Pt 24:4563-75.
- Bacher, A., Q. Le Van, P.J. Keller, and H.G. Floss. 1983. Biosynthesis of riboflavin. Incorporation of ¹³C-labeled precursors into the xylene ring. *J Biol Chem*. 258:13431-7.
- Bailer, S.M., S. Siniosoglou, A. Podtelejnikov, A. Hellwig, M. Mann, and E. Hurt. 1998. Nup116p and nup100p are interchangeable through a conserved motif which constitutes a docking site for the mRNA transport factor gle2p. *Embo J*. 17:1107-19.
- Baldin, V., J. Lukas, M.J. Marcote, M. Pagano, and G. Draetta. 1993. Cyclin D1 is a nuclear protein required for cell cycle progression in G1. *Genes Dev*. 7:812-21.
- Basco, R.D., M.D. Segal, and S.I. Reed. 1995. Negative regulation of G1 and G2 by S-phase cyclins of *Saccharomyces cerevisiae*. *Mol Cell Biol*. 15:5030-42.
- Baudin, A., O. Ozier-Kalogeropoulos, A. Denouel, F. Lacroute, and C. Cullin. 1993. A simple and efficient method for direct gene deletion in *Saccharomyces cerevisiae*. *Nucleic Acids Res*. 21:3329-30.
- Baumer, M., M. Kunzler, P. Steigemann, G.H. Braus, and S. Irniger. 2000. Yeast Ran-binding protein Yrb1p is required for efficient proteolysis of cell cycle regulatory proteins Pds1p and Sic1p. *J Biol Chem*. 275:38929-37.
- Becker, J., F. Melchior, V. Gerke, F.R. Bischoff, H. Ponstingl, and A. Wittinghofer. 1995. RNA1 encodes a GTPase-activating protein specific for Gsp1p, the Ran/TC4 homologue of *Saccharomyces cerevisiae*. *J Biol Chem*. 270:11860-5.
- Belhumeur, P., A. Lee, R. Tam, T. DiPaolo, N. Fortin, and M.W. Clark. 1993. GSP1 and GSP2, genetic suppressors of the prp20-1 mutant in *Saccharomyces cerevisiae*: GTP-binding proteins involved in the maintenance of nuclear organization. *Mol Cell Biol*. 13:2152-61.
- Booher, R.N., R.J. Deshaies, and M.W. Kirschner. 1993. Properties of *Saccharomyces cerevisiae* wee1 and its differential regulation of p34CDC28 in response to G1 and G2 cyclins. *Embo J*. 12:3417-26.
- Byers, B., and L. Goetsch. 1975. Behavior of spindles and spindle plaques in the cell cycle and conjugation of *Saccharomyces cerevisiae*. *J Bacteriol*. 124:511-23.
- Chen, K.C., A. Csikasz-Nagy, B. Gyorfy, J. Val, B. Novak, and J.J. Tyson. 2000. Kinetic analysis of a molecular model of the budding yeast cell cycle. *Mol Biol Cell*. 11:369-91.
- Cho, J.W., and H.W. Sauer. 1994. A non-cycling mitotic cyclin in the naturally synchronous cell cycle of *Physarum polycephalum*. *Eur J Cell Biol*. 65:94-102.
- Clutterbuck, A.J. 1970. Synchronous nuclear division and septation in *Aspergillus nidulans*. *J Gen Microbiol*. 60:133-5.
- Cross, F.R. 1988. DAF1, a mutant gene affecting size control, pheromone arrest, and cell cycle kinetics of *Saccharomyces cerevisiae*. *Mol Cell Biol*. 8:4675-84.
- Cross, F.R. 2003. Two redundant oscillatory

- mechanisms in the yeast cell cycle. *Dev Cell*. 4:741-52.
- Cross, F.R., V. Archambault, M. Miller, and M. Klovstad. 2002. Testing a mathematical model of the yeast cell cycle. *Mol Biol Cell*. 13:52-70.
- Cross, F.R., and C.M. Blake. 1993. The yeast Cln3 protein is an unstable activator of Cdc28. *Mol Cell Biol*. 13:3266-71.
- Cross, F.R., M. Hoek, J.D. McKinney, and A.H. Tinkelenberg. 1994. Role of Swi4 in cell cycle regulation of CLN2 expression. *Mol Cell Biol*. 14:4779-87.
- Cross, F.R., and M.D. Jacobson. 2000. Conservation and function of a potential substrate-binding domain in the yeast Clb5 B-type cyclin. *Mol Cell Biol*. 20:4782-90.
- Cross, F.R., L. Schroeder, M. Kruse, and K.C. Chen. 2005. Quantitative characterization of a mitotic cyclin threshold regulating exit from mitosis. *Mol Biol Cell*. 16:2129-38.
- Dahmann, C., J.F. Diffley, and K.A. Nasmyth. 1995. S-phase-promoting cyclin-dependent kinases prevent re-replication by inhibiting the transition of replication origins to a pre-replicative state. *Curr Biol*. 5:1257-69.
- De Bondt, H.L., J. Rosenblatt, J. Jancarik, H.D. Jones, D.O. Morgan, and S.H. Kim. 1993. Crystal structure of cyclin-dependent kinase 2. *Nature*. 363:595-602.
- De Souza, C.P., A.H. Osmani, S.B. Hashmi, and S.A. Osmani. 2004. Partial nuclear pore complex disassembly during closed mitosis in *Aspergillus nidulans*. *Curr Biol*. 14:1973-84.
- Deshaies, R.J., and M. Kirschner. 1995. G1 cyclin-dependent activation of p34CDC28 (Cdc28p) in vitro. *Proc Natl Acad Sci U S A*. 92:1182-6.
- Dietrich, F.S., S. Voegeli, S. Brachat, A. Lerch, K. Gates, S. Steiner, C. Mohr, R. Pohlmann, P. Luedi, S. Choi, R.A. Wing, A. Flavier, T.D. Gaffney, and P. Philippsen. 2004. The *Ashbya gossypii* genome as a tool for mapping the ancient *Saccharomyces cerevisiae* genome. *Science*. 304:304-7.
- Donaldson, A.D., and J.V. Kilmartin. 1996. Spc42p: a phosphorylated component of the *S. cerevisiae* spindle pole body (SPB) with an essential function during SPB duplication. *J Cell Biol*. 132:887-901.
- Edgington, N.P., and B. Futcher. 2001. Relationship between the function and the location of G1 cyclins in *S. cerevisiae*. *J Cell Sci*. 114:4599-611.
- Epstein, C.B., and F.R. Cross. 1992. CLB5: a novel B cyclin from budding yeast with a role in S phase. *Genes Dev*. 6:1695-706.
- Evans, T., E.T. Rosenthal, J. Youngblom, D. Distel, and T. Hunt. 1983. Cyclin: a protein specified by maternal mRNA in sea urchin eggs that is destroyed at each cleavage division. *Cell*. 33:389-96.
- Fabre, E., W.C. Boelens, C. Wimmer, I.W. Mattaj, and E.C. Hurt. 1994. Nup145p is required for nuclear export of mRNA and binds homopolymeric RNA in vitro via a novel conserved motif. *Cell*. 78:275-89.
- Fisher, D.L., and P. Nurse. 1996. A single fission yeast mitotic cyclin B p34cdc2 kinase promotes both S-phase and mitosis in the absence of G1 cyclins. *Embo J*. 15:850-60.
- Gilchrist, D., and M. Rexach. 2003. Molecular basis for the rapid dissociation of nuclear localization signals from karyopherin alpha in the nucleoplasm. *J Biol Chem*. 278:51937-49.
- Gladfelter, A.S., A.K. Hungerbuehler, and P. Philippsen. 2006. Asynchronous nuclear division cycles in multinucleated cells. *J Cell Biol*. 172:347-62.
- Glotzer, M., A. Murray, and M. Kirschner. 1991. Cyclin is degraded by the ubiquitin pathway. *Nature*. 349:132-138.
- Glotzer, M., A.W. Murray, and M.W. Kirschner. 1991. Cyclin is degraded by the ubiquitin pathway. *Nature*. 349:132-8.
- Haase, S.B., and S.I. Reed. 1999. Evidence that a free-running oscillator drives G1 events in the budding yeast cell cycle. *Nature*. 401:394-7.
- Hadwiger, J.A., C. Wittenberg, H.E. Richardson, M. de Barros Lopes, and S.I. Reed. 1989. A family of cyclin homologs that control the G1 phase in yeast. *Proc Natl Acad Sci U S A*. 86:6255-9.
- Hagting, A., C. Karlsson, P. Clute, M. Jackman, and J. Pines. 1998. MPF localization is controlled by nuclear export. *Embo J*. 17:4127-38.
- Hanahan, D. 1983. Studies on transformation of *Escherichia coli* with plasmids. *J Mol Biol*. 166:557-80.
- Hazan, I., M. Sepulveda-Becerra, and H. Liu. 2002. Hyphal elongation is regulated independently of cell cycle in *Candida albicans*. *Mol Biol Cell*. 13:134-45.
- Hodge, C.A., H.V. Colot, P. Stafford, and C.N. Cole. 1999. Rat8p/Dbp5p is a shuttling transport factor that interacts with Rat7p/Nup159p and Gle1p and suppresses the mRNA

- export defect of xpo1-1 cells. *Embo J*. 18:5778-88.
- Hoepfner, D., A. Brachat, and P. Philippsen. 2000. Time-lapse video microscopy analysis reveals astral microtubule detachment in the yeast spindle pole mutant *cnm67*. *Mol Biol Cell*. 11:1197-211.
- Hoepfner, D., F. Schaerer, A. Brachat, A. Wach, and P. Philippsen. 2002. Reorientation of mispositioned spindles in short astral microtubule mutant *spc72Delta* is dependent on spindle pole body outer plaque and Kar3 motor protein. *Mol Biol Cell*. 13:1366-80.
- Holloway, S.L., M. Glotzer, R.W. King, and A.W. Murray. 1993. Anaphase is initiated by proteolysis rather than by the inactivation of maturation-promoting factor. *Cell*. 73:1393-402.
- Hood, J.K., W.W. Hwang, and P.A. Silver. 2001. The *Saccharomyces cerevisiae* cyclin Clb2p is targeted to multiple subcellular locations by cis- and trans-acting determinants. *J Cell Sci*. 114:589-97.
- Iborra, F.J., D.A. Jackson, and P.R. Cook. 2001. Coupled transcription and translation within nuclei of mammalian cells. *Science*. 293:1139-42.
- Iovine, M.K., J.L. Watkins, and S.R. Wentz. 1995. The GLFG repetitive region of the nucleoporin Nup116p interacts with Kap95p, an essential yeast nuclear import factor. *J Cell Biol*. 131:1699-713.
- Iovine, M.K., and S.R. Wentz. 1997. A nuclear export signal in Kap95p is required for both recycling the import factor and interaction with the nucleoporin GLFG repeat regions of Nup116p and Nup100p. *J Cell Biol*. 137:797-811.
- Irniger, S., and K. Nasmyth. 1997. The anaphase-promoting complex is required in G1 arrested yeast cells to inhibit B-type cyclin accumulation and to prevent uncontrolled entry into S-phase. *J Cell Sci*. 110 (Pt 13):1523-31.
- Jackson, L.P., S.I. Reed, and S.B. Haase. 2006. Distinct mechanisms control the stability of the related S-phase cyclins Clb5 and Clb6. *Mol Cell Biol*. 26:2456-66.
- Jacobs, C.W., A.E. Adams, P.J. Szanislo, and J.R. Pringle. 1988. Functions of microtubules in the *Saccharomyces cerevisiae* cell cycle. *J Cell Biol*. 107:1409-26.
- Jacobson, M.D., S. Gray, M. Yuste-Rojas, and F.R. Cross. 2000. Testing cyclin specificity in the exit from mitosis. *Mol Cell Biol*. 20:4483-93.
- Jans, D.A., C.Y. Xiao, and M.H. Lam. 2000. Nuclear targeting signal recognition: a key control point in nuclear transport? *Bioessays*. 22:532-44.
- Jeffrey, P.D., A.A. Russo, K. Polyak, E. Gibbs, J. Hurwitz, J. Massague, and N.P. Pavletich. 1995. Mechanism of CDK activation revealed by the structure of a cyclinA-CDK2 complex. *Nature*. 376:313-20.
- Kellis, M., B.W. Birren, and E.S. Lander. 2004. Proof and evolutionary analysis of ancient genome duplication in the yeast *Saccharomyces cerevisiae*. *Nature*. 428:617-24.
- Kellis, M., N. Patterson, M. Endrizzi, B. Birren, and E.S. Lander. 2003. Sequencing and comparison of yeast species to identify genes and regulatory elements. *Nature*. 423:241-54.
- Kilmartin, J.V., and A.E. Adams. 1984. Structural rearrangements of tubulin and actin during the cell cycle of the yeast *Saccharomyces*. *J Cell Biol*. 98:922-33.
- Knechtle, P. 2002. AgSPA2 and AgBOI control landmarks of filamentous growth in the filamentous ascomycete *Ashbya gossypii*. In *Biozentrum*. Vol. Ph.D. Basel, Basel, Switzerland.
- Kobayashi, H., E. Stewart, R. Poon, J.P. Adamczewski, J. Gannon, and T. Hunt. 1992. Identification of the domains in cyclin A required for binding to, and activation of, p34cdc2 and p32cdk2 protein kinase subunits. *Mol Biol Cell*. 3:1279-94.
- Koch, C., and K. Nasmyth. 1994. Cell cycle regulated transcription in yeast. *Curr Opin Cell Biol*. 6:451-9.
- Laabs, T.L., D.D. Markwardt, M.G. Slattery, L.L. Newcomb, D.J. Stillman, and W. Heideman. 2003. ACE2 is required for daughter cell-specific G1 delay in *Saccharomyces cerevisiae*. *Proc Natl Acad Sci U S A*. 100:10275-80.
- Leslie, D.M., B. Grill, M.P. Rout, R.W. Wozniak, and J.D. Aitchison. 2002. Kap121p-mediated nuclear import is required for mating and cellular differentiation in yeast. *Mol Cell Biol*. 22:2544-55.
- Lew, D.J., and S.I. Reed. 1993. Morphogenesis in the yeast cell cycle: regulation by Cdc28 and cyclins. *J Cell Biol*. 120:1305-20.
- Lew, D.J., and S.I. Reed. 1995. A cell cycle checkpoint monitors cell morphogenesis in budding yeast. *J Cell Biol*. 129:739-49.
- Lew, D.J., T. Weinert, and J.R. Pringle. 1997.

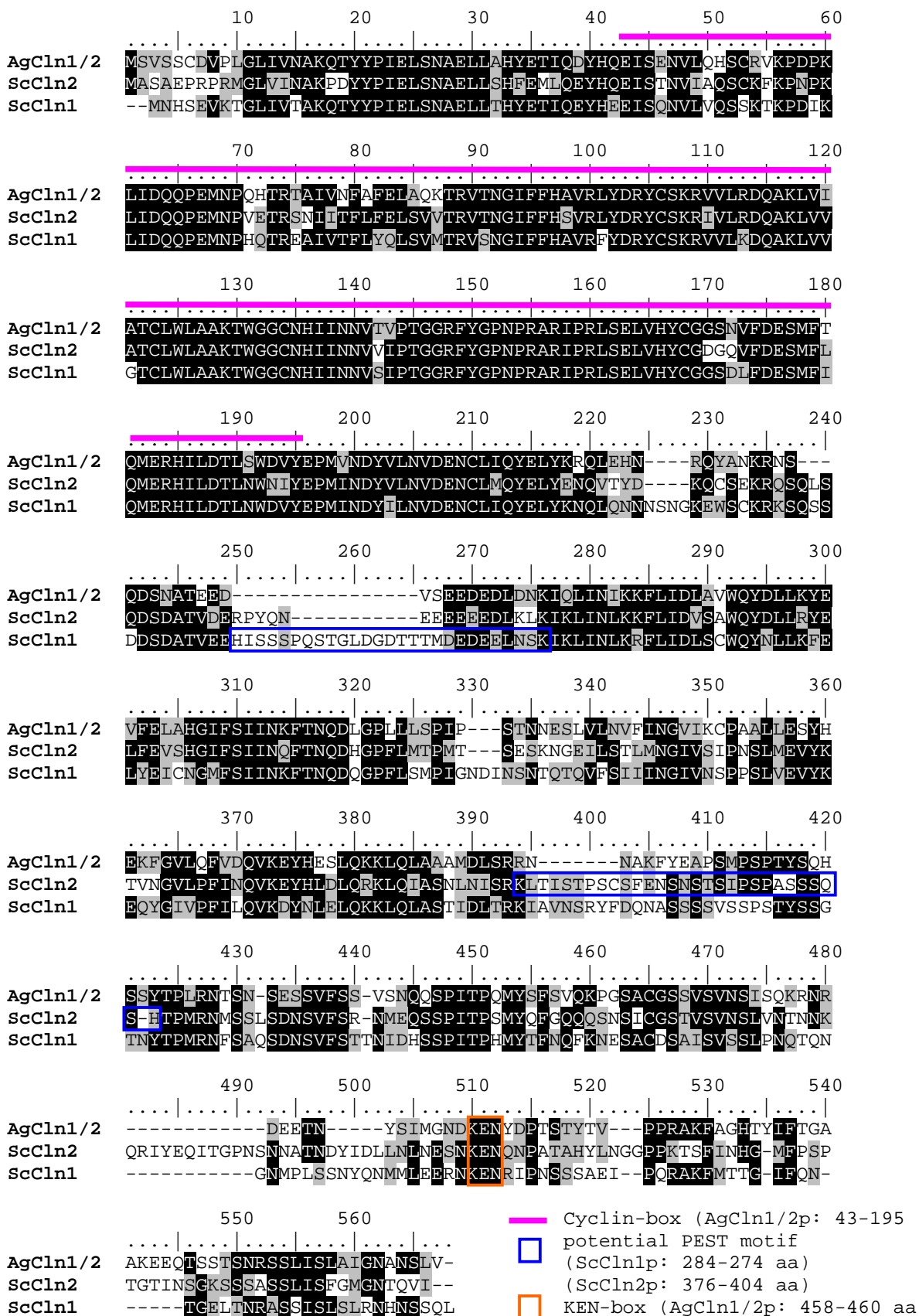
- Cell Cycle Control in *Saccharomyces cerevisiae*. Cold Spring Harbor Laboratory Press, NY. 607-695 pp.
- Lim, H.H., P.Y. Goh, and U. Surana. 1996. Spindle pole body separation in *Saccharomyces cerevisiae* requires dephosphorylation of the tyrosine 19 residue of Cdc28. *Mol Cell Biol*. 16:6385-97.
- Lodish, H., A. Berk, et al. 2000. Molecular Cell Biology. Freeman and Company, NY.
- Loeb, J.D., G. Schlenstedt, D. Pellman, D. Kornitzer, P.A. Silver, and G.R. Fink. 1995. The yeast nuclear import receptor is required for mitosis. *Proc Natl Acad Sci U S A*. 92:7647-51.
- Longtine, M.S., H. Fares, and J.R. Pringle. 1998. Role of the yeast Gin4p protein kinase in septin assembly and the relationship between septin assembly and septin function. *J Cell Biol*. 143:719-36.
- Makhnevych, T., C.P. Lusk, A.M. Anderson, J.D. Aitchison, and R.W. Wozniak. 2003. Cell cycle regulated transport controlled by alterations in the nuclear pore complex. *Cell*. 115:813-23.
- Marelli, M., J.D. Aitchison, and R.W. Wozniak. 1998. Specific binding of the karyopherin Kap121p to a subunit of the nuclear pore complex containing Nup53p, Nup59p, and Nup170p. *J Cell Biol*. 143:1813-30.
- Mendenhall, M.D., and A.E. Hodge. 1998. Regulation of Cdc28 cyclin-dependent protein kinase activity during the cell cycle of the yeast *Saccharomyces cerevisiae*. *Microbiol Mol Biol Rev*. 62:1191-243.
- Miller, M.E., and F.R. Cross. 2001. Mechanisms controlling subcellular localization of the G(1) cyclins Cln2p and Cln3p in budding yeast. *Mol Cell Biol*. 21:6292-311.
- Minke, P.F., I.H. Lee, and M. Plamann. 1999. Microscopic analysis of *Neurospora* ropy mutants defective in nuclear distribution. *Fungal Genet Biol*. 28:55-67.
- Morgan, D.O. 1995. Principles of CDK regulation. *Nature*. 374:131-4.
- Mosammamaparast, N., Y. Guo, J. Shabanowitz, D.F. Hunt, and L.F. Pemberton. 2002. Pathways mediating the nuclear import of histones H3 and H4 in yeast. *J Biol Chem*. 277:862-8.
- Murray, A.W. 2004. Recycling the cell cycle: cyclins revisited. *Cell*. 116:221-34.
- Nash, R., G. Tokiwa, S. Anand, K. Erickson, and A.B. Futcher. 1988. The WHI1+ gene of *Saccharomyces cerevisiae* tethers cell division to cell size and is a cyclin homolog. *Embo J*. 7:4335-46.
- Nasmyth, K. 1993. Control of the yeast cell cycle by the Cdc28 protein kinase. *Curr Opin Cell Biol*. 5:166-79.
- Nygaard, O.F., S. Guttus, and H.P. Rusch. 1960. Nucleic acid metabolism in a slime mold with synchronous mitosis. *Biochim Biophys Acta*. 38:298-306.
- Ouspenski, I. 1998. A RanBP1 mutation which does not visibly affect nuclear import may reveal additional functions of the ran GTPase system. *Exp Cell Res*. 244:171-83.
- Pearson, C.G., P.S. Maddox, E.D. Salmon, and K. Bloom. 2001. Budding yeast chromosome structure and dynamics during mitosis. *J Cell Biol*. 152:1255-66.
- Peter, M., and I. Herskowitz. 1994. Direct inhibition of the yeast cyclin-dependent kinase Cdc28-Cln by Far1. *Science*. 265:1228-31.
- Pfleger, C.M., and M.W. Kirschner. 2000. The KEN box: an APC recognition signal distinct from the D box targeted by Cdh1. *Genes Dev*. 14:655-65.
- Phaff, H.J., and W.T. Starmer. 1987. Yeasts associated with plants, insects and soil in Rose, A. a. H., J. (Ed). *The yeasts*:153-155.
- Pines, J., and T. Hunter. 1991. Human cyclins A and B1 are differentially located in the cell and undergo cell cycle-dependent nuclear transport. *J Cell Biol*. 115:1-17.
- Pomeroy, J.R., E.D. Sontag, and J.E. Ferrell, Jr. 2003. Building a cell cycle oscillator: hysteresis and bistability in the activation of Cdc2. *Nat Cell Biol*. 5:346-51.
- Prillinger, H., W. Schweigkofler, M. Breitenbach, P. Briza, E. Staudacher, K. Lopandic, O. Molnar, F. Weigang, M. Ibl, and A. Ellinger. 1997. Phytopathogenic filamentous (Ashbya, Eremothecium) and dimorphic fungi (Holleya, Nematosporea) with needle-shaped ascospores as new members within the Saccharomycetaceae. *Yeast*. 13:945-60.
- Pringle, J.R., A.E.M. Adams, D.G. Drubin, and B.K. Haarer. 1991. Immunofluorescence methods for yeast. *Methods Enzymol*. 194:565-602.
- Pringle, J.R., and L.H. Hartwell. 1981. *The molecular Biology of the Yeast Saccharomyces cerevisiae*.
- Prinz, S., E.S. Hwang, R. Visintin, and A. Amon. 1998. The regulation of Cdc20 proteolysis reveals a role for APC components Cdc23 and Cdc27 during S phase and early mitosis. *Curr Biol*. 8:750-60.

- Rao, P.N., and R.T. Johnson. 1970. Mammalian cell fusion: studies on the regulation of DNA synthesis and mitosis. *Nature*. 225:159-64.
- Rechsteiner, M., and S.W. Rogers. 1996. PEST sequences and regulation by proteolysis. *Trends Biochem Sci*. 21:267-71.
- Richardson, H., D.J. Lew, M. Henze, K. Sugimoto, and S.I. Reed. 1992. Cyclin-B homologs in *Saccharomyces cerevisiae* function in S phase and in G2. *Genes Dev*. 6:2021-34.
- Rogers, S., R. Wells, and M. Rechsteiner. 1986. Amino acid sequences common to rapidly degraded proteins: the PEST hypothesis. *Science*. 234:364-8.
- Rout, M.P., J.D. Aitchison, A. Suprpto, K. Hjertaas, Y. Zhao, and B.T. Chait. 2000. The yeast nuclear pore complex: composition, architecture, and transport mechanism. *J Cell Biol*. 148:635-51.
- Russell, P., S. Moreno, and S.I. Reed. 1989. Conservation of mitotic controls in fission and budding yeasts. *Cell*. 57:295-303.
- Ryan, K.J., and S.R. Wenthe. 2000. The nuclear pore complex: a protein machine bridging the nucleus and cytoplasm. *Curr Opin Cell Biol*. 12:361-71.
- Sambrook, J., and D.W. Russell. 2001. *Molecular Cloning: A Laboratory Manual*. Cold Spring Harbor, NY, Cold Spring Harbor Laboratory Press.
- Schlenstedt, G., E. Smirnova, R. Deane, J. Solsbacher, U. Kutay, D. Gorlich, H. Ponstingl, and F.R. Bischoff. 1997. Yrb4p, a yeast ran-GTP-binding protein involved in import of ribosomal protein L25 into the nucleus. *Embo J*. 16:6237-49.
- Schmitz, H.P., A. Kaufmann, M. Kohli, P.P. Laissue, and P. Philippsen. 2006. From function to shape: a novel role of a formin in morphogenesis of the fungus *Ashbya gossypii*. *Mol Biol Cell*. 17:130-45.
- Schneider, B.L., Q.H. Yang, and A.B. Futcher. 1996. Linkage of replication to start by the Cdk inhibitor Sic1. *Science*. 272:560-2.
- Schwob, E., T. Bohm, M.D. Mendenhall, and K. Nasmyth. 1994. The B-type cyclin kinase inhibitor p40SIC1 controls the G1 to S transition in *S. cerevisiae*. *Cell*. 79:233-44.
- Schwob, E., and K. Nasmyth. 1993. CLB5 and CLB6, a new pair of B cyclins involved in DNA replication in *Saccharomyces cerevisiae*. *Genes Dev*. 7:1160-75.
- Segal, M., D.J. Clarke, P. Maddox, E.D. Salmon, K. Bloom, and S.I. Reed. 2000. Coordinated spindle assembly and orientation requires Clb5p-dependent kinase in budding yeast. *J Cell Biol*. 148:441-52.
- Sigrist, S., H. Jacobs, R. Stratmann, and C.F. Lehner. 1995. Exit from mitosis is regulated by *Drosophila* fizzy and the sequential destruction of cyclins A, B and B3. *Embo J*. 14:4827-38.
- Spellman, P.T., G. Sherlock, M.Q. Zhang, V.R. Iyer, K. Anders, M.B. Eisen, P.O. Brown, D. Botstein, and B. Futcher. 1998. Comprehensive identification of cell cycle-regulated genes of the yeast *Saccharomyces cerevisiae* by microarray hybridization. *Mol Biol Cell*. 9:3273-97.
- Stern, B., and P. Nurse. 1996. A quantitative model for the cdc2 control of S phase and mitosis in fission yeast. *Trends Genet*. 12:345-50.
- Straight, A.F., A.S. Belmont, C.C. Robinett, and A.W. Murray. 1996. GFP tagging of budding yeast chromosomes reveals that protein-protein interactions can mediate sister chromatid cohesion. *Curr Biol*. 6:1599-608.
- Stuart, D., and C. Wittenberg. 1994. Cell cycle-dependent transcription of CLN2 is conferred by multiple distinct cis-acting regulatory elements. *Mol Cell Biol*. 14:4788-801.
- Surana, U., A. Amon, C. Dowzer, J. McGrew, B. Byers, and K. Nasmyth. 1993. Destruction of the CDC28/CLB mitotic kinase is not required for the metaphase to anaphase transition in budding yeast. *Embo J*. 12:1969-78.
- Sydorsky, Y., D.J. Dilworth, E.C. Yi, D.R. Goodlett, R.W. Wozniak, and J.D. Aitchison. 2003. Intersection of the Kap123p-mediated nuclear import and ribosome export pathways. *Mol Cell Biol*. 23:2042-54.
- Teixeira, M.T., E. Fabre, and B. Dujon. 1999. Self-catalyzed cleavage of the yeast nucleoporin Nup145p precursor. *J Biol Chem*. 274:32439-44.
- Thornton, B.R., K.C. Chen, F.R. Cross, J.J. Tyson, and D.P. Toczyski. 2004. Cycling without the Cyclosome: Modeling a Yeast Strain Lacking the APC. *Cell Cycle*. 3.
- Thornton, B.R., and D.P. Toczyski. 2003. Securin and B-cyclin/CDK are the only essential targets of the APC. *Nat Cell Biol*. 5:1090-4.
- Tyers, M. 1996. The cyclin-dependent kinase inhibitor p40SIC1 imposes the requirement for Cln G1 cyclin function at Start. *Proc Natl Acad Sci U S A*. 93:7772-6.
- Tyers, M., G. Tokiwa, R. Nash, and B. Futcher.

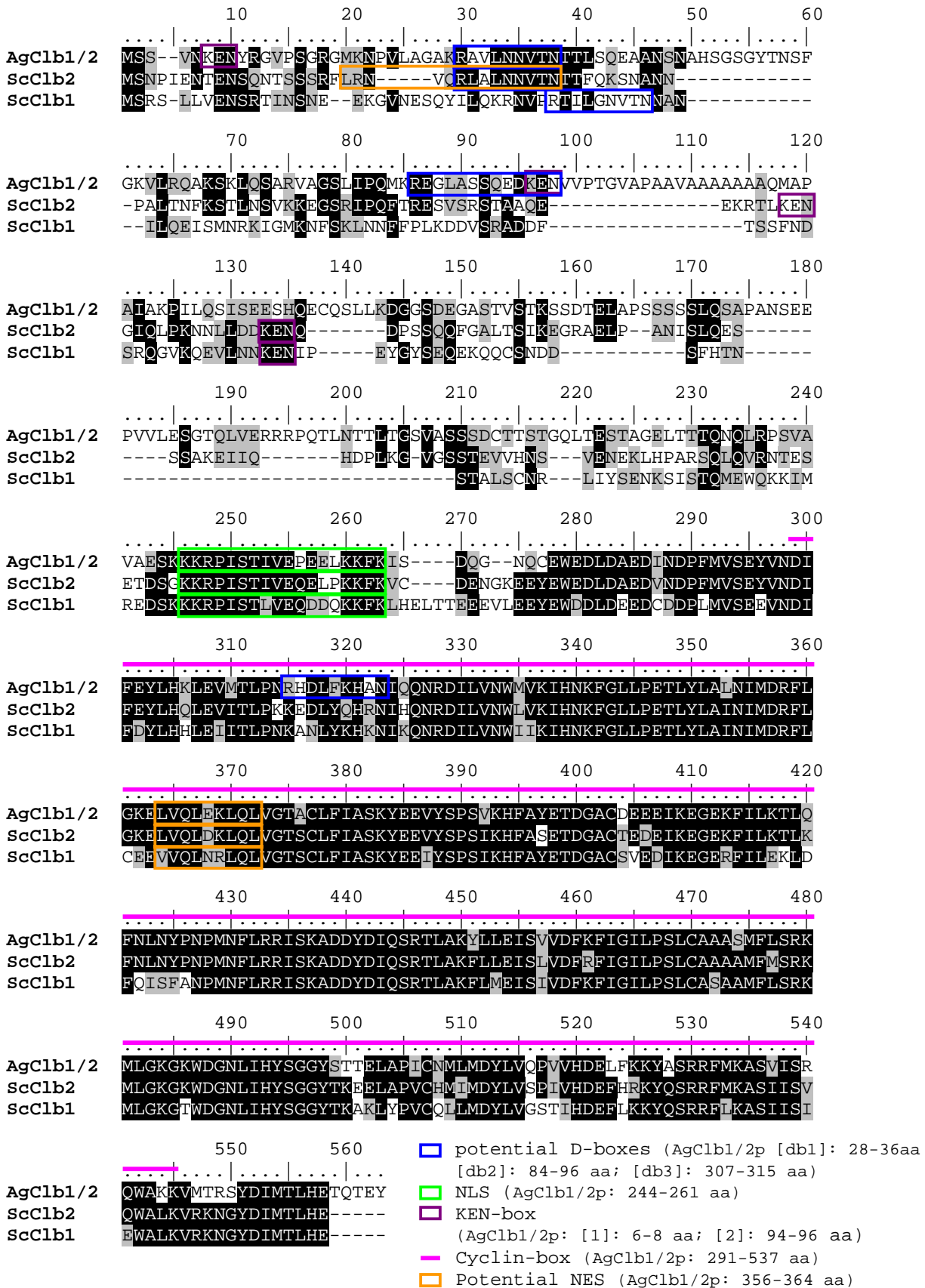
-
1992. The Cln3-Cdc28 kinase complex of *S. cerevisiae* is regulated by proteolysis and phosphorylation. *Embo J.* 11:1773-84.
- Verma, R., R.S. Annan, M.J. Huddleston, S.A. Carr, G. Reynard, and R.J. Deshaies. 1997. Phosphorylation of Sic1p by G1 Cdk required for its degradation and entry into S phase. *Science.* 278:455-60.
- Verma, R., R.M. Feldman, and R.J. Deshaies. 1997. SIC1 is ubiquitinated in vitro by a pathway that requires CDC4, CDC34, and cyclin/CDK activities. *Mol Biol Cell.* 8:1427-37.
- Wach, A., A. Brachat, R. Pohlmann, and P. Philippsen. 1994. New heterologous modules for classical or PCR-based gene disruptions in *Saccharomyces cerevisiae*. *Yeast.* 10:1793-808.
- Wasch, R., and F.R. Cross. 2002. APC-dependent proteolysis of the mitotic cyclin Clb2 is essential for mitotic exit. *Nature.* 418:556-62.
- Wendland, J., Y. Ayad-Durieux, P. Knechtle, C. Rebischung, and P. Philippsen. 2000. PCR-based gene targeting in the filamentous fungus *Ashbya gossypii*. *Gene.* 242:381-91.
- Wente, S.R., and G. Blobel. 1994. NUP145 encodes a novel yeast glycine-leucine-phenylalanine-glycine (GLFG) nucleoporin required for nuclear envelope structure. *J Cell Biol.* 125:955-69.
- Wente, S.R., M.P. Rout, and G. Blobel. 1992. A new family of yeast nuclear pore complex proteins. *J Cell Biol.* 119:705-23.
- Wilmes, G.M., V. Archambault, R.J. Austin, M.D. Jacobson, S.P. Bell, and F.R. Cross. 2004. Interaction of the S-phase cyclin Clb5 with an "RXL" docking sequence in the initiator protein Orc6 provides an origin-localized replication control switch. *Genes Dev.* 18:981-91.
- Yamano, H., J. Gannon, and T. Hunt. 1996. The role of proteolysis in cell cycle progression in *Schizosaccharomyces pombe*. *Embo J.* 15:5268-79.
- Yanisch-Perron, C., J. Vieira, and J. Messing. 1985. Improved M13 phage cloning vectors and host strains: nucleotide sequences of the M13mp18 and pUC19 vectors. *Gene.* 33:103-19.
- Zachariae, W., T.H. Shin, M. Galova, B. Obermaier, and K. Nasmyth. 1996. Identification of subunits of the anaphase-promoting complex of *Saccharomyces cerevisiae*. *Science.* 274:1201-4.
-

APPENDIX I

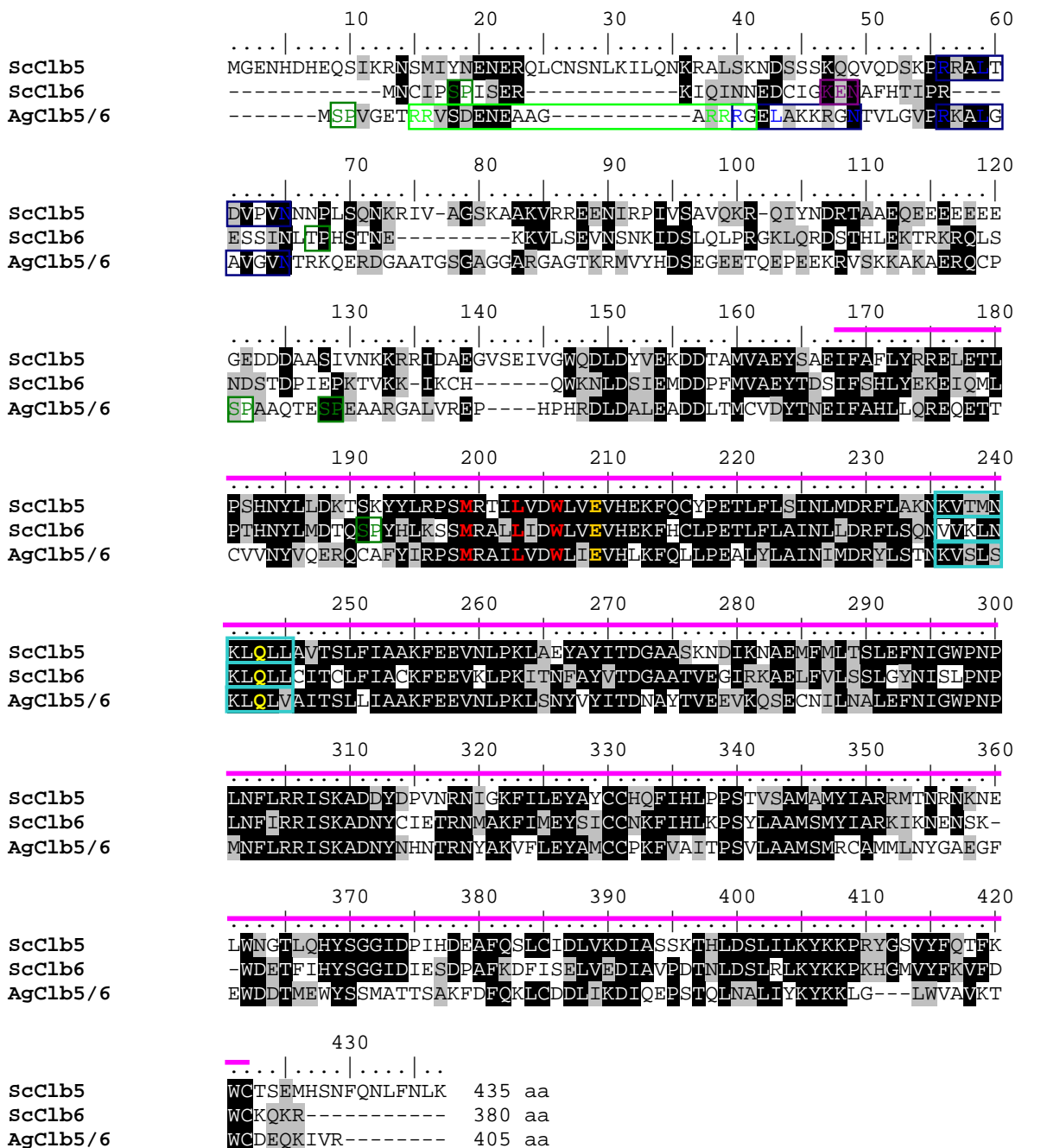
Appendix 1: Alignment of AgCln1/2p, ScCln2p and ScCln1p



Appendix 1: Alignment of AgClb1/2p, ScClb2p and ScClb1p



Alignment of ScClb5p, ScClb6p and AgClb5/6p



- Cyclin-box (AgClb5/6p: 145-399 aa)
 - Putative S/TP phosphorylation sites
 - Potential D-box (AgClb5/6p: db1: 22-31 aa; db2: 38-47 aa)
 - Potential bipartite Nuclear Localization Signal (NLS; AgClb5/6p: 8-24 aa)
 - Potential Nuclear Export Signal (NES; AgClb5/6p: 214-222 aa)
 - Hydrophobic patch (AgClb5/6p: 177, 181 and 184 aa)
 - Salt bridge (AgClb5/6p: 187 aa)
 - H-bond (AgClb5/6p: 221 aa)
- } Cross Jacobson, 2000

Appendix 1: Alignment of AgNup53/59p and ScNup59p and ScNup53p

```

      10      20      30      40      50      60
AgNup53  MSSLFSQNSSDSNR-FTNLSIKFPQ-----OQQTISQQQGSNLOPOSSQQAA
ScNup59  ---MFGIRSGNNGGFTNLSQAPQTTQMFQSQSLOLPQPPQPPQOQQOQHLOFNSSDAS
ScNup53  ---MADLQKQENSRRFTNVSVIAPES----OQOHEQQKQEQLEQQKOPTGLLKGLNGFP

      70      80      90      100     110     120
AgNup53  IASQGFVFPNEEKP-----PRWFNNPRKRTLPQ
ScNup59  SLRFGNSLSNTVNNYSSNIGNNSINNNNIKNGTNNISQHGQGNPNSWVNNPKKRFTPH
ScNup53  SAPQPLFMEDPPSTVSGELN-----DNPAWFNNPRKRAIPN

      130     140     150     160     170     180
AgNup53  NLIKRSKPTSSSEGPAPSSGNSSTSHSGFGSVTFGSKK-----SNIFNTRANTQ
ScNup59  TVIRRKTTKQNSSSDINQNDSSSMNATMRNFSKQNDSKH-----NERNKSAANNQ
ScNup53  SLIKRSNGQ--SLSPVRSDSADVPFASNSNGFNNTVTFGSKKDPRIILKNVSPNDNNSANN

      190     200     210     220     230     240
AgNup53  GHDMTPGNVIDSNEAPPKSLYDLQREDEFG---SVIPSGVGEQRQOPLALAKSKDAIL
ScNup59  INSLLS----NFNDIPPSVILQDQREDEFGSIPSLTQFVTDKYTAKKTNRSAYDSKN
ScNup53  AHSDDLGTVVFDSNEAPPKSLADWQKEDGIFS--SKTDNIEDPNLSSNITFDGKPTATP

      250     260     270     280     290     300
AgNup53  MRN-VFDR-----ELEPKKVKKDDQSAS-----ASASHNESAVLVFGYPESISNQ
ScNup59  TPN-VFDKDSYVRIANIEQNHLDDNYNTAETNNKVHETSCKSSSLSAIIVFGYPESISNE
ScNup53  SPFRPLEKTSRILNFFDKNTKTTNPNTASSEASAGSKEGASTNWDHAIILIFGYPETIANS

      310     320     330     340     350     360
AgNup53  VILHFSKFCNILEDFVLRGVSGMRP-----TAMKVSGRQHTEN
ScNup59  LIHFHSHFGHIMEDFOVLRRLGRGIPNTFRIFHNHDTGCDENDSTVNKSITLGRNNESEN
ScNup53  IILHFANFGEILEDFRVLKDFKKLNS-----KNMSKSPSLT

      370     380     390     400     410     420
AgNup53  RKKYPIFTGDGWIKLYDSPSSALRALQENGTVYGGCLVGCVPYSKQAVEQLASCHIEKA
ScNup59  NKKYPIFTGESWVKLTYNSPSSALRALQENGTIFRGLIGCLPYSKNAVEQLAGCKIDNV
ScNup53  AQKYPIYTG DGWVKLTYKSELKSRALQENGIIIMNGTLIGCVSYSPAALKQLASLKKSEE

      430     440     450     460     470     480
AgNup53  DDIGGVNFVSAQTPNNSLNAGHPNGDDQPVPG---SREDDHARFTFS-----
ScNup59  DDIGEFNVSMYQNSSTSSSTNTPSPPNVITDGTLLREDDNTPAGHAGNPTNISSPIVAN
ScNup53  IINNKTSSQTSLSKDLSNYRKTEGIFEKAKAKAVTSKVRNAEFKVSKNSTSFKN-----

      490     500     510     520     530     540
AgNup53  --TRMLDIKDGKSLLVHNG--NAHNQNFNKNLEDKMRHHDHAHTQAN--KGVLSKVNWNWLF
ScNup59  SPNKRLDVIDGKLPFMONAGPNSNIPNLLRNLESKMRQOEAKYRNNEPAGFTHKLSNWLK
ScNup53  --PRRLEIKDGRSLFLRNR--GKIHSGLVSSIESDLKKREQASKSK--KSWLNRLLNWNLF

      ....
AgNup53  GWNEL
ScNup59  GWNDL
ScNup53  GWNDL

```

Appendix 1: Alignment of AgNup116/100p and ScNup116p and ScNup100p

```

      10      20      30      40      50      60
AgNup116  MFGASRPAFGNTGAPAFGQQQTGSFG-----QPQSTTNAFGPSTGTNAHSGFGGFGNTQ
ScNup116  MFGVSRGAFPSATTQPFQSTGS-TFGGQQQQQPVAINTSAFGLSQQTINTTQAP-AFGNFQ
ScNup100  MFGNRRPMPFGGSNLSFGSNTSSFFGGQQSQQPNSLFGNSNNMNNSTSNNAQSGFGGFTSAA

      70      80      90      100     110     120
AgNup116  QQPAASPFQGMSTQPPASGPFQGTSSVSNPP-SLFSGNASGVAASG-----GT
ScNup116  NQTSNSPFGMSGSTTANGTTPFGQSQLTNNNASGSLFSGMGNNTALSAGSASVVPNSTACT
ScNup100  GSNSNSLFGNNN--TONNGAFGQSMGATQNSP---FGLNSNSNASNG

      130     140     150     160     170     180
AgNup116  SIKPFTAYTEKDAITGGINVVFOSITCMPEYKSFSEELRFQDYQANNKVGQAGGCVGGV
ScNup116  SIKPFTTFEEKDPTTGVINVVFOSITCMPEYRNFSEELRFQDYQAGRKFGTSQNGTG---
ScNup100  -----NTFSGSSSMGSGFGGNTNNAFNNSNSTNSPFGFNKPNITG---

      190     200     210     220     230     240
AgNup116  SSAFCAPSSTSPFGTNSQGTTFVGTTNAASTGGLFGQNNANTNNSPFGQSTSTNAFCQPA
ScNup116  -TTFNNPQGTNTNTEFGIMGN--NSITTSATTGGLFGQKPATGMFG--TGTGSGGFCG--
ScNup100  -TLFGS-----QNNNSAGTSSLFGQ-----STSTITGFCN--

      250     260     270     280     290     300
AgNup116  NSPFGQSNNTTNAFGQNTGMSINSPFGQGNAAANSPPFGMKTSTTSTGGLFGQNTTGGFG
ScNup116  ----GATNSTGLFGSSTNLSGNSAFGANKPATSGGLFGNTTNNPTNG----TNNITGLFG
ScNup100  -----TGSSFGTGLNGGNSNIFGAGNNSQS

      310     320     330     340     350     360
AgNup116  QAG-ATGTGLFGQSAGTNTSTPFGQSNTFNQAGTTSAGLFGQNTNRQSSGNLFGSTNQ-
ScNup116  QQNSNTNGGLFGQQNSFGANNVSNNGAFQGVN----RGAFFPQQQTQQSGGIFGQSNAN
ScNup100  ----NTTGSFLFGNQSSAFGTNNQQGSLFGQSS-----QNTNNAFNGNQ-

      370     380     390     400     410     420
AgNup116  QNGSMFGQNNQTTTGLFGSNPTN--TFQONTASG--NLFNKPATGGGLFGQNTTQPSG
ScNup116  ANGGAFGQ--QQGTGALFGAKPASGGLFGQSAGSKAFGMNTNPTGTTGGLFGQNTQQQSG
ScNup100  LGGSSFGSK-PVGSGLFGQ-----SNNTLGNNTNRRNGLFGQMNSSNQGSSN

      430     440     450     460     470     480
AgNup116  GGLFGQNNTTNAFGQSNPSSGGLFGQNNQSMPPQGMQLCGGTQQQNGFQGSNQQQQGLF
ScNup116  GGLFGQ-----QONSNAAGGLFGQNNQSQNSGLFGQ--QNSSNAFGQP--QQQGLF
ScNup100  SGLFGQ-----SMNSSTQGVFGQNNNQMQINNNNSLFGKANTFSNS--ASGGLF

      490     500     510     520     530     540
AgNup116  GQNMQQSQQQGGLFGQNSANNTFR---QNNNTGGLFGNKPAAGGLFGQNTTGSTFGQS
ScNup116  G-----SKPAGGLFGQQGASTFASGNAQNSIFGQNNQQQSTGGLFGQNNQS----Q
ScNup100  GQN--NQQQGSLFGQNSQTSGSSGLFGQNNQKQPNFTTQSNITGIGLFGQNNNQ----

      550     560     570     580     590     600
AgNup116  NNSGGLFGQTNNOQQGNVFGTN----NQQQGGLFGQNNNQQTGLFGQNSNPQQNGITLQ
ScNup116  SQPGGLFGQTN-QNNNQPFQQNGLQPPQNNSLFGAKPTGFGNTSLFSNSTTNQSNGLISG
ScNup100  QQSTGLFGAKPAGTTGSLFGGNS---STQPNLFGTTN-----VPTSNTQSQGNSLFG

```

```

        610      620      630      640      650      660
AgNup116  QNNQQQSGGLFGQNSNPQNNQQGGLFGSKPANTTGGGLFGNNSSTTGNGLFGANNQQQTQ
ScNup116  NNLQQQSGGLFQ---NKQQPASGGLFGSKPSTVCGGLFGNNO-----VANQNNPAS
ScNup100  -ATKLTNMPFGGNPTANQSGSGNSLFGTKPASTTG-SLFGNNTAS-----

        670      680      690      700      710      720
AgNup116  QAGGLFGNNNGQSTTGSGLFG--NKSA GASAGGGLFG--NNTTQTGSTCG--GLFGNNTS
ScNup116  TSGGLFG-----SKPATGSLFGGTNSTAPNASSGGIFGSNNASNTAATTNSTGLFGNKPV
ScNup100  -----TTVPSTNGLFGNNANNSTSTTNTGLFGAKPDSQSKPALCG-GLFGNSNS

        730      740      750      760      770      780
AgNup116  TGNITNGTGGGLFGSKPAHASSVTGGASGGLFAPKPAARLSGGLFASKPAATTGGGLFGSK
ScNup116  GAGASTSAGGLFGNNNNSSLNNSNGSTG-LFGSN-----NTSQSTNAGGLFQNN
ScNup100  NSSITIGQNKPVFGTTQN--TGLFGATG-----TNSAVGSTGKLFQGN

        790      800      810      820      830      840
AgNup116  PAGSATGGLFGNNSSTSNNTGIGALQOQSGINGAAVGAQQSNPYGTNELFSRVILPNSLT
ScNup116  TSINTSGGLFSGQPSQSMASQNALQQQ--QQQRLQIQNNNPYGTNELFSKATVTNTVVS
ScNup100  NNTLNVG-----TONVPPVNNTTQALLGTTAVPSLQQAPVTNEQLFSKISIPNSIT

        850      860      870      880      890      900
AgNup116  QPSKPSATKLNADNKKRASLTSAYRLAPKPLFTAKSKPATAMPGLTHRKASLSTSQESLR
ScNup116  YPIQPSATKIKADERKKASLTNAYKMTPKTLFTAKLKTNNVMDKAQIKVDPKLS-ISISD
ScNup100  NPVKATTSKVNADMKRNSLTSAYRLAPKPLFAPSSNGDAKFQWGWKTLE-----

        910      920      930      940      950      960
AgNup116  EKIPSPSTGSTVFSSETDEIILASCHLFPNPKKSFKNLVL--NSKKMEDAGAGYESEPK
ScNup116  KKNNQIAISNQQEENLDESILKASELLFPNPKRSFKNLIN--NRKMLIASEEKNNGSQNN
ScNup100  -RSDRGSSTSNSITDPESYLSNDLLEDPDRRYLKHLVIKNNKLNLVINHNDDEASKVK

        970      980      990      1000     1010     1020
AgNup116  RITTFAPADRE-----PSPAEPAPAPAPPKDSLSTEPAPAPAEQPSQAP-----
ScNup116  DMNFKSKSEEQETILGKPKMDEKETANGGERMVLSSKNDGEDSATKHHSRNMDEENKENV
ScNup100  LVTFTEFSAS-----KDDQASSSIAASKLTEKAHSPQTDLKDDEHDESTPDPQSKSPN

        1030     1040     1050     1060     1070     1080
AgNup116  -----GLLGDDIGFGDDGYIAPALDSLAAAMSLQLRRVSGLVVGGHH
ScNup116  ADLQKQEYSEDDKAVFADVAEKDASEFINENYIISPLDTLSSYLLQLRKVPHLVVGGHK
ScNup100  GSTSIPMIENEKISSKVPGLLSNDVTFPKNNYIISPSIETLGNKSLTELRLKINNVLVIGHR

        1090     1100     1110     1120     1130     1140
AgNup116  LHGRIEFLAPVDLSNIPLPAICGNLVRFTEKVCESYVVGSEPPAPGQLNVRARISLHNT
ScNup116  SYGKIEFLPVDLAGIPLTSLGGVIITFEPKTCIIYANLPNRPKRREGINVRARITCFNC
ScNup100  NYGKVEFLPVDLLNTPLDLCGLVTFGPKSCSIYENCSEIKPEKREGINVRCRVTLYS

        1150     1160     1170     1180     1190
AgNup116  FPTDKASRLPIKDPKHPILKRHIEKLLKLEHTRFEAYDVKTGTYTFIVDTPVA--
ScNup116  YPVDKSTRKPIKDPNHQLVKRHIEKLLKKNPNKSFESYDADSGTYVFIYNHAAEQT
ScNup100  FPIDKETRKPIKNITHPLLKRSTAKLKENPVYKSFESYDPVTGTYSYTIIDHPVLT-

```

□ Potential Gle2p-binding sequence (AgNup116/100p: 101-150 aa; GLEBS)

Appendix 1: Alignment of AgNup145p and ScNup145

```

      10      20      30      40      50      60
AgNup145 MFGAASGGNSLFGGANASTPTPTPAPAGNLFNFNKKPGEFAGAGQN-NVSTPSPAGDLL
ScNup145 MFNKS VNSGFTFGNQNTSTPTSTPAQPS SSSLOFPQKSTGLFGNVNVNANTSTPSPSGGLF

      70      80      90      100     110     120
AgNup145 GAKSTTTGGLFGPKTEQKPAGGLFGQSSAAPNGTGGGGLFASTGNSGSTQLCGLFGNSAA
ScNup145 NANSNAN-----SISQQPANNSLFGNKPAQPS-----GGLFGATNNTTSKSAAGSLFGNNNA

      130     140     150     160     170     180
AgNup145 GGGGS-LFGAGSAAANNAS-TSLGNLFGKPNPND---TAPAAGGGLFNSRPNATATNTVSSST
ScNup145 TANSTGSTGLFSGSNNIASSTQNGGLFGNSNNNITSTTQNGGLFG-----KPTTTPAGA

      190     200     210     220     230     240
AgNup145 NSLFSNNQNGAQNNGGLFGAKPTGGLFGNSTAQPOSSSLFGASSONNQQQQQTQQLSL
ScNup145 GGLFGNS--SSTNSTTGLFGSNNTQSSTGIFGQKPGASTTGGLFGNGASFPRSGETTGT

      250     260     270     280     290     300
AgNup145 LGSNPYGLNLTGVP--VTMPESITAAITSK--KKNELPLVHEKKRMFSTSSASN---VL
ScNup145 MSTNPYGINLSNVPMVAVADMRSITSSLSDVNGKSDAEPKPIENRRITYSFS SSVSGNAPL

      310     320     330     340     350     360
AgNup145 PLVSNOSTLISKLSRLNSGKNGESTRGLFSP--SRKVLS---QGPLVAADNTRDLNPPL
ScNup145 PLAS-QSSLVSRSLSTRLKATOKSTSPNEIFSPSYSKPWLNGAGSAPLVDDFFSSKMTSLA

      370     380     390     400     410     420
AgNup145 NHPSSSIPSRPLLSLAN-RIDLSDMRKLKLDPHRSAAKKLRLLNGQSATTKLKLIDTNYQ
ScNup145 PNENSIFPQNGFNFLSSQRADLTELRKLKIDSNRSAAKKLLLSGTPAITKKHMODEQDS

      430     440     450     460     470     480
AgNup145 SQREESSEIFVSTKTDROP-----LEEKCEVSSTTG---IPESDNGCDGYWC
ScNup145 SENPPIANADSVTINIDRKENRDNNLDNTYLNKKEQSNNLNKQD GENTLQHEKSSSFQGYWC

      490     500     510     520     530     540
AgNup145 SPSTEQQLQRITPQQLSAIPNFVIGRKGYSISFDLDVDLTAFSDDFKHALFGSVMFNEN
ScNup145 SPSPTEQLERLSLKQLAAVSNFVIGRRGYGCITFQHDVDLTAFTKSFREELFGKIVIFRSS

      550     560     570     580     590     600
AgNup145 KTVEVYPDDSLKPPITGLGLNVPATITLERIYPIDKKTNOPIITENS DLAKVQYFVKRLKSM
ScNup145 KTVEVYPDEATKPMIGHGLNVPATITLENVYPVDKTKKPKMDTTKFAEFQVDRKLRSM

      610     620     630     640     650     660
AgNup145 RDMEFISYNPYGGVWTFKVKHFSIWGLVNDSDVEIDDVLEAAREAEIKQRIVAIPKRPG
ScNup145 REMNYLSYNPFGGIWTFKVNHF SIWGLVNEEDAEI DEDDLS-----

      670     680     690     700     710     720
AgNup145 FGKQADSTVPGGFDQLVHIPSSVDIDMTQTSPDDYSLTSAPVDALHDEAMTDLIEEKPY
ScNup145 --KQED-----GGEQPLRKVRT---LAQSKPSDKEVILKTDGTFGTLSGKDDS-IVEEKAY

```

```

          730      740      750      760      770      780
AgNup145  EPSDVDEEDFEGLAEAPNLEVSSDWHQQLQLAADPYKSVFANSTSLN-RVNMKDDVIFNT
ScNup145  EP-DLSADDFEGIEASPKLVDVSKDWVEQLILAGSSLRVSVFATSKFEFDGPCQNEIDLLFSE

          790      800      810      820      830      840
AgNup145  FQKDMDEFKSTIRRQRRLDSAPSFVRFNNDSTITMKTDKSTSGCTVTASPLPLQTORSSID
ScNup145  CNDEIDNAKLIMKERRFTASYTFKFFSTGSMLLTKDIVGKSGVSIKRLPTELQRKFLFDD

          850      860      870      880      890      900
AgNup145  SVLKKSLIDSTIELRNNN-YPIVKQFSLTFDDIAAAKYPKIPAEYRTWKLASILFDPISVS
ScNup145  VYLDKEIEKVTIEARKSNPYQISESSLFKDALDYMEKTSSDYNLWKLSSILFDPVSYF

          910      920      930      940      950      960
AgNup145  KSRSHPDDAVKDVLVKKKQYELLCDWIINEINSEVGAKTASAG-PLEKIFLYLVKRDIIIG
ScNup145  YKTDN--DQVKMALLKKERHCRLLTSWIVSQIGPEIEEKIRNSSNEIEQIFLYLLNDVVR

          970      980      990      1000     1010     1020
AgNup145  ATTAAIASNNNHLAVLVTLGSDNPLVRELSTSHLSKIKKLGSSLDINIIKIYQLLTGSP
ScNup145  ASKLAIESKNGHLSVLI SYLGSNDPRIRDLAELQLQKWSTGCGSIDKNI SKIYKLLSGSP

          1030     1040     1050     1060     1070     1080
AgNup145  FAESAN-SVISEGLSWLATLGLQIFYGDDALSLRELI ERGLEYSCKDQWELNDISANTL
ScNup145  FEGLFSLKELESEFSWLCLLNLTLCYGQIDEYSLESLVQSHLD---KFSLPYDDPIGVIF

          1090     1100     1110     1120     1130     1140
AgNup145  RLYCSDVTPDILVGNLKISSNNLDVRLSWFFIQILTRDD---ISPSLRDHLTLQYVEQLK
ScNup145  QLYAANENTEKLYKEVRQRINALDVQFCWYLIQTLRFNGTRVFSKETSDEATFAFAAQLE

          1150     1160     1170     1180     1190     1200
AgNup145  LNRMFGEALFIMCFINDDRLLAKQQVDHLLSSQITFFSQDSNYELLTRLRIPKSSYYAFLA
ScNup145  FAQLHGHSLVSCFLNDDKAAEDTIKRLVMREITLLRASNNDHILNRLKIPSQLIFNAQA

          1210     1220     1230     1240     1250     1260
AgNup145  LLDKYNRNHLSEARNLLKAGHFQEA EKVVIVSVAPKLVLDGSAAN---LQTLRQLLETFP
ScNup145  LKDRYEGNYLSEVONLLLGSSYDLAEMAIVTSLGPRLLSNPNVQNNELKTLREILNEFP

          1270     1280     1290     1300     1310     1320
AgNup145  AQOMETWTHGLGVFEKYLQIALDNNHNQELLSDLV RVLPVLATDFGSHRELSVVCVMSK
ScNup145  DSERDKWSVSINVFEVYLKLVLDNVETQETIDSLISGMKIFYDQYKHCREVAACCNVMSQ

          1330     1340     1350     1360     1370
AgNup145  LVCHIILENYRQALETSPFKDRLLALPLGQPETIYKRALAST-----
ScNup145  EIVSKILEKNNPSIGDS--KAKLLELPLGQPEKAYLRGEFAQDLMKCTYKI

```

- GLFG-repeats
- NRM-domain (AgNup145p: 580-595 aa; *: conserved ser 588 aa)
- RNP-like motif (AgNup145p: 471-478 aa, Fabre et al., 1994)

Appendix 1: Alignment of AgOrc6p, KlOrc6p, ScOrc6p and CgOrc6p

	10	20	30	40	50	60
AgOrc6	MSVSQVRSVSEILGLNAQEETPDWNSGRLKRMATTAATLYNVSLNKVMLKQPEELARCH					
KlOrc6	MSTQQVRTCVDLLGVK-NDSNVDWQDQRLKKVASTTATLYNVSVKVMLKNSEELARCH					
ScOrc6	MSMQVQHCVAEVLRLD-PQEKPDWSSGYLKKLTNATSILYNTSLNKVMLKQDEEVARCH					
CgOrc6	MSSRQVQQSLQDILGYT-DREEVDWGGKYLKKLVTTTTLYNTSASKIVLTPDEEVARCH					
	70	80	90	100	110	120
AgOrc6	TCAYLAABKILSEKYEPELQYYREKIPLEPRKTVKLVGLFKQTLWTSPPVRNLN-----					
KlOrc6	ICALIAFQKLAEKYDNDLPYSQEKIPLPPDQVSKLVNIFKRNIWPHSPQKDTREGQLLKFD					
ScOrc6	ICAYIASQKMNKEHMPDLCYYIDSIPLEPKKAKHLMNLFQSLSNSSPMKQFA-----					
CgOrc6	ICAVLAAERLAEKHMPDLKYYTDKIPLQPSRVNMLMGYFKQNLFNMSPVKDKMS-----					
	130	140	150	160	170	180
AgOrc6	--LSPSPKK-----DGGRLSARDPVELRAELFGTPVKRAGAVTLPGAGELSPTKQLS					
KlOrc6	DTASPSVRKSA-----VKNARFTGIDPKSLQEQLFQTPSKSR---TKSGIQPLK-NVDLS					
ScOrc6	--WTPSPKKNK-RSPVKNNGRFTSSDPKELRNQLFGTPTKVR----KSNQNDSFVPEL					
CgOrc6	--WTPSPMKRRTRSPVKNNDRFTAQDPQSLKKQLFGTPTKST----GSPS--PFVVPQS					
	190	200	210	220	230	240
AgOrc6	PSKPMSPVKPSPRRRLAFEDDEDE-----DYEPD---ASPQSPRRS					
KlOrc6	PSK---GSRSSVRRKLVFEADTE-----NGLPLPILATPKNKTDMI					
ScOrc6	PPMQTNESPSITRRKLAFEDEDEDEE--EPGNDGLSLKSHSNKSITGTRNVDSDEYENH					
CgOrc6	PKSNNSNPRKIRKLAFEEDDDEADESVVPSND---SRSNSNNLREDESETPS-VIDSS					
	250	260	270	280	290	300
AgOrc6	IFPGGFEPDPDESEFDSPTKSPFKSPTRSPSTKSAQSS-PRKKRGEYNQ-----WNMLYK					
KlOrc6	NIPQVFGSVEDDPE-SPLRQSPFRD---SPSKYTSP--PRKKRKYNE-----WNMLYK					
ScOrc6	ESDPTSEEEPLGVQESRSGRTKQNKAVGKPKQSELKTAKALRKRGRIPN-----SLLVK					
CgOrc6	STAPVFGNVAITTPSKRVLDEDYKEDDESRESSVQTESSPRKR-RLESPRKKNLLSILEK					
	310	320	330	340	350	360
AgOrc6	KYRITPPEIIVGLCNQFELPSRVAFQVLDCEFGMHATYLVYPAQLVCGLVMLCCFVVHHRK					
KlOrc6	KYRIPSTAEVLVTLTNEFELPEEVTATIISEFNNNATYLAAPTQLVCGLVLLCSFVVFNQ					
ScOrc6	KYCKMTTEEIIRLCNDFELPREVAYKIVDEYNINASRLVCPWQLVCGLVNLCTEIVFNER					
CgOrc6	RHVNLISAADIIKICNIFELPKDVAHFVLEEYYARSSFLTYSWQLVAGLVINCVEIVFNER					
	370	380	390	400	410	420
AgOrc6	RASDPTIDDYLLKMKCALLRSNSTSDVLEAMKITKELLDGENWYRALKIEYDYDAADFE					
KlOrc6	RNQDSTIDNKLKMAAQMRRTTNDDEDIMEAIIKITKELIDGKQWYRELRVKFDYDYGSDFD					
ScOrc6	RRKDPRIDHFIVSKMCSLMLTSKVDDVIECVKLVKELIIGEKWFRDLQIRYDDEFGIRYD					
CgOrc6	RRKDPRIDHLILTRMQEKEMKSKDLSEVIDSTKMKVLELLEGGQWYRELEVKNYDFDGASYN					
	430	440	450	460		
AgOrc6	QSLAIRLGSMLQNSNVIASTEQFEWKKKVMVLDLSLRDGS					
KlOrc6	NALAVRIGSMLQDEYEVVSEEQYSNWKRRIMVDLSLRDGT					
ScOrc6	EILFRKLGSMLOTTNLTVDQYNIWKKRIEMDLALTEPL					
CgOrc6	EVLAKKLGSMLOPNNILATEDQYKNWSRRIREDISIREL-					

Ag: *A. gossypii* Kl: *K. lactis* Sc: *S. cerevisiae* Cg: *C. glabrata*
 : "RXL" motif involved in the interaction with Clb5p (Wilmes et al., 2004)

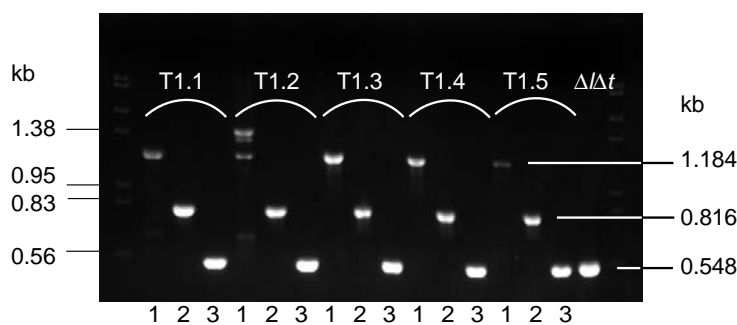
APPENDIX II

Appendix 2: Verification PCR of *A. gossypii* deletions



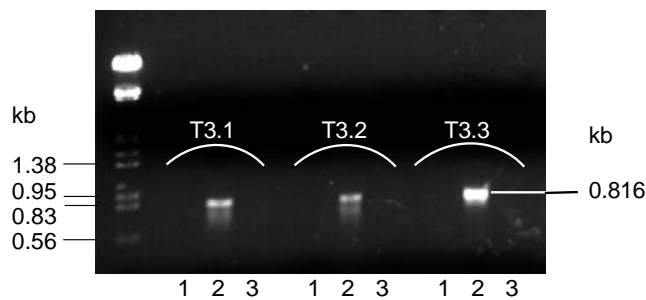
AKHAg1: *Agclb1/2Δ::GEN3, leu2Δ thr4Δ / AgCLB1/2 leu2Δ thr4Δ*

- | | | |
|----|------------------------|----------|
| 1: | CLB1/2-G1 - G2: | 1.184 kb |
| 2: | G3 - CLB1/2-G4: | 0.816 kb |
| 3: | CLB1/2-I1 - CLB1/2-G4: | 0.548 kb |



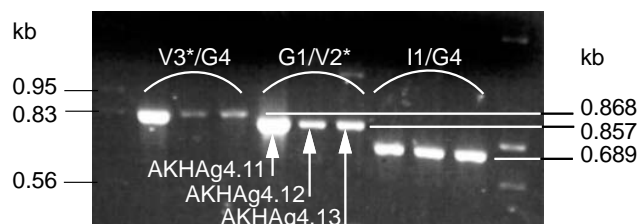
AKHAg3: *Agclb3/4Δ::GEN3, leu2Δ thr4Δ*

- | | | |
|----|------------------------|-------------------------|
| 1: | CLB3/4-G1 - G2: | 1.152 kb |
| 2: | G3 - CLB3/4-G4: | 0.868 kb |
| 3: | CLB3/4-G1 - CLB3/4-I1: | 0.727 kb (Heterokaryon) |



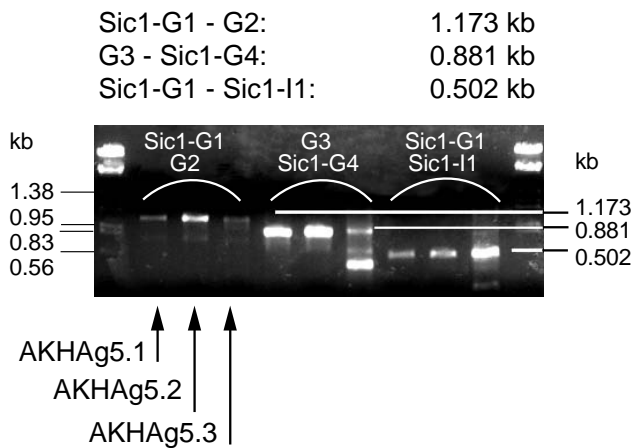
AKHAg4: *Agclb5/6Δ::NAT1, leu2Δ thr4Δ / AgCLB5/6 leu2Δ thr4Δ*

- | | |
|--------------------|----------|
| V3*NAT1 - CLB5-G4: | 0.868 kb |
| CLB5-G1 - V2*NAT1: | 0.857 kb |
| CLB5-I1 - CLB5-G4: | 0.689 kb |



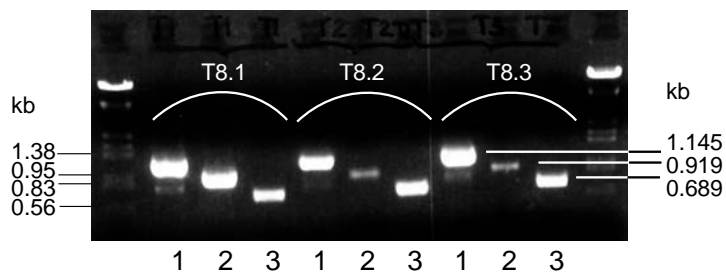
Appendix 2: Verification PCR of *A. gossypii* deletions

AKHAg5: *AgSic1* Δ ::*GEN3*, *leu2* Δ *thr4* Δ / *AgSIC1* *leu2* Δ *thr4* Δ (partial deletion)
Deletion of the N-terminal 405 bps of the *AgSIC1* (689 bp) gene.



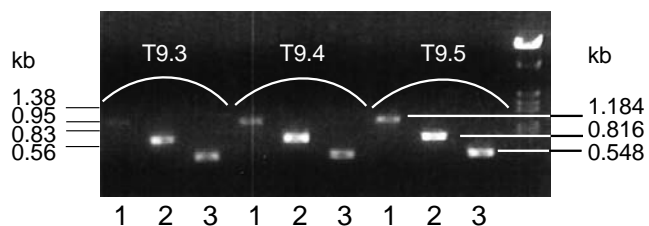
AKHAg8: *Agclb5/6* Δ ::*GEN3*, *leu2* Δ *thr4* Δ / *AgCLB5/6* *leu2* Δ *thr4* Δ

1. CLB5-G1 - G2: 1.145 kb
2. G3 - CLB5-G4: 0.919 kb
3. CLB5-I1 - CLB5-G4: 0.689 kb

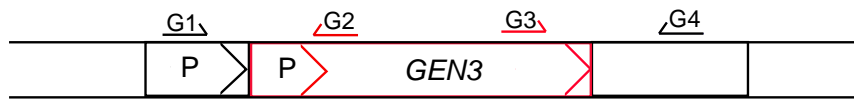


AKHAg9: *Agclb1/2* Δ ::*GEN3*, *leu2* Δ *thr4* Δ *ade2*::*ADE2-H4-GFP* / *AgCLB1/2* *leu2* Δ *thr4* Δ

1. CLB1/2-G1 - G2: 1.184 kb
2. G3 - CLB1/2-G4: 0.816 kb
3. CLB1/2-G4 - CLB1/2-I1: 0.548 kb

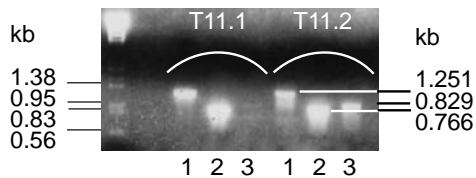


Appendix 2: Verification PCR of *A. gossypii* deletions



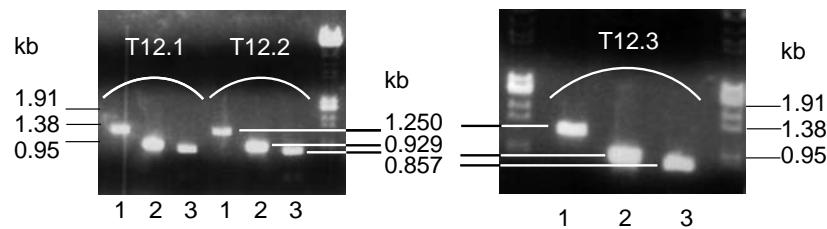
AKHAg11: *AgYrb1* Δ ::*GEN3*, *leu2* Δ *thr4* Δ / *AgYRB1 leu2* Δ *thr4* Δ

1:	AgYRB1-G1 - G2:	1.251 kb
2:	AgYRB1-I1 - AgYRB1-G1:	0.766 kb
3:	G3 - AgYRB1-G4:	0.829 kb



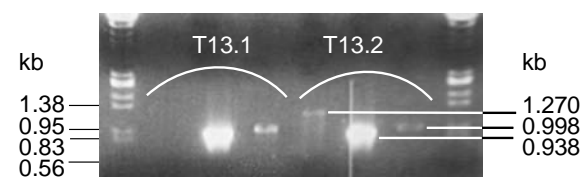
AKHAg12: *AgSrp1* Δ ::*GEN3*, *leu2* Δ *thr4* Δ / *AgSRP1 leu2* Δ *thr4* Δ

1:	AgSRP1-G1 - G2:	1.250 kb
2:	G3 - AgSRP1-G4:	0.929 kb
3:	AgSRP1-G1 - AgSRP1-I1:	0.857 kb

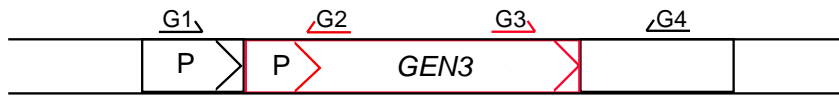


AKHAg13: *AgKAP95* Δ ::*GEN3*, *leu2* Δ *thr4* Δ / *AgKAP95 leu2* Δ *thr4* Δ

AgKAP95-G1 - G2:	1.270 kb
G3 - AgKAP95-G4:	0.938 kb
AgKAP95-I1 - AgKAP95-G1:	0.998 kb

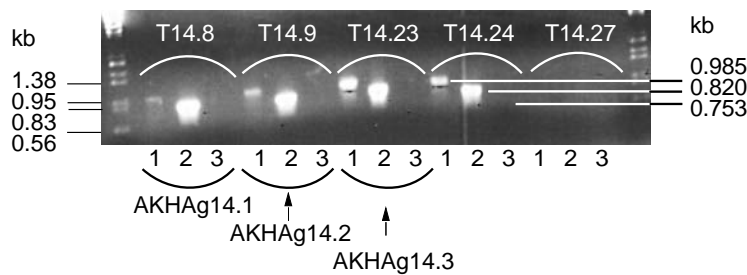


Appendix 2: Verification PCR of *A. gossypii* deletions



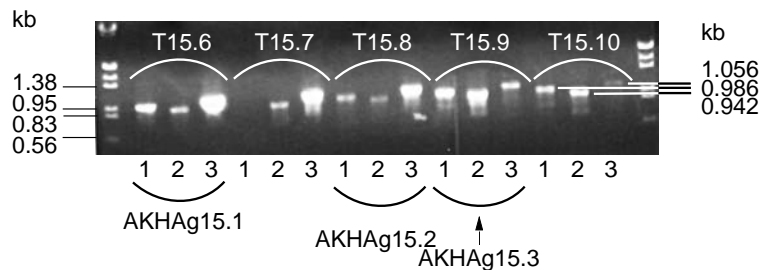
AKHAg14: *AgRNA1*Δ::*GEN3*, *leu2*Δ *thr4*Δ / *AgRNA1 leu2*Δ *thr4*Δ

- 1: AgRNA1-G1 - G2: 0.985 kb
- 2: G3 - AgRNA1-G4: 0.820 kb
- 3: AgRNA1-I1 - AgRNA1-G1: 0.753 kb



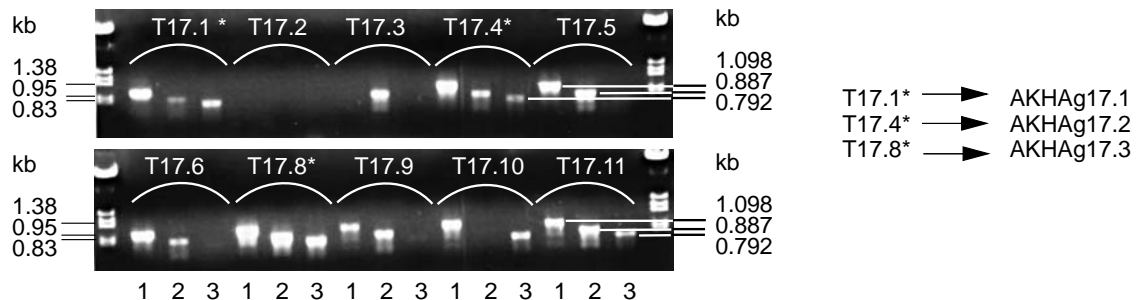
AKHAg15: *Agpse1*Δ::*GEN3*, *leu2*Δ *thr4*Δ / *AgPSE1 leu2*Δ *thr4*Δ

- 1: AgPSE1-G1 - G2: 0.986 kb
- 2: G3 - AgPSE1-G4: 0.942 kb
- 3: AgPSE1-G1 - AgPSE1-I1: 1.056 kb

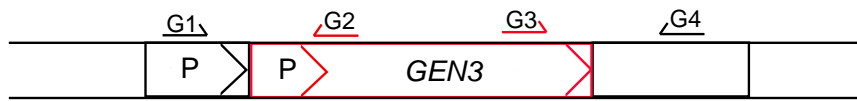


AKHAg17: *Agkap123*Δ::*GEN3*, *leu2*Δ *thr4*Δ / *AgKAP123 leu2*Δ *thr4*Δ

- AgKAP123-G1 - G2: 1.098 kb
- G3 - AgKAP123-G4: 0.887 kb
- AgKAP123-I1 - AgKAP123-G1: 0.792 kb

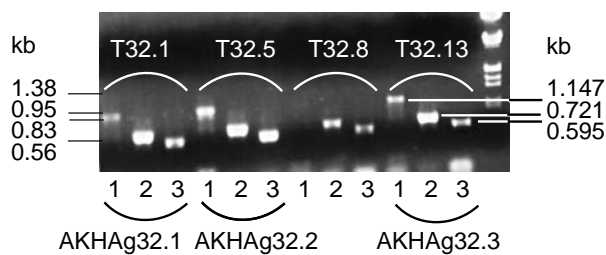


Appendix 2: Verification PCR of *A. gossypii* deletions



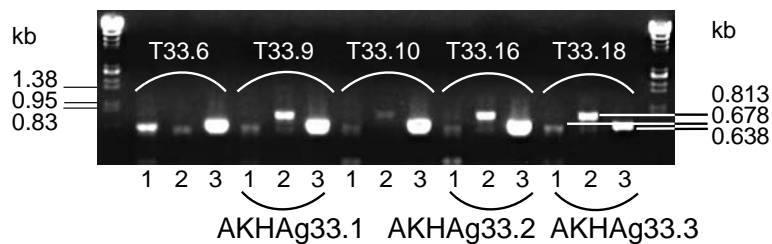
AKHAg32: *AgNUP116/100Δ::GEN3, leu2Δ thr4Δ* / *AgNUP116/100 leu2Δ thr4Δ*

1:	AgNUP116-G1 - G2:	1.147 kb
2:	G3 - AgNUP116-G4:	0.721 kb
3:	AgNUP116-I1 - AgNUP116-G4:	0.595 kb



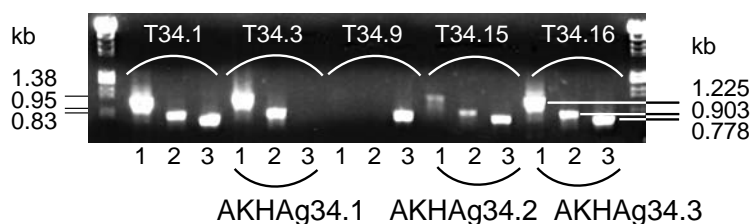
AKHAg33: *AgNUP53/59Δ::GEN3, leu2Δ thr4Δ* / *AgNUP53/59 leu2Δ thr4Δ*

1:	AgNUP53-G1 - G2:	0.678 kb
2:	G3 - AgNUP53-G4:	0.813 kb
3:	AgNUP53-I1 - AgNUP53-G4:	0.638 kb



AKHAg34: *AgNUP145Δ::GEN3, leu2Δ thr4Δ* / *AgNUP145 leu2Δ thr4Δ*

	AgNUP145-G1 - G2:	1.225 kb
	G3 - AgNUP145-G4:	0.903 kb
	AgNUP145-I1 - AgNUP145-G4:	0.778 kb



Appendix 2: Verification PCR of GFP-fusion

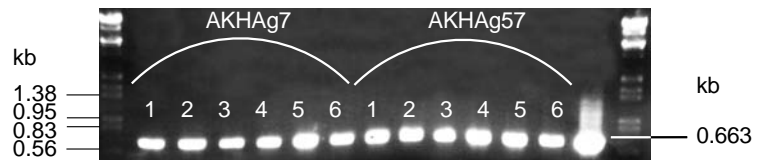


AKHAg7: *AgCLB1/2-GFP-GEN3, leu2Δ thr4Δ* (derived from pAKH7)

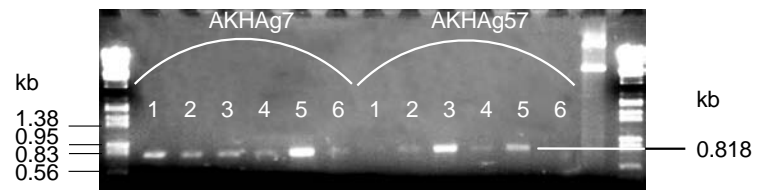
AKHAg57: *AgCLB1/2-GFP-GEN3, leu2Δ thr4Δ* (derived from pAKH9)

CLB1/2-I1* - GG2: 0.663 kb
 G3 - CLB1/2-G4: 0.818 kb
 CLB1/2-I1* - CLB1/2-G4: 0.703 kb (Heterokaryon)

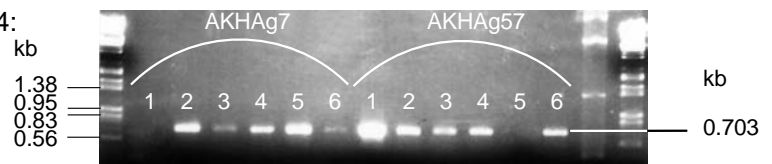
CLB1/2-I1* - GG2:



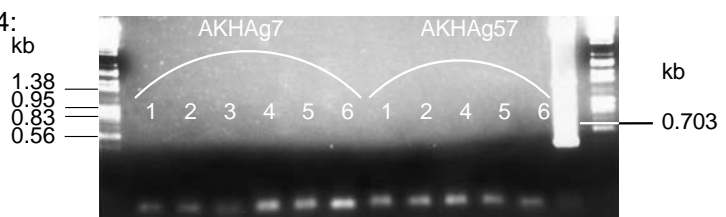
G3 - CLB1/2-G4:



CLB1/2-I1* - CLB1/2-G4:
(Heterokaryon)

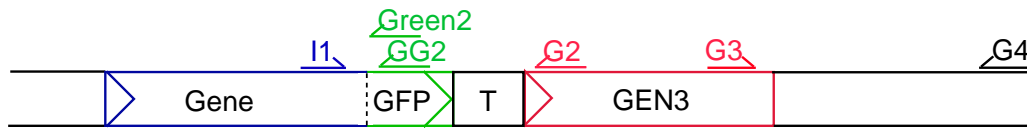


CLB1/2-I1* - CLB1/2-G4:
(Homokaryon)



↑ AKHAg7.2
 ↑ AKHAg7.3
 ↑ AKHAg7.5
 ↑ AKHAg57.2
 ↑ AKHAg57.4
 ↑ AKHAg57.6

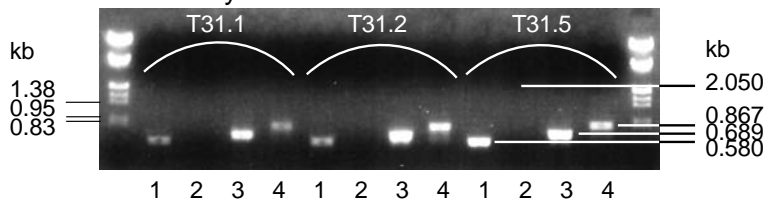
Appendix 2: Verification PCR of GFP-fusion



AKHAg31: *AgCLB5/6-GFP-GEN3, leu2Δ thr4Δ*

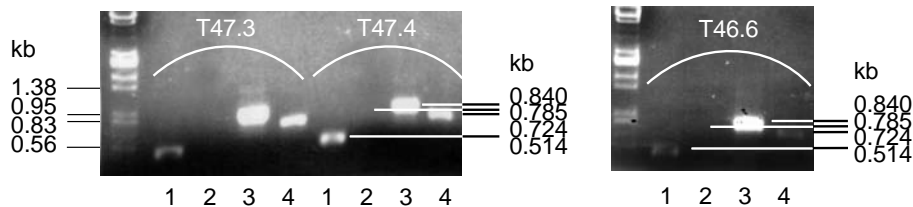
1. CLB5-I1 - Green2: 0.580 kb
2. CLB5-I1 - G2: 2.050 kb
3. CLB5-I1 - CLB5-G4: 0.689 kb (Heterokaryon)
4. CLB5-G4 - G3: 0.867 kb

Heterokaryon:



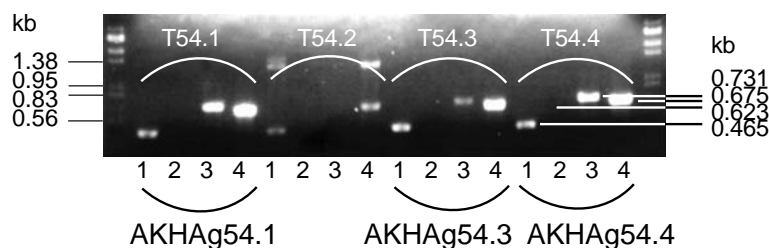
AKHAg47: *AgCLB3/4-GFP-GEN3, leu2Δ thr4Δ*

1. CLB3/4-I1 - Green2: 0.514 kb
2. CLB3/4-I1 - CLB3/4-G4: 0.785 kb (Heterokaryon)
3. G3 - CLB3/4-G4: 0.840 kb
4. CLB3/4-I1 - GG2: 0.724 kb

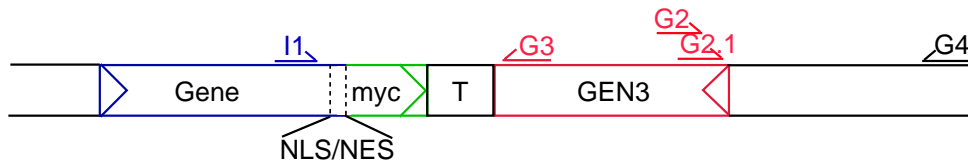


AKHAg54: *AgCLN3-GFP-GEN3, leu2Δ thr4Δ*

1. CLN3-I1 - Green2: 0.465 kb
2. CLN3-I1 - CLN3-G4: 0.623 kb (Heterokaryon)
3. G3 - CLN3-G4: 0.731 kb
4. CLN3-I1 - GG2: 0.675 kb



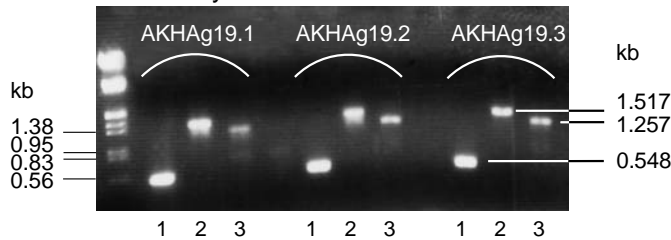
Appendix 2: Verification PCR of forced localization cassettes



AKHAg19: *AgCLB1/2-NESa-13myc-GEN3, leu2Δ thr4Δ*

1. CLB1/2-I1 - CLB1/2-G4: 0.548 kb (Heterokaryon)
2. G3 - CLB1/2-I1: 1.517 kb
3. G2 - CLB1/2-G4: 1.257 kb

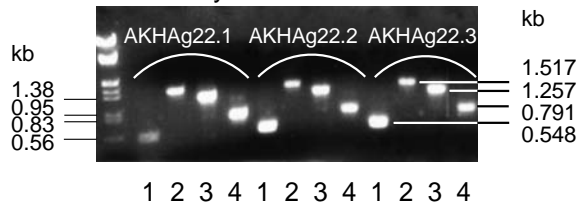
Heterokaryon:



AKHAg22: *AgCLB1/2-NESi-13myc-GEN3, leu2Δ thr4Δ*

1. CLB1/2-I1 - CLB1/2-G4: 0.548 kb (Heterokaryon)
2. G3 - CLB1/2-I1: 1.517 kb
3. G2 - CLB1/2-G4: 1.257 kb
4. G2.1-CLB1/2-G4: 0.791 kb

Heterokaryon:

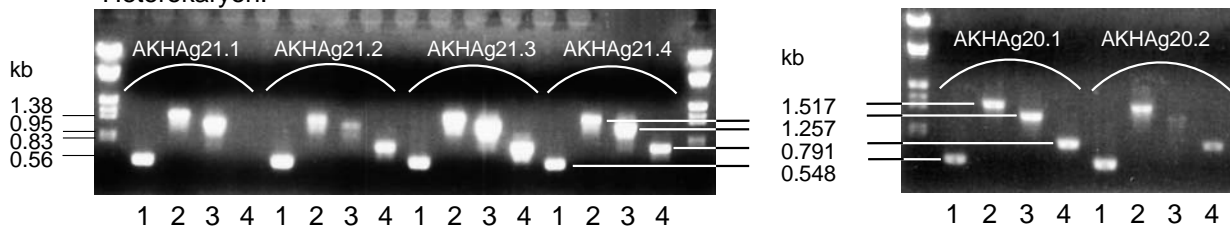


AKHAg20: *AgCLB1/2-NLSi-13myc-GEN3, leu2Δ thr4Δ*

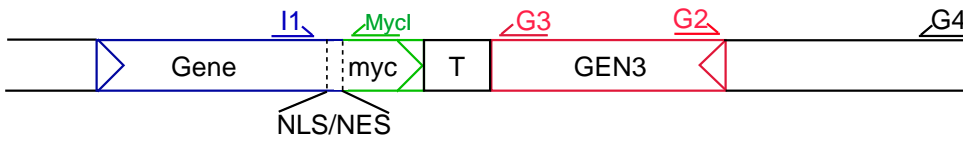
AKHAg21: *AgCLB1/2-NLSa-13myc-GEN3, leu2Δ thr4Δ*

1. CLB1/2-I1 - CLB1/2-G4: 0.548 kb (Heterokaryon)
2. G3 - CLB1/2-I1: 1.517 kb
3. G2 - CLB1/2-G4: 1.257 kb
4. G2.1-CLB1/2-G4: 0.791 kb

Heterokaryon:



Appendix 2: Verification PCR of forced localization cassettes

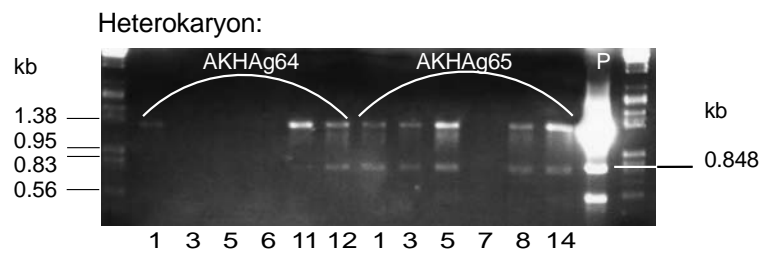


AKHAg64: *AgCLB5/6-NESa-13myc-GEN3, leu2Δ thr4Δ*

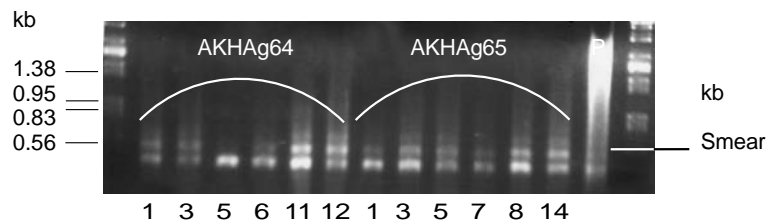
AKHAg65: *AgCLB5/6-NESi-13myc-GEN3, leu2Δ thr4Δ*

1. CLB5-G4 - G2: 0.848 kb
2. CLB5-I1 - Mycl: Smear
3. CLB5-I1 - CLB5-G4: 0.689 kb (Heterokaryon)

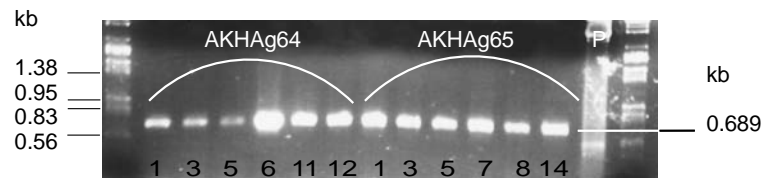
CLB5-G4 - G2:



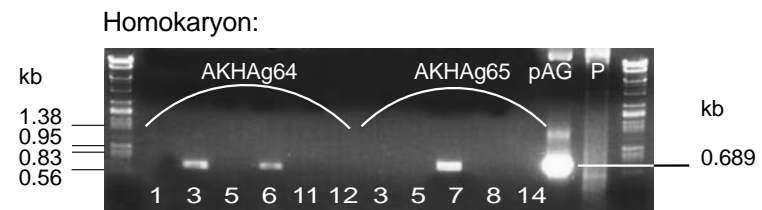
CLB5-I1 - Mycl:



CLB5-I1 - CLB5-G4:



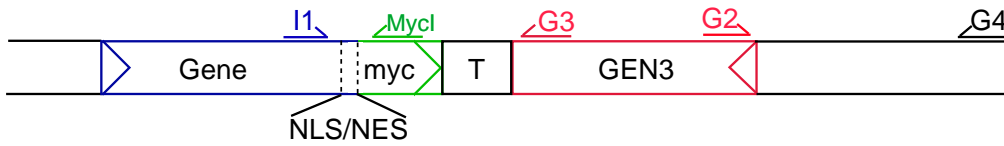
CLB5-I1 - CLB5-G4:



* = plasmidic

↑
AKHAg64.1 *
↑
AKHAg64.11
↑
AKHAg64.12
↑
AKHAg65.3
↑
AKHAg65.5 *
↑
AKHAg65.8

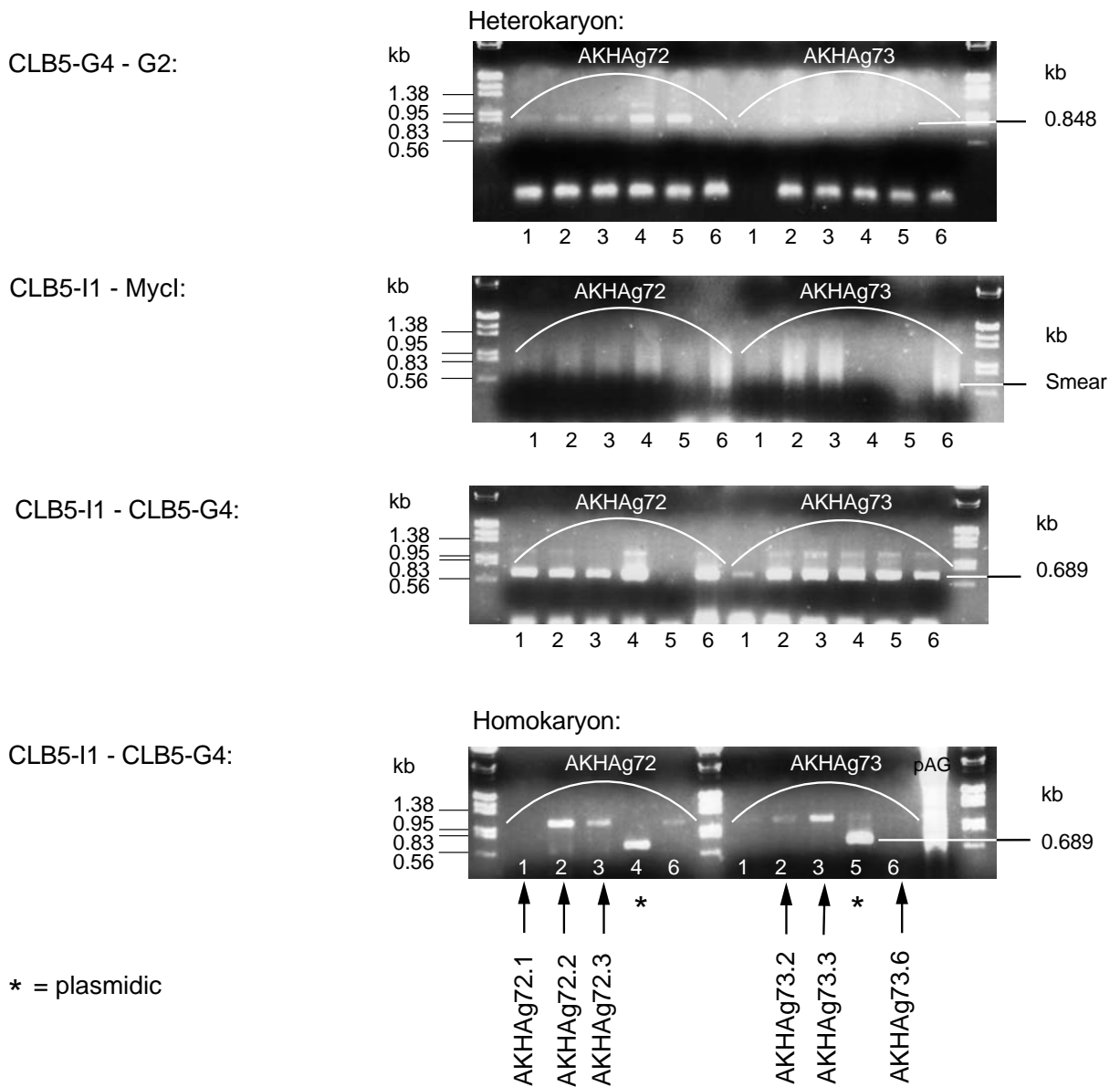
Appendix 2: Verification PCR of forced localization cassettes



AKHAg72: *AgCLB5/6-NLSa-13myc-GEN3, leu2Δ thr4Δ*

AKHAg73: *AgCLB5/6-NLSi-13myc-GEN3, leu2Δ thr4Δ*

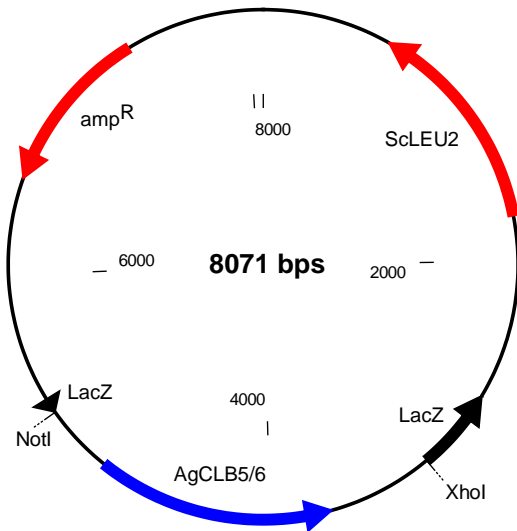
1. CLB5-G4 - G2: 0.848 kb
2. CLB5-I1 - Mycl: Smear
3. CLB5-I1 - CLB5-G4: 0.689 kb (Heterokaryon)



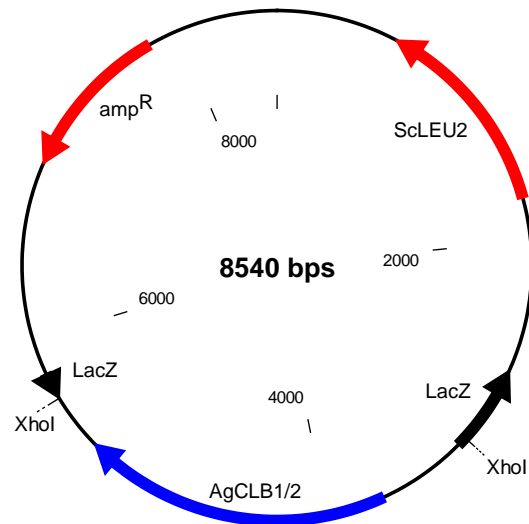
APPENDIX III

Appendix 3

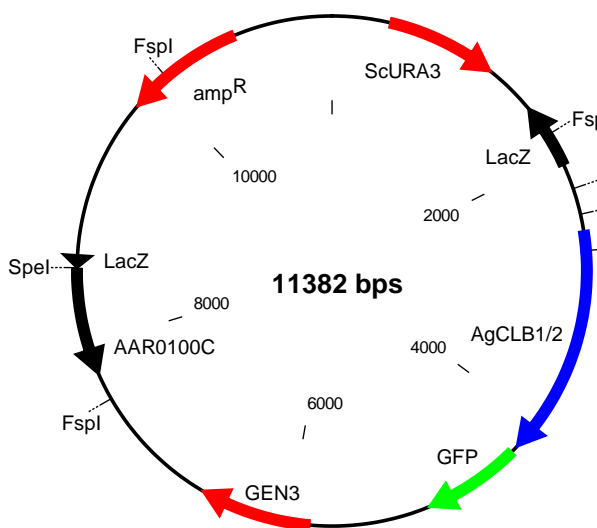
pAKH1



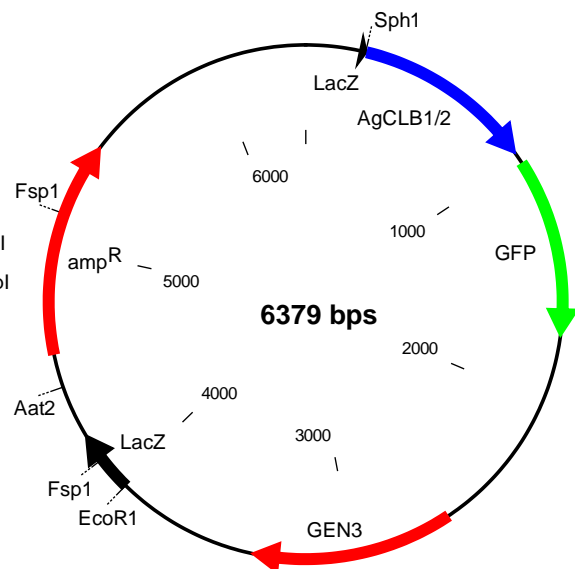
pAKH2



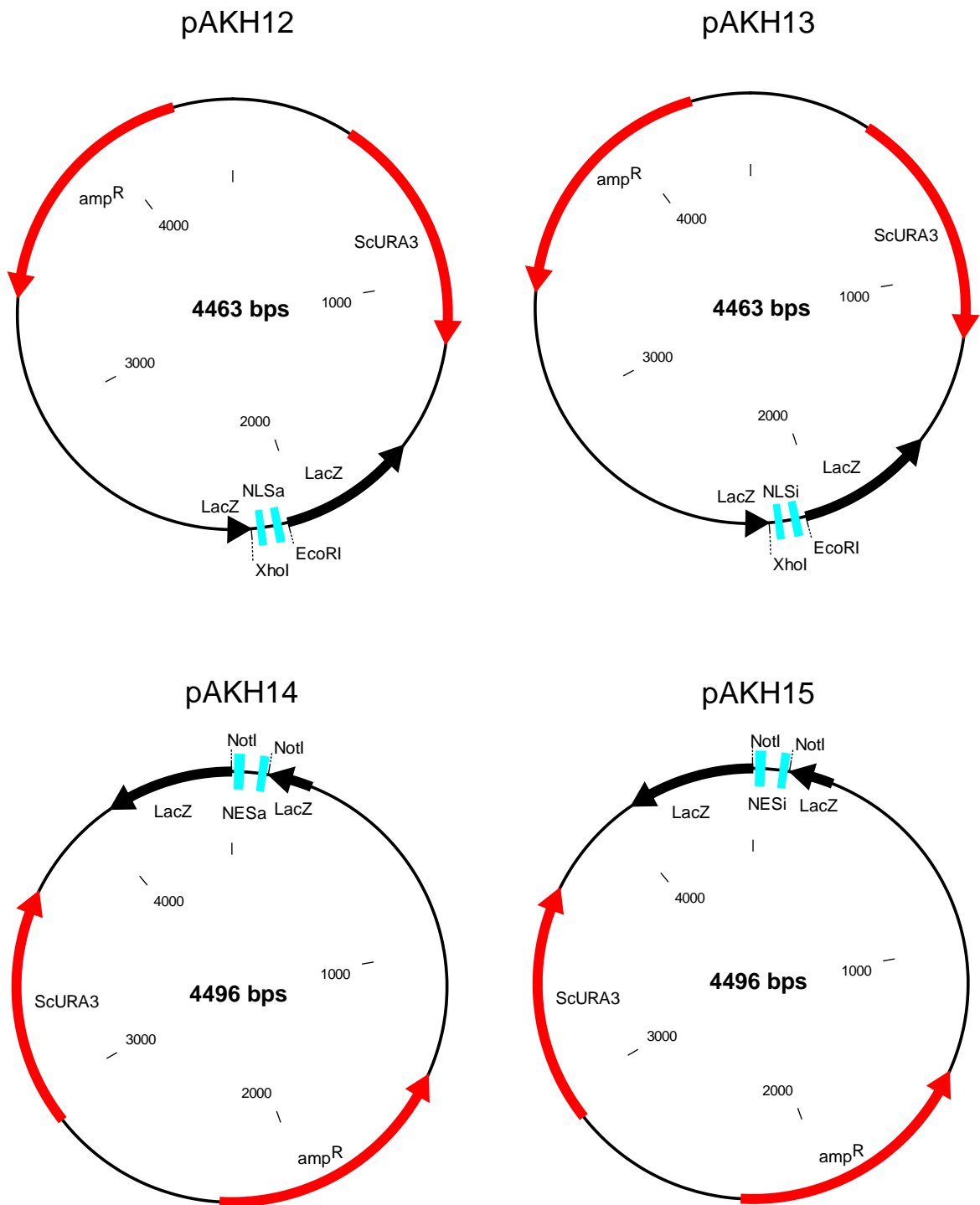
pAKH7



pAKH9

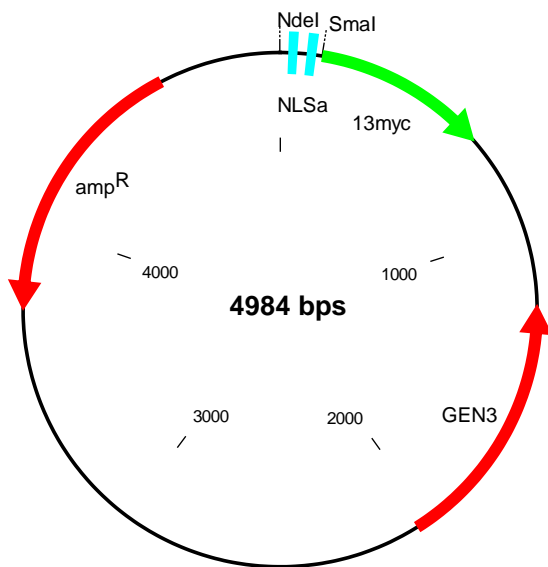


Appendix 3

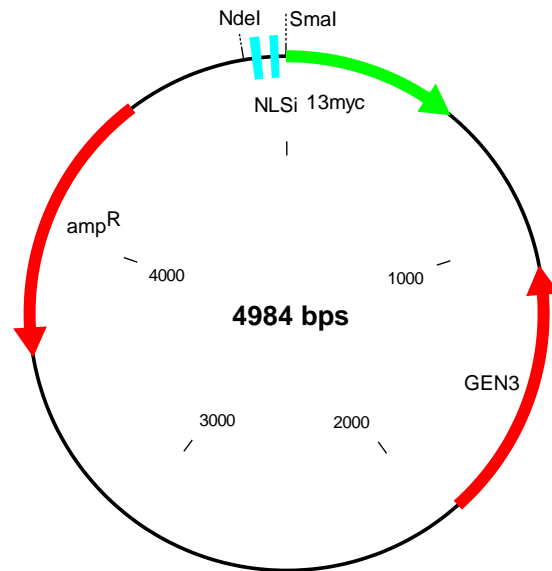


Appendix 3

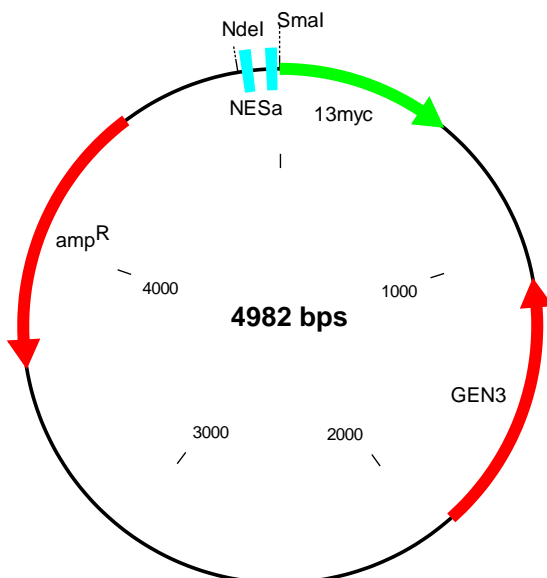
pAKH18



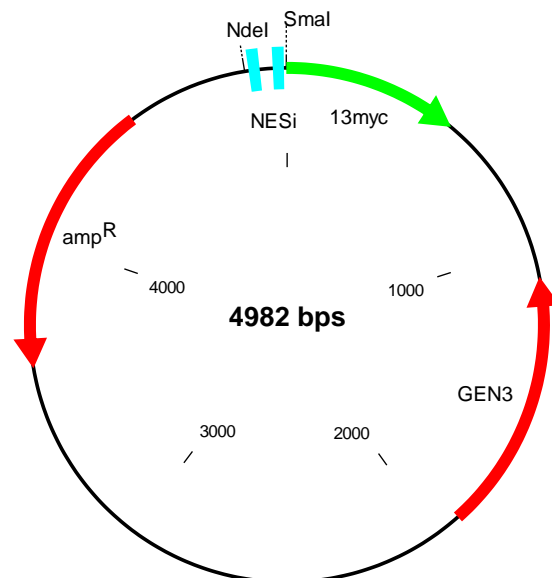
pAKH19



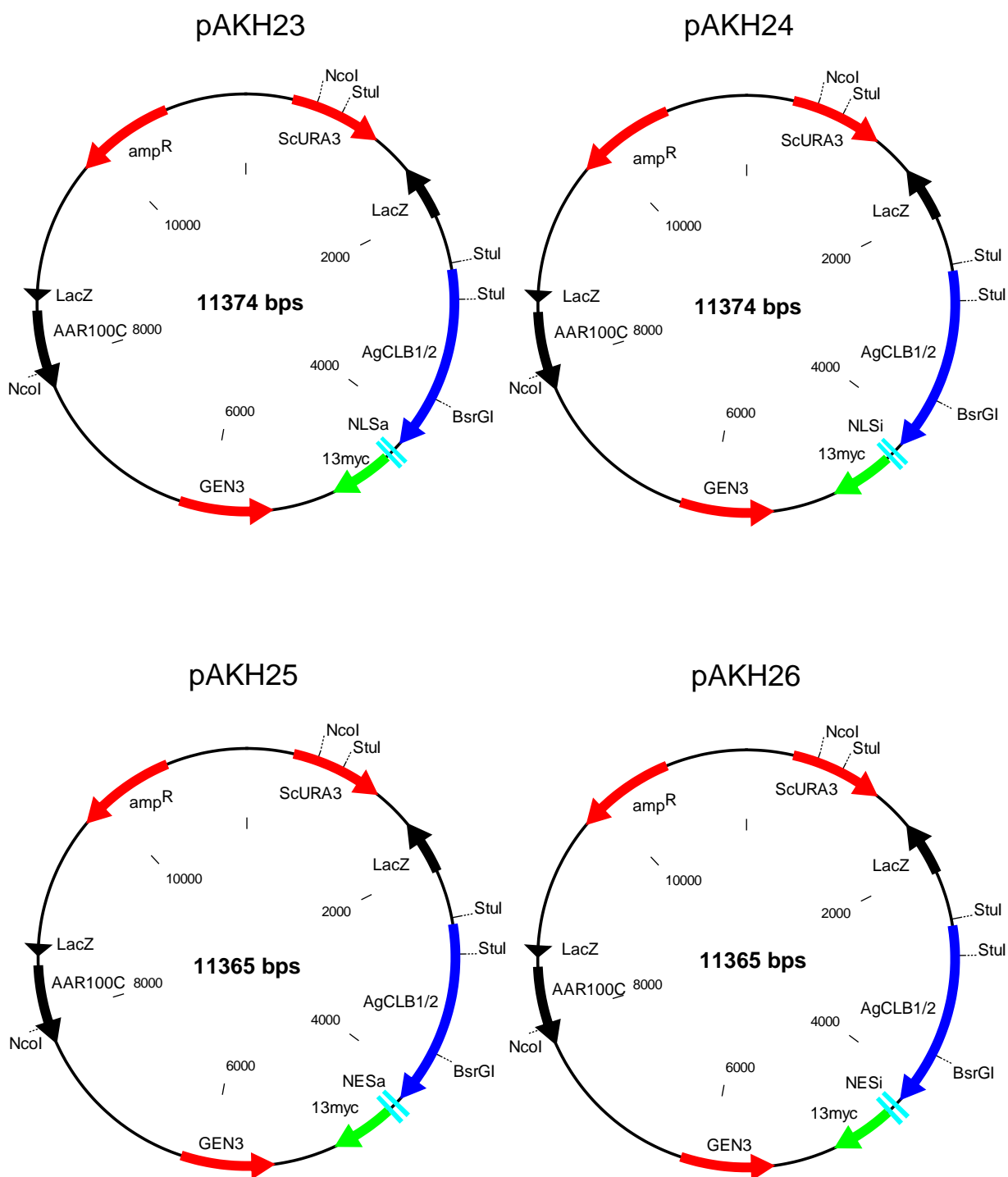
pAKH20



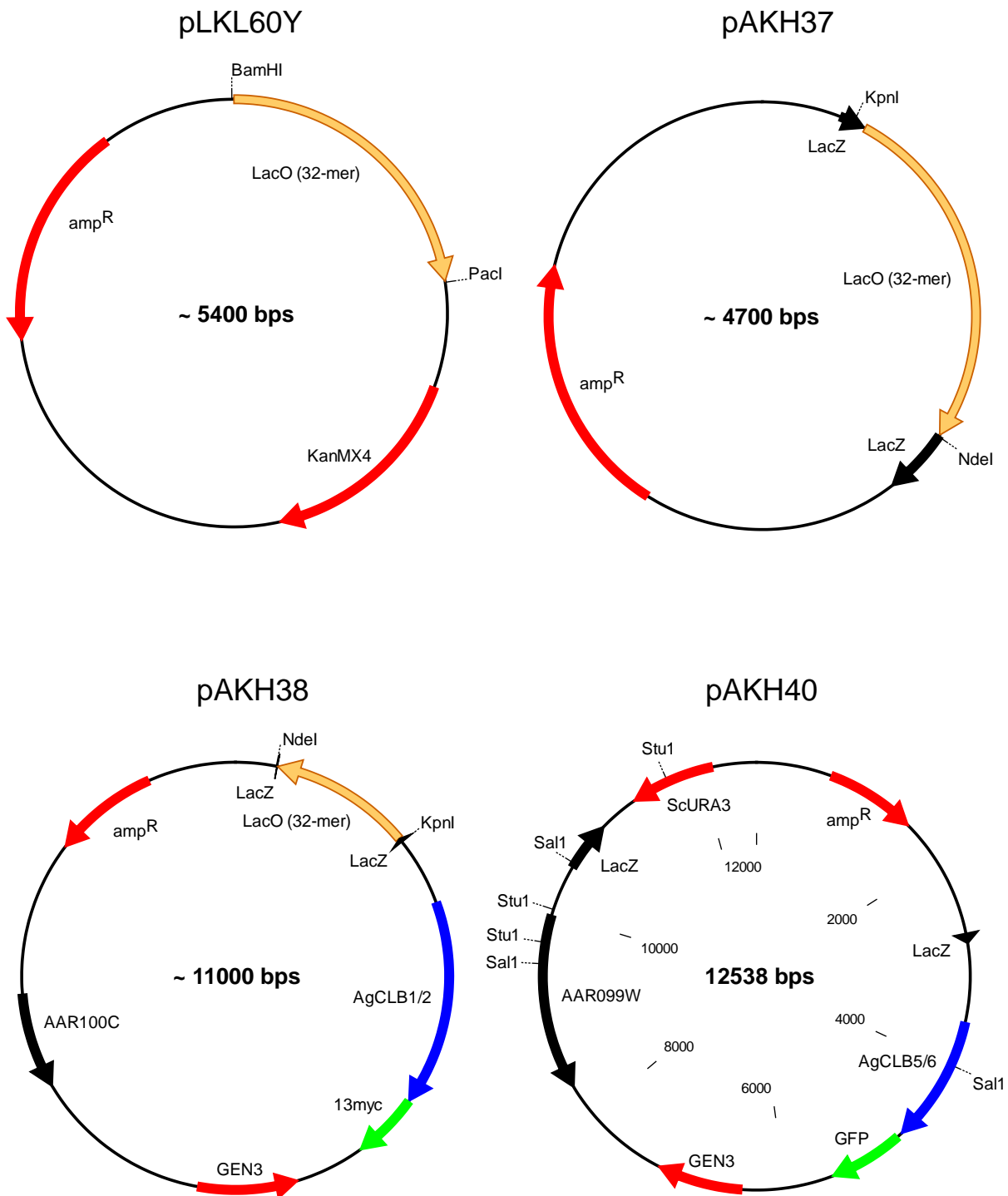
pAKH21



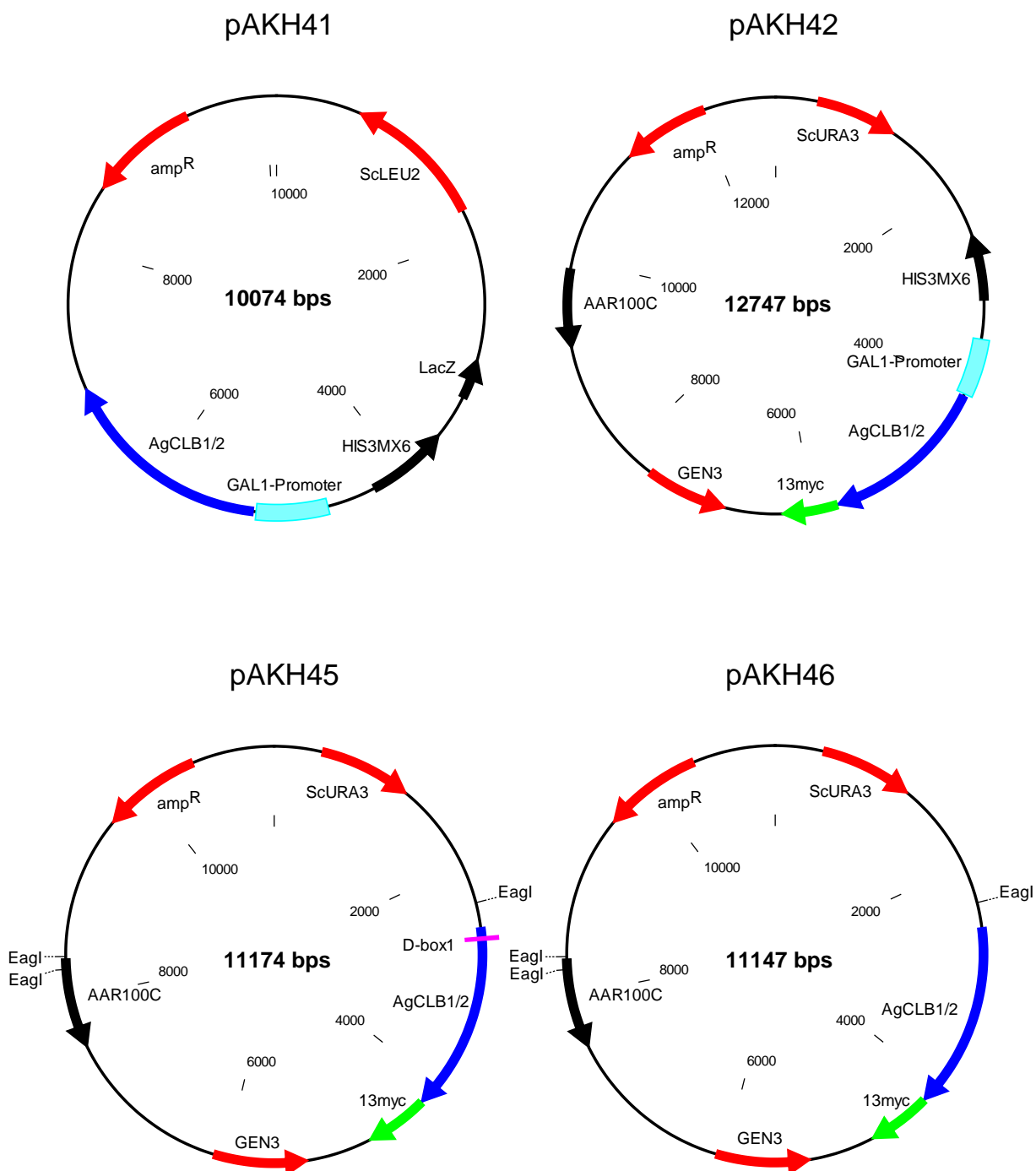
Appendix 3



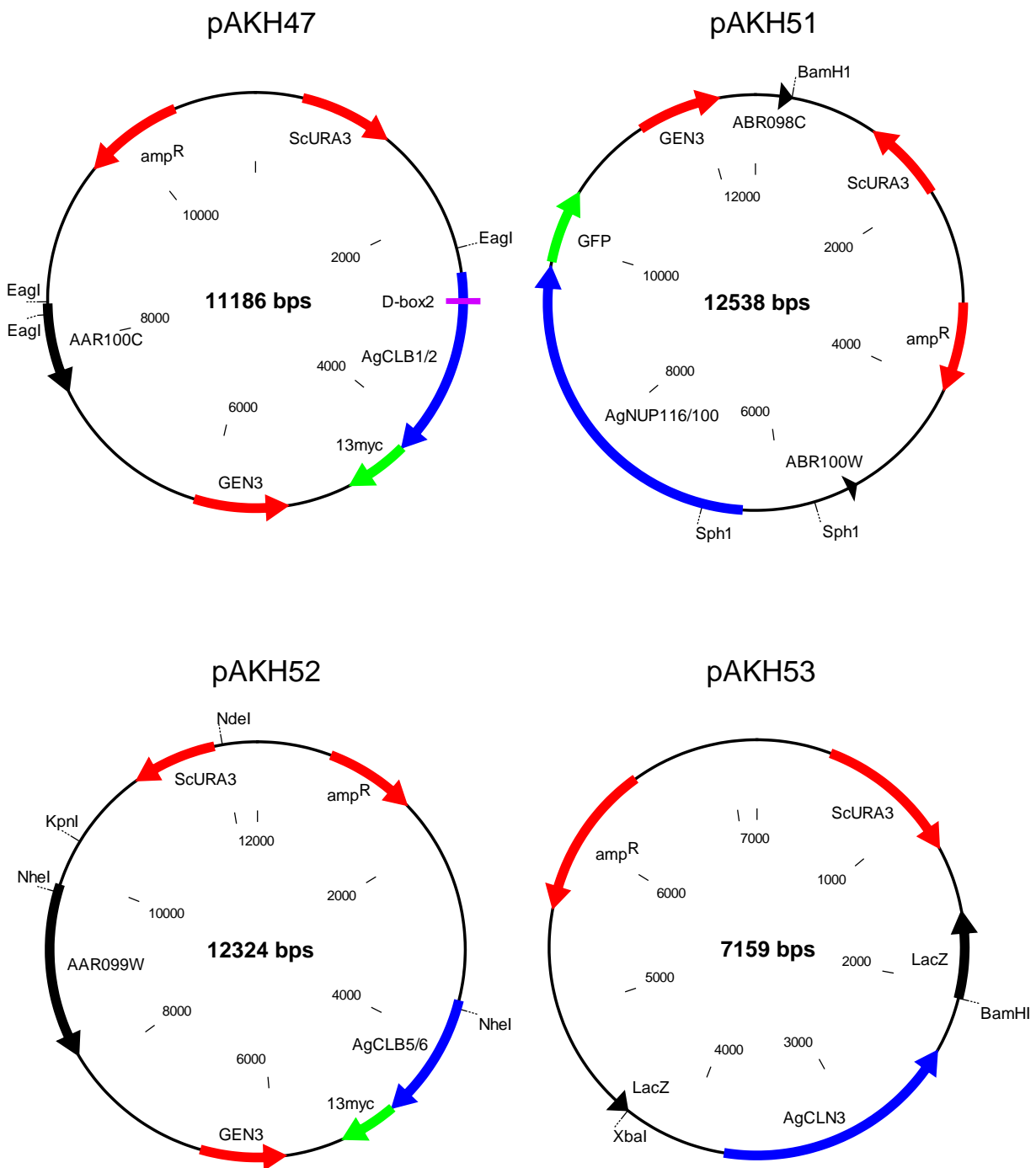
Appendix 3



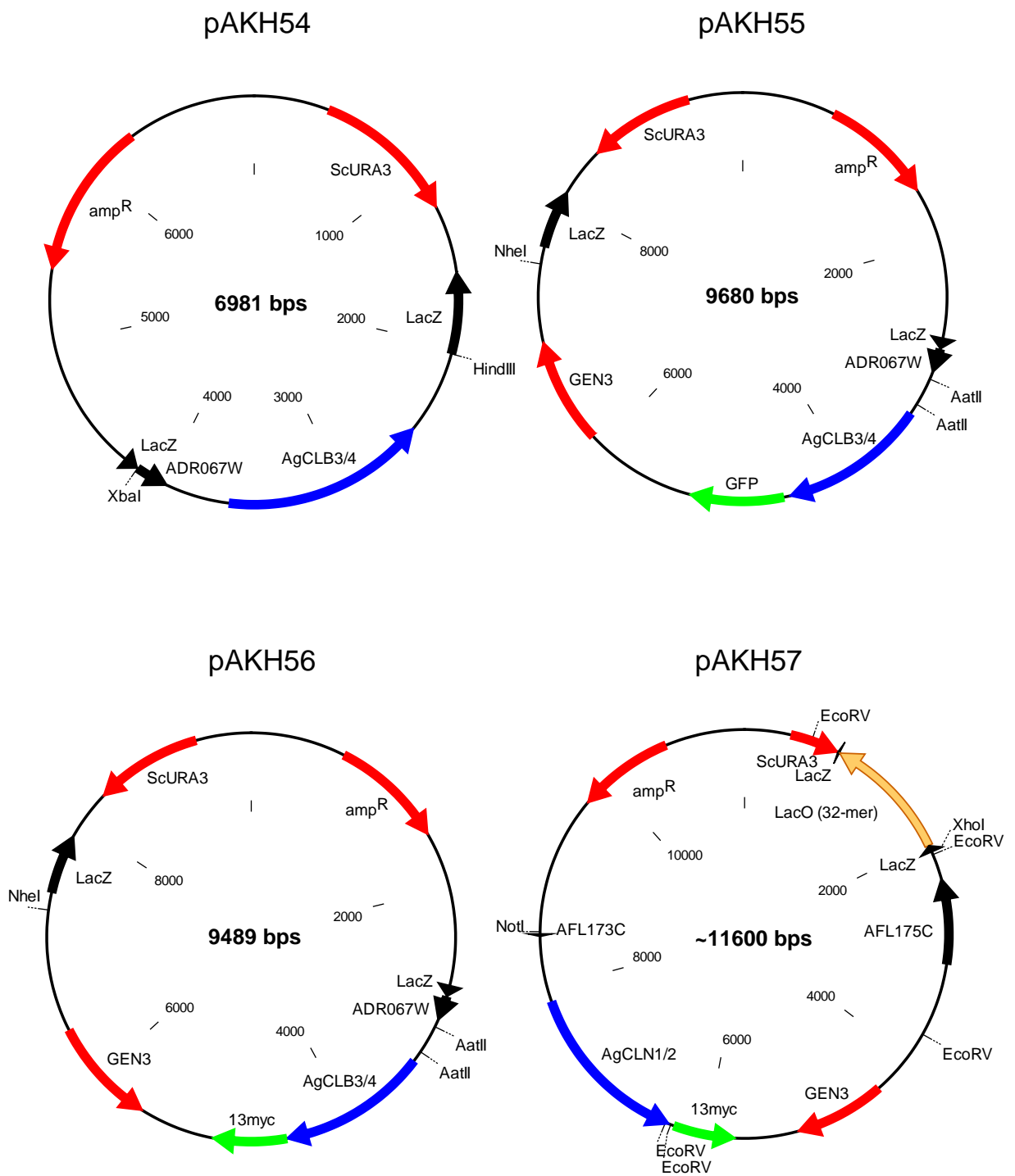
Appendix 3



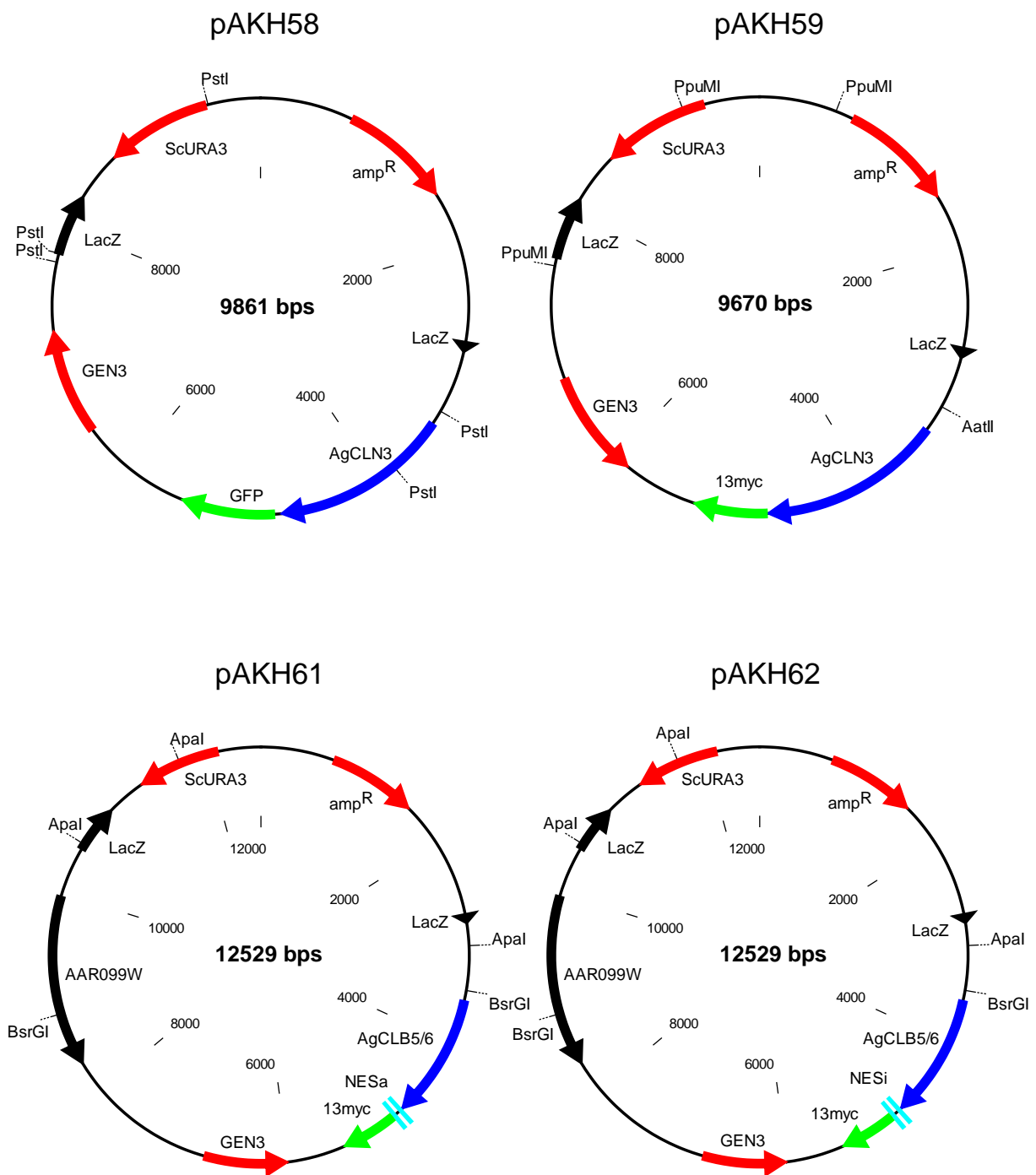
Appendix 3



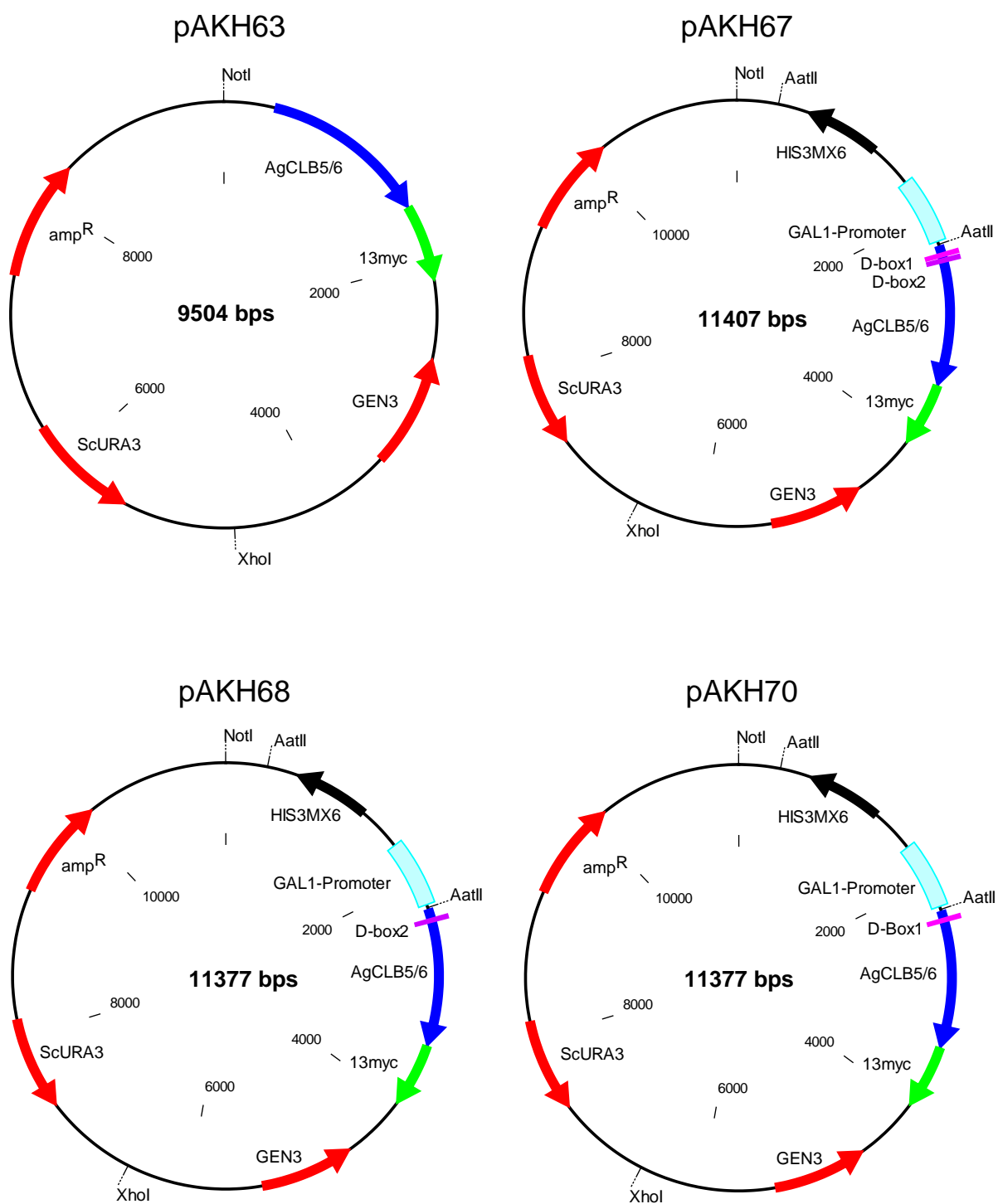
Appendix 3



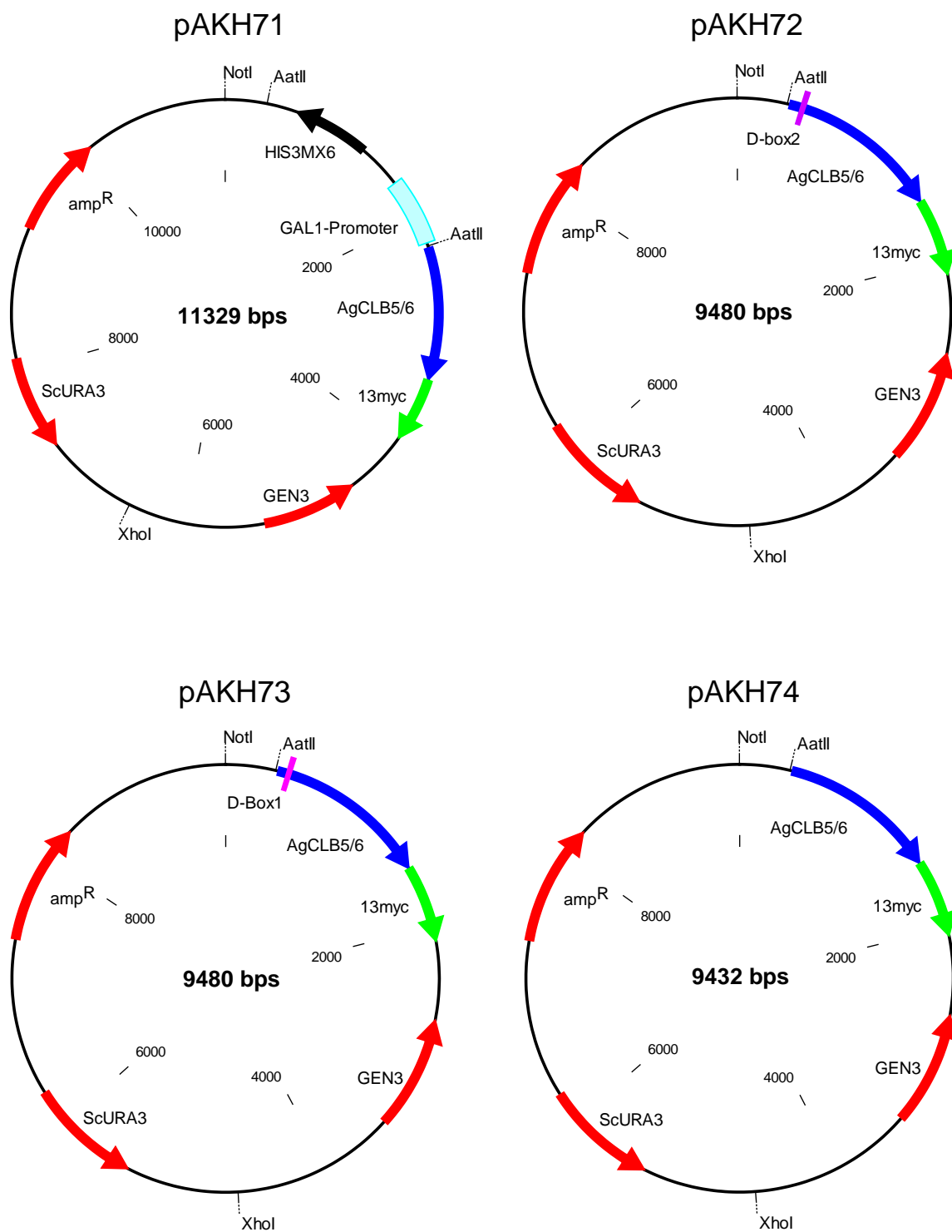
Appendix 3



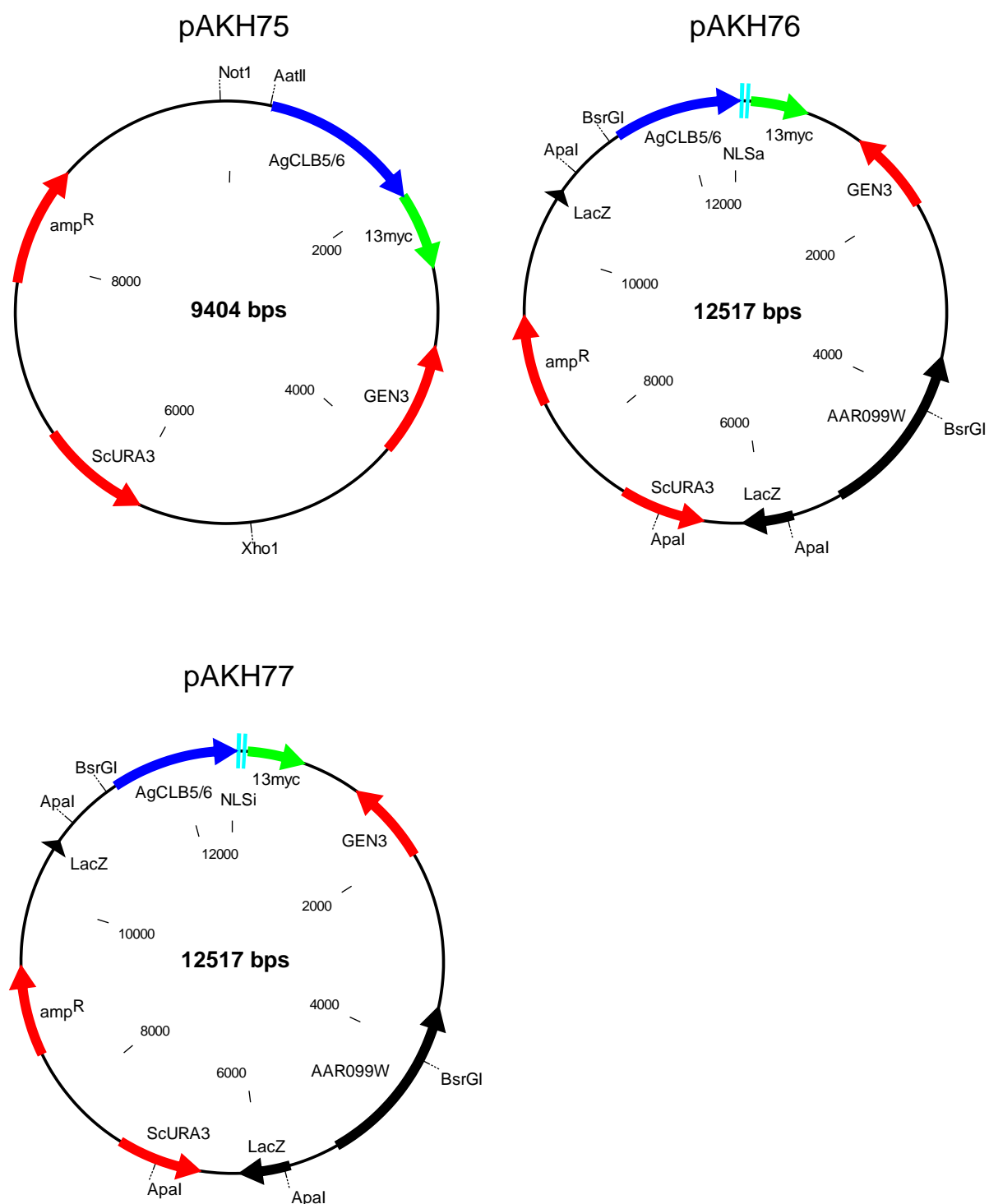
Appendix 3



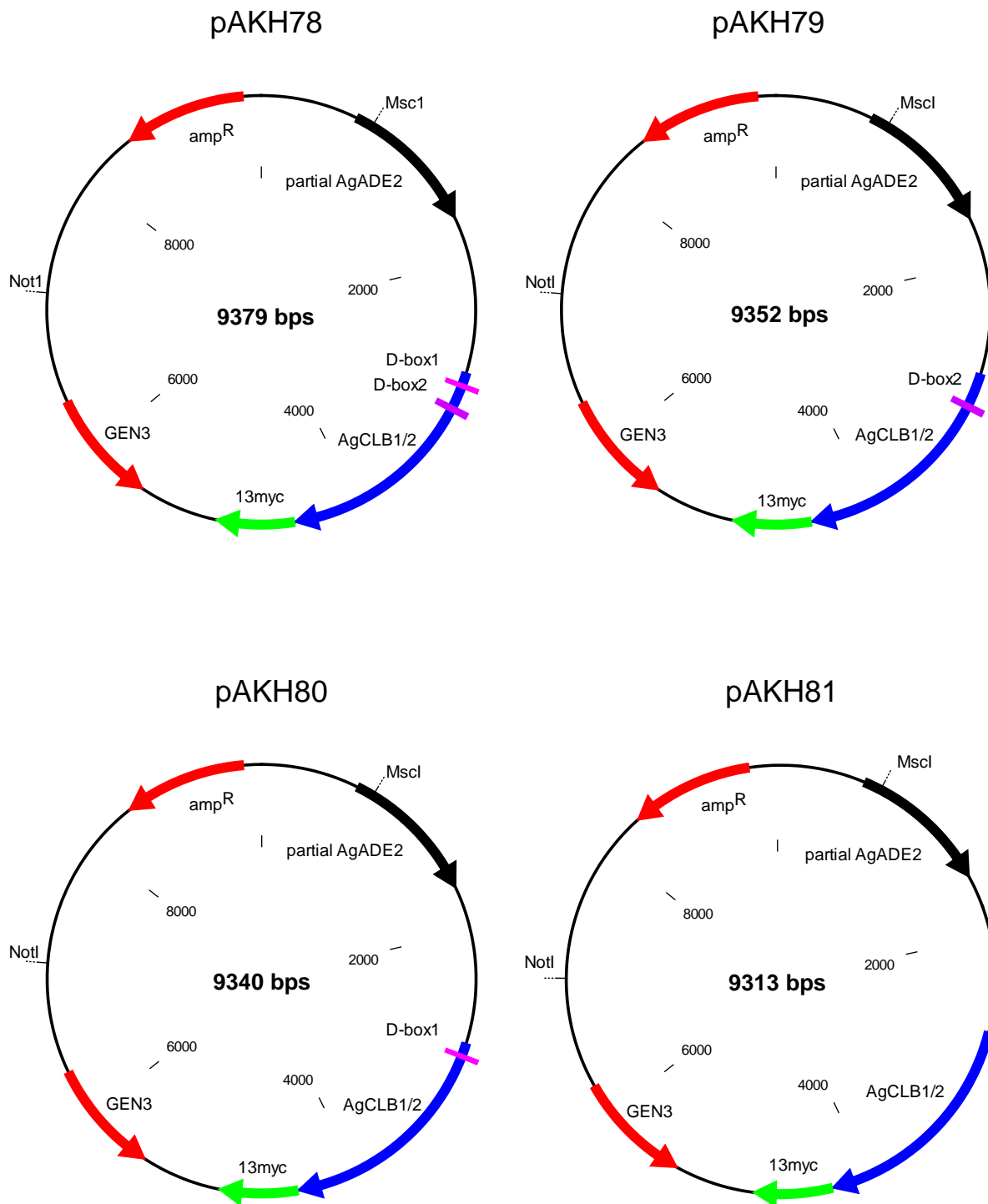
Appendix 3



Appendix 3



Appendix 3



Acknowledgements

I am very grateful to Prof. Peter Philippsen for giving me the opportunity to do my PhD on the fascinating field of the nuclear cycle. He offered me to study cyclin behaviour in *A. gossypii*, however he also gave me the freedom to decide which part of this area I wanted to investigate more closely. He supported me with many fruitful discussions and provided an excellent lab environment. In addition, he gave me the chance to participate on interesting conferences and meet special scientists.

I would like to thank Amy Gladfelter for supervising my work, for her stimulating discussions and her encouraging manners. She showed me the basics of scientific writing, taught me to be positive and convinced about data and supported me with great ideas. I very much enjoyed our close collaboration which was not only based on interesting science, but also friendship.

I would like to thank Prof. Yves Barral for participating as a member in my thesis committee, providing guidance and inspiring discussions. In addition I also would like to thank Prof. Jean Pieters, for being the representative of the Dean during my thesis defense.

Additionally I would like to acknowledge Michael Köhli, for his constant interest in my data, his good spirits and our adventures with Bonny and Clyde, Hans-Peter Schmitz for sharing his knowledge in the lab and helping me using the computer facilities, Andreas Kaufmann for being the good ghost with repairing and maintaining and doing what nobody else likes to do, Kamila Boudier for her friendship and discussions about life, Sylvia Voegeli and Virginie Galati for having relaxing times during lunch in the Mensa and all the other members or previous members in the lab who were all greatly involved in providing the warm and friendly atmosphere I enjoyed so much working in.

I also thank my family and friends, for their constant support during the ups and downs of this interesting time. Especially I would like to thank my parents for their confidence and love which has supported me for all my life.

Finally, I would like to thank Hanspeter Helfer. With his quiet and charming presence he made daily work an enjoyable experience. Even though it took me a long time to realize that he is much more than just a friend, I am very happy that he became a central part in my life. I would like to thank him for being the way he is, for his love and friendship.

Curriculum vitae

Anne Katrin Hungerbühler

Davidsrain 4
4056 Basel

Date of birth: 29.09.1978

Place of birth: Winterthur, Switzerland

Nationality: Swiss

Education:

1984-1989	Primary school Rheinfelden, Switzerland
1989-1993	Secondary school Rheinfelden, Switzerland
1993-1997	Grammar school Muttenz, Switzerland
1998-2003	Study of molecular biology at the University of Basel, including blockcourses in biochemistry, biophysical chemistry, microbiology cellbiology and microscopy.
2002-2003	Diploma Thesis in Microbiology "Cell Cycle Regulation in <i>Ashbya gossypii</i> : Analysis of B-type Cyclin Homologs". In the lab of Prof. P. Philippsen, Biozentrum Basel, Switzerland
2003-2006	PhD Thesis in Microbiology "Some cycle others do not" New views on cyclin function in the multinucleate hyphae of <i>A. gossypii</i> . In the lab of Prof. P. Philippsen, Biozentrum, Basel, Switzerland

Publications:

Gladfelter, A.S., **A.K. Hungerbuehler**, and P. Philippsen. 2006. Asynchronous nuclear division cycles in multinucleated cells. *J Cell Biol.* 172:347-62.

Conferences:

- April 2002, 6th European Conference on Fungal Genetics (EGFG VI), Pisa, Italy.
- July 2004, Yeast Genetics and Molecular Biology Meeting, University of Washington, Seattle, Washington, USA
- March 2005, 23 Fungal Genetics Conference, Asilomar, CA, USA.

Erklärung

Ich erkläre, dass ich die Dissertation

„Some cycle others do not“
New views on cyclin function in the multinucleate hyphae of *A. gossypii*

nur mit der darin angegebenen Hilfe verfasst und bei keiner anderen Fakultät eingereicht habe.

Basel, Mai 2006

Anne Katrin Hungerbühler